

Description of a new species of *Paraplehnia* (Polycladida, Stylochoidea) from Japan, with inference on the phylogenetic position of Plehniidae

Yuki Oya¹, Taeko Kimura², Hiroshi Kajihara³

1 Graduate School of Science, Hokkaido University, Sapporo 060-0810, Japan **2** Graduate School of Bio-resources, Mie University, Kurimamachiya-cho 1577, Tsu 514-8507, Japan **3** Faculty of Science, Hokkaido University, Sapporo 060-0810, Japan

Corresponding author: Yuki Oya (yoya@eis.hokudai.ac.jp)

Academic editor: Tom Artois | Received 19 February 2019 | Accepted 14 May 2019 | Published 15 July 2019

<http://zoobank.org/49229E2C-8630-48A6-81F7-6318511EFE31>

Citation: Oya Y, Kimura T, Kajihara H (2019) Description of a new species of *Paraplehnia* (Polycladida, Stylochoidea) from Japan, with inference on the phylogenetic position of Plehniidae. ZooKeys 864: 1–13. <https://doi.org/10.3897/zookeys.864.33955>

Abstract

We describe a new species of polyclad flatworm, *Paraplehnia seisuiae* **sp. nov.**, from 298–310 m depths in the Sea of Kumano, West Pacific, Japan. *Paraplehnia seisuiae* **sp. nov.** is characterized by i) a developed muscular wall proximally occupying about one-third of the prostatic vesicle, ii) no common duct between the spermiducal bulbs and the prostatic vesicle, and iii) a genital pit between the male and female gonopores. We provide a partial sequence (712 bp) of the mitochondrial cytochrome *c* oxidase subunit I gene as a DNA barcode for the species. Our phylogenetic analyses based on 603-bp 28S rDNA sequences indicate that *P. seisuiae* **sp. nov.** is nested in a clade consisting of stylochoid species along with unidentified species of *Stylochus*. It suggests that Plehniidae belongs to Stylochoidea, although this should be confirmed by future studies that contain *Plehnia arctica* (Plehn, 1896), the type species of the type genus of the family. The interfamily relationship among the superfamily Stylochoidea remains poorly resolved.

Keywords

28S rDNA, Acotylea, Bayesian inference, COI, marine flatworm, maximum likelihood, taxonomy

Introduction

Polyclad flatworms in the family Plehniidae Bock, 1913 are characterized by possessing sperm ducts or a common sperm duct entering the neck of a prostatic vesicle, the latter lacks an ejaculatory duct (Hyman 1953). The majority of plehniids have been reported from sublittoral zones by dredging (e.g. Bock 1913, 1923; Kato 1939; Hyman 1953; Hagiya 1993); some species were described from more than 200 m depths (Bock 1913; Hyman 1953).

The superfamilial affinity of Plehniidae has not been molecularly tested, while both Faubel (1983) and Prudhoe (1985) placed the family in Stylochoidea Poche, 1926 based on morphological characters. No plehniid has been represented in recent molecular phylogenetic analyses (Aguado et al. 2017; Bahia et al. 2017; Tsunashima et al. 2017; Litvaitis et al. 2019), although Bahia et al. (2017) indicated that Plehniidae possibly belongs to Cryptoceloidea Laidlaw, 1903. There has been a conflict between Faubel (1983) and Prudhoe (1985) as to the genus-level classification in Plehniidae. Faubel (1983) divided Plehniidae into three genera: *Diplehnia* Faubel, 1983, *Discocelides* Bergendal, 1893, and *Plehnia* Bock, 1913. Prudhoe (1985) separated this family into four genera: *Discocelides*, *Nephtheaplana* Prudhoe, 1985, *Paraplehnia* Hyman, 1953, and *Plehnia*. Later, Newman and Cannon (1997) established a new genus, *Myoramyxia*, within Plehniidae in the sense of Prudhoe (1985).

In this paper, we describe a new species of plehniid flatworm from Japan. We provide a partial sequence of the cytochrome *c* oxidase subunit I (COI) gene as a DNA barcode for the new species. We estimate the phylogenetic position of Plehniidae, represented by the new species, among other acotylean polyclads by molecular analyses using partial 28S rDNA sequences.

Material and methods

A single polyclad specimen was collected by dredging during the research cruise No. 1722 by Training/Research Vessel (TRV) *Seisui-maru*. The worm was anesthetized in a MgCl₂ solution prepared with tap water so that it had the same refractive index (or “salinity”) as the seawater, using an IS/Mill-E refractometer (AS ONE, Japan), and then photographed with a Nikon D5300 digital camera with external strobe lighting provided by a pair of Morris Hikaru Komachi Di flash units. For DNA extraction, a piece of the body margin was cut away from the specimen and fixed in 100% ethanol. The rest of the body was fixed in Bouin’s solution for 24 h and preserved in 70% ethanol. It was then cut into two (anterior and posterior) pieces. Both pieces were dehydrated in an ethanol series and cleared in xylene, then embedded in paraffin wax, sectioned at 7 μm thickness, stained with hematoxylin and eosin (HE), and embedded in Entellan New (Merck, Germany). They were observed under an Olympus BX51 compound microscope and photographed with a Nikon D5300 digital camera.

Sections containing part of copulatory apparatus, mounted on one of the slides, were re-stained by Mallory’s trichrome method to yield clear contrast between the muscular and connective tissues. The cover glass was removed by steeping the prepara-

Table 1. List of species that were used for the molecular phylogenetic analysis and respective GenBank accession numbers.

Species	GenBank accession number
Acotylea	
<i>Adenoplana evelinae</i> Marcus, 1950	KY263647
<i>Anemiyaita pacifica</i> Kato, 1944	LC100077
<i>Armatoplana leptalea</i> (Marcus, 1947)	KY263649
<i>Callioplana marginata</i> (Stimpson, 1857)	LC100082
<i>Discoplana gigas</i> (Schmarda, 1859)	LC100080
<i>Echinoplana celerrima</i> Haswell, 1907	HQ659020
<i>Hoploplana californica</i> Hyman, 1953	KC869850
<i>Hoploplana divae</i> Marcus, 1950	KY263692
<i>Hoploplana villosa</i> (Lang, 1884)	LC100076
<i>Idioplana australiensis</i> Woodworth, 1898	HQ659008
<i>Imogine ijimai</i> (Yeri & Kaburaki, 1918)	LC100079
<i>Imogine oculiferus</i> (Girard, 1853)	HQ659007
<i>Imogine refertus</i> (Du Bois-Reymond Marcus, 1965)	KY263694
<i>Imogine zebra</i> (Verrill, 1882)	AF342800
<i>Koinostylochus elongatus</i> (Kato, 1937)	LC100083
<i>Leptoplana tremellaris</i> (Müller, 1773)	KY263696
<i>Leptostylochus gracilis</i> Kato, 1934	LC100078
<i>Melloplana ferruginea</i> (Schmarda, 1859)	HQ659014
<i>Notocomplana humilis</i> (Stimpson, 1857)	LC100085
<i>Notoplana australis</i> (Schmarda, 1859)	HQ659015
<i>Notoplana</i> sp.	KY263651
<i>Paraplanocera oligoglena</i> (Schmarda, 1859)	KC869849
<i>Paraplanocera</i> sp.	KY263699
<i>Paraplehnia seisuiiae</i> sp. nov.	LC467000
<i>Phaenocelis medvedica</i> Marcus, 1952	KY263706
<i>Planocera multitentaculata</i> Kato, 1944	LC100081
<i>Pleioplana delicata</i> (Yeri & Kaburaki, 1918)	LC100088
<i>Pseudostylochus obscurus</i> (Stimpson, 1857)	LC100084
<i>Stylochus</i> sp.	KY263743
Outgroup (Cotylea)	
<i>Cestoplana rubrocincta</i> (Grube, 1840)	HQ659009
<i>Pericelis orbicularis</i> (Schmarda, 1859)	EU679116

tion in xylene for 24 h. The sections on the slide were hydrated in an ethanol series. HE staining was then removed by washing in 50% ethanol containing 0.5% HCl for 2 h. After Mallory's staining, the sections were likewise embedded in Entellan New.

Total DNA was extracted by using Boom et al.'s (1990) silica method. A fragment of the cytochrome *c* oxidase subunit I (COI) (712 bp) was amplified with primers *Acotylea_COI_F* and *Acotylea_COI_R* (Oya and Kajihara 2017) as a reference for DNA barcoding. A 1004-bp fragment of 28S rDNA was amplified with primers *fw1* and *rev2* (Sonnenberg et al. 2007) for molecular phylogenetic analyses; the primer pairs have been used in other phylogenetic studies of polyclads (e.g. Bahia et al. 2017; Litvaitis et al. 2019). Polymerase chain reaction (PCR) amplification conditions were 94 °C for 5 min; 35 cycles of 94 °C for 30 s, 50 °C (COI) or 52.5 °C (28S rDNA) for 30 s, and 72 °C for 1.5 min (COI) or 2 min (28S rDNA); and 72 °C for 7 min. All nucleotide sequences were determined by direct sequencing with a BigDye Terminator Kit ver. 3.1 and 3730 Genetic Analyzer (Life Technologies, California, USA); two internal primers, *fw2* and *rev4* (Sonnenberg et al. 2007), were used in sequencing 28S rDNA. Sequences were checked and edited using MEGA ver. 5.2 (Tamura et al. 2011).

Additional 28S rDNA sequences of *Acotylea* were downloaded from GenBank. Two cotylean species were chosen as outgroups (Table 1): *Cestoplana rubrocincta* (Grube, 1840) and *Pericelis orbicularis* (Schmarda, 1859), the former was transferred to *Cotylea* by Bahia et al. (2017). Sequences were aligned using MAFFT ver. 7 (Kato and Standley 2013), with the FFT-NS-i strategy selected by the “Auto” option. Ambiguous sites were removed with Gblocks ver. 0.91b (Castresana 2002) using a less stringent option. The optimal substitution models selected with Kakusan4 (Tanabe 2011) under the Akaike Information Criterion (AIC) (Akaike 1974) were GTR+G.

Phylogenetic analyses were performed with maximum-likelihood (ML) methods and Bayesian Inference (BI). The ML analysis was performed with RAxML ver. 8.2.3 (Stamatakis 2014). Nodal support within the ML tree was assessed by analyses of 1,000 bootstrap pseudoreplicates (Felsenstein 1985). BI was performed with MrBayes ver. 3.2.2 (Ronquist and Huelsenbeck 2003). The Markov chain Monte Carlo (MCMC) process used random starting trees and involved four chains for 1,000,000 generations. The first 25% of the trees were discarded as burn-in.

Type slides have been deposited in the Invertebrate Collection of the Hokkaido University Museum, Sapporo, Japan (ICHUM). The sequences determined in this study have been deposited in DDBJ/EMBL/GenBank databases with the accession numbers LC466999 (COI) and LC467000 (28S rDNA).

Results

Family Plehniidae Bock, 1913 sensu Prudhoe (1985)

Genus *Paraplehnia* Hyman, 1953

Paraplehnia seisiae sp. nov.

<http://zoobank.org/565559B6-CFC2-4CF6-A4F7-BFAFCCCF4EEDA>

Figures 1, 2

Etymology. The specific name is a noun in the genitive case and taken from the TRV *Seisui-maru*.

Material examined. One specimen: holotype, ICHUM 5345, 44 slides (14 slides for the anterior part and 30 slides for the posterior part of the body), dredged from 298–310 m depths, the Sea of Kumano, between 34°08.0'N, 136°37.8'E to 34°07.8'N, 136°37.9'E, Japan.

Description. Live specimen 26 mm in length, 11 mm in width. Body thick, elongate, oval, narrow toward posterior end (Fig. 1A, B). Anterior and posterior ends pointed. Body ground color translucent to whitish opaque. General appearance of body light brown. Dorsal body without any pattern. Body margin translucent. Tentacles lacking. Pharynx, ruffled in shape, 7.4 mm in length, located at center of body. Mouth opening at center of pharyngeal cavity (Fig. 1B). Intestine highly branched and not anastomosing, spreading throughout body except margin. Pair of sperm ducts and oviducts whitish, visible through



Figure 1. *Paraplehnia seisuiiae* sp. nov., ICHUM 5345 (holotype), photographs taken in life and eyespots observed in sections. **A** Dorsal view **B** ventral view **C** marginal eyespot (inset showing magnification of black box) **D** cerebral eyespot (inset showing magnification of black box). Abbreviations: **br** brain **ce** cerebral eyespot **fg** female gonopore **m** mouth **me** marginal eyespot **mg** male gonopore **ov** oviduct **ph** pharynx **sd** sperm duct. Scale bar: 10 mm (**A**, **B**); 600 μ m (**C**, **D**); 20 μ m (insets in **C**, **D**),.

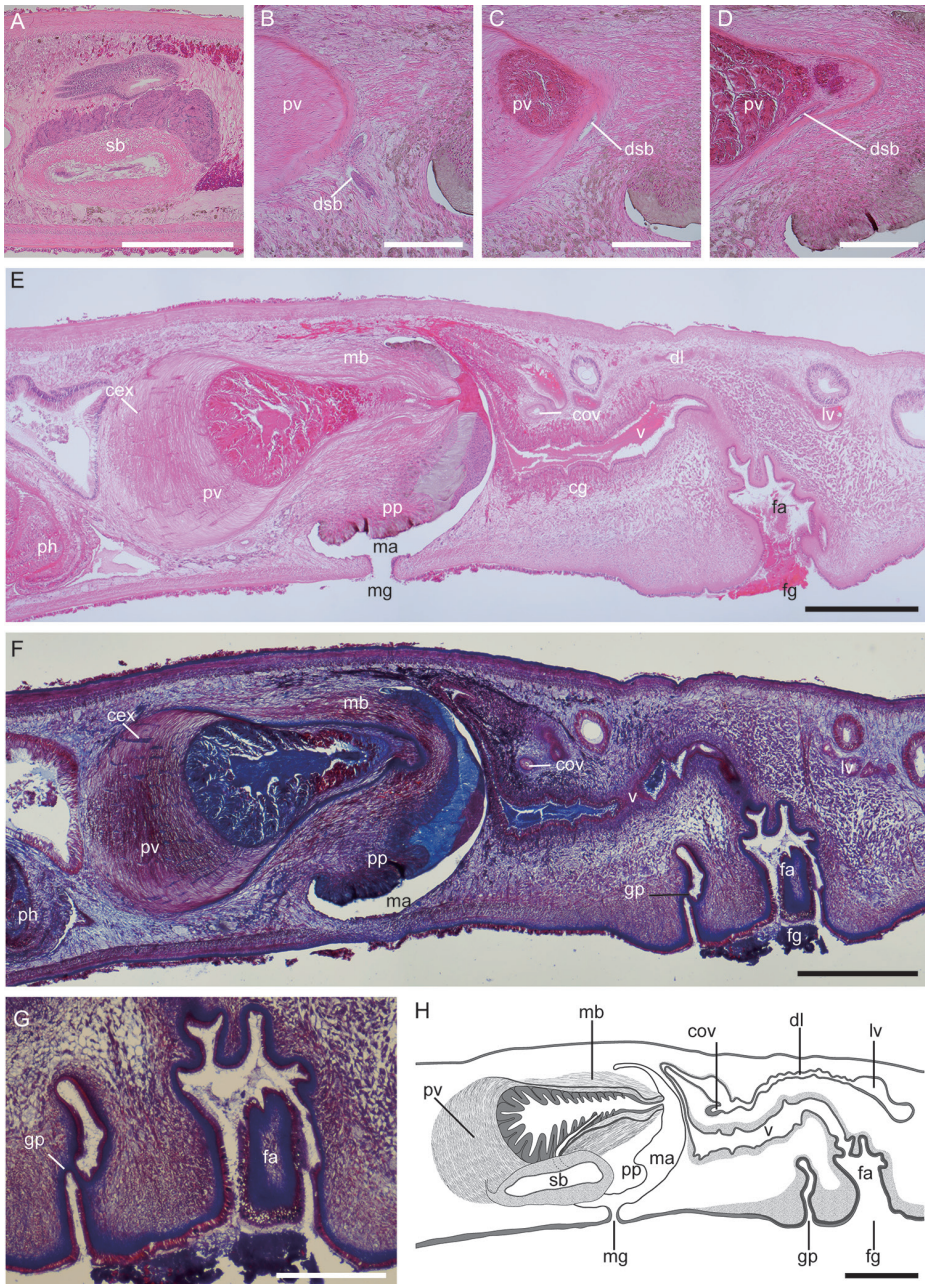


Figure 2. *Paraplehmia seisuiae* sp. nov., ICHUM 5345 (holotype), sagittal sections (**A–G**) and schematic diagram (**H**). **A** Spermiducal bulb **B–D** connection between spermiducal bulb and prostatic vesicle **E, F** copulatory apparatus **G** genital pit **H** schematic diagram of copulatory complex. Abbreviations: **cex** canal of extra-vesicular grand **cg** cement glands **cov** common oviduct **dl** duct of Lang's vesicle **dsb** duct of spermiducal bulb **fa** female atrium **fg** female gonopore **gp** genital pit **lv** Lang's vesicle **ma** male atrium **mb** muscular bulb **mg** male gonopore **ph** pharynx **pp** penis papilla **pv** prostatic vesicle **sb** spermiducal bulb **v** vagina. Scale bars: 600 μ m (**A, E, F, H**); 300 μ m (**B–D, G**). Staining: hematoxylin and eosin stain (**A–E**); Mallory's triple stain (**F, G**).

ventral surface. Male and female gonopores separate; male gonopore opening at 9 mm from posterior end; female gonopore situated 2.5 mm posterior to male gonopore.

Marginal and cerebral eyespots small and embedded in parenchyma (Fig. 1C, D). At least 47 and 28 eyespots arranged in anterior body margin and from just behind brain to anterior to brain, respectively, but detailed distribution of eyespots could not be observed.

Male copulatory apparatus located posteriorly to pharynx, consisting of pair of spermiducal bulbs, prostatic vesicle, and penis papilla (Fig. 2A–E). Distal end of each sperm duct forming oval spermiducal bulb, latter having thick muscular wall (Fig. 2A). Distal end of each spermiducal bulb slender and separately connecting to neck of prostatic vesicle (Fig. 2B–D). Prostatic vesicle pear-shaped, having strong muscular wall occupying its proximal one-third, distally coated with connective tissue and enclosed by muscular bulb (Fig. 2F). Canals of extra-vesicular gland penetrating prostatic-vesicle wall. Glandular epithelium with numerous teardrop-shaped cells folded in prostatic vesicle. Ejaculatory duct lacking; distal end of prostatic vesicle directly forming a part of penis papilla. Penis papilla large, conical, and projecting posteriorly into male atrium. Male atrium lined with thin, non-ciliated epithelium.

Pair of oviducts forming common oviduct, which run postero-dorsally to enter vagina (Fig. 2E). From this point, elongated duct of Lang's vesicle, lined with ciliated epithelium, running posteriorly. Lang's vesicle sac-shaped, lined with squamous cells, positioned posterior to female gonopore. Vagina lined with smooth ciliated epithelium, running antero-dorsally, curving postero-ventrally as it becomes slenderer, turning postero-dorsally as it becomes wider, eventually leading ventrally to exit at female atrium (or vagina externa). Medial part of vagina surrounded by numerous cement glands (Fig. 2E). Female atrium large, folded, with thick basement membrane opening at female gonopore.

Genital pit with smooth epithelium and basement membrane similar to those in vagina (Fig. 2G), located between male and female gonopores (Fig. 2F, H).

Habitat. Judging from the nature of the dredged material, the sediment type of the species' habitat is likely to be sandy mud.

Molecular phylogeny. The resulting BI and ML trees were almost identical to each other in topology. *Paraplehnia seisuiiae* sp. nov. was nested in a clade composed of stylochoids except *Koinostylochus elongatus* and *Pseudostylochus obscurus* (Fig. 3); the latter two appeared to be more closely related to leptoplanoids than to stylochoids, as indicated by Tsunashima et al. (2017). The majority of stylochoids except *Callioplana marginata*, *Koinostylochus elongatus*, and *Pseudostylochus obscurus* formed a clade which also included *Stylochus* sp. of Bahia et al. (2017) and was supported by 0.99 BI posterior probability and 73% ML bootstrap (Fig. 3). Given Bahia et al.'s (2017) generic identification of *Stylochus* sp., this clade can be regarded as representing the "true" Stylochoidea, because *Stylochus* is the type genus for this family-group name. While *Paraplehnia seisuiiae* sp. nov. appeared as sister to *Hoploplana* spp., its supporting values were low (0.64 BI posterior probability; 27% ML bootstrap). The inter-family relation of Plehniidae among Stylochoidea was thus not fully resolved in the present study.

Remarks. In this paper, we follow the classification system by Prudhoe (1985), in which Plehniidae consists of five genera (*Discocelides*, *Myorammyxa*, *Nephtheaplana*, *Paraplehnia*, and *Plehnia*); for Faubel's (1983) system, see Discussion below. Hyman (1953)

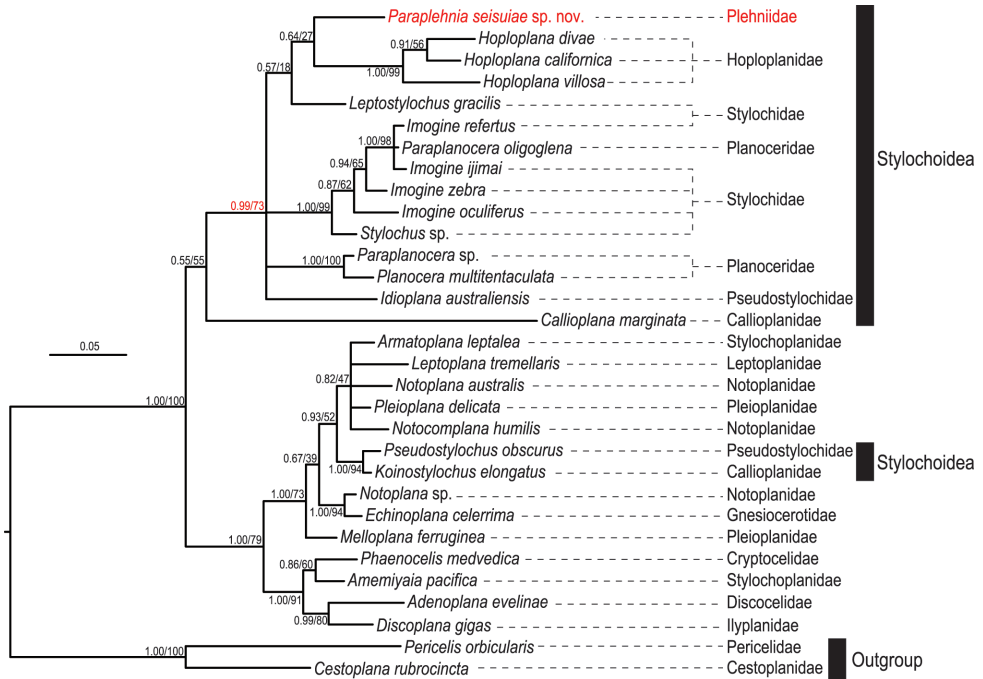


Figure 3. Bayesian phylogenetic tree based on 28S rDNA sequences (603 bp in total). Numbers near nodes are posterior probability and bootstrap value, respectively.

characterized *Paraplehnia* as possessing a prostatic vesicle that has i) a strong muscular wall in its proximal end and ii) a reduced glandular part. *Paraplehnia seisuiae* sp. nov. is characteristic of the genus by possessing these characteristics. By these characters, our new species cannot be placed in *Plehnia* sensu Prudhoe (1985), because the latter is diagnosed to have a prostatic vesicle whose proximal end is not particularly thick-walled. *Paraplehnia seisuiae* sp. nov. differs from *Discocelides* and *Myoramymxa* in that it does not have a vaginal duct (ductus vaginalis) and from *Nephtheaplana* in that our specimen has a pair of spermiducal bulbs.

Paraplehnia has contained two species, *P. japonica* (Bock, 1923) and *P. pacifica* (Kato, 1939), and both were originally described from the sublittoral zone in Japan. *Paraplehnia seisuiae* sp. nov. can be distinguished from the two congeners by the thickness of the muscular wall of the prostatic vesicle (about one-third of the prostatic vesicle in *P. seisuiae* sp. nov.; about one-half in *P. japonica* and *P. pacifica*), the presence/absence of a common duct between spermiducal bulbs and prostatic vesicle (absent in *P. seisuiae* sp. nov.; present in *P. japonica* and *P. pacifica*), and the presence/absence of a genital pit between the male and the female gonopores (present in *P. seisuiae* sp. nov.; absent in *P. japonica* and *P. pacifica*) (Table 2). In addition, *P. seisuiae* sp. nov. differs from *P. japonica* by the length of the Lang's duct (elongated in *P. seisuiae* sp. nov.; short in *P. japonica*) and from *P. pacifica* by the range of developed connective tissues in the female copulatory apparatus (from the female atrium to around the female gonopore and the genital pit in *P. seisuiae* sp. nov.; only around the female atrium in *P. pacifica*).

Table 2. Comparison of characters between species of *Paraplehnia*.

	<i>P. japonica</i> (Bock, 1923)	<i>P. pacifica</i> (Kato, 1939)	<i>P. seisuia</i> sp. nov.
Type locality	Kobe Bay, Japan	Tako-shima, Onagawa, Japan	Sea of Kumano, Japan
Depth	12–15 m	28 m (Kato 1939); 64, 78 m (Hagiya 1993)	298–310 m
Muscular wall in posterior end of prostatic vesicle	About 1/2 of the prostatic vesicle	About 1/2 of the prostatic vesicle	About 1/3 of the prostatic vesicle
Common duct between spermiducal bulbs and prostatic vesicle	Present	Present	Absent
Genital pit	Absent	Absent	Present
Duct of Lang's vesicle	Short	Elongated	Elongated
Developed connective tissues in the female copulatory apparatus	?	Only around the female atrium	From the female atrium to the genital pit and the female gonopore
Reference	Bock 1923	Kato 1939; Hagiya 1993	This study

The eyespots were invisible in the living specimen (Fig. 1A), probably because of the thickness and opaqueness of the body, as well as the small size of each eyespot. We noticed the presence of eyespots only after sectioning (Fig. 1C, D). Bock (1923: 3) also remarked for *Paraplehnia japonica* that eyespots were undetectable in the living specimens and became apparent only after histological sectioning. Because we failed to observe the arrangement of eyespots from dorsal view in intact body, we had to categorize each eyespot into marginal ones or cerebral ones according to the relative position from the body margin and the brain.

It is for the first time that a genital pit (or genital sucker) was found in a species of plehniid. Among Acotylea, genital pits have been known in *Itannia ornata* Marcus, 1947 (Hoploplanidae Stummer-Traunfels, 1933), three species of *Leptoplana* (*Leptoplana* Stimpson, 1857) (Gammoudi et al. 2012), and *Persica qeshmensis* Maghsoudlou, Bulnes, & Rahimian, 2015 (Pleioplanidae Faubel, 1983). Genital pits in *I. ornata* are present in a pair, situated on both sides of the female gonopore (Marcus 1952). On the other hand, a single genital pit is present between the male and female gonopores in three *Leptoplana* species and *Persica qeshmensis*, as well as in *Paraplehnia seisuia* sp. nov. (Fig. 2H, I).

Discussion

In this paper, we adopted Prudhoe's (1985) – instead of Faubel's (1983) – classification system as to the infrafamilial classification of Plehniidae because this system was followed by some of the subsequent researchers (e.g. Hagiya 1993; Newman and Cannon 1997). Faubel (1983) did not accept *Paraplehnia* because he considered that “the presence (*P. japonica*) or the absence (*P. pacifica*) of Lang's vesicle demands a separation of both these species” (Faubel 1983: 54–55) and classified *Paraplehnia pacifica* as a *Diplehnia*, which was characterized by lacking a Lang's vesicle (Faubel 1983). However, Kato (1939: 68, fig. 3) clearly stated that the “Lang's vesicle is small and irregularly elongated, disposed immediately behind the vagina bulbosa in the ventral part of the body” in the original description of *Paraplehnia pacifica* and also included

a line drawing of the Lang's vesicle as a schematic figure of the copulatory apparatus of *Paraplehnia pacifica*. The validity of *Diplehnia* should be tested by future molecular studies along with *Diplehnia caeca* (Hyman, 1953), the type species of the genus.

Our 28S rDNA analyses corroborate the taxonomic views by Faubel (1983) and Prudhoe (1985) in that Plehniidae, as represented by *Paraplehnia seisuia* sp. nov. in this study, should be placed in Stylochoidea (Fig. 3), rather than in Cryptoceloidea as Bahia et al. (2017) suggested. Faubel (1983) and Prudhoe (1985) placed Plehniidae in Stylochoidea based primarily on the reproductive-system morphology and the arrangement of eyespots, respectively. Bahia et al. (2017) carried out a 28S-rDNA-based molecular phylogenetic analysis covering 19 families and 32 genera of polyclads. Based on the analysis, Bahia et al. (2017: 674) circumscribed Cryptoceloidea as having “oval to elongated body, without tentacles, and with cerebral, nuchal, and marginal eyespots” and Stylochoidea as having “rounded body, nuchal tentacles, and cerebral, nuchal, and sometimes marginal eyespots”, among other super-familial redefinitions. Bahia et al. (2017: 675) stated that “Polyposthiidae and Plehniidae possibly belong to Cryptoceloidea”, probably because Plehniidae had been defined as having no tentacles (Bock 1913); our new species, *Paraplehnia seisuia* sp. nov., also lacks tentacles. Litvaitis et al. (2019) inferred the internal relationships of Polycladida using 28S rDNA sequences representing 22 families and 37 genera, and identified morphological characters for each clade recovered. Although Stylochoidea was found to be monophyletic, Litvaitis et al. (2019) concluded that this superfamily cannot be defined by any morphological or developmental synapomorphy. It was because in Litvaitis et al.'s (2019) analyses, Stylochoidea turned out to contain members that lack tentacles (e.g., Latocestidae) and have elongated body (e.g., Latocestidae and *Leptostylochus*), which do not fit to Bahia et al.'s (2017) circumscription for this superfamily. In our analysis, Stylochoidea was “split” into two clades (Fig. 3), and our new species *Paraplehnia seisuia* sp. nov., having no tentacles, appeared in one of the two stylochoid clades along with *Stylochus* sp. of Bahia et al. (2017). If we suppose that *Paraplehnia seisuia* sp. nov. is more closely related to *Plehnia arctica* (Plehn, 1896) (originally in *Acelis*; type species of *Plehnia*, which in turn is the type genus for Plehniidae) than any other type species of the type genera of all the nominal families potentially belonging to Stylochoidea, our new species should belong to Plehniidae. If so, and given that Bahia et al.'s (2017) identification of *Stylochus* sp. (see Molecular phylogeny above) was correct, Plehniidae should belong to Stylochoidea. Our study corroborates the opinion of Litvaitis et al. (2019) in that at least the presence/absence of tentacles is not appropriate to circumscribe Stylochoidea.

The inter-familial relation of Plehniidae was not resolved in this study. It is probably due to the shortness of the 28S rDNA sequence (603 bp) employed in the analyses. Future studies should be done with additional molecular markers and more extensive taxon sampling.

Acknowledgements

We thank the captain and crew of TRV *Seisui-maru*, and all the participants of the research cruise No. 1722 for help in collecting the specimen. YO is thankful to Dr Naoto

Jimi (National Institute of Polar Research) and Mr Akito Ogawa (The University of Tokyo) for inviting YO to this cruise; Dr Juliana Bahia (Ludwig-Maximilians-Universität München) for providing the sequence data. This study was funded by Research Institute of Marine Invertebrates (No. 2017 IKU-3) for YO.

References

- Aguado MT, Noreña C, Alcaraz L, Marquina D, Brusa F, Damborenea C, Almon B, Bleidorn C, Grande C (2017) Phylogeny of Polycladida (Platyhelminthes) based on mtDNA data. *Organisms Diversity & Evolution* 17(4): 767–778. <https://doi.org/10.1007/s13127-017-0344-4>
- Akaike H (1974) A new look at the statistical model identification. *IEEE Transactions on Automatic Control* 19: 716–723. <https://doi.org/10.1109/TAC.1974.1100705>
- Bahia J, Padula V, Schrödl M (2017) Polycladida phylogeny and evolution: integrating evidence from 28S rDNA and morphology. *Organisms Diversity & Evolution* 17(3): 653–678. <https://doi.org/10.1007/s13127-017-0327-5>
- Bergendal D (1893) Quelques observations sur *Cryptocelides loveni* mihi. (Note préliminaire). *Revue biologique du nord de la France* 5: 237–241.
- Bock S (1913) Studien über Polycladen. *Zoologische Bidrag från Uppsala* 2: 31–344.
- Bock S (1923) Two new acotylean polyclads from Japan. *Arkiv för Zoologi* 15(17): 1–41.
- Boom R, Sol CJ, Salimans MM, Jansen CL, Wertheim-van Dillen PM, van der Noordaa J (1990) Rapid and simple method for purification of nucleic acids. *Journal of Clinical Microbiology* 28: 495–503.
- Castresana J (2002) Gblocks, v. 0.91b. Online version. http://molevol.cmima.csic.es/castresana/Gblocks_server.html [Accessed on: 2019-1-18]
- Du Bois-Reymond Marcus E (1965) Drei neue neotropische Turbellaria. *Sitzungsberichte der Gesellschaft Naturforschender Freunde zu Berlin (NF)* 5: 129–135.
- Faubel A (1983) The Polycladida, Turbellaria. Proposal and establishment of a new system. Part I. The Acotylea. *Mitteilungen des hamburgischen zoologischen Museums und Instituts* 80: 17–121.
- Felsenstein J (1985) Confidence limits on phylogenies: an approach using the bootstrap. *Evolution* 39: 783–791. <https://doi.org/10.2307/2408678>
- Gammoudi M, Egger B, Tekaya S, Noreña C (2012) The genus *Leptoplana* (Leptoplanidae, Polycladida) in the Mediterranean basin. Redescription of the species *Leptoplana mediterranea* (Bock, 1913) comb. nov. *Zootaxa* 3178(1): 45–56. <https://doi.org/10.11646/zootaxa.3178.1.4>
- Girard CF (1853) Descriptions of new nemertean and planarians from the coast of the Carolinas. *Proceedings of the Academy of Natural Sciences of Philadelphia* 6: 365–367.
- Grube AE (1840) Actinien, Echinodermen und Würmer des adriatischen und Mittelmeers, nach eigenen Sammlungen beschreiben. Verlag von JH Bon, Königsberg, 92 pp. <https://doi.org/10.5962/bhl.title.23025>
- Hagiya M (1993) Note on some polyclad turbellarians (Platyhelminthes) from Otsuchi Bay and its vicinity, Iwate Prefecture. *Otsuchi Marine Research Center Report* 19: 31–51.

- Haswell WA (1907) Observations on Australian polyclads. Transactions of the Linnean Society of London, Zoology 9(2): 465–485. <https://doi.org/10.1111/j.1096-3642.1907.tb00455.x>
- Hyman LH (1953) The polyclad flatworms of the Pacific coast of North America. Bulletin of the American Museum of Natural History 100: 269–392.
- Kato K (1934) *Leptostylochus gracilis*, a new polyclad turbellarian. Proceedings of the Imperial Academy 10(6): 374–377. <https://doi.org/10.2183/pjab1912.10.374>
- Kato K (1937) Polyclads collected in Idu, Japan. Japanese Journal of Zoology 7: 211–232.
- Kato K (1939) Polyclads in Onagawa and vicinity. Science Reports of the Tohoku Imperial University, Fourth Series, Biology 14: 65–79.
- Kato K (1944) Polycladida of Japan. Journal of Sigenkagaku Kenkyusyo 1: 257–319.
- Katoh K, Standley DM (2013) MAFFT multiple sequence alignment software version 7: improvements in performance and usability. Molecular Biology and Evolution 30: 772–780. <https://doi.org/10.1093/molbev/mst010>
- Laidlaw FF (1903) On a collection of Turbellaria Polycladida from the Straits of Malacca. (Skeat Expedition 1899–1900). Proceedings of the Zoological Society of London 1: 301–318.
- Lang A (1884) Die Polycladen (Seeplanarien) des Golfes von Neapel und der angrenzenden Meeresabschnitte. Eine Monographie. Engelmann W, Leipzig, 688 pp. <https://doi.org/10.5962/bhl.title.10545>
- Litvaitis MK, Bolaños DM, Quiroga SY (2019) Systematic congruence in Polycladida (Platyhelminthes, Rhabditophora): are DNA and morphology telling the same story? Zoological Journal of the Linnean Society 20: 1–27. <https://doi.org/10.1093/zoolinnean/zlz007>
- Maghsoudlou A, Bulnes VN, Rahimian H (2015) *Persica qeshmensis* gen. nov. sp. nov. from the Persian Gulf (Platyhelminthes: Polycladida: Acotylea), with remarks on reproductive structures. Journal of Natural History 49(25–26): 1477–1491. <https://doi.org/10.1080/00222933.2015.1006278>
- Marcus E (1947) Turbelários marinhos do Brasil. Boletim da Faculdade de Filosofia, Ciências e Letras da Universidade de São Paulo Zoologia 12: 99–206. <https://doi.org/10.11606/issn.2526-4877.bsffclzoologia.1947.125220>
- Marcus E (1950) Turbellaria brasileiros (8). Boletim da Faculdade de Filosofia, Ciências e Letras da Universidade de São Paulo Zoologia 15: 69–190. <https://doi.org/10.11606/issn.2526-4877.bsffclzoologia.1950.125192>
- Marcus E (1952) Turbellaria brasileiros (10). Boletim da Faculdade de Filosofia, Ciências e Letras da Universidade de São Paulo Zoologia 17: 5–186. <https://doi.org/10.11606/issn.2526-4877.bsffclzoologia.1952.125189>
- Müller OF (1773) Vermium terrestrium et fluviatilium, seu animalium infusoriorum, helminthicorum et testaceorum, non marinorum, succincta historia. Voluminis primi pars prima. Heineck et Faber, Havnia et Lipsia (Copenhagen and Leipzig), 72 pp. <https://doi.org/10.5962/bhl.title.12733>
- Newman LJ, Cannon LRG (1997) A new semi-terrestrial acotylean flatworm, *Myoramixa pardalota* gen. et sp. nov. (Platyhelminthes, Polycladida) from southeast Queensland. Memoirs of the Queensland Museum 42: 311–314.
- Oya Y, Kajihara H (2017) Description of a new *Notocomplana* species (Platyhelminthes: Acotylea), new combination and new records of Polycladida from the northeastern Sea of Ja-

- pan, with a comparison of two different barcoding markers. *Zootaxa* 4282(3): 526–542. <https://doi.org/10.11646/zootaxa.4282.3.6>
- Plehn M (1896) Neue Polycladen, gesammelt von Herrn Kapitan Chierchia bei der Erdumschiffung der Korvett Vettor Pisani, von Herrn Prof. Dr. Kukenthal im nördlichem Eismeer und von Herrn Prof. Dr. Semon in Java. *Jenaische Zeitschrift für Naturwissenschaft* 30: 137–181.
- Poche F (1926) Das System der Platyzoa. *Archiv für Naturgeschichte Abteilung A* 91: 1–458.
- Prudhoe S (1985) A Monograph on Polyclad Turbellaria. Oxford University Press, Oxford, 253 pp.
- Ronquist F, Huelsenbeck JP (2003) MrBayes 3: Bayesian phylogenetic inference under mixed models. *Bioinformatics* 19: 1572–1574. <https://doi.org/10.1093/bioinformatics/btg180>
- Schmarda LK (1859) Neue wirbellose Thiere beobachtet und gesammelt auf einer Reise um die Erde 1853 bis 1857. Bd. I: Turbellarien, Rotatorien und Anneliden. Engelmann W, Leipzig, 66 pp. <https://doi.org/10.5962/bhl.title.85313>
- Sonnenberg R, Nolte AW, Tautz D (2007) An evaluation of LSU rDNA D1–D2 sequences for their use in species identification. *Frontiers in Zoology* 4(1): 1–12. <https://doi.org/10.1186/1742-9994-4-6>
- Stamatakis A (2014) RAxML version 8: a tool for phylogenetic analysis and post-analysis of large phylogenies. *Bioinformatics* 30: 1312–1313. <https://doi.org/10.1093/bioinformatics/btu033>
- Stimpson W (1857) *Prodromus descriptionis animalium evertibratorum, quae in Expeditione ad Oceanum Pacificum Septentrionalem a Republica Federata missa, Johanne Rodgers Duce, observavit et descripsit. Pars I, Turbellaria Dendrocoela.* Proceedings of the Academy of Natural Sciences of Philadelphia 9: 19–31. <https://doi.org/10.5962/bhl.title.51447>
- Stummer-Traunfels R (1933) Polycladida. In: Bronn HG (Ed.) *Klassen und Ordnungen des Tierreichs, Vierter Band, Abteilung 1c (Volume 4, Part 1c).* Akademische Verlagsgesellschaft, Leipzig, 3485–3596.
- Tamura K, Peterson D, Peterson N, Stecher G, Nei M, Kumar S (2011) MEGA5: molecular evolutionary genetics analysis using maximum likelihood, evolutionary distance, and maximum parsimony methods. *Molecular Biology and Evolution* 28: 2731–2739. <https://doi.org/10.1093/molbev/msr121>
- Tanabe AS (2011) Kakusan4 and Aminosan: two programs for comparing nonpartitioned, proportional and separate models for combined molecular phylogenetic analyses of multilocus sequence data. *Molecular Ecology Resources* 11(5): 914–921. <https://doi.org/10.1111/j.1755-0998.2011.03021.x>
- Tsunashima T, Hagiya M, Yamada R, Koito T, Tsuyuki N, Izawa S, Kosoba K, Itoi S, Sugita H (2017) A molecular framework for the taxonomy and systematics of Japanese marine turbellarian flatworms (Platyhelminthes, Polycladida). *Aquatic Biology* 26: 159–167. <https://doi.org/10.3354/ab00682>
- Verrill AE (1882) Notice of the remarkable marine fauna occupying the outer banks off the southern coast of New England, no. 7, and of some additions to the fauna of Vineyard Sound. *American Journal of Science* 24: 1–360. <https://doi.org/10.2475/ajs.s3-24.143.360>
- Woodworth WM (1898) Some planarians from Great Barrier Reef of Australia. *Bulletin of the Museum of Comparative Zoology of Harvard College* 32(4): 61–67.
- Yeri M, Kaburaki T (1918) Bestimmungsschlüssel für die japanischen Polycladen. *Annotationes Zoologicae Japonenses* 9: 431–442.

Insights into the morphology and molecular characterisation of glacial relict *Eurytemora lacustris* (Poppe, 1887) (Crustacea, Copepoda, Calanoida, Temoridae)

Łukasz Sługocki^{1,2}, Anna Rymaszewska¹, Lucyna Kirczuk^{1,2}

1 University of Szczecin, Faculty of Biology, Szczecin, Poland **2** University of Szczecin, Center of Molecular Biology and Biotechnology, Szczecin, Poland

Corresponding author: Łukasz Sługocki (lukasz.slugocki@usz.edu.pl)

Academic editor: Danielle Defaye | Received 6 March 2019 | Accepted 13 June 2019 | Published 15 July 2019

<http://zoobank.org/AC42B1B8-AB4B-4364-9F6F-49357BBAC6F3>

Citation: Sługocki L, Rymaszewska A, Kirczuk L (2019) Insights into the morphology and molecular characterisation of glacial relict *Eurytemora lacustris* (Poppe, 1887) (Crustacea, Copepoda, Calanoida, Temoridae). ZooKeys 864: 15–33. <https://doi.org/10.3897/zookeys.864.34259>

Abstract

Eurytemora lacustris (Poppe, 1887) is a stenothermic glacial relict whose narrow environmental requirements make it an indicator species for good ecological conditions. The primary threats to this species are eutrophication and global warming. Many authors have described *E. lacustris* in taxonomic keys; however, its morphological description is unsatisfactory. Therefore, in this study, we aimed to review morphological characteristics of *E. lacustris* that were previously undescribed in the literature and to provide the molecular characteristics based on the two conservative mitochondrial genes: cytochrome *c* oxidase I (*COI*) and cytochrome *b* (*cytb*). The new record of *E. lacustris* indicates that it is a more widespread species than previously hypothesized. Width-to-length ratio of the last female endopod segment of legs indicates variation among the widely distributed species of the genus in Europe (i.e., *E. lacustris*, *E. velox* (Lilljeborg, 1853), and *E. affinis* (Poppe, 1880)). We also found variability of number of setae on the second segment of male endopod. Furthermore, our analysis confirms the occurrence of species in different than exclusively freshwater habitats.

Keywords

Brackish water, crustaceans, genetics, lake, rare species, zooplankton

Introduction

The marine, estuarine, and freshwater genus *Eurytemora* is represented in Europe by eight species (22 worldwide) (Błędzki and Rybak 2016). Recently, Alekseev and Souissi (2011) described a new species, *Eurytemora carolleeae*, from the North American waters, which is invasive in European waters. Depending on the salinity of the water, *Eurytemora* shows highly evolvable traits (Lee 1999; Souissi et al. 2016). Most studies on *Eurytemora* concerns estuarine clade *Eurytemora affinis* (Poppe, 1880), which presents adaptations to freshwater habitats. The large morphological plasticity of *Eurytemora* in relation to its habitat can lead to confusion regarding the identification of the species. In contrast to the widely distributed species such as *E. affinis*, in Europe, other species of the genus are also present that represent relicts of *Eurytemora* on a global scale.

Eurytemora lacustris (Poppe, 1887) is a glacial relict that evolved from a marine ancestor in the ancient Holocene Ancylus Lake into an exclusively freshwater species (Ekman 1922; Segerstråle 1957). Distributions of crustacean glacial relicts are restricted to the North European and North American lakes in regions that were covered by water after the ice age. This stenothermic copepod is restricted to lakes that are deeper than 30 m and where oxygen concentration in the hypolimnion is higher than 1 mg L⁻¹ (Weiler et al. 2003; Kasprzak et al. 2005). *E. lacustris* is a dioecious and perennial species, unable to produce resting eggs (Kiefer 1978). Therefore, dispersion of the species is restricted mainly to the connected lakes (Maier et al. 2011). Its narrow environmental requirements make it an indicator species for waters with low trophy and good ecological condition (Karpowicz and Kalinowska 2018).

During the 20th century, environmental impact resulted in the decline of the population of *E. lacustris*, which made the species more difficult to obtain than before (Maier et al. 2011; Vezhnovets et al. 2012). *Eurytemora lacustris* was recorded from eight Norwegian lakes (Spikkeland et al. 2016), five Lithuanian lakes (Arbačiauskas and Kalytytė 2010), five Latvian lakes (Paidere et al. 2011), two Belarusian lakes (Vezhnovets et al. 2012), and Russian Ladoga Lake (Avinsky et al. 2006). Lakes of Sweden and Finland probably have many lakes in which *E. lacustris* occur; however, the latest reports on this topic was published at the last century (Silfverberg 1999; Northcote and Hammar 2006). Formerly, *E. lacustris* was recorded from several German lakes, which at present is absent from some of them (Maier et al. 2011). Defaye and Dussart (2002) also recorded *E. lacustris* from the Danube and Volga basins and from North America (North Western Territories, Massachusetts). The presence of *E. lacustris* in Polish lakes has not been reviewed, but its distribution could be similar to the known distribution of malacostracan glacial relicts, which is also becoming less frequent in Polish lakes (Żmudziński 1990). Reports on the occurrence of *E. lacustris* in Poland mainly refer to North Eastern and Northern Poland (Lityński 1925; Czczuga 1960; Karpowicz and Górniak 2013; Karpowicz and Kalinowska 2018) and rarely refer to Western Poland (Sługocki and Czerniawski 2018). A recent report from the Great Masurian Lakes (North Eastern Poland) showed high abundance of *E. lacustris* in three lakes, presumably as result of improvement of their trophic conditions (Karpowicz and Kalinowska 2018). The primary threats to this species are eutrophication and global warming

(Weiler et al. 2003), and Belarusian, Lithuanian, (Vezhnovets et al. 2012), Estonian (Lilleleht 1998), and Norwegian (Kålås et al. 2010) red lists assessed *E. lacustris* as an endangered or vulnerable species.

Eurytemora lacustris was found beyond the reach of the glaciation ice sheet, which suggests that this species could not be considered as a typical postglacial relict (Spikkeland et al. 2016). Records of *E. lacustris* outside the glaciation area might have resulted from posterior colonization to new localities or due to lack of proper identification. The lack of resting eggs and its environmental requirements makes dispersion of this species very difficult. Therefore, records outside their natural habitat should be verified by morphological and molecular analyses.

Despite the fact that many authors have identified the species in taxonomic keys (Poppe 1887; Sars 1895; Dussart 1967; Einsle 1993; Błędzki and Rybak 2016), the morphological description of *E. lacustris* is unsatisfactory. Recent studies on the genus *Eurytemora* show that morphological techniques have great potential in copepod taxonomy (Lajus et al. 2015). In this article, we supplement the knowledge about this species with incompletely known characters, including legs morphology and the characteristics of the feeding appendages. The connection of morphological and molecular analysis allows to determine the proper taxonomic status of the specimens under study. The DNA barcoding methods, using amplification of the selected genes of the mtDNA, are commonly used to identify species of copepods. These gene sequences are used to distinguish between sibling species, identify species based on the remains of organisms, but they are also successfully used to describe unknown species. In molecular analysis, gene coding cytochrome *c* oxidase I (*COI*) and gene coding protein or complex III in oxidative phosphorylation (*cytb*) are used for the identification of species (Merritt et al. 1998; Costa et al. 2007; Thum and Derry 2008; Thum and Harrison 2008; Sukhikh et al. 2013; Blanco-Bercial et al. 2014; Gasmi et al. 2014). Such integrative studies using *COI* sequences and morphology of species were applied during the study of *E. carolleae* (Vasquez et al. 2016) and *E. affinis* (Lee and Frost 2002). The use of both molecular and morphological analyses for the population of *E. lacustris* will lead to a better understanding of the population of *E. lacustris* and its natural history. So far, the molecular analysis of *E. lacustris* refers to several individuals from the Baltic Sea (GenBank; Alekseev and Sukhikh, unpublished), which is not a typical habitat for *E. lacustris*. Our study of the relict population of *E. lacustris* at Lake Cieszęcino in Poland is the first report from the lake and the first from Poland based on both morphology and molecular analysis of *COI* and *cytb* genes, which are commonly used for barcoding. These studies provide basis for further analysis of intraspecific diversity of the populations of *E. lacustris*. Therefore, in this study, we aimed to determine the morphological and molecular characteristics of *E. lacustris*.

Materials and methods

Specimens of *E. lacustris* were obtained in September 2017 from Lake Cieszęcino (53°55'41.7"N, 16°49'29.6"E) (Fig. 1), north western Poland at an altitude of 154 m a.s.l. The lake has a surface of 102 ha; its deepest point reaches 39 m. The lake's catch-

ment area is 18.2 km², of which 80% are forests and semi-natural areas (Corine Land Cover 2012). Anthropogenic and agricultural areas cover less than 1% of the catchment area, and the rest are wetlands.

Sampling station was set up at the deepest point, based on bathymetric maps (Jańczak 1996). In order to collect the specimens, a zooplankton net (mesh size 100 µm, d = 20 cm) was towed vertically from the bottom to the surface. Concentrated samples were poured into a 110-mL tube and fixed in a buffered 4% formalin solution (for morphological purposes), and a second sample was fixed in 70% alcohol (for genetic purpose). Zooplankton was analysed in plankton chambers using a Nikon Eclipse 50i microscope (Japan) and a Zeiss Primo Vert reverse microscope (Germany). The species was identified using taxonomic keys (Sars 1895; Einsle 1993; Błędzki and Rybak 2016).

Body size of the specimens was measured without caudal setae. Appendages were dissected using glycerine as the dissecting fluid, and measured under a microscope at 400 × magnification. Morphological description is based on adult female specimens. In two cases, the morphology of males is also mentioned (if so, it is emphasized). Specimens are stored at the collections of the University of Szczecin, Poland. Each variable was measured from digital photographs, using the software ToupView (ToupTek Photonics, China). The significance of differences in size between sexes was calculated using nonparametric Mann-Whitney *U* test (Statistica 12, StatSoft). For molecular analysis, individuals were transferred to PBS tubes (phosphate buffered saline) (n=80), followed by DNA isolation using the ready-made Tissue Genomic Extraction Mini Kit (with Proteinase K, Genoplast). Until the analyses were performed, the DNA was stored in a freezer (−70 °C).

Polymerase chain reaction (PCR) was performed twice for each specimen: amplification of the cytochrome *c* oxidase subunit I gene (*COI*, *cox1*) and *cytb*. Both genes are located in mtDNA and belong to the group of conservative genes that allow species identification. PCR amplification was conducted using the following primers: COIF-PR115 and COIR-PR114 for *COI* (Folmer et al. 1994) and UCYTB151F and UCYTB272R for *cytb* (Merritt et al. 1998). The results of PCR amplification were visualized by performing electrophoresis with 5 µL sample each in 1.5% agarose gels with GPB Gold View Nucleic Acid Stain (GenoPlast, Biochemicals, Poland).

Sequential analysis was performed for all samples. Sequencing was performed in MacroGen Europe (the Netherlands) with the same sets of primers that were used to obtain amplicons. The results were analysed using the Finch TV, BLAST, and Mega 7 software. Phylogenies were constructed using the Minimum Evolution method algorithm with Tamura–3-parameter model. A 1000-replicate bootstrapping was performed to obtain a measure of robustness of tree topology. *COI* and *cytb* sequences of *E. lacustris* have been reported to the GenBank (*cox1*: MH316160, MH316161; *cytb*: MH316162–MH316164). Due to the lack of data concerning deposited type specimens (Poppe 1887) genetic and morphological analyses were difficult to perform. Therefore, morphological traits that are described in this article based on specimens from population (Lake Cieszęcino) for which molecular characterization was performed.

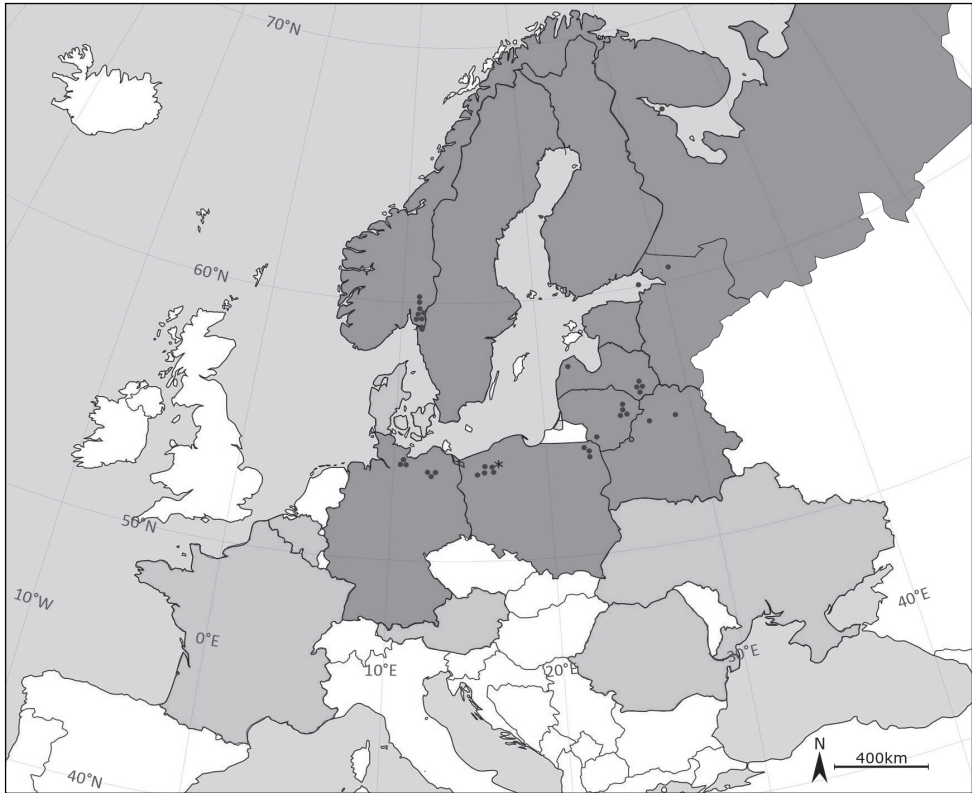


Figure 1. Distribution map of *Eurytemora lacustris*. Dark grey colour indicates present distribution of *E. lacustris*. Light grey colour demonstrates countries in which occurrence of this species is uncertain. Black dots indicate records in 21st century, asterisk indicates a new record of *E. lacustris* in Lake Cieszęcino (Poland). The map does not include recent records in Volga basins (Popov 2011) and North America (Dussart and Defaye 2002).

Results

Morphology

Length of 40 adult specimens (20 females and 20 males) ranging from 1.274 to 1.483 mm. No significant differences in the body size between the two sexes ($p > 0.05$). Antennules of 24 segments with variable setation. Male right antennule with 21 segments. Most segments with two and more setae provided with one aesthetasc and distal segment with six setae and one aesthetasc. Antenna biramous, composed of two-segmented protopod, two-segmented endopod and seven-segmented exopod. First exopod segment with one seta, second segment with three setae, third to sixth segments with one seta each, seventh (distal) segment with four setae. First endopodal segment with two setae, second with nine setae laterally, and seven setae at distal end. Mandible (Fig. 2A) with sharp ventralmost tooth that corresponds to the largest tooth of the mandible. Size and shape of teeth (pars molaris) varied from a molar shape to

acute teeth. Trident-shaped teeth from third to seventh. Distal tooth long and thin (spike-like), at least two times longer than seventh tooth. Coxa heavily sclerotized medially; basis with four setae. Exopod four-segmented with one seta on the first segment, second, and third segment and three setae on the fourth segment. Endopod two-segmented, with 4 and 11 setae. Maxilla (Fig. 2B) uniramous, precoxa with two endites, first endite with five setae, distal endite with three setae; coxa with two endites bearing three setae each; 5-segmented endopod including basal endite with one long, and four short segments bearing one or two long distal setae. Maxilliped (Fig. 2C) with syncoxa consisting of three lobes with respectively two, two, three setae; basis with five setae (two on a distal medial lobe). Endopod five-segmented with 2, 2, 2, 2, 4 setae. Maxillule (Fig. 2D) composed of precoxa with medial arthrite bearing nine strong spines; coxa with elongated endite bearing four setae and outer outgrowth with six strong sub-equal in length setae and three thin setae. Basis composed of basal endite, one-segmented exopod with nine long subequal setae and four-segmented endopod bearing 5–5–4–7 (distally) long setae.

First pair of legs (Fig. 3A) having coxa with medial seta. Exopod three-segmented with 2, 2, 7 setae. All segments with row of denticles toward distal edge. Endopod one-segmented with six setae. Second pair of legs (Fig. 3B) having coxa with medial seta. Exopod three-segmented, first and second segments each with one seta on the inner margin and one spine on the outer margin, third segment with five setae on inner margin, two spines on the outer margin and one terminal strong spine; first and third segments with row of denticles toward distal edge. Endopod two-segmented, first segment with three setae, second segment with six setae (adult male: endopod two-segmented; first segment with three setae, second segment with five or six setae Fig. 4). Third pair of legs (Fig. 3C) having coxa with medial seta. Exopod three-segmented; posterior face of the segments with denticles toward distal edge. Endopod two-segmented; posterior face of segments with denticles toward distal edge. Fourth pair of legs (Fig. 3D) having coxa with medial seta. Exopod three-segmented with 2, 2, 8 setae and spines; posterior face of segments with denticles toward distal edge. Endopod two-segmented with 3, 5 setae. Female fifth pair of legs three-segmented (Fig. 5C). Second segment with strong inner outgrowth and two spines, distal segment with long apical seta about four times longer than lateral spine. Distal segment about 1.5 length of lateral spine. Male fifth pair of legs three-segmented and asymmetric. Right leg basipodal segment with distally located smooth bulge on inner side about 1.2 times long as wide. Left leg basipod with smooth bulge on inner side as long as wide or slightly wider. The three most widely distributed species among the genus in Europe (*E. lacustris*, *E. affinis* and *E. velox*) were chosen for comparison of selected morphological characters. Females of *E. lacustris* and *E. affinis* are characterized by similar ratio of length to width of caudal rami (Tab. 1). *Eurytemora velox* is characterized by a lower ratio of this parameter compared with females of *E. lacustris* and *E. affinis* (Tab. 1). In case of males, the differences of the discussed parameter were higher in each species considered; therefore, this parameter cannot be considered as indicative. Concerning the length to width ratio of the last endopod segment

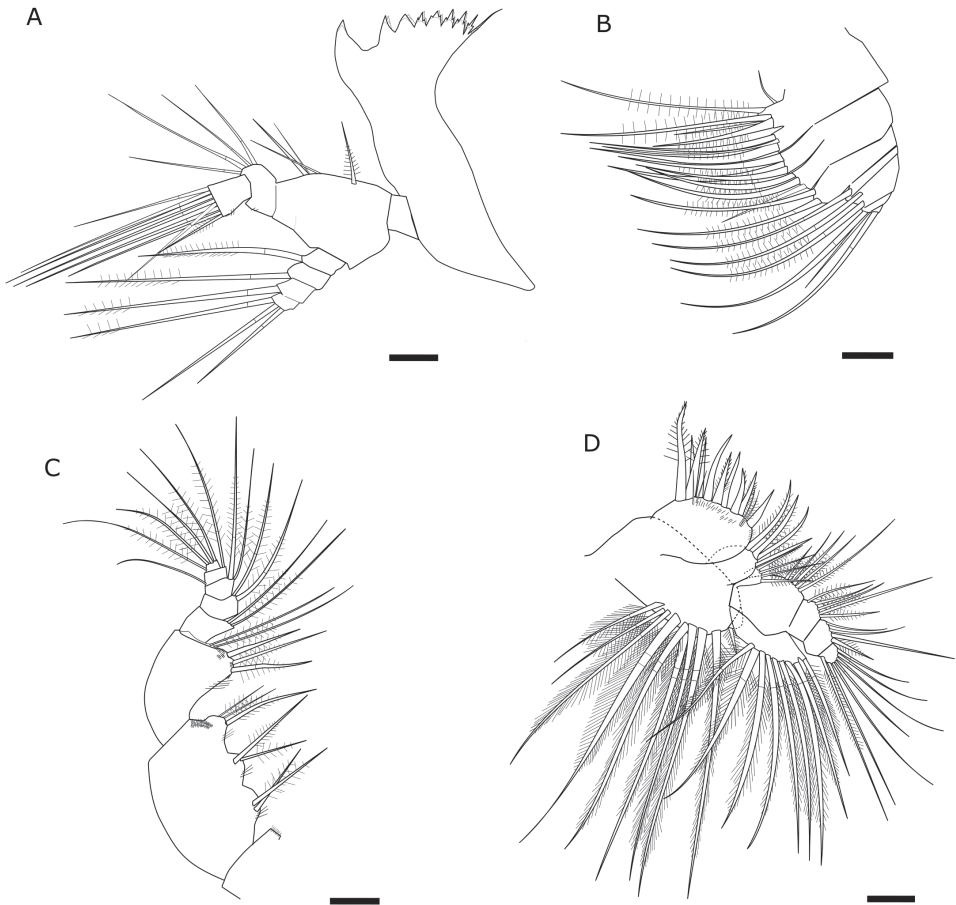


Figure 2. Feeding appendages of *Eurytemora lacustris* **A** mandible **B** maxilla **C** maxilliped **D** maxillule. Scale bars: 20 μm .

of the legs, *E. lacustris* shows the highest value among the three compared taxa (Tab. 1). In the case of the parameter referring to the ratio of the length of the last endopod segment to the length of the spine, there was greater variability.

Molecular analysis

For each specimen of *E. lacustris*, amplicons of the expected length were obtained, of approximately 612 bp for the *COI* gene and 369 bp for the *cytb*. Subsequently, we performed nucleotide sequence analysis. *Cox1* gene analysis showed high degree of similarity in the nucleotide sequences for the population from Lake Cieszęcino (Poland). Two haplotypes were distinguished: one of them, described as CX-01 (MH316161)

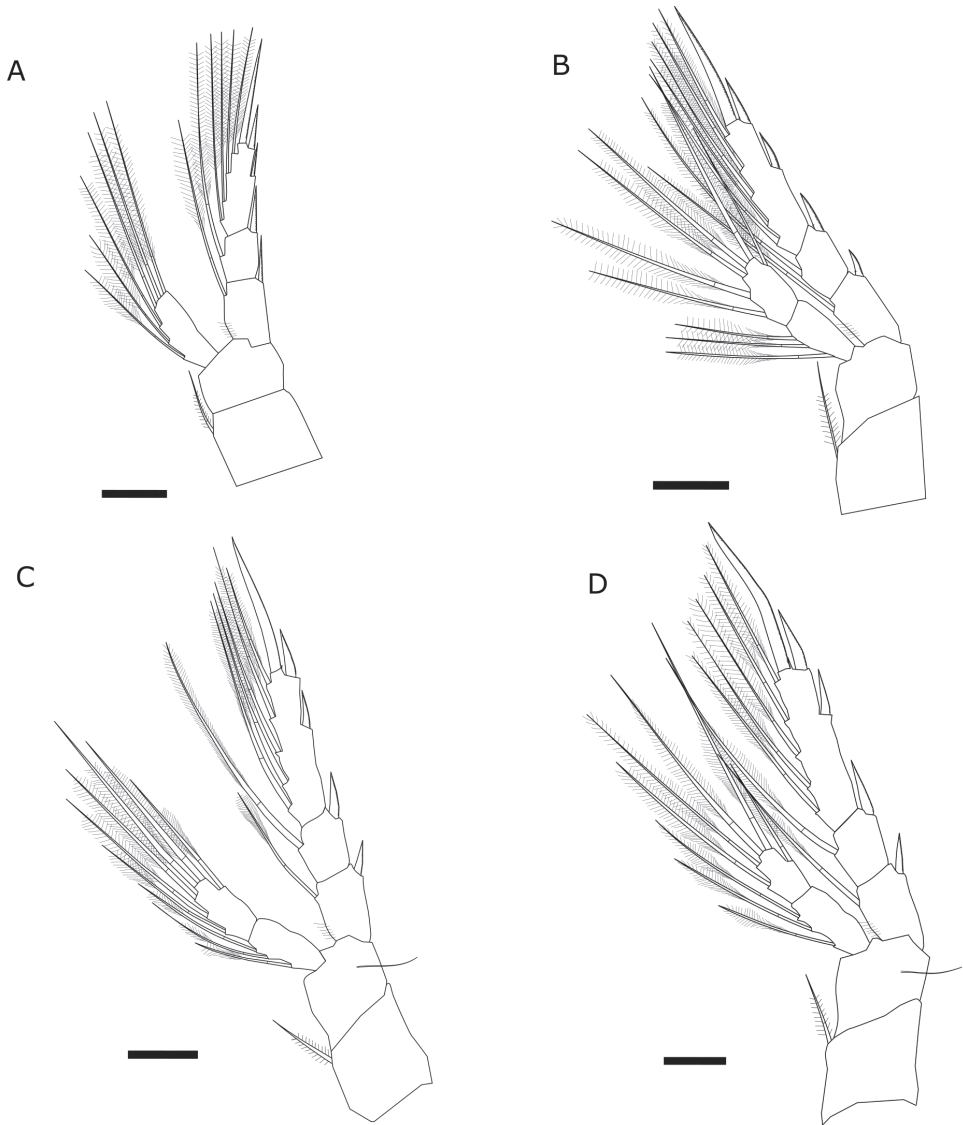


Figure 3. Legs of *Eurytemora lacustris* **A** first pair **B** second pair **C** third pair **D** fourth pair. Scale bars: 20 μ m.

was represented only by 12.5% of the population (10 individuals). Sequencing of the *cox1* gene resulted in 612 bp, of which differences were related to the five nucleotide positions (Tab. 2). The four substitutions were transitions (3: A \leftrightarrow G and 1: T \leftrightarrow C), whereas one was transversion (A \leftrightarrow C). All substitutions were synonymous and they did not cause amino acid substitutions in the protein. The obtained sequences were compared to analogous sequences deposited in the GenBank, derived from *E. lacustris* from Russia (Table 3; Alekseev and Sukhikh, Russia, Baltic See, St Petersburg, Vyborg

Table 1. Selected characteristics of the three related *Eurytemora* species (*E. affinis*, *E. velox*, and *E. lacustris*). The value indicates the normalized ratio for size of the body parts.

	<i>E. affinis</i>			<i>E. velox</i>			<i>E. lacustris</i>			
	Sars 1895	Einsle 1993	Błędzki and Rybak 2016	Sars 1895	Einsle 1993	Błędzki and Rybak 2016	Sars 1895	Einsle 1993	Błędzki and Rybak 2016	present study
endopod 1 (length-width) ♀				100/36.1				100/33.7		100/31.9
endopod 1 (spine length-width) ♀				100/102				100/96.4		100/119
endopod 2 (length-width) ♀										100/24.2
endopod 2 (spine length-width) ♀										100/93.4
endopod 3 (length-width) ♀	100/24.6			100/39.8			100/21.8			100/21.6
endopod 3 (spine length-width) ♀	100/104			100/103.9			100/96.4			100/92.5
endopod 4 (length-width) ♀		100/31.9		100/35.3						100/24.9
endopod 4 (spine length-width) ♀		100/97.4		100/100						100/102
furca (length-width) ♂	100/8.1		100/11.4		100/16.3	100/12.3		100/14.6	100/10.6	100/14.2
furca (length-width) ♀	100/11.1	100/14	100/13.1	100/24.6	100/25.1	100/26.4	100/13.5	100/14.6	100/13.8	100/19
body length (µm) ♂	1150	1200–1800	800–1900	2200	1300–2200	1100–2200	1300	1000–1500	1100–1500	1272–1456
body length (µm) ♀		1100–1700	750–1650	1850	1000–1900	1500–1850		<1400	1000–1400	1274–1483

Table 2. Variability in the nucleotide sequences of the gene *cox1* for *Eurytemora lacustris* from Cieszcino Lake (NW Poland) and Baltic Sea, Vyborg Gulf (Alekseev and Sukhikh, unpublished).

Accession number	58	69	210	303	309	399	405	759	582	612
T	T	T	G	A	C	A	A	T	T	C
CX-02*
CX-01**	.	.	A	G	A	G	.	C	.	.
HM474035	C	.	A	.	.	.	G	.	.	T
HM474034	C	.	A	T
HM474033	.	.	A	T
HM474032	.	.	A	T
HM474031	.	.	A	C	.	T
HM474030	.	C	A	C	C	T
SUBSTITUTION	TZ	TZ	TZ	TZ	TW	TZ	TZ	TZ	TZ	TZ

CX-02* (GenBank accession number: MH316160), CX-01** (MH316161); TZ-transition, TW-transversion;



Figure 4. Variability of number of setae on second segment of endopod on second pair of male leg of *Eurytemora lacustris*. Scale bar: 20 μm .

Table 3. The most commonly used markers in the determination of selected Copepoda species.

Species	COI	cytb	rRNA genes	TGDNA	ISSR-PCR	Authors
<i>Calanus finmarchicus</i> , <i>C. glacialis</i> , <i>C. helgolandicus</i> , <i>Neocalanus</i> <i>crustatus</i> , <i>N. flemingeri</i> , <i>N. plumchrus</i> , <i>Pseudocalanus</i> <i>moultoni</i> , <i>P. newmani</i>	×					Bucklin et al. 1999
<i>Leptocaris canariensis</i>	×			×		Fazhan et al. 2016; Waiho et al. 2013
<i>Leptodiaptomus garciai</i>	×					Montiel-Martínez et al. 2008; Ortega-Mayagoitia et al. 2018
<i>L. minutus</i> , <i>Onychodiaptomus</i> <i>sanguineus</i>	×					Thum and Derry 2008
<i>Pseudocalanus moultoni</i>	×					Aarbakke et al. 2011
<i>Skistodiaptomus pallidus</i>	×	×				Thum and Derry 2008
<i>S. reighardi</i>	×					Thum and Derry 2008
<i>S. oregonensis</i> , <i>S. pygmaeus</i>	×	×	×			Thum and Harrison 2009
<i>Tigriopus japonicus</i>			×			Ki et al. 2009
Species of family Temoridae incl. <i>T. discaudata</i> , <i>T. longicornis</i>	×	×	×	×		Blanco-Bercial et al. 2011, 2014; Khodami et al. 2017
<i>Eurytemora affinis</i>					×	Gasmi et al. 2014
<i>Eurytemora affinis</i>	×					Gorokhova et al. 2013; Sukhikh et al. 2013; Vasquez et al. 2016
<i>Eurytemora carolleae</i>	×					Sukhikh et al. 2013; Vasquez et al. 2016
<i>Eurytemora lacustris</i>	×					GenBank Alekseev and Sukhikh, unpublished
<i>Eurytemora lacustris</i>	×	×				Present study

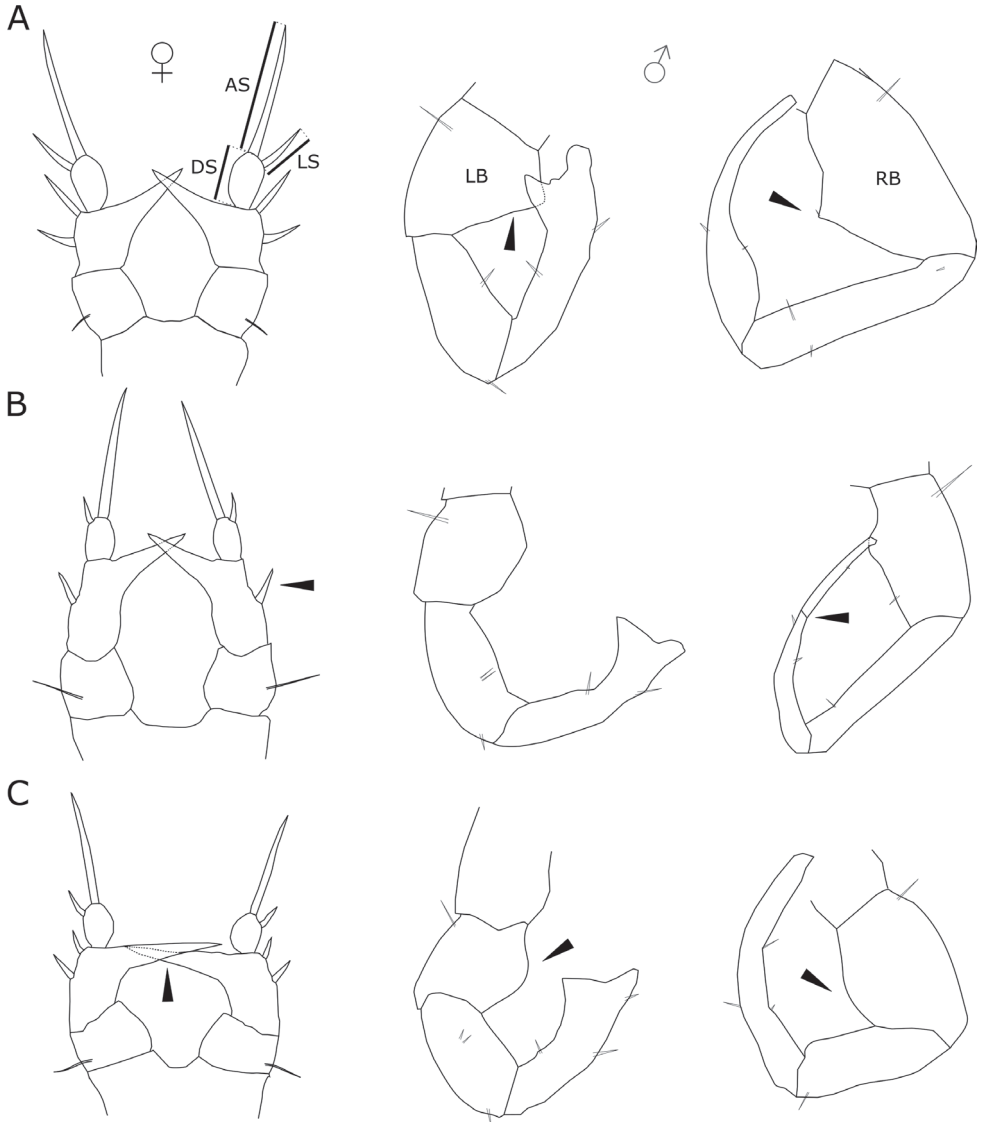


Figure 5. Fifth pair of legs of related *Eurytemora* species **A** *E. affinis* **B** *E. velox* **C** *E. lacustris*. Abbreviations: AS – apical seta, DS – distal segment, LS – lateral spine, LB – left basipod, RB – right basipod. Arrows indicate important characteristics of fifth pair of legs.

Table 4. Variability in the nucleotide sequences of the gene *cytb* for *Eurytemora lacustris* from Lake Cieszęcino, NW Poland.

Position in sequences/ Accession Number	205	211	316
	T	G	C
CY-03*	.	.	T
CY-02**	.	.	.
CY-01***	C	A	.

CY-01*** (GenBank accession number: MH316162); CY-02** (MH316163); CY-03*(MH316164).

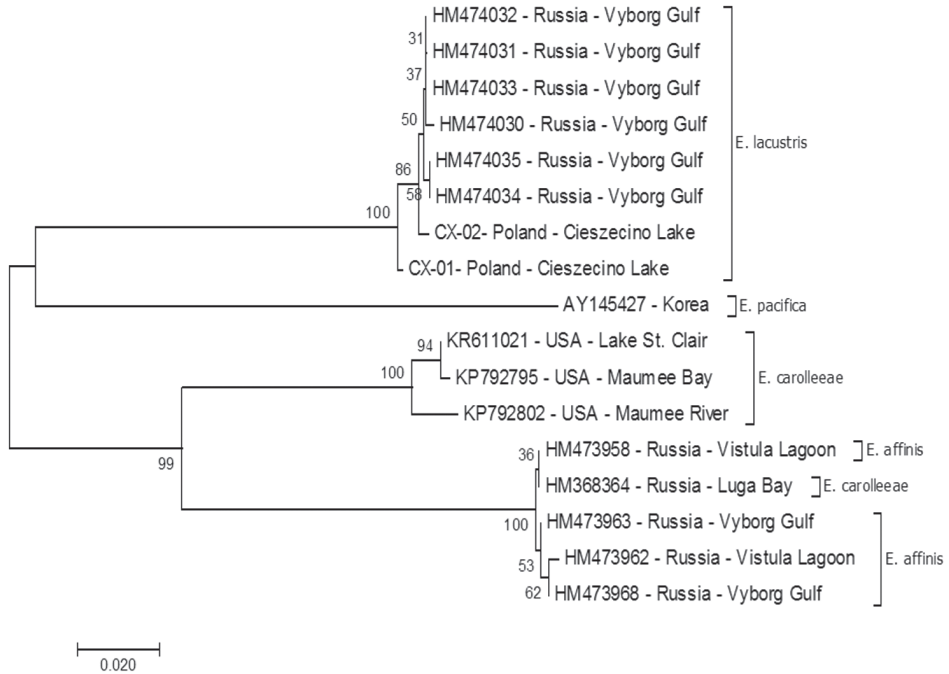


Figure 6. Evolutionary relationship of taxa based on *mCOI* sequences. The phylogenetic tree was inferred using the Minimum Evolution method (MEGA 10.0.5, Kumar et al. 2018). The evolutionary distances were computed using the Tamura 3-parameter method [3] and are in the units of the number of base substitutions per site. Sequences deposited at GenBank from Sukhikh et al. (2013, 2018), Vasquez et al. (2016), and Alekseev and Sukhikh (unpublished).

Gulf). In total, there were ten substitutions between the Polish and Russian sequences, which also had no consequences at the protein level. Calculations based on the Kimura-2-parameter model revealed distance ranging from 0.000-0.002 to 0.011 (CX-01 vs HM474030) and an overall distance of 0.005 (S.E. 0.001). An analysis of kinship (Fig. 6) was made using the nucleotide sequences of *E. lacustris* from Lake Cieszęcino and sequences of *E. lacustris* and related species (*E. affinis* and *E. carolleae*) caught in Russia (GenBank). All nucleotide sequences of the *COI* gene form a separate clad, with the sequence from Poland designated as CX-01 (MH316160) by us as the initial for them. Molecular analysis based on *COI* showed that our collection belongs to the same species of *E. lacustris* inhabiting the waters of the Baltic Sea.

Analysis of the *cytb* gene sequence from the *E. lacustris* population from Lake Cieszęcino revealed three haplotypes: designated as CY-01*** (MH316162); CY-02** (MH316163), and CY-03* (MH316164). These haplotypes were determined based on the analysis of substitution in the nucleotide sequence, in which three substitutions (transitions) were observed on the 369 bp section, at positions 205, 211, and 316 (Tab. 4). Overall mean distance was 0.005. None of the changes caused substitution

of amino acids in the protein. Due to the lack of analogous sequences in GenBank of the *cytb* gene (the reported sequences are the first for the genus *Eurytemora*), it was not possible to perform similarity analysis within the species using that gene, as well as phylogenetic analysis between closely related species.

Discussion

The occurrence of *E. lacustris* in the Lake Cieszęcino has not been recorded so far (NW Poland). The lake in which the new record of the species was obtained is one of the smallest in terms of surface area (Sars 1895; Czeczuga 1960; Kasprzak et al. 2005; Maier et al. 2011; Karpowicz and Kalinowska 2018). *Eurytemora lacustris* does not have the ability to produce resting eggs and was not observed in the river network upstream and downstream. Therefore, we assume that these are stable populations in this lake. Another location of occurrence of this species indicates that it is more widespread species in the lakes of Western Pomerania (Poland) than previously assumed. Presently, *E. lacustris* is recorded in at least six West Pomeranian lakes (Lakes Cieszęcino, Drawsko, Ińsko, Lubie, Siecino, and Żerdno).

Morphology

Eurytemora lacustris and *E. affinis* are similar in morphological terms. Sars (1895) described the genus *Eurytemora* and indicated that except to the construction of the fifth pair of legs on both species and wings on the fifth thoracic segment on *E. affinis* on females, both taxa are very similar. Therefore, particularly for younger specimens with fifth pair of not fully developed legs, these species can be misidentified. Hence *E. lacustris* has been sometimes reported in the typical habitats of *E. affinis*, i.e., in the estuaries of the southern Baltic.

Swimming legs may not differ on the number of setae on female and male individuals (except P2 endopod 2). It is not yet determined whether this phenomenon is specific for the population from Cieszęcino Lake, or whether it is common for that species. Gaviria and Forró (2000) studying the populations of *E. velox* (Lilljeborg, 1853) of Europe showed changes in the leg spinulation pattern of some individuals of the Austrian and Hungarian populations. They stated that a possible explanation could include effects of pollution (Gaviria and Forró 2000). The catchment of Cieszęcino Lake is anthropogenically less transformed, which allows us to suppose that there is no excessive pollution of the lake's waters; hence, the polymorphism observed within this species is probably not the result of anthropogenic changes.

The parameters of some appendages differ between related species (*E. lacustris*, *E. affinis* and *E. velox*). At the same time, differences are also observed between different authors. However, the parameter concerning the width-to-length ratio of the last endopod segment in females indicates variation between the indicated species

(*E. lacustris*, *E. velox*, and *E. affinis*). Therefore, this parameter seems to be able to serve as an auxiliary parameter in morphological identification.

The most indicative features among *Eurytemora* species are related to fifth pairs of legs (Aleksiev and Souissi 2011). Female of *E. lacustris* has strong inner outgrowth almost at right angle in relation to the basipodite. Two spines on second segment distinguish *E. lacustris* from *E. velox*, that has one spine (Fig. 5A–C). However, Gaviria and Forró (2000) found variability in the number of spines on female first exopod segments. Female (*E. lacustris*) distal segment with long apical seta about four times longer than lateral spine, while at *E. affinis* lateral spine is less than three times long as apical seta. Male *E. lacustris* fifth pair of legs three-segmented what distinguish that species from *E. velox* that has four segments at right leg. Legs basipod segments with smooth bulges on inner side distinguish *E. lacustris* from *E. velox* and *E. affinis* that have sharp shape basipodal inner side.

Molecular analysis

Morphology is the primary criterion in the determination of species affiliation. However, the small size of copepods could be an obstacle in terms of morphological determination. Genetic analysis among such species allowed to verify the species within morphologically similar specimens and hence give indication of cryptic species (Lee 2000; Lajus et al. 2015). Sometimes morphological differences are imperceptible and are not indicated on taxonomic keys. Therefore, collection of molecular data allows the identification of species (Thum 2006). The invasion of the American species *E. carolleae* in the Gulf of Finland was found through morphological studies, as well as through molecular genetic tools (Sukhikh et al. 2013). In addition, the analysis of morphological and molecular features allows to determine whether the methods of morphological identification include those features that are important to identify species (Thum and Harrison 2008).

COI is a unique diagnostic tool for identifying copepods at the species level with barcoding (Bucklin et al. 2003; Costa et al. 2007; Sukhikh et al. 2013; Blanco-Bercial et al. 2014; Sukhikh et al. 2018). Costa et al. (2007) noted that the level of genetic variation between congeneric species on crustaceans is 17.16% on average, which is extremely high compared to variation in other groups of animals. In addition, the level of intraspecific variability in crustaceans (average 0.46%) is only slightly higher than in other groups of animals. According to our results, the average variation between Polish and Russian populations of *E. lacustris* is 0.5%, which would confirm the hypothesis of Costa et al. (2007) about intraspecific variability on crustaceans. At the same time, between the compared species of *Eurytemora*, the genetic distance is high with ranges from 23.1% between *E. affinis* and *E. lacustris*, to 21.3% between *E. carolleae* and *E. lacustris* and to 13.6% between *E. carolleae* and *E. affinis*.

Sars (1895) stated that *E. lacustris* is “a perfectly freshwater” species. Nevertheless, there are cases where *E. lacustris* is recorded in brackish waters (Vekhov 2001; Sukhikh et al. 2019). This is most likely a result of drifting of individuals from lakes that are relatively close to estuarine waters. The drift can be particularly effective during the night when

low intensity of light limits the pressure of the planktivorous fish on drifting plankton (Czerniawski et al. 2016). Probably in this way, individuals of *E. lacustris* drifting from Lake Ladoga arrived at Vyborg Gulf. Hence, Sukhikh et al. (2019) indicated Vyborg Gulf as the location for obtaining individuals of *E. lacustris*. Our research confirms that this is the same species. However, the question is whether populations that reach the bay acquire the ability to survive in low-salinity waters, which would be the beginning of speciation of population entering the waters with low salinity, such as the Gulf of Finland. We can state that *E. lacustris* is not a purely freshwater species as Sars (1895) and others believed. Further research should be conducted to explain this phenomenon.

Cytb also belongs to conservative mitochondrial genes that are successfully used to identify species of vertebrates (Lopez-Oceja et al. 2016) and invertebrates (Merritt et al. 1998; Thum and Derry 2008; Thum and Harrison 2008; Blanco-Bercial et al. 2014). In previous studies on *Eurytemora*, no data was found on *cytb* analysis. The *cytb* sequences reported by us are the first for this genus; hence, the comparison to the closest related species was not possible.

The use of molecular and morphological analyses allows for a reliable determination of species affiliation and further research. The identification of juvenile stages is possible primarily with molecular analysis. Bucklin et al. (2003) also suggested the use of molecular methods to analyse unsorted zooplankton to determine species affiliation. When analysing the genetic structure and phenotypic traits of *E. lacustris*, we obtained data that may be useful for further monitoring of this species and for research concerning the origin of individual populations. Accurate taxonomic identification of species at all stages of life is crucial for understanding and predicting processes that determine the dynamics of planktonic communities.

Acknowledgments

The research was supported by the funds of the National Science Center granted on the basis of decision number DEC-2017/01/X/NZ8/00793.

References

- Aarbakke ONS, Bucklin A, Halsband C, Norrbin F (2011) Discovery of *Pseudocalanus moultoni* (Frost, 1989) in Northeast Atlantic waters based on mitochondrial COI sequence variation. *Journal of Plankton Research* 33: 1487–1495. <https://doi.org/10.1093/plankt/fbr057>
- Alekseev VR, Souissi A (2011) A new species within the *Eurytemora affinis* complex (Copepoda: Calanoida) from the Atlantic Coast of USA, with observations on eight morphologically different European populations. *Zootaxa* 2767: 41–56. <https://doi.org/10.11646/zootaxa.2767.1.4>
- Arbačiauskas K, Kalutyte D (2010) Occurrence and interannual abundance variation of glacial relict calanoids *Limnocalanus macrurus* and *Eurytemora lacustris* in Lithuanian Lakes. *Acta Zoologica Lituanica* 20: 61–67. <https://doi.org/10.2478/v10043-010-0009-4>

- Avinsky V, Rahkola-Sorsa M, Viljanen M (2006) Seasonal succession of zooplankton of Lake Ladoga (NW Russia). *Internationale Vereinigung für theoretische und angewandte Limnologie: Verhandlungen* 29: 1149–1152. <https://doi.org/10.1080/03680770.2005.11902865>
- Blanco-Bercial L, Bradford-Grieve J, Bucklin A (2011) Molecular phylogeny of the Calanoida (Crustacea: Copepoda). *Molecular Phylogenetics and Evolution* 59: 103–113. <https://doi.org/10.1016/j.ympev.2011.01.008>
- Blanco-Bercial L, Cornils A, Copley N, Bucklin A (2014) DNA barcoding of marine copepods: assessment of analytical approaches to species identification. *PLoS Currents* 6: 1–22. <https://doi.org/10.1371/currents.tol.cdf8b74881f87e3b01d56b43791626d2>
- Błędzki LA, Rybak JI (2016) *Freshwater crustacean zooplankton of Europe*. Springer, Switzerland, 918 pp. <https://doi.org/10.1007/978-3-319-29871-9>
- Bucklin A, Frost B, Bradford-Grieve J, Allen L, Copley N (2003) Molecular systematic and phylogenetic assessment of 34 calanoid copepod species of the Calanidae and Clausocalanidae. *Marine Biology* 142: 333–343. <https://doi.org/10.1007/s00227-002-0943-1>
- Bucklin A, Guarnieri M, Hill RS, Bentley AM, Kaartvedt S (1999) Taxonomic and systematic assessment of planktonic copepods using mitochondrial COI sequence variation and competitive, species-specific PCR. In: Zehr JP, Voytek MA (Eds) *Molecular Ecology of Aquatic Communities*. Springer, Dordrecht, 239–254. https://doi.org/10.1007/978-94-011-4201-4_18
- Costa FO, DeWaard JR, Boutillier J, Ratnasingham S, Dooh RT, Hajibabaei M, Hebert PD (2007) Biological identifications through DNA barcodes: the case of the Crustacea. *Canadian Journal of Fisheries and Aquatic Sciences* 64: 272–295. <https://doi.org/10.1139/f07-008>
- Czeczuga B (1960) Zmiany płodności niektórych przedstawicieli zooplanktonu. I. Crustacea Jezior Rajgrodzkich. *Polskie Archiwum Hydrobiologii* 7: 61–89.
- Czerniawski R, Ślugocki Ł, Kowalska-Górska M (2016) Diurnal changes of zooplankton community reduction rate at lake outlets and related environmental factors. *PLoS ONE* 11: e0158837. <https://doi.org/10.1371/journal.pone.0158837>
- Dussart B (1967) *Les copépodes des eaux continentales d'Europe occidentale*. Tome I: Calanoides et Harpacticoides. Ed. N. Boubée & Cie, Paris, 266 pp.
- Dussart B, Defaye D (2002) *World Directory of Crustacean Copepods*. I- Calaniformes. Backhuys Publishers, Leiden, 276 pp.
- Einsle U (1993) *Crustacea: Copepoda, Calanoida und Cyclopoida* (Vol. 4). Gustav Fischer Verlag, Stuttgart, 209 pp.
- Fazhan H, Waiho K, Shahreza MS (2016) A simple and efficient total genomic DNA extraction method for individual zooplankton. *Springer Plus* 5: 2049. <https://doi.org/10.1186/s40064-016-3724-x>
- Folmer O, Black M, Hoen W, Lutz R, Vrijenhoek R (1994) DNA primers for amplification of mitochondrial cytochrome c oxidase subunit I from diverse metazoan invertebrates. *Molecular Marine Biology and Biotechnology* 3: 294–299.
- Gasmi S, Ferval M, Pelissier C, D'amico F, Maris T, Tackx M, Legal L (2014) Genetic diversity among the *Eurytemora affinis* species complex in the Scheldt estuary and its tributaries using ISSR-PCR marker assay. *Estuarine, Coastal and Shelf Science*. 145: 22–30. <https://doi.org/10.1016/j.ecss.2014.04.005>

- Gaviria S, Forró L (2000) Morphological characterization of new populations of the copepod *Eurytemora velox* (Lilljeborg, 1853) (Calanoida, Temoridae) found in Austria and Hungary. *Hydrobiologia* 438: 205–216. <https://doi.org/10.1023/A:1004173704289>
- Gorokhova E, Löf M, Reutgard M, Lindström M, Sundelin B (2013) Exposure to contaminants exacerbates oxidative stress in amphipod *Monoporeia affinis* subjected to fluctuating hypoxia. *Aquatic toxicology* 127: 46–53. <https://doi.org/10.1016/j.aquatox.2012.01.022>
- Jańczak J (1996) Atlas jezior Polski. Bogucki Wydawnictwo Naukowe (IMGW), Poznań, 269 pp.
- Kålås JA, Viken Å, Henriksen S, Skjelseth S (2010) Norsk rødliste for arter 2010. The 2010 Norwegian Red List for Species. Artsdatabanken, Norway, 480 pp.
- Karpowicz M, Górniak A (2013) Zooplankton skorupiakowy jezior harmonijnych Wigierskiego Parku Narodowego a trofia wód. *Monitoring Środowiska Przyrodniczego* 14: 97–101.
- Karpowicz M, Kalinowska K (2018) Vertical distribution of the relic species *Eurytemora lacustris* (Copepoda, Calanoida) in stratified mesotrophic lakes. *Biologia* 73: 1197–1204. <https://doi.org/10.2478/s11756-018-0138-y>
- Kasprzak P, Reese C, Koschel R, Schulz M, Hambaryan L, Mathes J (2005) Habitat characteristics of *Eurytemora lacustris* (Poppe, 1887) (Copepoda, Calanoida): the role of lake depth, temperature, oxygen concentration and light intensity. *International Review of Hydrobiology* 90: 292–309. <https://doi.org/10.1002/iroh.200410769>
- Khodami S, McArthur JV, Blanco-Bercial L, Arbizu PM (2017) Molecular phylogeny and revision of copepod orders (Crustacea: Copepoda). *Scientific Reports* 7: 9164. <https://doi.org/10.1038/s41598-017-06656-4>
- Ki JS, Raisuddin S, Lee KW, Hwang DS, Han J, Rhee JS, Kim IC, Park HG, Ryu JC, Lee JS (2009) Gene expression profiling of copper-induced responses in the intertidal copepod *Tigriopus japonicus* using a 6K oligochip microarray. *Aquatic Toxicology* 93: 177–187. <https://doi.org/10.1016/j.aquatox.2009.04.004>
- Lajus D, Sukhikh N, Alekseev V (2015) Cryptic or pseudocryptic: can morphological methods inform copepod taxonomy? An analysis of publications and a case study of the *Eurytemora affinis* species complex. *Ecology and Evolution* 5: 2374–2385. <https://doi.org/10.1002/ece3.1521>
- Lee CE (1999) Rapid and repeated invasions of fresh water by the copepod *Eurytemora affinis*. *Evolution* 53: 1423–1434. <https://doi.org/10.1111/j.1558-5646.1999.tb05407.x>
- Lee CE (2000) Global phylogeography of a cryptic copepod species complex and reproductive isolation between genetically proximate “populations”. *Evolution* 54: 2014–2027. <https://doi.org/10.1111/j.0014-3820.2000.tb01245.x>
- Lee CE, Frost BW (2002) Morphological stasis in the *Eurytemora affinis* species complex (Copepoda: Temoridae). *Hydrobiologia* 480: 111–128. <https://doi.org/10.1023/A:1021293203512>
- Lilleleht V (1998) Red Data Book of Estonia. Threatened Fungi, Plants and Animals. Eesti Teaduste Akadeemia, Tartu, 150 pp.
- Lityński A (1925) Próba klasyfikacji biologicznej jezior Suwalszczyzny na zasadzie składu zooplanktonu. *Sprawozdania Stacji Hydrobiologicznej na Wigrach*. 1: 37–56.
- Lopez-Oceja A, Gamarra D, Borrigan S, Jiménez-Moreno S, De Pancorbo MM (2016) New cyt b gene universal primer set for forensic analysis. *Forensic Science International: Genetics* 23: 159–165. <https://doi.org/10.1016/j.fsigen.2016.05.001>
- Maier G, Speth B, Wolfgang ARP, Bahnwart M, Kasprzak P (2011) New records of the rare glacial relict *Eurytemora lacustris* (Poppe, 1887) (Copepoda; Calanoida) in atypical lake habi-

- tats of northern Germany. *Journal of Limnology* 70: 145–148. <https://doi.org/10.4081/jlimnol.2011.145>
- Merritt TJS, Shi L, Chase MC, Rex MA, Etter RJ, Quattro JM (1998) Universal cytochrome b primers facilitate intraspecific studies in molluscan taxa. *Molecular Marine Biology and Biotechnology* 7: 7–11.
- Montiel-Martínez A, Ciros-Pérez J, Ortega-Mayagoitia E, Elías-Gutiérrez M (2008) Morphological, ecological, reproductive and molecular evidence for *Leptodiatomus garciai* (Osorio-Tafall, 1942) as a valid endemic species. *Journal of Plankton Research* 30: 1079–1093. <https://doi.org/10.1093/plankt/fbn067>
- Northcote TG, Hammar J (2006) Feeding ecology of *Coregonus albula* and *Osmerus eperlanus* in the limnetic waters of Lake Mälaren, Sweden. *Boreal Environment Research* 11: 229–246.
- Ortega-Mayagoitia E, Hernández-Martínez O, Ciros-Pérez J (2018) Phenotypic plasticity of life-history traits of a calanoid copepod in a tropical lake: Is the magnitude of thermal plasticity related to thermal variability? *PLoS One* 13: e0196496. <https://doi.org/10.1371/journal.pone.0196496>
- Paidere J, Brakovska A, Stepanova M (2011) *Limnocalanus macrurus* G.O.Sars 1863 and *Eurytemora lacustris* (Poppe 1887) as indicator of the Latvian salmonid water lakes trophy. In: II International Conference. Bioindication in monitoring of freshwater ecosystems, St. Petersburg (Russia), October 2011. Russian Academy of Sciences, 1: 122
- Popov AI (2011) Alien species of zooplankton in Saratov reservoir (Russia, Volga River). *Russian Journal of Biological Invasions* 2: 126. <https://doi.org/10.1134/S2075111711020093>
- Poppe SA (1887) Beschreibung einiger neuer Entomostraken aus norddeutschen Seen. *Zeitschrift für wissenschaftliche Zoologie*, 45 278–281.
- Sars GO (1895) An account of the Crustacea of Norway: with short descriptions and figures of all the species (Vol. 4). A. Cammermeyer, Christiania, 120 pp. <https://doi.org/10.5962/bhl.title.1164>
- Segerstråle SG (1957) On the immigration of the glacial relicts of Northern Europe, with remarks on their prehistory. *Societas scientiarum Fennica, Helsingfors*, 117 pp.
- Silfverberg H (1999) A provisional list of Finnish Crustacea. *Memoranda-Societas Pro Fauna et Flora Fennica* 75: 15–37.
- Ślugocki Ł, Czerniawski R (2018) Trophic state (TSISD) and mixing type significantly influence pelagic zooplankton biodiversity in temperate lakes (NW Poland). *PeerJ* 6: e5731. <https://doi.org/10.7717/peerj.5731>
- Souissi A, Souissi S, Hwang JS (2016) Evaluation of the copepod *Eurytemora affinis* life history response to temperature and salinity increases. *Zoological Studies* 55: 2016–55.
- Spikkeland I, Kinsten B, Kjellberg G, Nilssen JP, Väinölä R (2016) The aquatic glacial relict fauna of Norway—an update of distribution and conservation status. *Fauna Norvegica* 36: 51–65. <https://doi.org/10.5324/fn.v36i0.1994>
- Sukhikh N, Souissi A, Souissi S, Alekseev V (2013) Invasion of *Eurytemora* sibling species (Copepoda: Temoridae) from north America into the Baltic Sea and European Atlantic coast estuaries. *Journal of Natural History* 47: 753–767. <https://doi.org/10.1080/00222933.2012.716865>

- Sukhikh NM, Castric V, Polyakova NV, Souissi S, Alekseev VR (2016) Isolated populations of *Eurytemora americana* Williams (Crustacea, Copepoda) in the White Sea rock pools – postglacial relicts or anthropogenic invasions? *Russian Journal of Biological Invasions* 7: 396–404. <https://doi.org/10.1134/S2075111716040093>
- Sukhikh N, Souissi A, Souissi S, Holl AC, Schizas NV, Alekseev V (2019) Life in sympatry: coexistence of native *Eurytemora affinis* and invasive *Eurytemora carolleeae* in the Gulf of Finland (Baltic Sea). *Oceanologia* 61: 227–238. <https://doi.org/10.1016/j.oceano.2018.11.002>
- Thum RA, Derry AM (2008) Taxonomic implications for diaptomid copepods based on contrasting patterns of mitochondrial DNA sequence divergences in four morphospecies. *Hydrobiologia* 614: 197. <https://doi.org/10.1007/s10750-008-9506-x>
- Thum RA, Harrison RG (2008) Deep genetic divergences among morphologically similar and parapatric *Skistodiaptomus* (Copepoda: Calanoida: Diaptomidae) challenge the hypothesis of Pleistocene speciation. *Biological Journal of the Linnean Society* 96: 150–165. <https://doi.org/10.1111/j.1095-8312.2008.01105.x>
- Vasquez AA, Hudson PL, Fujimoto M, Keeler K, Armenio PM, Ram JL (2016) *Eurytemora carolleeae* in the Laurentian Great Lakes revealed by phylogenetic and morphological analysis. *Journal of Great Lakes Research* 42: 802–811. <https://doi.org/10.1016/j.jglr.2016.04.001>
- Vekhov VN (2001) Crustaceans in rock water reservoirs of islands and coast of the Kandalaksha Bay, White Sea, *Biol. Vnutr. Vod* 3: 20–28
- Vezhnovets VV, Zaidykov IY, Naumova EY, Sysova EA (2012) Biological peculiarities of two copepod species (Crustacea, Copepoda, Calanoida) as possible causes of changes in their geographical ranges. *Russian Journal of Biological Invasions* 3: 243–250. <https://doi.org/10.1134/S2075111712040054>
- Waiho K, Fazhan H, Shahreza MS (2013) Isolation and characterization of partial mitochondrial CO1 gene from harpacticoid copepod, *Leptocaris canariensis* (Lang, 1965). *African Journal of Biotechnology* 12: 6901–6906. <https://doi.org/10.5897/AJB11.2064>
- Weiler W, Kasprzak P, Schulz M, Flössner D (2003) Habitat requirements of *Eurytemora lacustris* (Copepoda, Calanoida) and implications for its distribution. *Ergebnisse der Limnologie* 201–214.
- Żmudziński L (1990) Past and recent occurrence of Malacostraca glacial relicts in Polish lakes. In: Salemaa H (Ed) *Biology and ecology of glacial relict Crustacea*. Nordic research conference, April 1988, Finnish Zoological Publishing Board, Finland, 227–230.

A new genus and two new species of miniature clingfishes from temperate southern Australia (Teleostei, Gobiesocidae)

Kevin W. Conway^{1,2}, Glenn I. Moore^{3,4}, Adam P. Summers^{5,6}

1 Department of Wildlife and Fisheries Sciences and Biodiversity Research and Teaching Collections, Texas A&M University, College Station, TX 77843, USA **2** Research Associate, Ichthyology, Australian Museum Research Institute, 1 William Street, Sydney, NSW 2010, Australia **3** Fish Section, Department of Aquatic Zoology, Western Australian Museum, Locked Bag 49 Welshpool DC WA 6986, Australia **4** School of Biological Sciences, University of Western Australia, Nedlands, WA 6907, Australia **5** Friday Harbor Laboratories, University of Washington, Friday Harbor, Washington 98250, USA **6** Burke Museum of Natural History and Culture, University of Washington, Seattle, WA 98105, USA

Corresponding author: Kevin W. Conway (kevin.conway@tamu.edu)

Academic editor: David Morgan | Received 15 March 2019 | Accepted 31 May 2019 | Published 15 July 2019

<http://zoobank.org/5B236AA0-725A-478D-96D4-6B8F366126D4>

Citation: Conway KW, Moore GI, Summers AP (2019) A new genus and two new species of miniature clingfishes from temperate southern Australia (Teleostei, Gobiesocidae). ZooKeys 864: 35–65. <https://doi.org/10.3897/zookeys.864.34521>

Abstract

A new genus and two new species of miniature clingfishes are described based on specimens collected from dense stands of macroalgae in intertidal and shallow subtidal areas along the coast of southern Australia. The new genus, *Barryichthys*, is distinguished from other genera of the Gobiesocidae by unique features of the adhesive disc, including elongate papillae in adhesive disc regions A and B, the reduction and/or loss of several elements of the cephalic lateral line canals, the lower gill arch skeleton, and the neurocranium, and by having two distinct types of pectoral-fin rays. *Barryichthys hutchinsi* is described based on 19 specimens (12.4–18.7 mm SL) from Western Australia and South Australia. *Barryichthys algicola* is described based on 22 specimens (9.0–21.0 mm SL) from Victoria, New South Wales and Tasmania. The new species are distinguished from each other by characters of body and head shape, vertebral counts, and aspects of live colour pattern. The new genus shares several characters in common with *Parvicrepis*, another genus of miniature gobiesocids from southern Australia that also inhabits macroalgae habitats. The many reductions and novel characters of *Barryichthys* are discussed within the context of miniaturisation.

Keywords

Macroalgae, miniaturisation, osteology, reduction, taxonomy

Introduction

The family Gobiesocidae contains 50 genera and more than 170 species of predominately marine fishes found in coastal areas of the Atlantic and Indo-Pacific oceans, from the intertidal zone to ~500 meters depth (Briggs 1955; Hastings and Conway 2017). Seven species are known to inhabit freshwater streams in the Neotropics (Briggs and Miller 1960; Conway et al. 2017a). Commonly referred to as clingfishes, members of this family generally exhibit a well-developed ventral adhesive disc (formed by elements of the paired fins and paired-fin girdles; Guitel 1888), with which they can attach to smooth or even heavily structured substrates with great tenacity (Wainwright et al. 2013; Ditsche et al. 2014). Although some clingfishes may reach body lengths over 200 mm in standard length (SL) (e.g., *Sicyases sanguineus* Müller & Troschel in Müller 1843), the majority are small-bodied and do not exceed 50 mm SL (Briggs 1955; Brandl et al. 2018). Several small-bodied clingfishes are not known to exceed 26 mm SL and are considered miniature species following the criteria of Weitzman and Vari (1988).

A number of temperate species of clingfishes, including several small-bodied or miniature species, are known to exhibit intimate (potentially obligate) associations with macroalgae and/or seagrasses. This includes members of the genus *Rimicola* Jordan and Evermann in Jordan, 1896 in the western Pacific (Roland 1978; Lamb and Edgell 2010), *Acyrtops* Schultz, 1951 in the western central Atlantic (Gould 1965), *Opeatogenys* Briggs, 1955 in the eastern central Atlantic (Hofrichter and Patzner 2000; Gonçalves et al. 2005), *Eckloniaichthys* Smith, 1942 in South Africa (Allen and Griffiths 1981), *Parvicrepis* Whitley, 1931, *Posidonichthys* Briggs, 1993, and two species of *Cochleocephalus* (*C. spatula* (Günther, 1861) and *C. viridis* Hutchins, 1991) in southern Australia (Briggs 1993; Hutchins 1983, 1991, 1994a, 2008), and *Gastrocyathus* Briggs, 1955, *Gastrocymba* Briggs, 1955, *Gastroscyphus* Briggs, 1955, and *Haplocylix* Briggs, 1955 in New Zealand (Paulin and Roberts 1992; Stewart 2015). All these taxa share a number of characteristics that may represent adaptations for dwelling on the surface of macroalgae and/or seagrass blades, including narrow, elongate bodies and relatively narrow heads, short dorsal and anal fins, modified pectoral fins in which the lower rays are generally notably shorter than the upper rays (Briggs 1955), and live colour patterns comprised predominately of different shades of green, brown, orange or red. This type of colouration likely facilitates crypsis on the fronds of macroalgae or blades of seagrass to which they adhere (Paulin and Roberts 1992; Hofrichter and Patzner 2000).

Several undescribed species of macroalgae and/or seagrass inhabiting clingfishes have been known from the southern coast of Australia since at least the 1980s (Hutchins 1983, 1991a, b; Last et al. 1983; Kuitert 1993). They are considered to represent at least four different genera, three of which have yet to be formally described (viz. Genus A, B, and C sensu Hutchins 1994a, 2008). Hutchins (1994a, 2008) considered the undescribed Genus B to be monotypic and comprised of a single undescribed species (referred to using the common name “Rat Clingfish”; Hutchins 1991b, 1994a, 2008) with a disjunct distribution in shallow coastal areas along the southern coast of Australia, including Western Australia in the west and Victoria and Tasmania in the east (Hutchins 2008). Members of Genus B are very small (≤ 21 mm SL) and similar in

general appearance to members of *Parvicrepis*, with which they are sympatric in shallow coastal areas rich in “weed” (Hutchins 1994a, 2008). Examination of unidentified and unsorted material of gobiesocids as well as material identified previously as *Parvicrepis*, from the southern coast of Australia held within the Western Australian Museum (Perth) and the Australian Museum (Sydney) produced additional specimens of the undescribed Genus B for study. Based on differences in vertebral counts, body and head shape, and colouration in life, we consider this material of Genus B to represent two different species, both of which are undescribed. In the present paper, we provide descriptions for these two new miniature species, and provide a formal description for the undescribed Genus B, which we name *Barryichthys* gen. nov.

Materials and methods

Specimens used in this study were obtained from the following museum collections: Australian Museum, Sydney (**AMS**); Biodiversity Research and Teaching Collections, Texas A&M University, College Station (**TCWC**); and Western Australian Museum, Perth (**WAM**). Head and body measurements and counts reported follow Conway et al. (2014) and are expressed as percent of standard length (SL) or head length (HL). Adhesive disc papillae terminology follows Briggs (1955) and Hutchins (2008). Cephalic lateral line pore terminology follows Shiogaki and Dotsu (1983), except that we also use numbers to refer to individual pores following Conway et al. (2017b), with pores numbered along a particular canal from anterior to posterior or dorsal to ventral. General osteological terminology follows that of Springer and Fraser (1976), except that we use the term anguloarticular instead of articular, anterior ceratohyal instead of ceratohyal, autopalatine instead of palatine, epicentral instead of epipleural (following Gemballa and Britz 1998), endopterygoid instead of mesopterygoid, pharyngobranchial instead of infrapharyngobranchial, posterior ceratohyal instead of epihyal, and retroarticular instead of angular.

Selected specimens were cleared and double stained (C&S) for bone and cartilage investigation using the protocol of Taylor and Van Dyke (1985). Computed tomography (CT) scans of select specimens were also obtained at the Karel F. Liem BioImaging Center (Friday Harbor Laboratories, University of Washington) using a Bruker (Billerica, MA) SkyScan 1173 scanner with a 1 mm aluminium filter at 60 kV and 110 μ A on a 2240 x 2240 pixel CCD at a resolution of 8.8 μ m. Specimens were scanned simultaneously in a 50ml plastic Falcon tube (Corning, NY), in which they were wrapped with cheesecloth moistened with ethanol (70%) to prevent movement during scanning. The resulting CT data were visualised, segmented, and rendered in Horos (www.horosproject.org) and Amira (FEI). Select specimens were reversibly stained using cyanine blue following Saruwatari et al. (1997) to aid examination of adhesive disc papillae and cephalic lateral line canal pores. Specimens or parts thereof were observed and photographed using a ZEISS SteREO Discovery V20 stereomicroscope equipped with a ZEISS Axiocam MRc5 digital camera. Digital images were typically stacked using ZEISS Axiovision software. All digital images were processed using Adobe Photoshop and Adobe Illustrator.

Taxonomy

Barryichthys gen. nov.

<http://zoobank.org/505099BF-E797-43FC-BEC0-B433A0398707>

Genus B Hutchins 1994a: 309; 2008: 725.

Diagnosis. A genus of the Gobiesocidae differing from all other genera by the following unique characters: a double adhesive disc with elongate papillae in regions A and B (Fig. 1A), few enlarged papillae (with circular or elongate cuboid margins) in disc region D, and papillae absent from region C; two distinct types of ray in the pectoral fin including a longer ray comprising a pair of poorly ossified and unsegmented hemitrichia (uppermost 10–12 rays) and a shorter, stouter ray comprising a pair of well-ossified and segmented hemitrichia (lowermost 4–5 rays); anterior part of parasphenoid a narrow strut of bone, $\sim 1/4$ width of wider posterior part of bone; a greatly reduced gill-arch skeleton in which the hypobranchial and basibranchial elements (including cartilages) and lower pharyngeal jaw teeth are absent; and a sexually dimorphic urogenital papilla that is housed within a shallow groove posterior to the anus that is either flanked by a pair of swollen skin folds (male) or not (female). The following characters are also diagnostic, although not unique to the genus: a well-developed skin pad covering base of lower pectoral-fin rays and girdle; a thick,

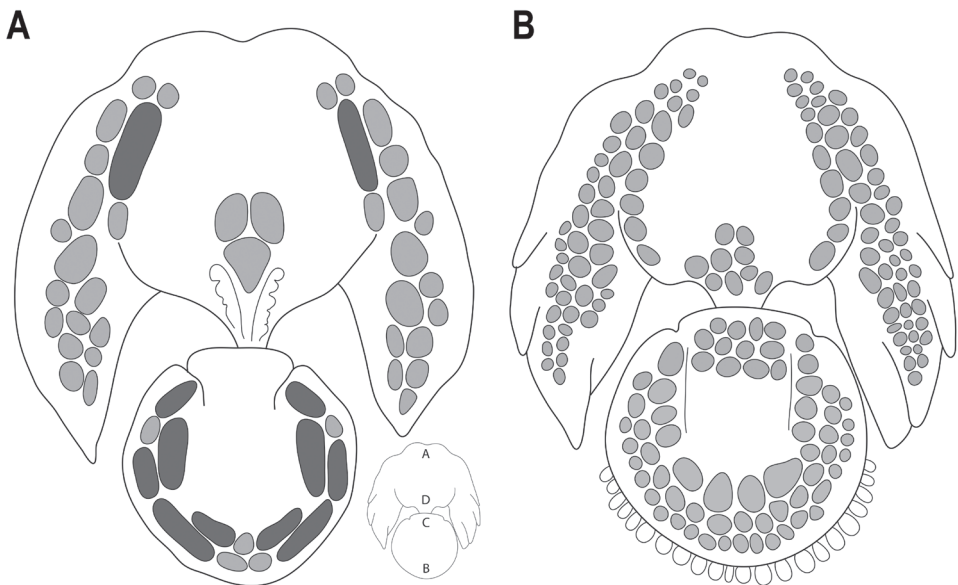


Figure 1. Schematic outline drawings of the adhesive disc of *Barryichthys* (A) and *Parvicrepis* (B). Both redrawn from Hutchins (1994: fig. 1). Typical circular-cuboid papillae in light grey (A and B); elongate papillae in dark grey (A). Disc regions A–D shown in inset figure.

fleshy upper lip that is thicker along midline than at lateral margins; the absence of preoperculo-mandibular and lachrymal lateral line canals; a single lateral line canal pore (PO1) posterior to orbit; gill filaments of the first gill arch comprising a hemibranch of 5–6 poorly developed gill filaments; branchiostegal rays 5 or 6; dorsal and anal fins with 4–6 rays, well separated from caudal fin; 4+4 principal caudal-fin rays; and 1–2 procurrent caudal-fin rays.

Etymology. Named for Barry Hutchins, in honour of his work on Australian clingfishes. Masculine.

Type species. *Barryichthys hutchinsi* sp. nov.

Remarks. Hutchins (1994a) provided a brief overview of *Barryichthys* (his Genus B) based on relatively few specimens from the coasts of Victoria and Tasmania. Later, Hutchins (2008) provided a more in-depth summary of the characteristics that he considered important for separating his Genus B from other genera of gobiesocids inhabiting the southern coast of Australia and extended the range of the genus to Western Australia.

***Barryichthys hutchinsi* sp. nov.**

<http://zoobank.org/DE65B196-C878-4524-850E-1DA1C8CB3548>

Figs 2A, 3A–C, 4A, 5A, 6–8, 9A, C–E, 10

Common name: Brown rat clingfish

Genus B sp. Hutchins 2008: 725.

Holotype. WAM P.28981-004, male, 15.4 mm SL; Western Australia, Cottesloe Reef platform, Perth (31°59'00.0"S, 115°45'00.0"E), 16 January 1986, J. Keesing et al., CT scan: <https://doi.org/10.17602/M2/M78748>.

Paratypes. *Western Australia:* WAM P.28981-003, 4, 16.0–16.9 mm SL; same data as holotype. – WAM P.34510-001, 5 (2 C&S), 14.2–16.3 mm SL; Western Australia, Cottesloe Reef platform, Perth (31°58'59"S, 115°45'00"E), 29 January 1985, J. Keesing. – WAM P. 34940-001, 1, female, 18.7 mm SL; Trigg Reef platform, Perth (31°52'46.5"S, 115°45'04.7"E), 13 January 1986, J. Keesing et al.

Other material. *South Australia:* AMS I.20171-012, 6 (2 C&S), 12.4–13.1 mm SL (immature); South Australia; Kangraoo Island, Vivonne Bay (36°00'00.0"S, 137°10'48.0"E), D. Hoese & K. Handley. – AMS I.49000-001, 2 (1 CT <https://doi.org/10.17602/M2/M80016>), 14.0–14.6 mm SL; Victor Harbor, Bluff Jetty (35°35'19.1"S, 138°36'16.5"E), 25 March 2015, G. Short.

Diagnosis. *Barryichthys hutchinsi* is distinguished from *B. algicola* (below) by a shorter, deeper body (body depth at dorsal-fin origin 10–11% SL vs. 7–8% SL), a wider, deeper head (head width at widest point 66–75% HL vs. 55–61%; depth at orbit 30–32% HL vs. 27–29%; interorbital width 27–33% HL vs. 20–24%), ventral margin of the orbit obscured by cheek in ventral view (vs. entire ventral margin of orbit visible in ventral view), by having a shorter abdominal region with fewer vertebrae (ab-



Figure 2. Specimens of *Barryichthys* **A** *B. hutchinsi*, WAM P.28981-004, holotype, male, 15.4 mm SL; Western Australia, Cottesloe Reef Platform, Perth **B** *B. algicola*, WAM P.27127-016, holotype, female, 16.9 mm SL; Victoria, Jubilee Point.

dominal vertebrae 17 vs. 21) and fewer ribs (11–12 vs. 15), fewer epicentrals (14–15 vs. 18–19), and a lower total number of vertebrae (total number of vertebrae 38–39 vs. 42–44), and by features of live colour pattern, including body background colour golden-yellow to olive-brown (vs. uniform green), the presence (vs. absence) of a variable number of irregularly shaped light to dark brown markings along dorsal midline, and the presence (vs. absence) of a series of light to dark brown elongate lateral markings forming an incomplete or complete horizontal stripe.



Figure 3. Live or freshly dead individuals of *Barryichthys* **A–C** *B. hutchinsi*, WAM P.28981-003, Western Australia, Cottesloe Reef Platform, Perth; male in dorsal view (**A**) female in dorsal (**B**) and lateral view (**C**). **D, E** *B. algicola*, WAM P.27559-007, Tasmania, St. Helens; in dorsal (**D**) and lateral (**E**) view. Photographs by B. Hutchins.

Description. General body shape as in Figs 2A, 3A–C. Select morphometric and meristic characters are listed in Tables 1, 2. Largest specimen examined 18.7 mm SL. Body moderately elongate, circular in cross-section anteriorly, becoming increasingly laterally compressed posteriorly. Widest point of body midway between head and dorsal-fin origin, corresponding with centre of abdominal cavity. Body width and depth tapering gradually posteriorly from widest point. Caudal peduncle thin, elongate (approximately 1/5 of SL). Head relatively large (approximately 1/3 of SL), slightly dorsoventrally compressed anteriorly, becoming increasingly circular in cross-section posteriorly. Widest point of head midway between orbit and opercular opening; wider than widest point of body. Eye large, positioned on dorsolateral surface of head; ventral margin of orbit not visible in ventral view (Fig. 5A). Snout of moderate length, triangular, narrowest anteriorly. Anterior nostril a small tubular opening (Fig. 5A). Posterior nostril surrounded by a low fleshy rim; situated along anterodorsal margin of orbit (Fig. 5A). Gill membranes united across midline, free from isthmus.

Mouth subterminal, small; posterior tip of upper jaw not reaching imaginary vertical line through anterior margin of orbit when mouth closed. Articulation between

Table 1. Select morphometric characters obtained from the holotype and four paratypes of *Barryichthys hutchinsi* and *B. algicola*. Ranges include values from holotype.

	<i>Barryichthys hutchinsi</i> (n = 5)				<i>Barryichthys algicola</i> (n = 5)			
	Holotype	Range	Mean	St. Dev.	Holotype	Range	Mean	St. Dev.
Standard Length (SL)	15.4	15.4–18.7			16.9	13.1–16.9		
In % of SL								
Head length (HL)	28.3	26.2–30.3	27.9	1.8	28.8	26.6–31.6	29.1	2
Body depth	10	9.6–11.6	10.3	0.9	8.3	7.4–8.3	7.8	0.4
Predorsal length	70.9	67.4–70.9	69.2	1.8	68.7	68.3–71.3	69.8	1.5
Preanal length	67.8	61.4–67.9	65.1	3.3	69.4	68.3–71.0	69.3	1.2
Preanus length	60.7	54.1–61.0	57.6	3.7	62.3	59.0–62.6	61.2	1.7
Anus to disc	25.1	16.6–25.1	20	4.5	26.2	22.9–26.8	25.2	1.7
Anus to anal fin	6.8	6.8–9.1	8.2	1.1	7.3	5.5–9.0	7.1	1.5
Caudal peduncle length	21.6	20.1–22.3	21.3	0.9	20.4	20.0–25.1	22.1	2.4
Caudal peduncle depth	5.8	5.2–6.2	5.7	0.4	4.9	4.1–4.9	4.5	0.4
Disc length	15	15.0–17.7	16.1	1.2	16.1	13.5–16.1	14.5	1.2
Disc width	12.6	12.6–15.0	14.1	1.3	13.2	12.1–13.4	12.8	0.6
In % of HL								
Head depth at orbit	31	28.2–32.5	30.4	1.9	26.1	25.3–27.3	26.3	0.8
Head width at orbit	36.9	33.8–38.2	35.9	1.9	32.7	32.7–38.2	34.9	2.4
Head width at widest point	65.8	65.3–74.9	69.1	4.5	56.6	55.2–60.9	57.1	2.6
Interorbital width	32.9	26.5–32.9	28.8	2.9	20.6	19.5–23.8	21.7	2
Snout length	25.8	24.4–25.8	24.9	0.7	30	27.7–31.1	29.5	1.4
Eye diameter	24	21.0–24.0	22.1	1.4	22.4	21.4–24.9	23.3	1.6

anguloarticular and quadrate located directly along imaginary vertical line through anterior margin of orbit. Upper lip fleshy (Fig. 5A); in dorsal view appearing uniform in thickness around entire anterior margin of snout; in lateral and ventral view upper lip appearing markedly thicker anteriorly, tapering in thickness posteriorly. Lower lip restricted to lateral margin of lower jaw only; separated along ventral midline by a fleshy pad of skin at symphysis of lower jaw. Lower lip narrower than upper lip, with poorly developed skin flap anteromedially. Fleshy pad of skin at symphysis of lower jaw bordered anterolaterally by a shallow groove; confluent posteriorly with skin of isthmus (Fig. 5A). Upper jaw longer and wider than lower jaw (Fig. 7A), creating a narrow gap between teeth of upper and lower jaw when jaws closed. Premaxilla with an outer row of 6–8 small conical teeth with slightly recurved tips, arranged along anteromedial edge, adjacent to symphysis, and a small patch of 2–4 tiny conical teeth on lingual surface posterior to teeth of outer row. Dentary with a single row of 5–6 conical teeth; anteriormost 3–4 teeth dagger-like, only slightly recurved and orientated at a 180° angle to dentary, with cusp directed anteriorly; posteriormost 2–3 teeth strongly recurved and orientated at a 90° angle to dentary, with cusp directed posterodorsally (Fig. 7A). Teeth on dentary slightly larger than largest teeth on premaxilla. Ascending process of premaxilla narrow, elongate (Fig. 7A); extending posteriorly along dorsal surface of neurocranium to a point slightly anterior to epiphyseal commissure of supraorbital lateral line canal when jaws closed. Pharyngeal jaws comprising patch of

Table 2. Total number of vertebrae in specimens of *Barryichthys*. Number obtained from holotype indicated with an asterisk.

Species	N	Number of Vertebrae						
		38	39	40	41	42	43	44
<i>B. hutchinsi</i>	8	3	5*	–	–	–	–	–
<i>B. algicola</i>	11	–	–	–	–	3	4*	4

3–4 tiny conical teeth with slightly recurved tips on pharyngobranchial 3 toothplate only (Fig. 7C); teeth absent from ceratobranchial 5 (Fig. 7B). 3–5 tiny, gnarled gill rakers along anterior and posterior edge of ceratobranchials 2–3 and anterior edge of ceratobranchial 4; ceratobranchial 1 without gill rakers (one gill raker along posterior edge of ceratobranchial 1 of left side only in one C&S specimen). Gill filaments associated with gill arches I–III only (three gill filaments of Briggs, 1955); restricted to lower (ceratobranchial) portion of gill arches only; ceratobranchial 2 and 3 with paired rows of filaments (holobranch); ceratobranchial 1 with single row (hemibranch) of 4–5 poorly developed gill filaments. Basihyal a short club-like element; capped with cartilage anteriorly (Fig. 7B). Ceratobranchials 1–4 rod-like elements; ceratobranchial 5 a short plate-like element, wider and shorter than more anterior ceratobranchial elements (Fig. 7B). Epibranchials 1–2 short rod-like elements; epibranchial 3 a club-like element, broadest anteriorly; epibranchial 4 a single splint like element (epibranchial 4 fused to epibranchial 3 on left side only in one C&S specimen; Fig. 7C). Five or six branchiostegal rays (Fig. 7D). In specimens with five, first ray articulating medially with hyoid bar along anterior ceratohyal; posterior rays articulating with hyoid bar laterally, including two along posteriormost part of anterior ceratohyal, one straddling junction between anterior and posterior ceratohyals, and one along anteriormost part of posterior ceratohyal. In specimens with six, an additional small ray without contact to hyoid bar located anterior to ray articulating with medial face of hyoid bar.

Superficial neuromasts on surface of head not observed in material other than a pair of large superficial neuromasts housed within a pair of shallow depressions at centre of symphyseal pad on lower jaw. Cephalic lateral-line system comprising supraorbital lateral-line canal only; 2 nasal pores; 1 postorbital pore. Canal pores minute; flush with surface of skin and difficult to locate. Supraorbital lateral line canals connected across midline via epiphyseal commissure (Fig. 6A). Lachrymal, a small paddle-like bone, without canal ossification, articulating with anterolateralmost point of lateral ethmoid. Nasal elongate, approximately half length of frontal, with canal ossification restricted to posteriormost part of bone adjacent to olfactory capsule. Nasal bones extending far anterior to ethmoid region of neurocranium over dorsal surface of upper jaw; terminating anterior to anteriormost point of upper jaw (Fig. 4A). Parasphenoid widest posteriorly ventral to occipital region of neurocranium; tapering anteriorly and abruptly to a narrow strut of bone along ventral midline of neurocranium (Fig. 6).

Dorsal-fin rays 4 or 5(*). Anal-fin rays 4, 5 or 6(*). All dorsal- and anal-fin rays unbranched and segmented; each in serial association with a narrow, rod-like pterygiophore, comprising proximal-middle radial only. Principal caudal-fin rays

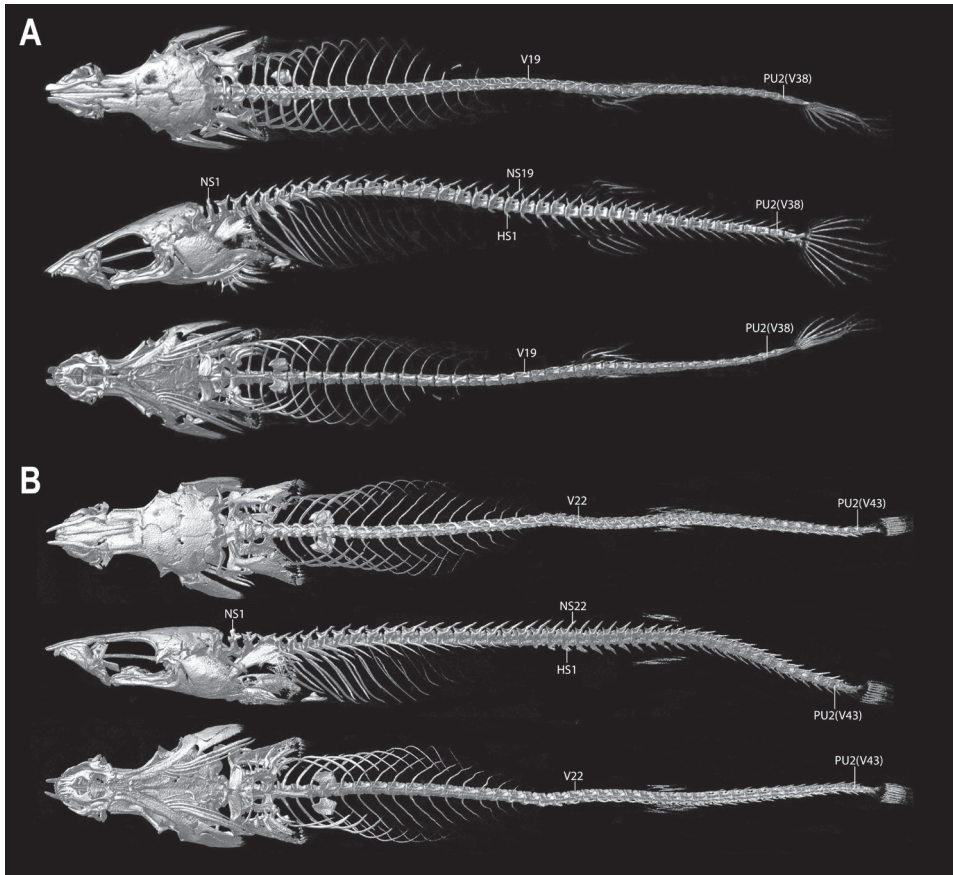


Figure 4. CT scanned skeleton of *Barryichthys* in dorsal, lateral and ventral view **A** *B. hutchinsi*, AMS I.49000-001, 14.0 mm SL **B** *B. algicola*, WAM P.27127-016, holotype, female, 16.9 mm SL. Abbreviations: HS, hemal spine; NS, neural spine; PU2, preural centrum 2; V, vertebra.

4+4, dorsal procurrent rays 1 or 2, ventral procurrent rays 1 or 2. Principal caudal-fin rays and posteriormost dorsal and ventral procurrent rays unbranched and segmented; anteriormost dorsal and ventral procurrent ray unsegmented. Pectoral-fin rays 15 or 17; uppermost ray typically a tiny splint-like element comprised of a single hemitrichium; present on right side only in one C&S specimen (WAM P.34510-001). Lowermost 4–5 pectoral-fin rays more heavily ossified and approximately half length of upper rays, with foreshortened segments in each hemitrichium (sensu Lundberg & Marsh 1976) (Fig. 8). Remaining pectoral-fin rays (uppermost 10–12 rays) poorly ossified, without segmentation of hemitrichia (Fig. 8). Pelvic-fin rays I.4. Distal tip of spinous pelvic-fin ray narrow; strongly bifurcated proximally, embracing a small circular cartilaginous pelvic-radial cartilage. Pelvic-fin rays 1–3 increasing in length and width posteriorly. Caudal fin marginally truncate, tips of principal caudal-fin rays extended slightly beyond fin margin. Caudal-fin skeleton comprised of narrow upper and lower hypural plates (Fig. 10B); lower hypural plate

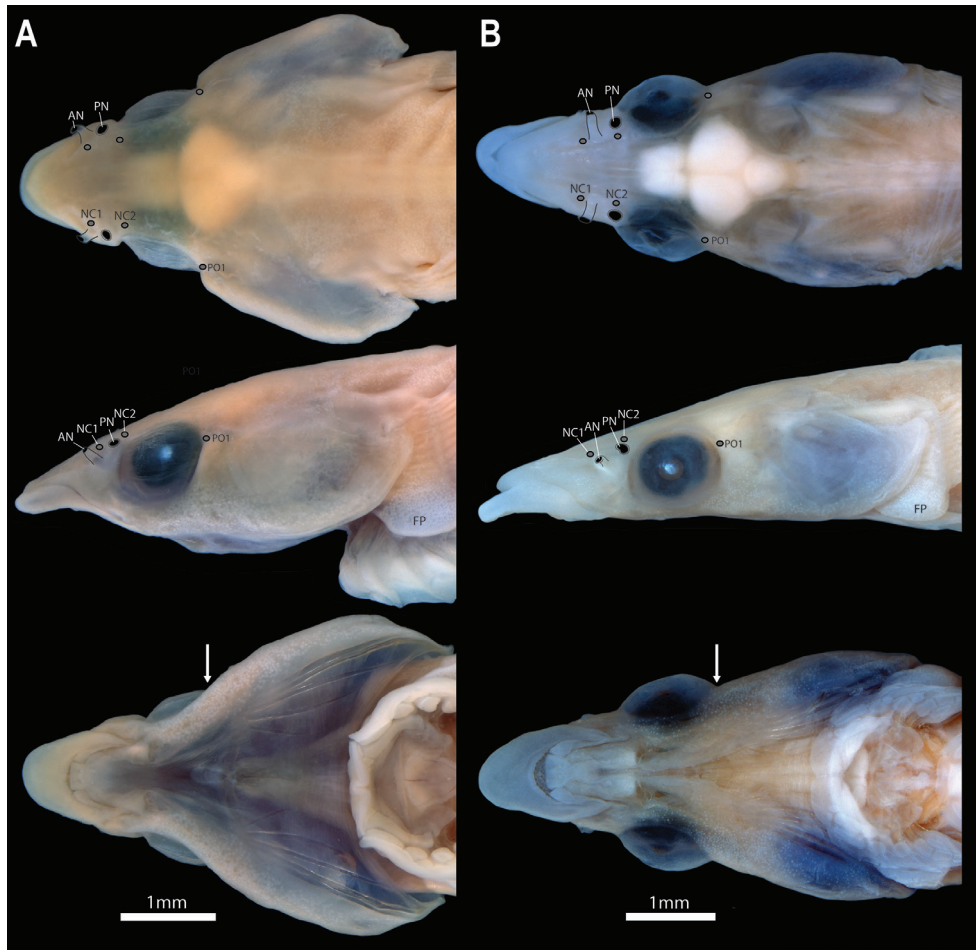


Figure 5. Head (in dorsal, lateral, and ventral views) in members of *Barryichthys* highlighting position of cephalic lateral line canal pores (grey circles) on head surface **A** *B. hutchinsi*, WAM P.28981-004, holotype, male, 15.4 mm SL **B** *B. algicola*, WAM P.27127-016, holotype, female, 16.9 mm SL. Outline of anterior and posterior nostril highlighted by grey solid line. White arrow points to posterior margin of orbit. Abbreviations: AN, anterior nostril; FP, fleshy pad at base of pectoral fin; NC1–2, nasal canal pores 1–2; PN, posterior nostril; PO1, postorbital canal pore 1.

with short antero- and posteroventral processes along ventral surface; tip of posteroventral process capped with cartilage. Epural a narrow, roughly triangular element, wider posteriorly than anteriorly, with broad cartilaginous posterodorsal margin; parhypural cartilage a small irregular element located at tip of posteroventral process of lower hypural plate (Fig. 10B). Dorsal-fin origin opposite anal-fin origin (Figs 2A, 4A). First dorsal-fin pterygiophore inserted between neural spines of vertebrae 20/21 or 21/22. First anal-fin pterygiophore inserted between hemal spines of vertebrae 19/20 or 20/21. Proximal-middle radials of dorsal- and anal-fin pterygiophores rod-like, without cup-like anterior process (Fig. 10A). Total number of vertebrae 38 or

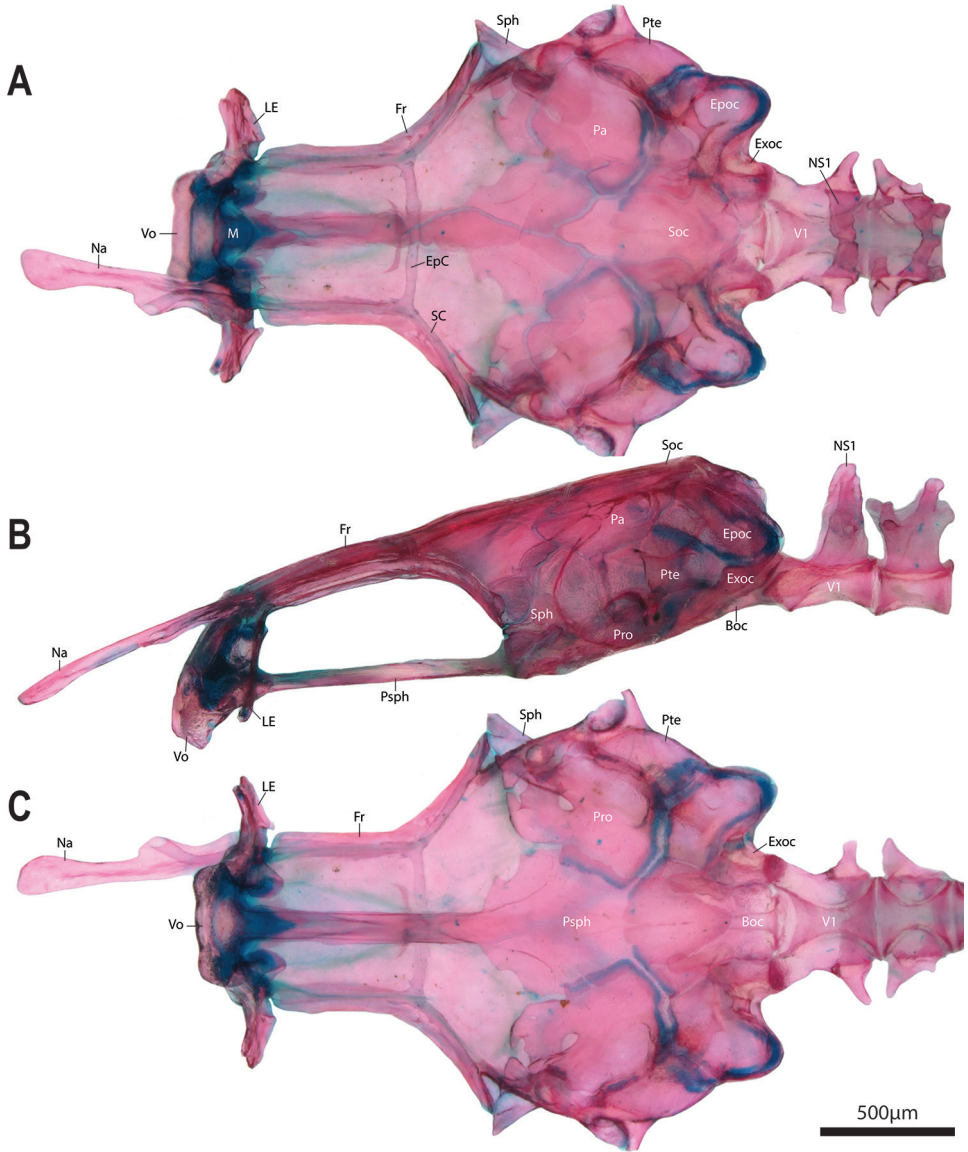


Figure 6. Neurocranium of *Barryichthys hutchinsi*, WAM P.34510-001, paratype, 15.5 mm SL **A** dorsal view **B** lateral view (left side) **C** ventral view. Lachrymal not shown. Nasal of right side removed. Abbreviations: Boc, basioccipital; EpC, epiphyseal commissure of supraorbital canal; Epoc, epiotic; Exoc, exoccipital; Fr, frontal; LE, lateral ethmoid; M, mesethmoid; Na, nasal; NS1, neural spine of vertebral centrum 1; Pa, parietal; Pro, prootic; Psph, parasphenoid; Pte, pterotic; SC, supraorbital canal; Soc, supraoccipital; Sph, sphenotic; V1, vertebral centrum 1; Vo, vomere.

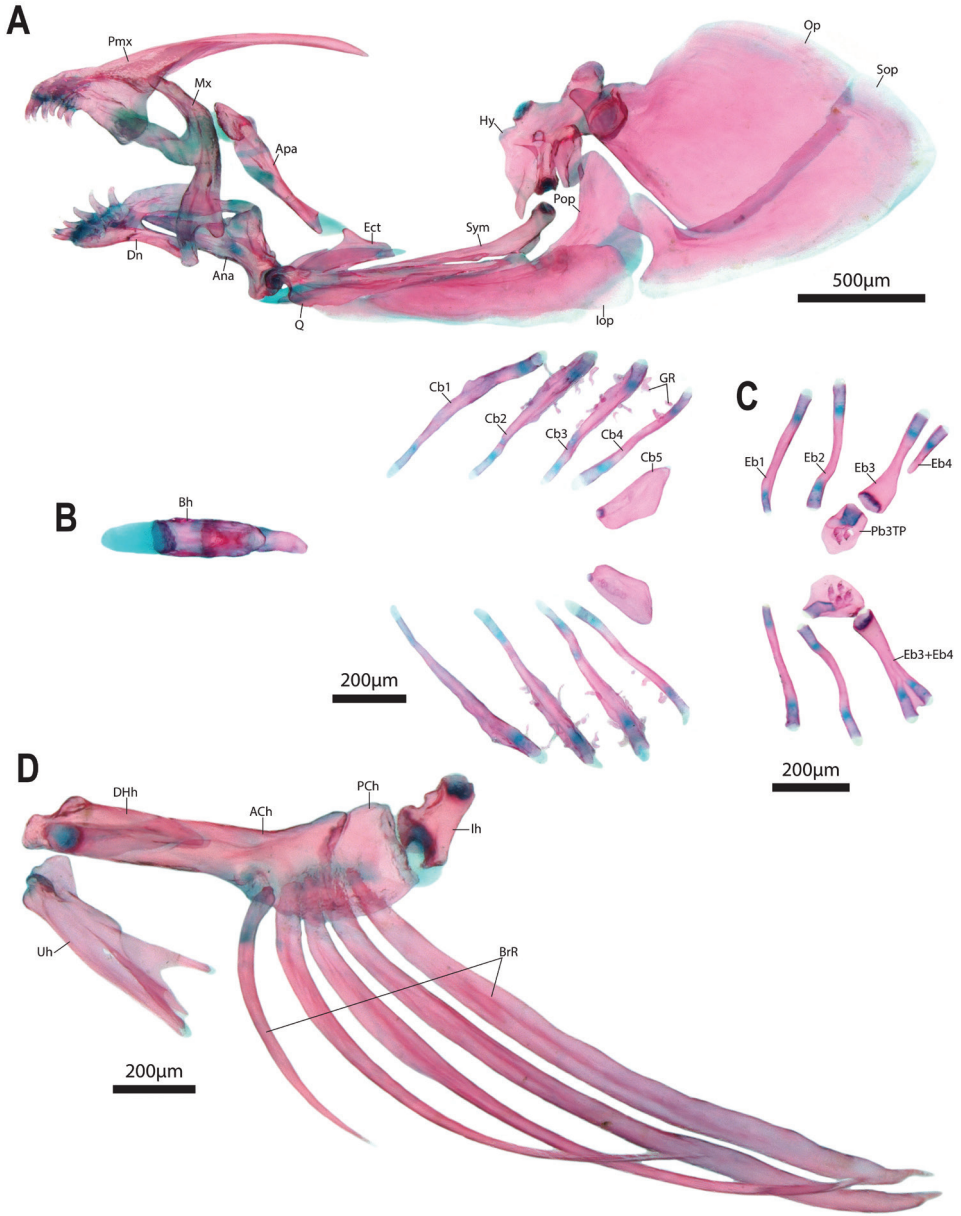


Figure 7. Viscerocranium of *Barryichthys hutchinsi*, WAM P.34510-001, paratype, 15.5 mm SL **A** hyopalatine arch and opercular series, right side in lateral view (image reversed) **B** lower gill-arch elements in dorsal view, gill filaments removed **C** upper gill-arch elements in ventral view **D** hyoid bar, right side in medial view and urohyal. Abbreviations: ACh, anterior ceratohyal; Ana, anguloarticular; Apa, autopalatine; Bh, basihyal; BrR, branchiostegal rays; Cb1-5, ceratobranchial 1-5; DHh, dorsal hypohyal; Dn, dentary; EB1-4, epibranchials 1-4; EB3+4, compound element comprising EB3 and EB4; Ect, ectopterygoid; GR, gill raker; Hy, hyomandibular; Iop, interopercle; Mx, maxilla; Op, opercle; Pb3TP, pharyngobranchial 3 toothplate; Pop, preopercle; Q, quadrate; Sop, subopercle; Sym, symplectic; Uh, urohyal.

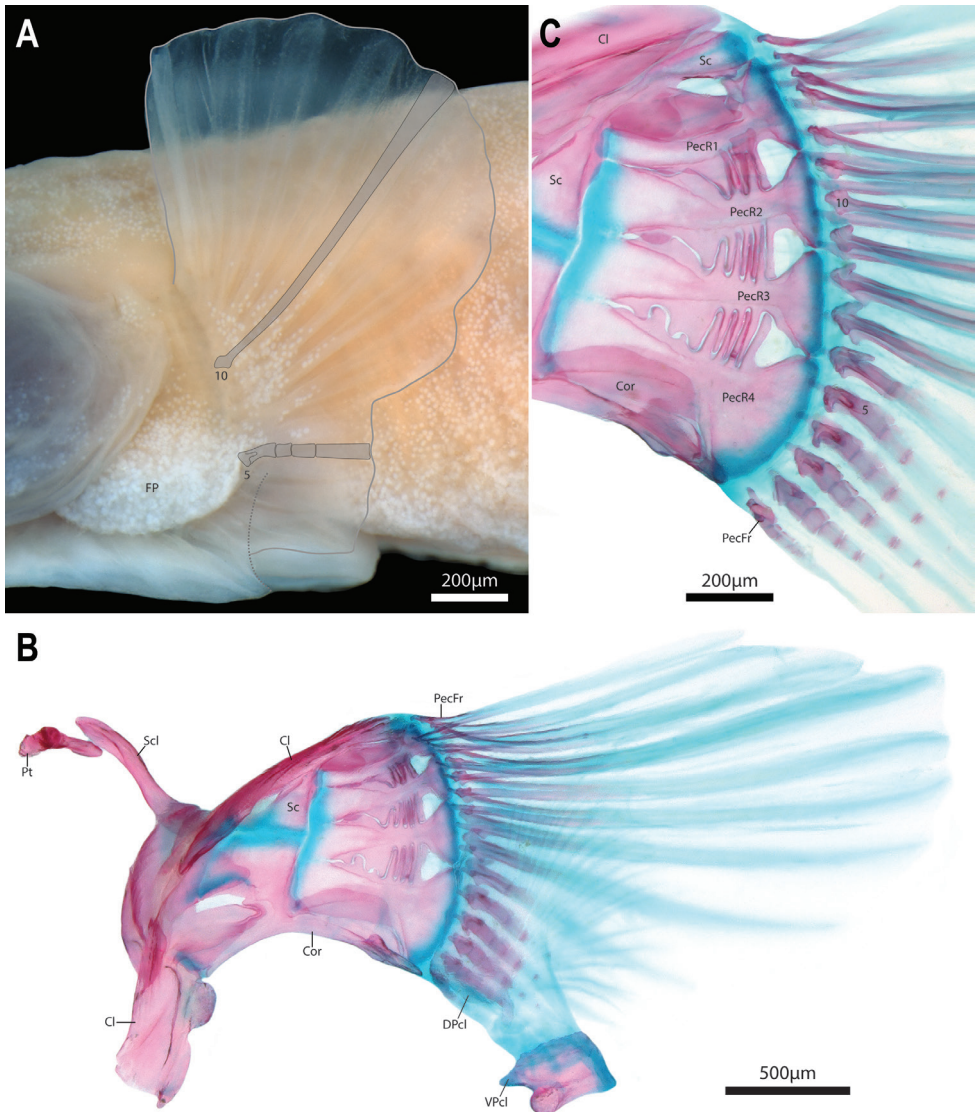


Figure 8. Pectoral fin and pectoral-fin girdle of *Barryichthys hutchinsi* **A** pectoral fin, left side in lateral view, WAM P.28981-004, holotype, male, 15.4 mm SL. Outline of fin margin highlighted by thin grey line. Schematic representation of 5th and 10th pectoral-fin rays (counted from ventral to dorsal) overlay rays **B** pectoral-fin girdle, right side in medial view, WAM P.34510-001, paratype, 15.5 mm SL **C** close-up of area of articulation between pectoral-fin rays and girdle, right side in medial view (image reversed; same specimen as in B). Postcleithra removed. Abbreviations: Cl, cleithrum; Cor, coracoid; DPcl, dorsal postcleithrum; PecR1–4, pectoral radial 1–4; PecFR, pectoral-fin ray; Pt, posttemporal; Sc, scapula; Scl, supra-cleithrum; VPcl, ventral postcleithrum; 5, 10, 5th and 10th pectoral-fin ray (counted from ventral to dorsal).

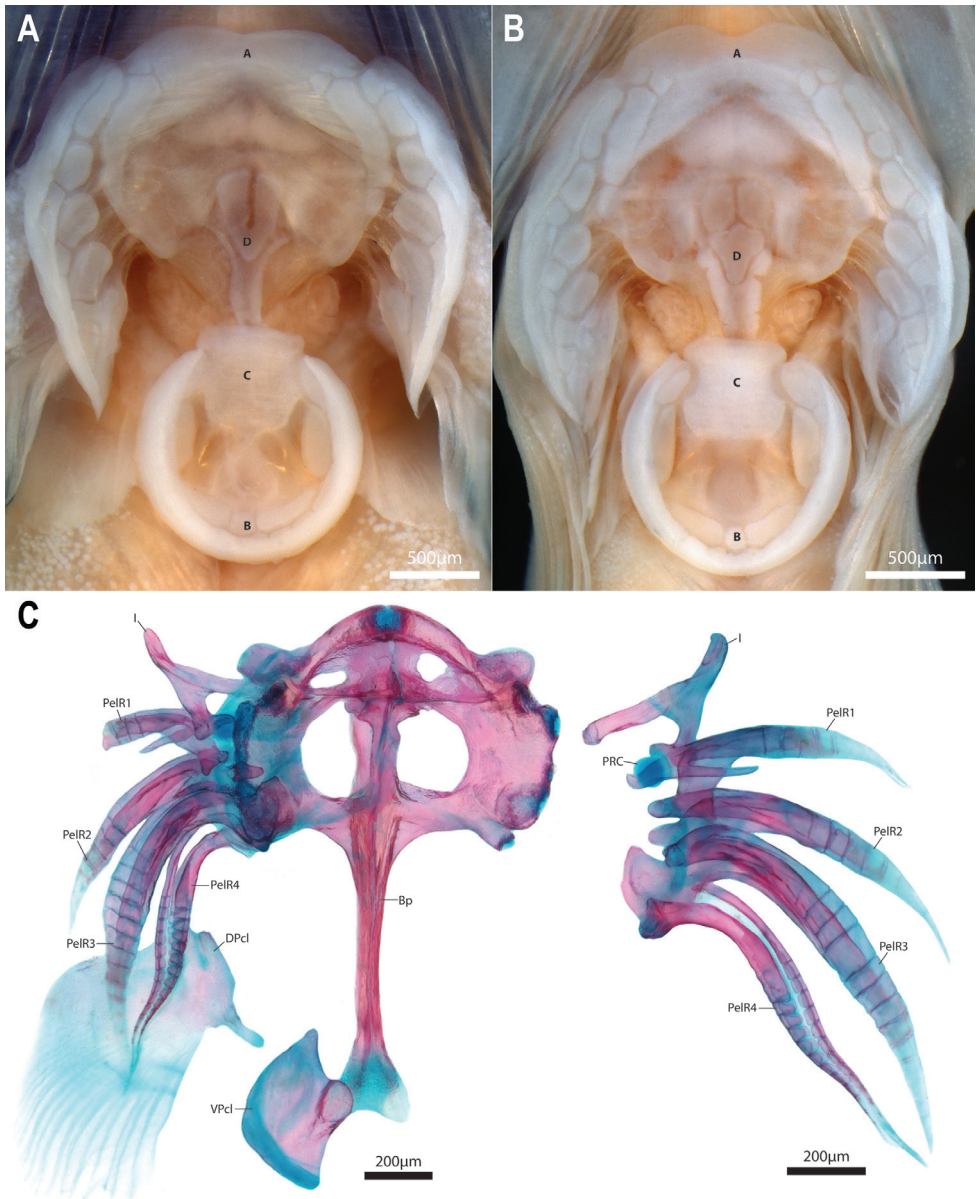


Figure 9. Surface features (**A, B**) and internal supporting skeleton (**C, D**) of the adhesive disc of *Barryichthys* **A** adhesive disc of *Barryichthys hutchinsi* (WAM P.28981-004, holotype, male, 15.4 mm SL), ventral view (anterior to top of page) **B** adhesive disc of *B. algicola* (WAM P.27127-016, holotype, female, 16.9 mm SL), ventral view (anterior to top of page) **C** adhesive disc supporting skeleton, including elements of the pelvic and pectoral-fin girdle of *B. hutchinsi* (WAM P.34510-001, paratype, 15.5 mm SL), ventral view (anterior to top of page). Postcleithra and pelvic-fin rays of the right side removed (image reversed) **D** pelvic-fin spine and rays of right side of *B. hutchinsi* (same specimen as in C), dorsal view (anterior to top of page). Abbreviations: A, disc region A; B, disc region B; Bp, basipterygium; C, disc region C; D, disc region D; DPcl, dorsal postcleithrum; I, pelvic-fin spine; PelR1–4, pelvic-fin rays 1–4; PRC, pelvic-radial cartilage; VPcl, ventral postcleithrum.

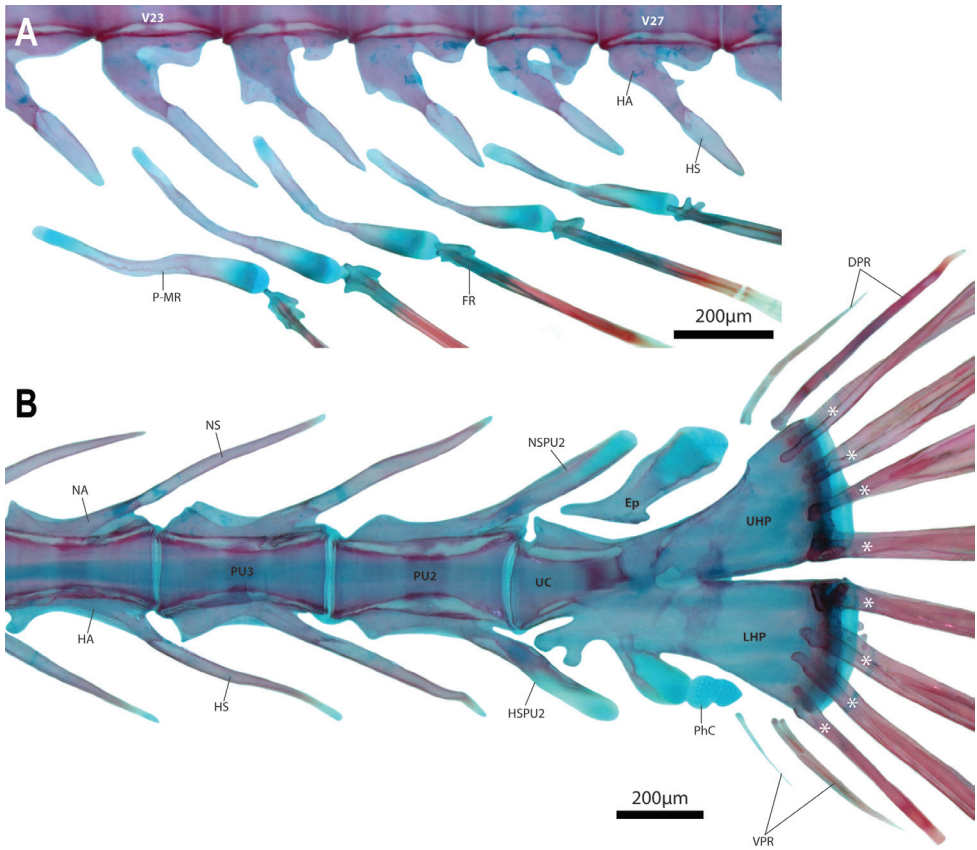


Figure 10. Anal- and caudal-fin skeleton of *Barryichthys hutchinsi*, WAM P.34510-001, paratype, 15.5 mm SL **A** anal-fin skeleton, left side in lateral view **B** caudal-fin skeleton, left side in lateral view. Principal caudal-fin rays are labelled with an asterisk (*). Abbreviations: DPR, dorsal procurrent rays; Ep, epural; FR, fin ray; HA, hemal arch; HS, hemal spine; HSPU2, hemal spine of preural centrum 2; LHP, lower hypural plate; NA, neural arch; NS, neural spine; NSPU2, neural spine of preural centrum 2; PhC, parhypural cartilage; P-MR, proximal-middle radial; PU2-3, preural centrum 2, 3; UC, ural centrum; UHP, upper hypural plate; VPR, ventral procurrent rays.

39, consisting of 17 abdominal vertebrae and 21 or 22 caudal vertebrae (Fig. 4A). Ribs 11 or 12 associated with vertebrae 3–13/14. Epicentrals 14 or 15, associated with vertebrae 3–16/17.

Adhesive disc small (15–18% of SL), double (Fig. 9A); outer margin of disc smooth. Outline of anterior margin of disc slightly irregular, concave at midline. Posterior margin of smaller inner disc bordered by narrow flap of dense skin which has rolled inward in majority of specimens, concealing outer papillae of disc region B. Disc region A without papillae at centre; inner margin with single row of elongate papillae, transitioning to smaller papillae with circular or cuboid margins posterolaterally over ventral surface of pectoral-fin rays. Apapillate region of disc region A equal in width

or slightly narrower than width of smaller inner disc. Disc region B with 2 transverse rows of papillae, comprised largely of elongate papillae with few smaller papillae with circular or cuboid margins scattered between elongate papillae. Disc region C covered in a thick pad of skin; apapillate. Disc region D with an irregular U-shaped papilla (Fig. 9A) or 2–3 circular to cuboid papillae at centre (Fig. 1A). Smaller inner disc connected to larger outer disc anteriorly via a narrow frenum of thick skin along ventral midline. Skin of frenum confluent with posterior margin of disc region D; lateral margins of frenum smooth to weakly crenate (Fig. 9A). Dorsal postcleithrum a poorly ossified sheet of bone with ~20 long, poorly ossified fimbriae along posterior margin (Fig. 9C). Medial edge of dorsal postcleithrum with a short peg-like strut of bone, directed towards ventral midline. Ventral postcleithrum well ossified, irregular in shape; approximately half size of dorsal postcleithrum (Fig. 9C). Posterior margin of ventral postcleithrum smooth, without fimbriae. Anteromedial edge of ventral postcleithrum with a concave facet that articulates with a dense pad of connective tissue located at posterior tip of basipterygium (Fig. 9C). Skin associated with last pelvic-fin ray attaching to base of pectoral fin opposite 4th–5th lowermost pectoral-fin rays. Skin over base of ventral pectoral-fin rays and lower half of shoulder girdle swollen and creating an obvious skin pad; epidermis of pad with a dense aggregation of club cells, giving skin pad a whitish appearance in preserved specimens (Fig. 8A). Pectoral radials with well-developed bony struts along ventral (pectoral radial 1), dorsal (pectoral radial 4), or both ventral and dorsal margins (pectoral radials 2 and 3) that interdigitate with struts borne on element(s) directly above and/or below (Fig. 8B, C).

Colouration. In alcohol, head and body background colour uniformly pale cream to yellow (Fig. 2A). In life, head and body background colour golden-yellow to olive-brown (Fig. 3A–C). Dorsal midline with variable number (10–14) of irregularly shaped light to dark brown markings; markings largest dorsal to centre of body, becoming smaller anterior or posterior to this point. Body side with a series of light to dark brown elongate markings forming an incomplete or complete horizontal stripe. Horizontal light to dark brown stripe along side of body continuing on side of head, through lower half of eye, to snout. Dorsal margin of light to dark brown stripe on head bordered by a lighter stripe, ranging from light yellow to white. Lighter stripe more pronounced in males. Iris red to orange. Fins uniform in colour without markings; colour matching body background colour.

Sexual dimorphism. External sexual dimorphism largely restricted to urogenital papilla. Urogenital papilla of male with a blunt tip, located within a deep groove posterior to the anus and flanked anterolaterally by a pair of swollen skin folds, termed here accessory folds. Each accessory fold is roughly triangular in shape and appears to be confluent anteromedially with the heavily plicate skin surrounding the anus (Fig. 11A, B). Urogenital papilla of female with a needle-like tip, located along the dorsal surface of a robust tube-like structure which also bears the anus (Fig. 11C, D). This entire structure is accommodated within a deep pocket anterior to the anal-fin origin. In several specimens, the posteriormost tip of this structure is located within the pocket, suggesting some degree of mobility.

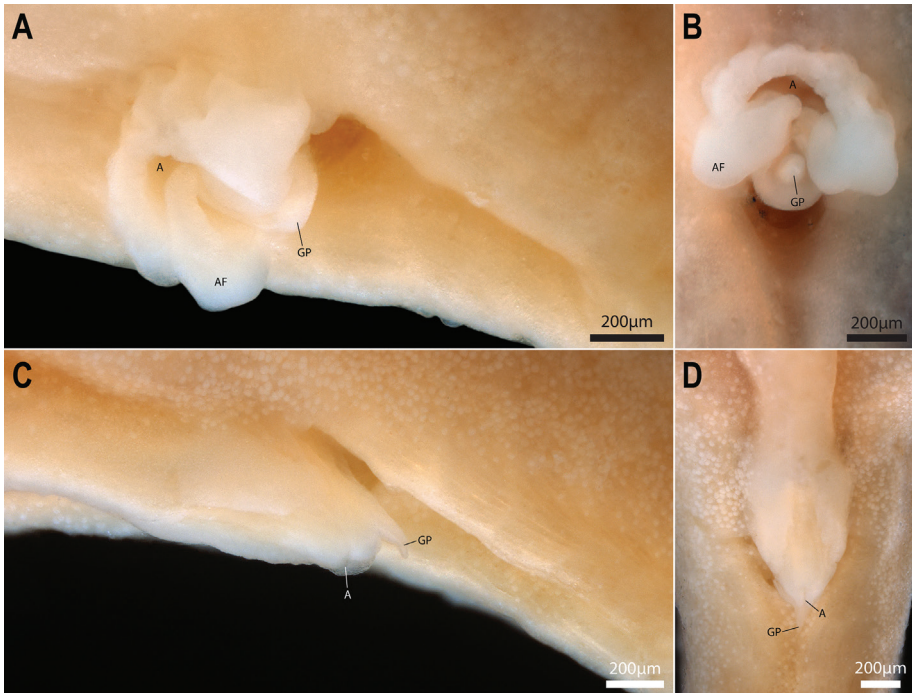


Figure 11. Genital papilla of *Barryichthys hutchinsi* **A** WAM P.28981-004, holotype, male, 15.4 mm SL, oblique lateral view **B** same specimen as in A, ventral view, anterior to top of page **C** WAM P.28981-003, paratype, female, 16.9 mm SL, oblique lateral view **D** same specimen as in D, ventral view, anterior to top of page. Abbreviations: A, anus; AF, accessory folds; GP, genital papilla.

Eggs. A female of 14.2 mm SL from WAM P.34510-001 contained ca. 20 mature eggs (ca. 10 within each ovary) of ca. 0.3–0.6 mm diameter. The largest eggs in each ovary exhibited a dark orange cap that may represent an “attachment apparatus” at the animal pole as described from the eggs of three species of European gobiesocid by Breining and Britz (2000).

Distribution. Known presently only from two close sites in Western Australia (Cottesloe Reef and Trigg Reef platforms, Perth) and two sites in South Australia (Vivonne Bay and Victor Harbor) (Fig. 12). At the type locality (Cottesloe Reef platform), *B. hutchinsi* was collected from dense mats of macroalgae attached to rocky substrate in water up to 1 meter depth.

Etymology. Named for Barry Hutchins, who discovered the new species. A noun in the genitive.

Remarks. Hutchins (2008: 725) illustrated a specimen of *Barryichthys hutchinsi* from Western Australia, likely from the type locality at Cottesloe Reef platform (Perth). Specimens from South Australia (AMS I.20171-012, AMS I.49000-001) exhibit vertebral counts within the range of *B. hutchinsi* and are referred to this species. These specimens have been excluded from the type series but data obtained from these specimens has contributed to the description above.

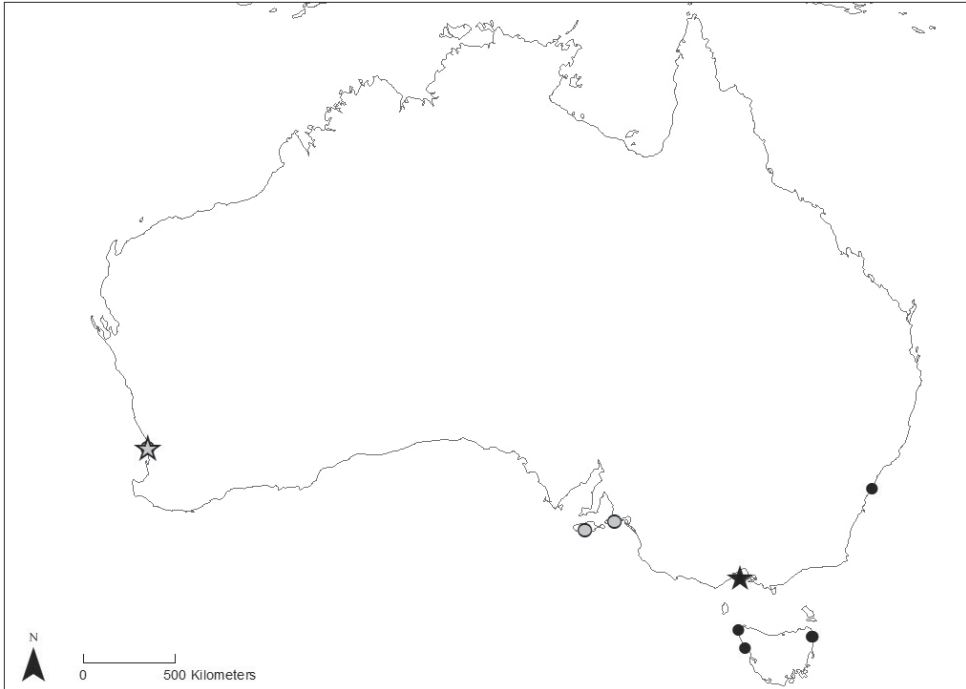


Figure 12. Distribution of material of *Barryichthys hutchinsi* (grey symbols) and *B. algicola* (black symbols) used in this study. Stars indicate type localities.

***Barryichthys algicola* sp. nov.**

<http://zoobank.org/ACAC214A-2D61-40B4-82E3-DBB5C55474A2>

Figures 2B, 3D, E, 4B, 5B, 6B

Common name: Green rat clingfish

Genus B sp., Hutchins 1994a: 310

Holotype. WAM P.27127-016, female, 16.8 mm SL; Victoria, Jubilee Point, Sorrento (38°20'00"S, 144°45'00"E), 3 March 1981, J.B. Hutchins, CT scan <https://doi.org/10.17602/M2/M78489>.

Paratypes. *New South Wales:* AMS I.137167-002, 1, 14.2 mm SL; Cape Banks, Botany Bay (34°00'00.0"S, 151°15'00.0"E), 01 March 1992–06 July 1993, N Gallahar. *Victoria:* WAM P.27127-001, 2, 16.0–21.0 mm SL; Same as holotype. *Tasmania:* AMS I.17555-002, 3, 15.5–15.7 mm SL; The Gardens, north of Binalong Bay (41°14'21.3"S, 148°17'35.8"E), D. Hoese & W. Ivanstoff. – AMS I.17576-012, 1, 19.0 mm SL; The Gardens, north of Binalong Bay (41°14'21.3"S, 148°17'35.8"E), D. Hoese & W. Ivanstoff. – AMS I.46787-001, 1, 15.6 mm SL; Coles Bay (42°07'28.0"S, 148°16'54.0"E), H. Lloyd. – WAM P.27572-004, 2, 10.0–13.0 mm SL; West Point, Marrawah (40°55'00"S, 144°42'00"E), 13 March 1982, J.B. Hutchins. – WAM P.27576-003, 1, 14.0 mm SL; north side of Granville Harbour (41°49'00"S, 145°01'00"E), 18 March

1982, J.B. Hutchins. – WAM P.27559-007, 10 (2C&S), 9.0–12.0 mm SL; St. Helens Point (41°16'00"S, 148°22'00"E), 25 February 1982, J.B. Hutchins.

Diagnosis. *Barryichthys algicola* is distinguished from *B. hutchinsi* by a longer, narrower body (body depth at dorsal-fin origin 7–8% SL vs. 10–11% SL), a more slender head (head width at widest point 55–61% HL vs. 66–75%; depth at orbit 27–29% HL vs. 30–32%; interorbital width 20–24% vs. 27–33% HL), the entire ventral margin of the orbit visible in ventral view (vs. ventral margin of orbit obscured by cheek in ventral view), by having a longer abdominal region with more vertebrae (abdominal vertebrae 21 vs. 17) and more ribs (15 vs. 11–12), a higher number of epicentrals (18–19 vs. 14–15), and a higher total number of vertebrae (42–44 vs. 38–39), and by features of live colour pattern, including body background colour green (vs. golden-yellow to olive-brown) without darker markings along dorsal midline or body side (vs. dorsal midline and lateral body side with darker markings).

Description. General body shape as in Figs. 2B, 3D–E. Select morphometric and meristic characters are listed in Tables 1, 2. As described for *B. hutchinsi* except for the following differences. Largest specimen examined 21.0 mm SL. Head narrow; widest point of head only slightly wider than widest part of body. Entire ventral margin of orbit visible in ventral view (Fig. 5B). Dorsal-fin rays 5 or 6. Anal-fin rays 6. Pectoral-fin rays 17. First dorsal-fin pterygiophore inserted between neural spines of vertebrae 23/24. First anal-fin pterygiophore inserted between hemal spines of vertebrae 20/21 or 22/23. Total number of vertebrae 42, 43(*) or 44, consisting of 21 abdominal vertebrae and 21, 22(*) or 23 caudal vertebrae (Fig. 4B). Ribs 15, associated with vertebrae 3–17. Epicentrals 18 or 19, associated with vertebrae 3–20/21.

Sexual Dimorphism. As described for *B. hutchinsi*.

Eggs. A female of 17.2 mm SL from WAM P.27127-001 contained multiple mature eggs (number not counted) in the right ovary. A single excised egg (ca. 0.6 mm in diameter) exhibited a dark orange cap that may represent an “attachment apparatus” at the animal pole as described from the eggs of three species of European gobiesocid by Breining and Britz (2000).

Colouration. In alcohol, head and body background colour pale cream (Fig. 2B). In life, head and body uniformly green (Fig. 3D, E). A lighter green stripe on side of head, extending from tip of snout to upper part of gill opening, passing through eye. Iris orange. Pectoral fin light green. Dorsal- and anal-fin rays green; fin membranes hyaline. Caudal-fin rays green; fin membranes light green.

Distribution. Known presently from multiple sites along the northern and northeastern coast of Tasmania, and two sites along the coast of mainland Australia, including Jubilee Point (Victoria; type locality) and Botany Bay (New South Wales) (Fig. 12). The majority of specimens have been collected from subtidal fields of macroalgae, 0–2 meters depth.

Etymology. Neologism combining the Latin *alga* and *colare*, who inhabits the algae, in reference to the habitat preference of the new species. A noun in apposition.

Remarks. The specimen of “Rat clingfish” illustrated in Hutchins (1994a: 310, fig. 273) represents *Barryichthys algicola*. An elongate gobiesocid larva (AMS I.48745-008) collected along the coast of New South Wales have been tentatively identified as *B. algicola* (T. Miskiewicz, pers. comm.)

Discussion

Specimens of *Barryichthys* have been known since at least the mid-1980s and referred to either as an undescribed genus (Last et al. 1983), as “Genus B” (Hutchins 1994a, 2008), or simply as “rat clingfish” (Hutchins 1991b). Hutchins (2008) considered his Genus B (here *Barryichthys*) to be monotypic, with a single undescribed species exhibiting a disjunct distribution along the southern coast of Australia, including Western Australia to the west and Victoria and Tasmania to the east. Our examination of material in museum collections has resulted in additional material of *Barryichthys* not known to Hutchins (2008) and from additional localities outside of the suspected range of the genus, including those in South Australia (Kangaroo Island and Victor Harbor) and New South Wales (Botany Bay). As we have shown herein, this material comprises two distinct species, with non-overlapping distributions along the southern coast, including the more western distributed *B. hutchinsi*, with specimens known from Western Australia and South Australia, and the more eastern distributed *B. algicola*, with specimens known from New South Wales, Victoria, and Tasmania. This disjunct distribution of *Barryichthys* is another example of numerous geminate species divided by the Bass Strait (see Moore 2012). The most parsimonious explanation for the presence of so many geminate pairs across a wide range of taxa is repeated vicariant isolations by an ephemeral biogeographic barrier in the form of a landbridge between southern Australia and Tasmania during historic glacial cycles (Hutchins 1994b; BurrIDGE 2000; Waters et al. 2004; Moore and Chaplin 2014). Species endemic to the west of the Bass Strait may have distributions restricted to the south-west corner or be widespread across southern Western Australia and South Australia (Hutchins 1994b). Based on this and our morphological evidence, we believe the South Australian specimens included here do represent *B. hutchinsi*, but further work on specimens from this region may be warranted.

The two species of *Barryichthys* are similar in overall appearance but differ in aspects of head shape, number of vertebrae and aspects of live colouration. The most obvious external difference between *B. hutchinsi* and *B. algicola* relates to the eye, the entire ventral margin of which is visible in ventral view in *B. algicola* (Fig. 5B) but not in *B. hutchinsi*, in which only the lateralmost part of the eye is visible in ventral view with the ventral eye margin obscured by the cheek (Fig. 5A). *Barryichthys hutchinsi* exhibits fewer vertebrae than *B. algicola* (38–39 vs. 42–44; Table 2) and these differences appear to be related to differences in the length of the abdominal region of the vertebral column, which is comprised of fewer vertebrae in *B. hutchinsi* (17) than in *B. algicola* (21). *Barryichthys hutchinsi* also exhibits fewer epicentrals than *B. algicola* (14–15 vs. 18–19) and there are also fewer ribs surrounding the abdominal cavity of *B. hutchinsi* compared to that of *B. algicola* (11–12 vs. 15). In contrast, the number of caudal vertebrae is similar in both species (21–22 in *B. hutchinsi* vs. 21–23 in *B. algicola*). In life, *B. hutchinsi* exhibits an overall golden-yellow to olive-brown body background colour combined with a variable number of irregular shaped light to dark brown markings along the dorsal and lateral body surface whereas the body background colour of *B. algicola* is uniform green in life and without obvious markings. Photographs of live or freshly dead specimens of *B. hutchinsi* from the type locality in Western Australia reveal the

presence of an obvious light yellow to white stripe along the side of the head that is not obvious in photographs of live or freshly dead specimens of *B. algicola*. This stripe may represent an additional diagnostic character between the two species but more observations are needed to confirm this, including information on live colouration of individuals of *B. hutchinsi* from South Australia.

Comparisons with other genera

Hutchins (1994a, 2008) noted that specimens of *Barryichthys* (referred to as Genus B) are often found with members of *Parvicrepis* and several of the specimens of *Barryichthys* that we examined as part of this study were originally identified as *Parvicrepis parvipinnis* (Waite, 1906) or *Parvicrepis* sp. As previously pointed out by Hutchins (1994a, 2008), the two genera can be distinguished by features of the adhesive disc (see Fig. 1), including margin of disc region B smooth in *Barryichthys* vs. surrounded by small fleshy tabs in *Parvicrepis*, papillae absent from disc region C in *Barryichthys* vs. present in *Parvicrepis*, and disc region D with a patch of 2–3 larger circular-cuboid papillae (Fig. 1A, 9B) or a single, large, irregular-shaped papilla (Fig. 9A) in *Barryichthys* vs. a patch of 7–10 smaller circular-cuboid papillae in *Parvicrepis*. Notably, the adhesive disc in species of *Barryichthys* exhibits two distinct types of papillae (Fig. 1A), including a smaller, more ‘typical’ papilla with a circular-cuboid margin; and a larger, more elongate papilla that is approximately three to four times larger than the former. Both types of papillae exhibit smooth surfaces without obvious grooves and we suspect (though cannot confirm based on available material) that each larger, elongate papilla, develops as a single unit (i.e., the larger papillae are not the result of ontogenetic fusion between multiple smaller papillae). Small papillae with circular-cuboid margins are almost ubiquitous across the disc-bearing gobiesocids (i.e., all genera excluding *Alabes* Cloquet, 1816), with few exceptions (papillae are reported to be absent only in *Gymnoscyphus ascitus* Bohlke & Robins, 1970; Bohlke and Robins 1970, Conway and Prestridge 2011), and likely represent the plesiomorphic condition at the level of the Gobiesocidae. The elongate papillae present in disc regions A and B of *Barryichthys* are unique to this genus among the disc-bearing gobiesocids and interpreted as an apomorphic condition.

In addition to features of the adhesive disc, *Barryichthys* is further distinguished from the superficially similar looking *Parvicrepis* by the presence (vs. absence) of a well-developed fleshy pad at the base of the lower pectoral-fin rays (Fig. 2, 8B), and features of the snout and jaws, including upper lip thicker at centre than at lateral margins in ventral view in *Barryichthys* vs. upper lip of uniform thickness in both dorsal and ventral view in *Parvicrepis*, and upper jaw longer than lower jaw in *Barryichthys* vs. upper and lower jaws equal in length or lower jaw only slight shorter than the upper in *Parvicrepis*.

A suite of absences and reductions also serve to distinguish *Barryichthys* from *Parvicrepis* (and also the majority of other gobiesocids), including: (1) lachrymal lateral line canal absent in *Barryichthys* vs. lachrymal lateral line canal present with two openings in *Parvicrepis* (canal absent or present with 2 or 3 openings in other gobiesocids); (2) anterior half of parasphenoid reduced to a thin strut of bone in *Barryichthys* vs. anterior

half of parasphenoid broad in *Parvicrepis* (and the majority of other gobiesocids); (3) lower pharyngeal jaw teeth absent in *Barryichthys* vs. lower pharyngeal jaw teeth present, comprising a single row of 4–5 teeth on ceratobranchial 5 in *Parvicrepis* (present or absent in other gobiesocids); (4) hypobranchial and basibranchial elements (including cartilages) absent in *Barryichthys* vs. hypobranchial elements 1–3 and basibranchial cartilages 3–4 present in *Parvicrepis* (elements highly variable across Gobiesocidae; see below); and (5) uppermost 10–12 pectoral-fin rays each comprising a pair of poorly ossified and unsegmented hemitrichia in *Barryichthys* vs. hemitrichia of uppermost pectoral-fin rays comprising multiple segments in *Parvicrepis* (and other gobiesocids). The first three of these aforementioned reductions are not unique to *Barryichthys* amongst gobiesocids. For example, lachrymal sensory pores (and potentially also the lachrymal lateral line canal) are absent in *Lepadichthys akiko* Allen and Erdmann, 2012 (Fujiwara and Motomura 2018), the anterior part of the parasphenoid is reduced to a thin strut of bone in *Alabes* (Springer and Fraser 1976: Fig. 1c) and *Diademichthys* Pfaff, 1942 (Hayashi et al. 1986), and lower pharyngeal jaw teeth are absent in *Discotrema* Briggs, 1976 and *Lepadichthys lineatus* Briggs, 1966 (Conway pers. obs.). There is considerable variation in the composition of the ventral gill arch elements across the Gobiesocidae, particularly the basibranchial and hypobranchial elements (Springer and Fraser 1976). The two anteriormost basibranchial cartilages are invariably absent in all members of the Gobiesocidae (Springer and Fraser 1976) and the two posterior elements (referred to as basibranchial 3 and 4 cartilages by Springer and Fraser 1976) are variably absent (e.g., only one [typically the third] may be absent or rarely both). The most common condition of the hypobranchial elements in gobiesocids is for all three to be present and ossified (e.g., see Springer and Fraser 1976: Fig. 4b) although other conditions exist, including one in which all three hypobranchial cartilages are present but only the first is ossified as hypobranchial 1 (e.g., see Conway et al. 2018: Fig. 8C) and another in which the first element is absent and the second and third elements are present and ossified as hypobranchials 2 and 3, respectively (as in *Alabes*; see Springer and Fraser 1976: Fig. 8a). The combined absence of hypobranchial and basibranchial elements in *Barryichthys* is, as far as we are aware, unique amongst gobiesocids and is reminiscent of the extreme condition found in some members of the Anguilliforms in which all hypobranchial and basibranchial elements are absent (e.g., *Gymnothorax* Bloch, 1795 or *Cyema* Günther, 1878; Nelson 1966). The poorly ossified uppermost 10–12 pectoral-fin rays that are each comprised of a pair of unsegmented hemitrichia is another unique character of *Barryichthys* amongst gobiesocid fishes in which the hemitrichia of the pectoral-fin rays are invariably segmented in the adult stage, as is the case in most teleosts (Lundberg and Marsh 1976; Marsh 1977; Grandel and Schulte-Merker 1998).

Despite the long list of differences between *Barryichthys* and *Parvicrepis*, the two genera share a number of characteristics, including: (1) the absence of the preoperculo-mandibular lateral line canal; (2) the absence of the otic lateral line canal (=postorbital canal of Shioyaki and Dotsu 1983), with only a single sensory canal pore (PO1) posterior to orbit; (3) the absence of papillae from the centre of disc region A; (4) 4+4 principal caudal-fin rays; (5) lower 5–6 pectoral-fin rays notably shorter than upper rays, with segments foreshortened; (6) first gill arch with a few (4–5) gill filaments arranged

as a hemibranch; (7) absence of filaments on the 4th gill arch; (8) a double adhesive disc; and (9) gill membranes united and free from isthmus. The question of whether this long list of shared characters between *Barryichthys* and *Parvicrepis* is the result of shared common ancestry or the result of convergence is a difficult one to answer and must await the outcome of phylogenetic analysis (which is beyond the scope of this paper). The majority of the characters listed above are reductive in nature and may not be useful for grouping small-bodied taxa because the shared absences may be linked to independent cases of reduction (e.g., see Britz et al. 2014). The fact that many of these reductive characters are common to many small-bodied gobioid fishes (especially reductions in the cephalic lateral line canal system; Shiogaki and Dotsu 1983) lends some weight to this argument.

Miniaturisation

Miniaturisation, the evolution of tiny adult body size, is a common phenomenon in animal taxa, especially in non-amniote vertebrates (Hanken and Wake 1993), with many notable examples from teleost fishes (e.g., Winterbottom and Emery 1981; Springer 1983; Iwata et al. 2001; Watson and Walker 2004; Kottelat et al. 2006; Britz et al. 2009). In their review of miniaturisation, Hanken and Wake (1993) noted that it is common for miniature taxa to exhibit higher numbers of morphological reductions and greater levels of morphological variability (e.g., asymmetry) in comparison to larger-bodied close relatives. They also noted that miniature taxa typically exhibited morphological novelties compared to larger-bodied close relatives and considered the evolution of morphological novelty a common consequence of the miniaturisation process (Hanken and Wake 1993). In ichthyological circles, miniature taxa are typically identified as those that mature at ≤ 20 mm SL or, when information on size at maturity is not available, are not known to exceed a maximum SL of 26 mm (following Weitzman and Vari 1988). Using these criteria, ichthyologists have identified several hundred species of miniature freshwater fishes, mostly from temperate and tropical regions (e.g., Weitzman and Vari 1988; Kottelat and Vidthayanon 1993; Conway and Moritz 2006; Bennett and Conway 2010; Toledo-Piza et al. 2014). We expect that similar numbers of marine fishes would also be identified as miniature using these criteria, if or when they are applied in the same way to the marine ichthyofauna.

Rüber et al. (2007) and Britz and Conway (2009) identified two distinct types of miniature taxa amongst cyprinid fishes, comprising: (1) proportioned dwarfs, representing scaled down replicas of closer relatives, with few reductions and few or no morphological novelties compared to their close relatives; and (2) developmentally truncated (= progenetic) miniatures, resembling earlier developmental stages of closer relatives, with high numbers of reductions and many morphological novelties. Based on these earlier observations, Britz and Conway (2016) concluded that the evolution of morphological novelty in miniature cyprinid fishes may be tied to extreme developmental truncation, which may work to release developmentally truncated taxa from

the evolutionary constraints imposed on larger bodied close relatives and facilitate the evolution of novel structures. Though there is compelling evidence from miniature cyprinid fishes to support this hypothesis (e.g., Britz and Conway 2009; Britz et al. 2009; Conway et al. 2017c), as of yet there are few examples of progenetic miniatures from other groups of fishes.

With maximum recorded sizes of 18.7 mm SL (*B. hutchinsi*) and 21.0 mm SL (*B. algicola*), the two species of *Barryichthys* are clearly miniature species (sensu Weitzman and Vari 1988) and some of the smallest gobiesocids described to date. Female individuals of *B. hutchinsi* and *B. algicola* as small as 14.2 mm SL and 17.2 mm SL, respectively, contain eggs demonstrating that they are mature and capable of reproduction at these small sizes. The high number of reductive characters exhibited by the two species of *Barryichthys*, including the absence of much of the cephalic sensory system and the lower gill-arch skeleton, are exceptional among the disc-bearing gobiesocids and may be attributed to targeted developmental truncation, at least within these character complexes. In stark contrast to these reductions, the adhesive disc of *Barryichthys* exhibits unusual, elongate papillae that are unique to this taxon amongst the disc bearing gobiesocids and may offer another, though less striking, example of the link between miniaturisation and morphological novelty from the world of fishes and the first from the Gobiesocidae.

Comparative material

Parvicrepis parvipinnis – *New South Wales*. AMS I.16233-009, 2, Dee Why, Long Reef, 12 January 1972. – AMS I.166467-012, 1, 16.0 mm SL; Minnie Waters, 14 February 1965. – AMS I.16915-002, 1, 13.4 mm SL; Clovelly Pool, 30 March 1967. – AMS I.34582-001, 16, 8.0–25.4 mm SL; Nadgee, north side of Black Head, 08 June 1970. – AMS I.44125-041, 2, 19.7 mm SL; Broken Bay, North side of Lion Island, 09 May 2007. – AMS I.43799-001, 1, 18.4 mm SL; Bellambi, 14 February 2006. – AMS I.45027-038, 1, 8.5 mm SL; Mollymock, Jones Beach. – AMS I.45630-057, 8, 11.5–18.5 mm SL; Bendalong, north of boat ramp, 14 March 2011. – AMS I.45631-032, 1, 17.0 mm SL; Monument Beach, 15 March 2011. – AMS I.45935-001, 1, 12.1 mm SL; north of Tathra, south of Baronda Head, 05 April 2008. – AMS I.45633-077, 9, 10.0–15.4 mm SL; Washerwomans Beach, 16 March 2011. – AMS I.46788-001, 1, 17.0 mm SL; Ulladulla, 2012. – AMS I.46923-001, 1, 12.0 mm SL; Burrill Rocks, south of Ulladulla, 15 May 2013. – TCWC 17169.01, 40 (4 C&S, 1 CT [<https://doi.org/10.17602/M2/M30713>]), 14.0–23.0 mm SL; Forresters Beach, 22 February 2015. *South Australia*. AMS I.20175-008, 1, 17.2 mm SL; Kangaroo Island, Admirals Arch, 07 March 1978. *Tasmania*. AMS I.17555-003, 4 (3 male, 1 female), 12.0–19.4 mm SL; The Gardens, 6 December 1972. – AMS I.46787-002, 2, 17.0–18.0 mm SL; Coles Bay, 2012. *Victoria*. AMS I.16981-001, 16, 10.3–22.6 mm SL; Bell's Beach AMS I.16984-004, 2, 12.7–12.8 mm SL; Anglesea, 19 March 1972. – AMS I.16988-001, 2, 20.6–22.5 mm SL; Children's Cove, 22 March 1972.

Acknowledgements

We would like to thank A. Hay, S. Reader, M. McGrouther (AMS), H. Prestridge (TCWC), and M. Allen (WAM) for providing access to material under their care, G. Short for arranging access to specimens from South Australia, A. Pinion for making the map used in Figure 12, R. Britz, A. Pinion, K. Kubicek, and G. Short for proof reading an earlier version of the manuscript, and R. Britz, T. Miskiewicz, G.D. Johnson, T. Gill, and M. Kottelat for helpful discussions and suggestions. Finally, we thank B. Hutchins for sharing unpublished data and his knowledge of Australian endemic gobiesocids. This research was supported by funding from NSF (IOS 1256793, DBI 1702442 to KWC; IOS 1256602, DBI 1701665 to APS) and Texas A&M Agrilife Research (TEX09452 to KWC). Much of this work was completed while KWC held an Australian Museum Foundation/AMRI Visiting Collections Fellowship based at the Australian Museum and hosted by A. Hay. This is publication number 1603 of the Biodiversity and Research Collections of Texas A&M University.

References

- Allen GR, Erdmann MV (2012) Reef Fishes of the East Indies. Vols. I–III. Tropical Reef Research, Perth, 1292 pp.
- Allen JC, Griffiths CL (1981) The fauna and flora of a kelp bed canopy. *African Zoology* 16: 80–84. <https://doi.org/10.1080/02541858.1981.11447737>
- Bennett MG, Conway KW (2010) An overview of North America's diminutive freshwater fish fauna. *Ichthyological Exploration of Freshwaters* 21: 63–72. https://pfeil-verlag.de/wp-content/uploads/2015/05/ief21_1_05.pdf
- Bloch ME (1795) *Naturgeschichte der ausländischen Fische* 9. Merinoand Co., Berlin, 192 pp. [pl. 397–429]
- Böhlke JE, Robins CR (1970) A new genus and species of deep-dwelling clingfish from the Lesser Antilles. *Notulae Naturae* 434: 1–12.
- Brandl SJ, Goatley CH, Bellwood DR, Tornabene L (2018) The hidden half: ecology and evolution of cryptobenthic fishes on coral reefs. *Biological Reviews* 93: 1846–1873. <https://doi.org/10.1111/brv.12423>
- Breining T, Britz R (2000) Egg surface structure of three clingfish species, using scanning electron microscopy. *Journal of Fish Biology* 56: 1129–1137. <https://doi.org/10.1111/j.1095-8649.2000.tb02128.x>
- Briggs JC (1955) A monograph of the clingfishes (Order Xenopterygii). *Stanford Ichthyological Bulletin*, 6: 1–224.
- Briggs JC (1966) A new clingfish of the genus *Lepadichthys* from the Red Sea. (Contribution to the knowledge of the Red Sea, no. 35). *Bulletin, Ministry of Agriculture, Department of Fisheries, Sea Fisheries Research Station Haifa* 42: 37–40.
- Briggs JC (1976) A new genus and species of clingfish from the western Pacific. *Copeia* 1976: 339–341. <https://doi.org/10.2307/1443956>

- Briggs JC (1993) New genus and species of clingfish (Gobiesocidae) from southern Australia. *Copeia* 1993: 196–199. <https://doi.org/10.2307/1446310>
- Briggs JC, Miller RR (1960) Two new freshwater clingfishes of the genus *Gobiesox* from southern Mexico. *Occasional Papers of the Museum of Zoology University of Michigan* 616: 1–15. <http://hdl.handle.net/2027.42/57053>
- Britz R, Conway KW (2009) Osteology of *Paedocypris*, a miniature and highly developmentally truncated fish (Teleostei: Ostariophysi: Cyprinidae). *Journal of Morphology* 270: 389–412. <https://doi.org/10.1002/jmor.10698>
- Britz R, Conway KW (2016) *Danionella dracula*, an escape from the cypriniform Bau-plan via developmental truncation? *Journal of Morphology* 277: 147–166. <https://doi.org/10.1002/jmor.20486>
- Britz R, Conway KW, Rüber L (2009) Spectacular morphological novelty in a miniature cyprinid fish, *Danionella dracula* n. sp. *Proceedings of the Royal Society B* 276: 2179–2186. <https://doi.org/10.1098/rspb.2009.0141>
- Britz R, Conway KW, Rüber L (2014) Miniatures, morphology and molecules: *Paedocypris* and its phylogenetic position (Teleostei, Cypriniformes). *Zoological Journal of the Linnean Society* 172: 556–615. <https://doi.org/10.1111/zoj.12184>
- Burridge CP (2000) Biogeographic history of geminate cirrhitoids (Perciformes: Cirrhitidae) with east-west allopatric distributions across southern Australia, based on molecular data. *Global Ecology and Biogeography* 9: 517–525. <https://doi.org/10.1046/j.1365-2699.2000.00204.x>
- Cloquet H (1816) *Alabes*. Pages 99–100 in supplement of volume 1 of *Dictionnaire des Sciences Naturelles*.
- Conway KW, Baldwin CC, White MD (2014) Cryptic diversity and venom glands in the western Atlantic clingfishes of the genus *Acyrtus* (Teleostei: Gobiesocidae). *PLoS ONE* 9: e97664. <https://doi.org/10.1371/journal.pone.0097664>
- Conway KW, Kim DM, Rüber L, Espinosa-Perez H, Hastings PA (2017a) Molecular phylogenetics of the New World clingfish genus *Gobiesox* (Teleostei: Gobiesocidae) and the origin of a freshwater clade. *Molecular Phylogenetics and Evolution* 112: 138–147. <https://doi.org/10.1016/j.ympev.2017.04.024>
- Conway KW, Kubicek KM, Britz R (2017c) Morphological novelty and modest developmental truncation in *Barbooides*, Africa's smallest vertebrates (Teleostei: Cyprinidae). *Journal of Morphology* 278: 750–767. <https://doi.org/10.1002/jmor.20670>
- Conway KW, Moritz T (2006) *Barbooides britzi*, a new species of miniature cyprinid from Benin (Ostariophysi: Cyprinidae), with neotype designation for *B. gracilis*. *Ichthyological Exploration of Freshwaters* 17: 73–84. https://pfeil-verlag.de/wp-content/uploads/2015/05/ief17_1_07.pdf
- Conway KW, Prestridge H (2011) Multiple new records of *Gymnoscyphus ascitus* Böhlke and Robins, 1970 (Perciformes: Gobiesocidae) from the western Central Atlantic. *Check List* 7: 581–582. <https://doi.org/10.15560/7.5.581>
- Conway KW, Stewart AL, King CD (2017b) A new species of the clingfish genus *Trachelochismus* (Teleostei: Gobiesocidae) from bays and estuaries of New Zealand. *Zootaxa* 4319: 531–549. <https://doi.org/10.11646/zootaxa.4319.3.6>

- Conway KW, Stewart AL, Summers AP (2018) A new genus and species of clingfish from the Rangitāhua Kermadec Islands of New Zealand (Teleostei, Gobiesocidae). *ZooKeys* 786: 75–104. <https://doi.org/10.3897/zookeys.786.28539>
- Ditsche P, Wainwright DK, Summers AP (2014). Attachment to challenging substrates—fouling, roughness and limits of adhesion in the northern clingfish (*Gobiesox maeandricus*). *Journal of Experimental Biology* 217: 2548–2554. <https://doi.org/10.1242/jeb.100149>
- Fujiwara K, Motomura H (2018) Revised diagnosis and first Northern Hemisphere records of the rare clingfish *Lepadichthys akiko* (Gobiesocidae: Diademichthyinae). *Species Diversity* 23: 87–93. <https://doi.org/10.12782/specdiv.23.87>
- Gemballa S, Britz R (1998) Homology of intermuscular bones in acanthomorph fishes. *American Museum Novitates* 3241: 1–25. <http://hdl.handle.net/2246/3238>
- Gonçalves EJ, Beldade R, Henriques M (2005) *Opeatogenys gracilis* (Pisces: Gobiesocidae): an overlooked species or another ‘Mediterranean endemism’ found in Atlantic waters? *Journal of Fish Biology* 67: 481–489. <https://doi.org/10.1111/j.0022-1112.2005.00739.x>
- Gould WR (1965) The biology and morphology of *Acyrtops beryllinus*, the emerald clingfish. *Bulletin of Marine Science* 15: 165–188. <https://www.ingentaconnect.com/contentone/umrsmas/bullmar/1965/00000015/00000001/art00004>
- Grandel H, Schulte-Merker S (1998) The development of the paired fins in the zebrafish (*Danio rerio*). *Mechanisms of Development* 79: 99–120. [https://doi.org/10.1016/S0925-4773\(98\)00176-2](https://doi.org/10.1016/S0925-4773(98)00176-2)
- Guitel F (1888) Recherches sur les *Lepadogaster*. *Archives de Zoologie Expérimentale et Générale* 2: 423–480. <https://doi.org/10.5962/bhl.title.13650>
- Günther A (1861) Catalogue of the acanthopterygian fishes in the collection of the British Museum. Gobiidae, Discoboli, Pediculati, Blenniidae, Labyrinthici, Mugilidae, Notacanthi. *Catalogue of the fishes in the British Museum, London* 3: 1–586.
- Günther A (1878) Preliminary notices of deep-sea fishes collected during the voyage of H. M. S. Challenger. *Annals and Magazine of Natural History (Series 5)* 2: 17–28, 179–187, 248–251. <https://doi.org/10.1080/00222937808682417>
- Hanken J, Wake DB (1993) Miniaturization of body size: organismal consequences and evolutionary significance. *Annual Review of Ecology and Systematics* 24: 501–519. <https://doi.org/10.1146/annurev.es.24.110193.002441>
- Hastings PA, Conway, KW (2017) *Gobiesox lanceolatus*, a new species of clingfish (Teleostei: Gobiesocidae) from the Los Frailes submarine canyon, Gulf of California, Mexico. *Zootaxa* 4221: 393–400. <https://doi.org/10.11646/zootaxa.4221.3.8>
- Hayashi M, Hagiwara K, Hayashi H (1986) Osteology of the cling fishes in Japan (Family: Gobiesocidae). *Science Report of the Yokosuka City Museum* 34: 39–66.
- Hofrichter R, Patzner RA (2000) Habitat and microhabitat of Mediterranean clingfishes (Teleostei: Gobiesociformes: Gobiesocidae). *Marine Ecology* 21: 41–53. <https://doi.org/10.1046/j.1439-0485.2000.00689.x>
- Hutchins JB (1983) Redescription of the clingfish *Cochleocephalus spatula* (Gobiesocidae) from Western Australia and South Australia, with the description of a new species from Victoria and Tasmania. *Records of the Western Australian Museum* 11: 33–47. <http://museum.wa.gov.au/research/records-supplements/records/redescription-clingfish-cochleocephalus-spatula-gobiesocidae-wester>

- Hutchins JB (1991a) Descriptions of three new species of gobioid fishes from southern Australia, with a key to the species of *Cochleoceps*. Records of the Western Australian Museum 15: 655–672. <http://museum.wa.gov.au/research/records-supplements/records/description-three-new-species-gobiesocid-fishes-southern-austra>
- Hutchins JB (1991b) Southern Australia's enigmatic clingfishes. Australian Natural History 23: 626–633.
- Hutchins JB (1994a) Gobioidae. In: Goman MF, Glover JCM, Kuitert RH (Eds) The Fishes of Australia's South Coast. The Flora and Fauna of South Australia Handbook Committee, Adelaide, 992 pp.
- Hutchins JB (1994b) A survey of the nearshore reef fish fauna of Western Australia's west and south coasts – the Leeuwin Province. Records of the Western Australian Museum Supplement 46: 1–66. <http://museum.wa.gov.au/research/records-supplements/records/survey-nearshore-reef-fish-fauna-western-australias-west-and-so>
- Hutchins JB (2008) Family Gobioidae Clingfishes, shore-eels. In: Gomon MF, Bray DJ, Kuitert RH (Eds) Fishes of Australia's Southern Coast. New Holland Publishers, Sydney, 722–742.
- Iwata A, Hosoya S, Larson HK (2001) *Paedogobius kimurai*, a new genus and species of goby (Teleostei: Gobioidae: Gobiidae) from the west Pacific. Records of the Australian Museum 53: 103–112. <https://doi.org/10.3853/j.0067-1975.53.2001.1326>
- Jordan DS (1896) Notes on fishes, little known or new to science. Proceedings of the California Academy of Sciences (Series 2) 6: 201–244.
- Kottelat M, Vidhyanon C (1993) *Boraras micros*, a new genus and species of minute freshwater fish from Thailand (Teleostei: Cyprinidae). Ichthyological Exploration of Freshwaters 4: 161–176.
- Kottelat M, Britz R, Tan HH, Witte K-E (2006) *Paedocypris*, a new genus of southeast Asian cyprinid fish with a remarkable sexual dimorphism, comprises the world's smallest vertebrate. Proceedings of the Royal Society of London B 273: 895–899. <https://doi.org/10.1098/rspb.2005.3419>
- Kuitert RH (1993) Coastal fishes of south-eastern Australia. University of Hawaii Press, Honolulu, 437 pp.
- Lamb A, Edgell P (2010) Coastal Fishes of the Pacific Northwest. Harbour Publishing Co., Madeira Park, British Columbia, 335 pp.
- Last PR, Scott EOG, Talbot FH (1983) Fishes of Tasmania. Tasmanian Fisheries Development Authority, Hobart, 563 pp.
- Lundberg JG, Marsh E (1976) Evolution and functional anatomy of the pectoral fin rays in cyprinoid fishes, with emphasis on the suckers (family Catostomidae). American Midland Naturalist 96: 332–349. <https://doi.org/10.2307/2424074>
- Marsh E (1977) Structural modifications of the pectoral fin rays in the order Pleuronectiformes. Copeia 1977: 575–578. <https://doi.org/10.2307/1443282>
- Moore GI (2012) Aspects of the evolutionary history of a pair of fish species (Arripidae: *Arripis*) on either side of a biogeographic barrier in southern Australian seas. Ph.D. Thesis. Centre for Fish and Fisheries Research, School of Biological Sciences and Biotechnology, Murdoch University, Western Australia.

- Moore GI, Chaplin JA (2014) Contrasting demographic histories in a pair of allopatric, sibling species of fish (Arripidae) from environments with contrasting glacial histories. *Marine Biology* 161: 1543–1555. <https://doi.org/10.1007/s00227-014-2439-1>
- Müller J (1843) Beiträge zur Kenntniss der natürlichen Familien der Fische. *Archiv für Naturgeschichte* 9: 292–330.
- Nelson GJ (1966) Gill arches of teleostean fishes of the order Anguilliformes. *Pacific Science* 20: 391–408.
- Paulin C, Roberts CD (1992) The rockpool fishes of New Zealand. *Te ika aaria o Aotearoa*. Museum of New Zealand Te Papa Tongarewa, Wellington, 177 pp.
- Pfaff JR (1942) Papers from Dr. Th. Mortensen's Pacific expedition 1914–16. LXXI. On a new genus and species of the family Gobiesocidae from the Indian Ocean, with observations on sexual dimorphism in the Gobiesocidae, and on the connection of certain gobiesocids with echinids. *Videnskabelige Meddelelser fra Dansk Naturhistorisk Forening, Kjøbenhavn* 105: 413–422.
- Roland W (1978) Feeding behaviour of the kelp clingfish *Rimicola muscarum* residing on the kelp *Macrocystis integrifolia*. *Canadian Journal of Zoology* 56: 711–712. <https://doi.org/10.1139/z78-099>
- Rüber L, Kottelat M, Tan HH, Ng PK, Britz R (2007) Evolution of miniaturization and the phylogenetic position of *Paedocypris*, comprising the world's smallest vertebrate. *BMC evolutionary biology* 7: 38. <https://doi.org/10.1186/1471-2148-7-38>
- Saruwatari T, López JA, Pietsch TW (1997) Cyanine blue: a versatile and harmless stain for specimen observation. *Copeia* 1997: 840–841. <https://doi.org/10.2307/1447302>
- Schultz LP (1951) A nomenclatorial correction for “A revision of the American clingfishes, family Gobiesocidae, with descriptions of new genera and forms”. *Copeia* 1951: 244. <https://doi.org/10.2307/1439108>
- Shiogaki M, Dotsu Y (1983) Two new genera and two new species of clingfishes from Japan, with comments on head sensory canals of the Gobiesocidae. *Japanese Journal of Ichthyology* 30: 111–121. <https://doi.org/10.11369/jji1950.30.111>
- Smith JLB (1943) Interesting new fishes of three genera new to South Africa, with a note on *Mobula diabolus* (Shaw). *Transactions of the Royal Society of South Africa* 30: 67–77. <https://doi.org/10.1080/00359194309519831>
- Springer VG (1983) *Tyson belos*, new genus and species of Western Pacific fish (Gobiidae, Xenisthminae): with discussions of gobioid osteology and classification. *Smithsonian Contributions to Zoology* 390: 1–39. <https://doi.org/10.5479/si.00810282.390>
- Springer VG, Fraser TH (1976) Synonymy of the fish families Cheilobranchidae (Alabetidae) and Gobiesocidae, with descriptions of two new species of *Alabes*. *Smithsonian Contributions to Zoology* 234: 1–23. <https://doi.org/10.5479/si.00810282.234>
- Stewart AL (2015) 218 Family Gobiesocidae. In: Roberts CD, Stewart AL, Struthers CD (Eds) *The Fishes of New Zealand*. Te Papa Press, Wellington, 1539–1555.
- Taylor WR, Van Dyke GG (1985) Revised procedure for staining and clearing small fishes and other vertebrates for bone and cartilage study. *Cybio* 9: 107–119. <http://sfi-cybio.com/en/node/2423>

- Toledo-Piza M, Mattox GMT, Britz R (2014) *Priocharax nanus*, a new miniature characid from the rio Negro, Amazon basin (Ostariophysi: Characiformes), with an updated list of miniature Neotropical freshwater fishes. *Neotropical Ichthyology* 12: 229–246. <https://doi.org/10.1590/1982-0224-20130171>
- Wainwright DK, Kleinteich T, Kleinteich A, Gorb SN, Summers AP (2013) Stick tight: suction adhesion on irregular surfaces in the northern clingfish. *Biology Letters* 9: 20130234. <https://doi.org/10.1098/rsbl.2013.0234>
- Waite ER (1906) Descriptions of and notes on some Australian and Tasmanian fishes. *Records of the Australian Museum* 6: 194–210. <https://doi.org/10.3853/j.0067-1975.6.1906.1000>
- Waters JM, O’Loughlin PM, Roy MS (2004) Cladogenesis in a starfish species complex from southern Australia: evidence for vicariant speciation? *Molecular Phylogenetics and Evolution* 32: 236–245. <https://doi.org/10.1016/j.ympev.2003.11.014>
- Watson W, Walker HJ (2004) The world’s smallest vertebrate, *Schindleria brevipinguis*, a new paedomorphic species in the family Schindleriidae (Perciformes: Gobioidae). *Records of the Australian Museum* 56: 139–142. <https://doi.org/10.3853/j.0067-1975.56.2004.1429>
- Weitzman SH, Vari RP (1988) Miniaturization in South American freshwater fishes; an overview and discussion. *Proceedings of the Biological Society of Washington* 101: 444–465. <https://repository.si.edu/handle/10088/901?show=full>
- Winterbottom R, Emery AR (1981) A new genus and two new species of gobiid fishes (Perciformes) from the Chagos Archipelago, Central Indian Ocean. *Environmental Biology of Fishes* 6: 139–149. <https://doi.org/10.1007/BF00002777>

A new species of *Tipulodina* (Diptera, Tipulidae) from China, with description of the female internal reproductive system

Guo-Xi Xue¹, Qiu-Lei Men², Jia Zhang², Qing Zhao²,
Nan Sheng², Hai-Xiao Wang², Ji-Feng Long³

1 School of Food and Bioengineering, Zhengzhou University of Light Industry, No. 5 Dongfeng Road, Zhengzhou, Henan 450002, China **2** School of Life Sciences, Research Center of Aquatic Organism, Conservation and Water Ecosystem Restoration in Anhui Province, Anqing Normal University, Anqing, Anhui 246011, China **3** Administration of Nonggang National Nature Reserve of Guangxi, Longzhou, Guangxi, 532400, China

Corresponding author: *Qiu-Lei Men* (menqiuLei888@126.com)

Academic editor: *C. Borkent* | Received 5 December 2018 | Accepted 30 June 2019 | Published 16 July 2019

<http://zoobank.org/66AE47A9-94BD-4264-8CD2-068B8FA63D02>

Citation: Xue G-X, Men Q-L, Zhang J, Zhao Q, Sheng N, Wang H-X, Long J-F (2019) A new species of *Tipulodina* (Diptera, Tipulidae) from China, with description of the female internal reproductive system. ZooKeys 864: 67–77. <https://doi.org/10.3897/zookeys.864.31755>

Abstract

A new species of the genus *Tipulodina* Enderlein, 1912, *Tipulodina bifurcata* Xue & Men, **sp. nov.** (Guangxi, South China) is described and illustrated. A key to the known species in China is provided. The morphological description of the female internal reproductive system of the new species is provided, which represents the first description for this genus.

Keywords

Crane flies, key, Nematocera, semen pump, Tipuloidea

Introduction

The genus *Tipulodina* was established by Enderlein (1912) with the type species *Tipulodina magnicornis* Enderlein, 1912 from Indonesia by original designation. It is a relatively large genus with 52 species worldwide, mainly restricted to the Oriental and Palearctic regions (Oosterbroek 2018). Five species of this genus have been reported

to occur in China before this study, four of which are distributed in southern China, and one from a northern part of the country (Oosterbroek 2018). *Tipulodina* can be separated from other tipulid genera by the following combination of characters: slender legs with femora and tibia having white rings (the tibia sometimes possessing two rings); wing transparent with a very short R_s and a dark pattern on apex; R_3 reduced; gonocoxite generally with elongate appendage (Enderlein 1912, Young 1999).

A previously unknown species of *Tipulodina* was noticed while sorting and identifying crane fly specimens collected from Nonggang National Nature Reserve of Guangxi, China. In the present paper, the new species is described and illustrated, which represents the first record of a *Tipulodina* species from Guangxi. A key to separate the known species in China is given.

Materials and methods

The specimens were collected using an insect net. All dissections and the photographs of the male body parts were performed using a SOIF XTZ-E stereo microscope (SOIF, Shanghai, China). The hypopygium of the male and ovipositor of the female were dissected in distilled water with the aid of two very fine needles, scissors and fine-tipped tweezers, and macerated in 10% NaOH for one hour in a 50 °C water bath. The structures were then observed and illustrated in glycerin under the stereo microscope. Body length measurements are from the vertex of head to the tip of the hypopygium. All measurements were made in millimeters (mm) with the aid of a digital caliper. The terminology and methods of description and illustration follow those of Alexander and Byers (1981), Frommer (1963) and de Jong (2017). The type specimens are deposited in the Systematics and Evolution Laboratory, School of Life Sciences, Anqing Normal University, Anhui Province, P. R. China.

The first and corresponding authors were responsible for the taxonomic portion of this paper, and are therefore the authors of the new species. The key was principally constructed from descriptions in the literature without examination of the types or other specimen of most of these species, and should be considered preliminary.

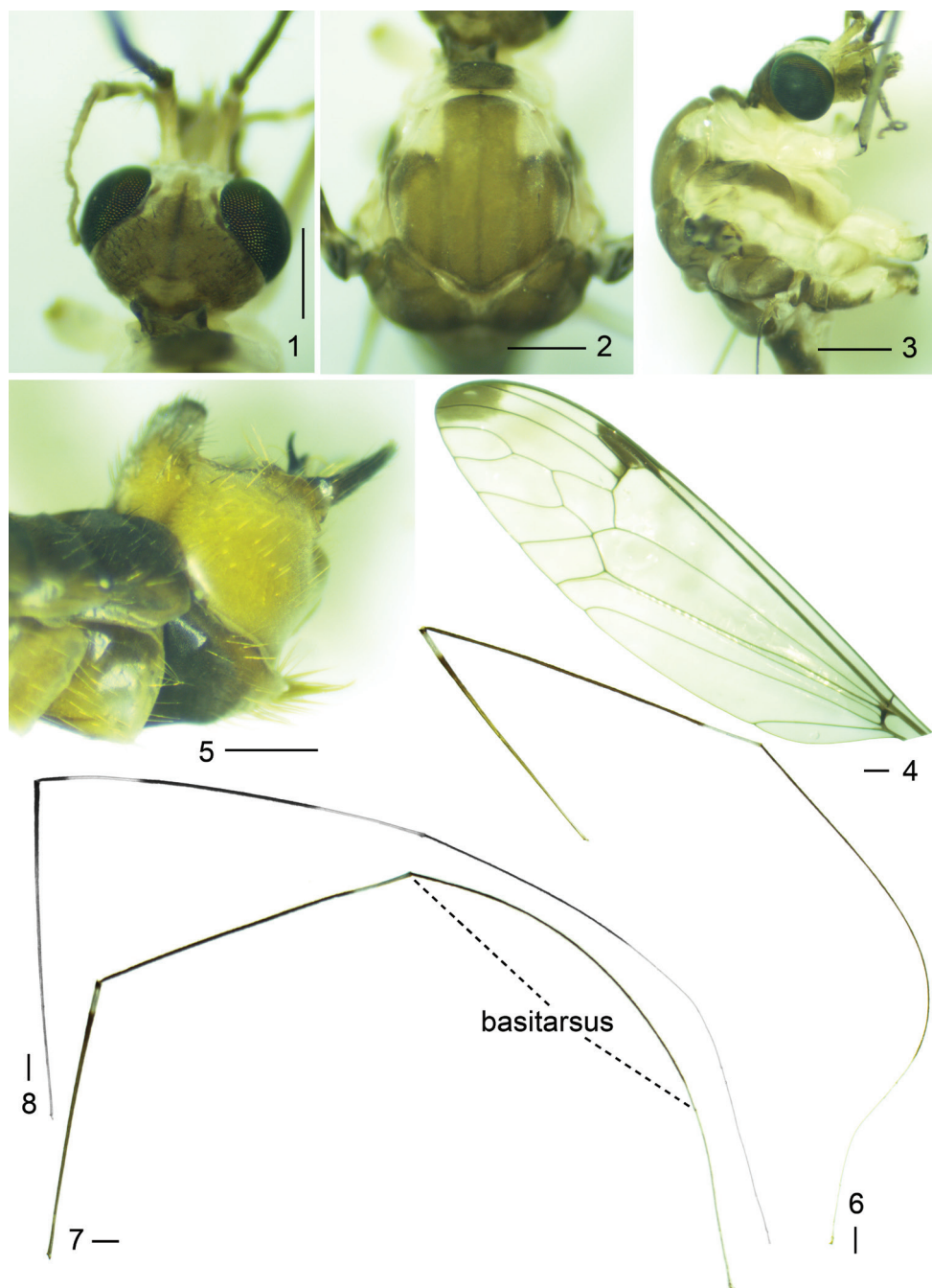
Taxonomy

Tipulodina bifurcata Xue & Men, sp. nov.

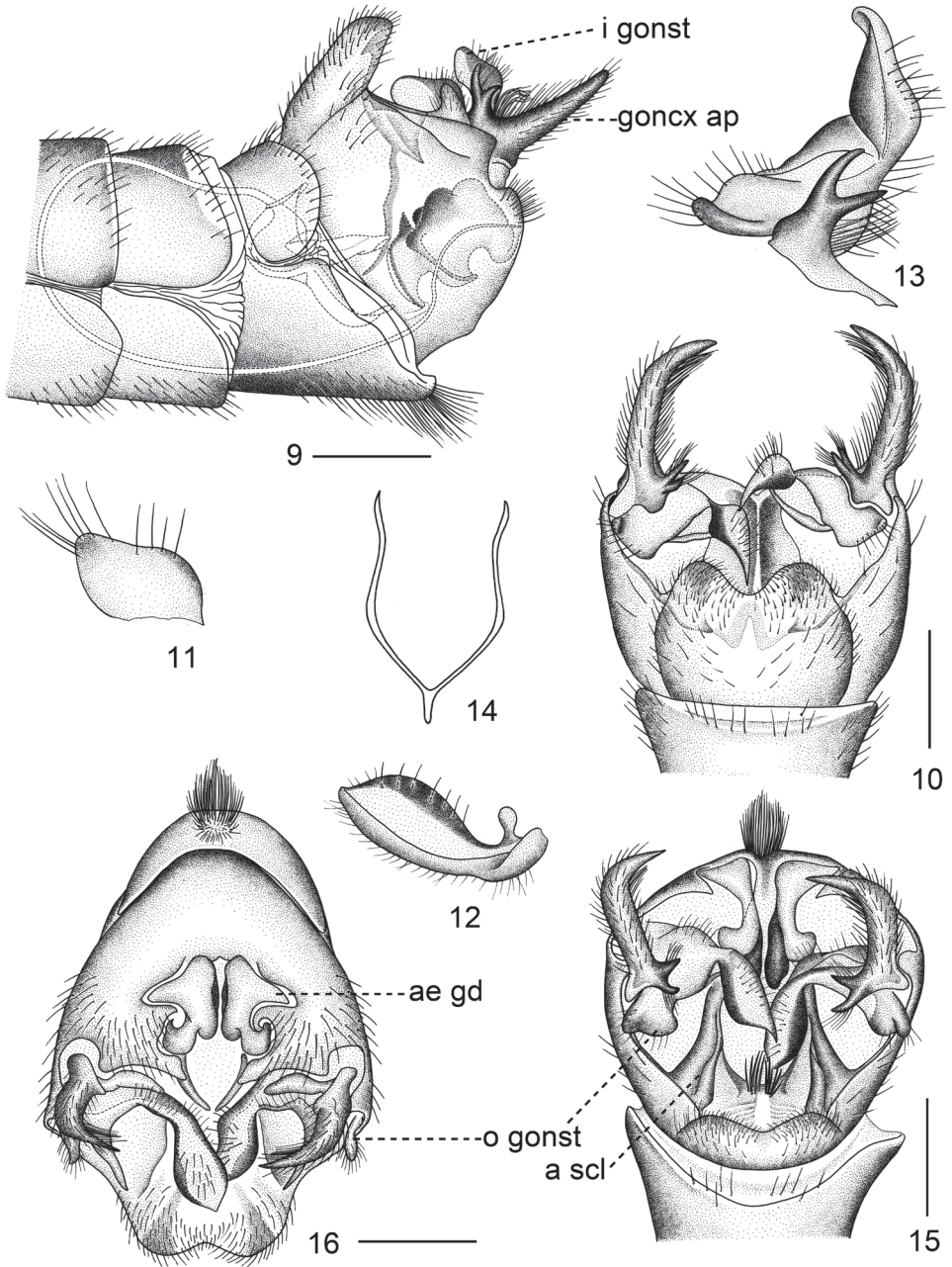
<http://zoobank.org/E14D124D-1789-4326-9C08-7B896BE3CA95>

Figs 1–20, 22–24

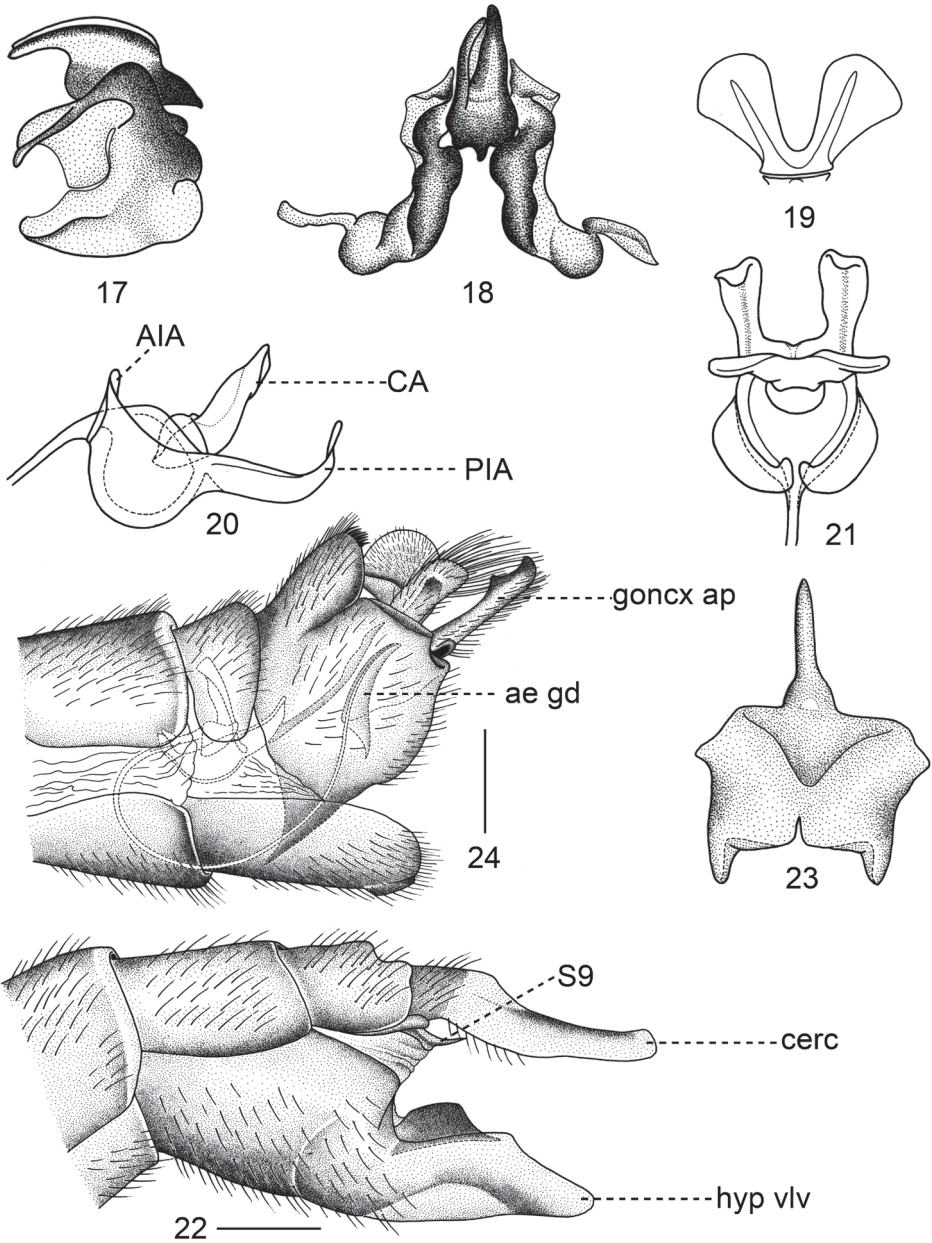
Material examined. Holotype: male. **CHINA:** Guangxi, Longzhou County, Nonggang National Nature Reserve, 9 April 2018, leg. Guoxi Xue. **Paratype:** 1 female, same data to holotype.



Figures 1–8. *Tipulodina bifurcata* Xue & Men, sp. nov. **1** head, dorsal view **2** thorax, dorsal view **3** thorax, lateral view **4** wing **5** hypopygium, lateral view **6** fore leg **7** middle leg **8** hind leg. Scale bars: 0.5 mm (**1–5**); 1.0 mm (**6–8**).



Figures 9–16. *Tipulodina bifurcata* Xue & Men, sp. nov. **9** hypopygium, lateral view **10** hypopygium, dorsal view **11** outer gonostylus, lateral view **12** inner gonostylus, lateral view **13** inner gonostylus and bifurcate process on appendage of gonocoxite, lateral view **14** genital bridge, dorsal view **15** hypopygium, caudal view **16** hypopygium, caudal view. Abbreviations: a scl = anal sclerite; ae gd = aedeagal guide; goncx ap = appendage of gonocoxite; i gonst = inner gonostylus; o gonst = outer gonostylus. Scale bars: 0.5 mm.



Figures 17–24. 17–23 *Tipulodina bifurcata* Xue & Men, sp. nov. 17 aedeagal guide, lateral view 18 aedeagal guide, dorsal view 19 compressor apodeme, dorsal view 20 semen pump, lateral view 21 semen pump, dorsal view 22 ovipositor, lateral view 23 sternite nine, dorsal view 24 *Tipulodina xyris*, hypopygium, lateral view. Abbreviations: ae gd = aedeagal guide; AIA = anterior immovable apodeme; CA = compressor apodeme; cerc = cercus; goncx ap = appendage of gonocoxite; hyp vlv = hypogynial valve; PIA = posterior immovable apodeme; S9 = sternite 9. Scale bars: 0.5 mm.

Diagnosis. The only male specimen of *Tipulodina* with the following combination of characters: antenna with scape white on basal two thirds, black on apical third, remaining segments black; prescutum with three brown stripes, median one divided by a narrow black vitta; wing transparent, stigma black, wing tip suffused with black on outer ends of cells r_1 , r_4 and r_5 ; fore and mid tibia with one white ring near apex, hind femora with two white rings; tergite nine shallowly emarginated on hind margin, densely covered with black setae; appendage of gonocoxite with a long horn-shaped rod, curved, black, sharply acute at apex, fringed with long yellow setae, with black bifurcate process inserted basally.

Description. Male. Length: body 13.1 mm (not including antenna, $n = 1$); wing 12.3 mm ($n = 1$); antenna 3.3 mm ($n = 1$).

Head. Rostrum white with white nasus, densely covered with black setae. Eye black. Occiput light brown (Fig. 1). Vertex light brown, medially with narrow pale line (Fig. 1). Antenna: bent backward extended beyond base of first abdominal segment; scape white on proximal two thirds, gradually changed to black on distal third, cylindrical, slightly expanded at apex; pedicel black, very short; flagellum entirely black, first flagellomere longest, subequal in length to scape, remaining segments progressively shortened, bases of each flagellomere with five black verticils, of which longest one significantly shorter than its corresponding flagellomere, surface of each flagellomere densely covered with short black setae. Palpus white, three basal segments distinctly thicker than apical segment.

Thorax. Pronotum white laterally, black on middle third (Fig. 2). Prescutum white with three brown stripes; median one with lateral margins parallel, anterior margin suffused with black, black median vitta dividing by median stripe into two parts; lateral stripes half the length of median one, their apices also black (Fig. 2). Scutum white anteriorly and medially, with two light brown markings connected to each other, upper one distinctly smaller than lower one. Scutellum entirely white (Fig. 2). Postnotum wholly dark brown. Pleuron white, with two brown stripes, anterior stripe extending throughout the anterior spiracle, anepisternum and katepisternum, posterior stripe throughout posterior spiracle, laterotergite and hind coxa (Fig. 3). Legs very slender, coxae and trochanters white, the latter narrowly margined with black at apex (Figs 6–8); fore and mid legs with femora brown at base, gradually changed into black, with white ring near apex, tibiae black with white ring at apex, basitarsi black on proximal four fifths, white on distal fifth, remaining segments white (Figs 6, 7); hind leg with femur brown at base, brown becoming darker on distal portion, tibia black with two white rings, basal one slightly shorter than apical one, the latter reaching end of tibia, basitarsus black on basal four fifths, white on apical fifth, remaining tarsomeres white (Fig. 8). Halter with stem brown, knob darker. Wing glassy and transparent, stigma black, wing tip tinged with black on outer ends of cells r_1 , r_4 and r_5 , light spot situated in middle of black region of cell r_4 ; discal cell transparent, broadened. Venation: R_s very short, R_3 reduced, petiole of cell m_1 slightly shorter than discal cell, the latter slightly longer than cell m_1 (Fig. 4).

Abdomen. Tergite 1 yellowish brown, dark on both anterior corners, tergite 2 yellowish brown, encircled in yellow medially and ringed with yellow at base, tergites 3 and 4 yellowish brown, narrowly suffused with yellow at base, tergites 5 to 8 entirely brown, all tergites narrowly bordered with black on lateral and hind margins, sternites yellowish brown; hypopygium yellow (Fig. 5). Hypopygium with tergite nine and sternite nine almost separated from each other, only fused at base (Figs 5, 9, 10, 12). Tergite nine U-shaped and emarginated at hind margin, densely covered with small black setae (Figs 10, 15); median area extended with pair of anal sclerites, between them with membranous area invisible from above, a few long yellow setae placed in the middle of this membranous area (Fig. 15). Appendage of gonocoxite bearing two parts: a big horn-shaped rod tapered to sharply acute and curved black apex, fringed with many long and yellow setae on lateral margin, and black bifurcated process originating from the base of the horn-shaped rod (Figs 5, 9, 10, 15, 16). Outer gonostylus small oval lobe, obtuse apically, tightly connected to base of inner gonostylus, bearing several long setae on outer margin (Figs 10, 11, 15, 16). Inner gonostylus, a fusiform lobe, with long setae on inner side, edged in black on both margins (Figs 12, 13, 15, 16). Sternite nine broader than tergite nine, deeply concave on posterior border (Fig. 16). Sternite eight shallowly concave on posterior border, medially with a group of long setae pointing caudally (Figs 5, 9, 15, 16). Genital bridge connected with base of gonocoxite, S-shaped, converged posteriorly into small common stem (Fig. 14). Aedeagal guide broad basally, narrowed apically, curved caudad, separated at apical half, with pair of lateral arms with inner margins expanded and variegated with black (Figs 9, 17, 18).

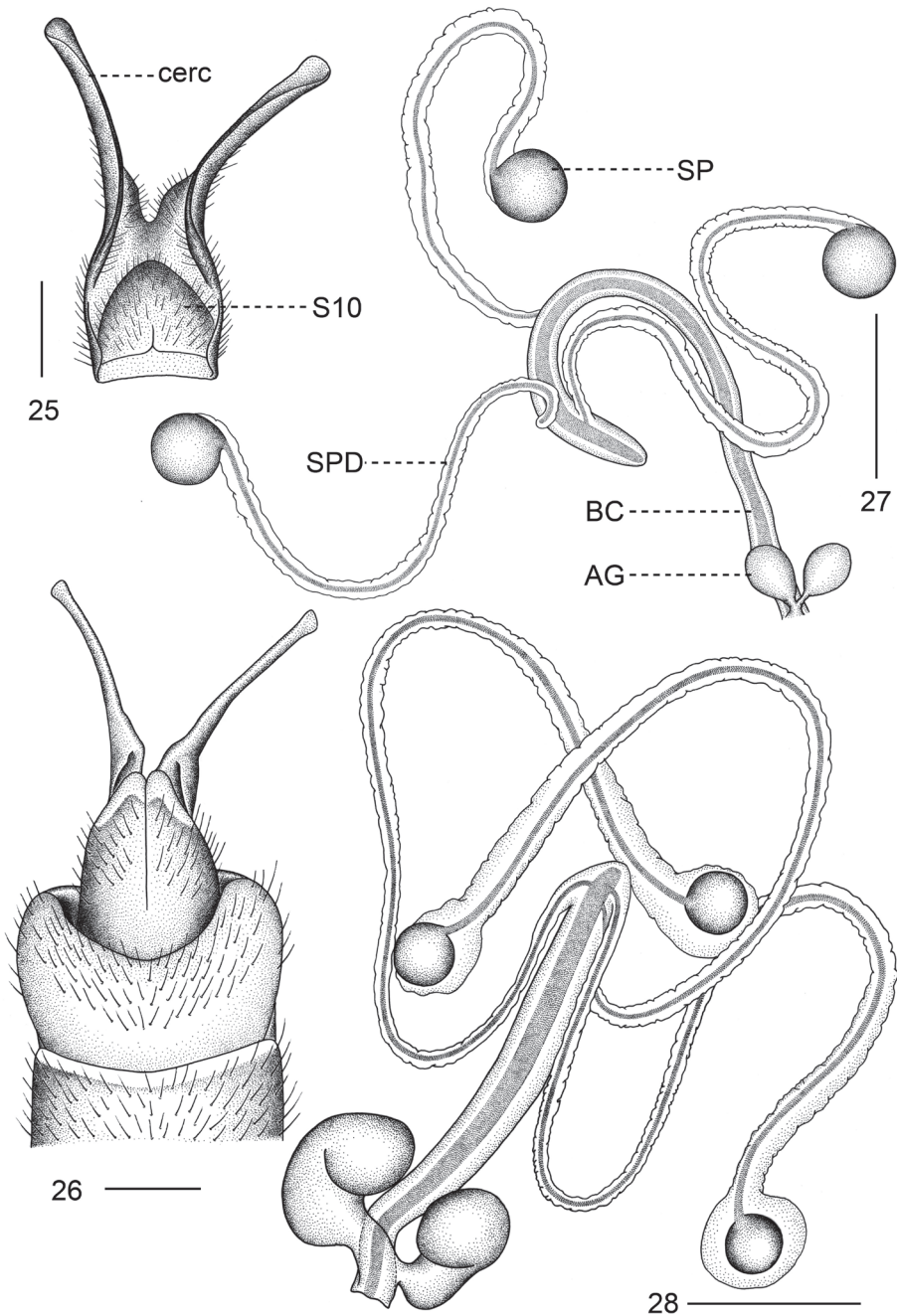
Semen pump. Compressor apodeme divided into two lobes by V-shaped notch, each lobe expanded apically with median ridge (Fig. 19). Posterior immovable apodeme with two arms elongated and curved dorsally (Figs 20, 21). Anterior immovable apodeme flattened and short, rounded in dorsal view (Figs 20, 21). Aedeagus elongated, tubular, thick basally, gradually narrowed to apex, more than 5.0 times longer than length of semen pump (Fig. 9).

Female. Length: body 15.3 mm (not including antenna, $n = 1$); wing 15.4 mm ($n = 1$); antenna 2.5 mm ($n = 1$).

Coloration. General coloration of head, thorax, and abdomen similar to male.

Ovipositor. Yellowish brown in general. Sternite nine broad basally, acute apically; tergite nine broad, longer than tergite ten in lateral view (Fig 22); sternite ten obtuse apically, densely covered with small setae, tergite ten broad at base, gradually narrowed to apex, the latter divided by suture (Figs 22, 25, 26). Cercus long, slight curved, widened at basal fourth, narrowed towards apex, slightly expanded apically, surpassing end of hypogynial valve (Figs 22, 25, 26). Hypogynial valve distinctly broader than cercus, rounded apically, broadened medially, bearing a black lobe on dorsal margin (Fig. 22).

Female internal reproductive system. Consisting of pair of accessory glands, bursa copulatrix, and three spermathecae with respective spermathecal duct (Fig. 27). Bursa copulatrix relatively elongate and narrow, rounded apically (Fig. 27). Accessory



Figures 25–28. **25–27** *Tipulodina bifurcata* Xue & Men, sp. nov. **25** cerci and sternite ten, ventral view **26** ovipositor, dorsal view **27** female internal reproductive system **28** *Tipulodina xyris*, female internal reproductive system . Abbreviations: AG = accessory gland; BC = bursa copulatrix; cerc = cercus; SP = spermatheca; SPD = spermathecal duct; S10 = sternite 10. Scale bars: 0.5 mm.

gland arising from base of bursa copulatrix, as pair of oval and swollen balls, terminating in small common stem (Fig. 27). Spermatheca spherical, black, bigger than the accessory gland (Fig. 27). Spermathecal duct slender, distinctly narrower than bursa copulatrix, flexible, generated from distal part of bursa copulatrix; connection points of three spermathecal ducts with bursa copulatrix not at same level (Fig. 27).

Distribution. China (Guangxi).

Remarks. The new species is generally similar to *Tipulodina xyris* (Alexander, 1949) by its colorations of the wing and legs (Alexander 1949, Men et al. 2016). The new species can be separated from related species by the appendage of the gonocoxite possessing a basal horn-shaped rod and a bifurcate process (not present in *T. xyris*), by the hind leg with basitarsus black on basal four fifths (hind leg with basitarsus black at basal third in *T. xyris*), by the aedeagus more than 5.0 times longer than the length of semen pump (about 3.0 times longer than the length of its semen pump in *T. xyris*) and by the shape of the aedeagal guide (Figs 9, 24). This new species also differs from *T. xyris* in organs of female internal reproductive system, including bigger spermathecae and accessory gland, and a narrower bursa copulatrix (Figs 27, 28).

Etymology. The specific epithet is an adjective derived from the Latin *furcata* meaning forked, with the Latin prefix *bi*, referring to the presence of a bifurcate process on the appendage of the gonocoxite.

Key to Chinese *Tipulodina* species (Fig. 29)

- 1 Hind tibia with single white ring (Alexander 1923: 76)
..... ***T. taiwanica* Alexander, 1923** (Taiwan, Xinzhu)
- Hind tibia with two white rings **2**
- 2 Middle femur with white ring immediately before apex (Alexander 1949: 524;
Men et al. 2016: 96) **5**
- Middle femur without white ring..... **3**
- 3 Hind tarsus with apical 3 segments not white (Alexander 1936: 175; Yang 1999:
39)
..... ***T. hopeiensis* (Alexander, 1936)** (Hebei, Tangshan, Qingdongling)
- Hind tarsus with apical 3 segments white..... **4**
- 4 Flagellum entirely black; cell sc and stigma black (Yang 1999: 39)
..... ***T. jigongshana* Yang, 1999** (Henan, Jigongshan)
- Flagellum bicolored; cell sc and stigma dark brown (Alexander 1938: 444, 445)....
***T. cantonensis* (Alexander, 1938)** (Guangdong, Honam Island = Haizhu District)
- 5 Appendage of gonocoxite without a bifurcate process.....
... ***T. xyris* (Alexander, 1949)** (Anhui, Huangshan, Tangkou; Fujian, Wuyishan)
- Appendage of gonocoxite with a bifurcate process on lateral side.....
***T. bifurcata* Xue & Men, sp. nov.** (Guangxi, Nonggang National Nature Reserve)

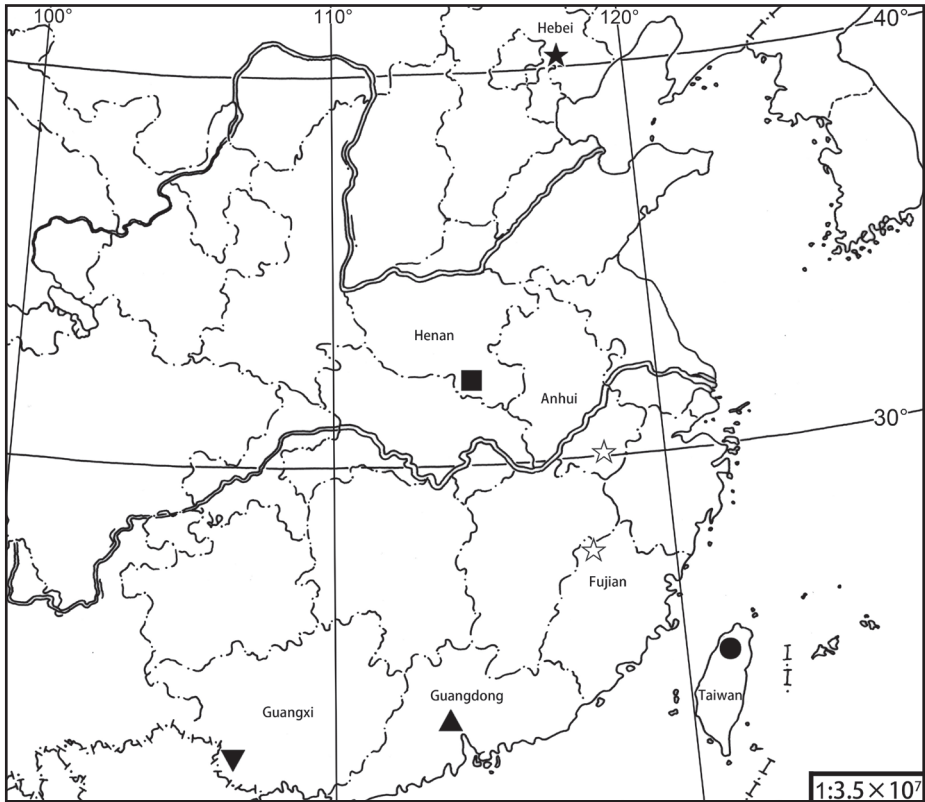


Figure 29. Geographic distribution of *Tipulodina* species in China. Key to symbols: *T. taiwanica* (circle), *T. hopeiensis* (black star), *T. jigongshana* (square), *T. cantonensis* (up-pointing triangle), *T. xyris* (white star), *T. bifurcata* (down-pointing triangle).

Acknowledgements

We thank Dr. Pjotr Oosterbroek, University of Amsterdam, Amsterdam, the Netherlands, for his valuable web site, the Catalogue of the Craneflies of the World (<http://ccw.naturalis.nl/index.php>), which provides much valuable information about distribution and taxonomy. We also thank Dr. Jon Gelhaus (Academy of Natural Science, Philadelphia, USA) and Dr. Jaroslav Stary (Olomouc-Nedvězí and Silesian Museum, Czech Republic) for their valuable comments. This study is supported by grants from the National Natural Science Foundation of China (No. 31300551), and the Anhui Outstanding Young Talent Support Program (No. gxfx2017059).

References

Alexander CP (1923) Undescribed species of Japanese crane-flies (Tipulidae, Diptera). Part III. *Annals of the Entomological Society of America* 16: 57–76. <https://doi.org/10.1093/aesa/16.1.57>

- Alexander CP (1936) New or little-known Tipulidae from eastern Asia (Diptera). Vol. 30. Philippine Journal of Science 60: 165–204.
- Alexander CP (1938) New or little-known Tipulidae from eastern Asia (Diptera). Vol. 39. Philippine Journal of Science 66: 439–478.
- Alexander CP (1949) New or little-known Tipulidae (Diptera). Vol. 85. Oriental-Australasian species. Annals and Magazine of Natural History 2(12): 512–538. <https://doi.org/10.1080/00222934908654002>
- Alexander CP, Byers GW (1981) Tipulidae. In: McAlpine JF, Peterson BV, Shewell GE, Teskey HJ, Vockeroth JR, Wood DM (Eds) Manual of Nearctic Diptera. Vol. 1. Biosystematics Research Institute, Ottawa, Ontario, 153–190.
- de Jong H (2017) Limoniidae and Tipulidae (Crane Flies). In: Kirk-Spriggs AH, Sinclair BJ (Eds.), Manual of Afrotropical Diptera. Volume 2. Nematocerous Diptera and lower Brachycera. Suricatas. South African National Biodiversity Institute, Pretoria, 427–477.
- Enderlein G (1912) Studien über die Tipuliden, Limoniiden, Cylindrotomiden und Ptychopteriden. Zoologische Jahrbücher, Abteilung für Systematik, Geographie und Biologie der Tiere 32: 1–88.
- Frommer SI (1963) Gross morphological studies of the reproductive system in representative North American crane flies (Diptera: Tipulidae). Kansas University Science Bulletin 44(12): 535–625.
- Men QL, Xue GX, Wang F (2016) Taxonomy on crane flies from Mountain Huang, China, with descriptions of two new species (Diptera: Tipulidae). Zoological Systematics 41(1): 89–101.
- Oosterbroek P (2018) Catalogue of the Craneflies of the World, (Diptera, Tipuloidea: Pediciidae, Limoniidae, Cylindrotomidae, Tipulidae). <http://ccw.naturalis.nl/index.php> [Accessed 6 September 2018]
- Yang D (1999) Two new species of Tipulidae from Jigongshan, Henan (Diptera: Tipuloidea). In: Shen X, Shi Z (Eds.), Fauna and Taxonomy of Insects in Henan. Vol. 3. China Agricultural Science and technology Press, Beijing, China, 37–40.
- Young CW (1999) New species and immature instars of crane flies of subgenus *Tipulodina* Enderlein from Sulawesi (Insecta: Diptera: Tipulidae: *Tipula*). Annals of the Carnegie Museum 68: 81–90.

Sinopyrophorinae, a new subfamily of Elateridae (Coleoptera, Elateroidea) with the first record of a luminous click beetle in Asia and evidence for multiple origins of bioluminescence in Elateridae

Wen-Xuan Bi^{1,2*}, Jin-Wu He^{1*}, Chang-Chin Chen³, Robin Kundrata⁴, Xue-Yan Li¹

1 State Key Laboratory of Genetic Resources and Evolution, Kunming Institute of Zoology, Chinese Academy of Sciences, Kunming 650223, China **2** Room 401, No. 2, Lane 155, Lianhua South Road, Shanghai, 201100, China **3** NPS office, Tianjin New Wei San Industrial Company, Ltd., Tianjing, China **4** Department of Zoology, Faculty of Science, Palacky University, 17. listopadu 50, 77146, Olomouc, Czech Republic

Corresponding author: Xue-Yan Li (lixxy@mail.kiz.ac.cn), Wen-Xuan Bi (insectb@163.com)

Academic editor: Hume Douglas | Received 15 May 2018 | Accepted 15 May 2019 | Published 17 July 2019

<http://zoobank.org/AA8F1ECD-15EF-4EC7-9F32-6AA081370598>

Citation: Bi W-X, He J-W, Chen C-C, Kundrata R, Li X-Y (2019) Sinopyrophorinae, a new subfamily of Elateridae (Coleoptera, Elateroidea) with the first record of a luminous click beetle in Asia and evidence for multiple origins of bioluminescence in Elateridae. ZooKeys 864: 79–95. <https://doi.org/10.3897/zookeys.864.26689>

Abstract

The new subfamily Sinopyrophorinae within Elateridae is proposed to accommodate a bioluminescent species, *Sinopyrophorus schimmeli* Bi & Li, **gen. et sp. nov.**, recently discovered in Yunnan, China. This lineage is morphologically distinguished from other click-beetle subfamilies by the strongly protruding frontoclypeal region, which is longitudinally carinate medially, the pretarsal claws without basal setae, the hind wing venation with a well-defined wedge cell, the abdomen with seven (male) or six (female) ventrites, the large luminous organ on the abdominal sternite II, and the male genitalia with median lobe much shorter than parameres, and parameres arcuate, with the inner margin near its apical third dentate. Molecular phylogeny based on the combined 14 mitochondrial and two nuclear genes supports the placement of this taxon far from other luminescent click-beetle groups, which provides additional evidence for the multiple origin of bioluminescence in Elateridae. Illustrations of habitus and main diagnostic features of *S. schimmeli* Bi & Li, **gen. et sp. nov.** are provided, as well as the brief description of its luminescent behavior.

Keywords

China, mitochondrial genome, molecular phylogeny, new genus, new species, taxonomy

* These authors contributed equally to this work.

Introduction

The cosmopolitan family Elateridae currently contains approximately 600 genera and almost 10,000 species (Costa et al. 2010, Kunderata and Bocak 2011). Based on a synthesis of the work over the past several decades, Costa et al. (2010; and references therein) provided the main characteristics of adult and larval elaterid morphology and recognized 17 subfamilies. Thereafter, slight modifications of the above classification were proposed by Kunderata and Bocak (2011), Kunderata et al. (2016, 2018), Bocak et al. (2018), and Douglas et al. (2018) based on molecular analyses. Currently, 18 subfamilies and 37 tribes of Elateridae are recognized (Kunderata et al. 2018).

Approximately 200 species of Elateridae are able to emit light, and these belong to Agrypninae: Pyrophorini (most species), Thylacosterninae (*Balgus schnusei* Heller) and Campyloxeninae (*Campyloxenus pyrothorax* Fairmaire) (Costa et al. 2010). The vast majority of bioluminescent species is known from the Neotropical region, with several species occurring in small Melanesian islands (Costa 1975, 1984b; Costa et al. 2010). The position of the luminous organs varies among adults of different elaterid lineages; they can be found on both prothorax and abdomen (Pyrophorini: Hapsodrilina and Pyrophorina), only on the prothorax (*Balgus* Fleutiaux, *Campyloxenus* Fairmaire, Pyrophorini: Nyctophyxina), or only on the abdomen (Pyrophorini: *Hifo* Candèze) (Costa 1975; 1984a, b; Costa et al. 2010).

In 2017, during an expedition to the western Yunnan in China, in which the first author participated, a remarkable dusk-active bioluminescent click beetle with a single luminous organ on the abdomen was discovered. Since no bioluminescent representative of Elateridae has been recorded in Asia to date, morphological study and molecular phylogenetic analysis were undertaken simultaneously to clarify the identity and phylogenetic placement of the new taxon. He et al. (2019) published the mitochondrial genome of this species and provided a preliminary phylogenetic hypothesis for it based on the analysis of 13 protein-coding genes. Here, we formally describe this species in a new genus, which we propose to place into a new subfamily within Elateridae, and provide more robust phylogenetic hypothesis for this taxon.

Materials and methods

Morphology

All specimens of the new species were collected from the vicinity of Longchuan County and Yingjiang County in western Yunnan, in subtropical evergreen broadleaf forests by searching for flashes or by setting light traps during the night. Specimens are deposited in the following collections: Kunming Institute of Zoology, Chinese Academy of Sciences, Kunming, China (**KIZ-CAS**), The Insect Collection of Shanghai Normal University, Shanghai, China (**SNUC**), collection of Wen-Xuan Bi, Shanghai, China (**CBWX**), and the collection of Chang-Chin Chen, Tianjin, China (**CCCC**). Morphological terminology follows Calder (1996) and Costa et al. (2010), except for the wing venation, for which we follow Kukalova-Peck and Lawrence (1993, 2004).

Phylogenetic analysis

To explore the phylogenetic position of the new Chinese luminescent click beetle, we newly generated 14 mitochondrial genes (13 protein-coding genes and *16S*) and two nuclear rRNA genes (*18S* and *28S*) for this species and merge them with the available four-gene Elateridae dataset (*18S*, *28S*, *16S*, *cox1*) by Kunderata et al. (2016, 2018) and Douglas et al. (2018) plus all publicly available Elateridae mitochondrial genomes downloaded from the GenBank (altogether 179 terminals representing 13 subfamilies). Four species of Phengodidae were used as outgroups following Kunderata et al. (2016, 2018) (Suppl. material 1, Table S1).

The mitogenome of the new species was obtained from GenBank (accession number MH065615) (He et al. 2019). Because we were not able to obtain high quality reference sequences of *18S* and *28S* from the Illumina reads previously used for assembling the mitogenome, we assembled *18S* and *28S* based on another batch of Illumina reads sequenced using fresh specimens collected from type locality later in June 13, 2018, and immediately frozen in liquid nitrogen and stored at -80 °C before use. Total genomic DNA (gDNA) was isolated from two male adults with Sodium Dodecyl Sulfonate method. Library (150-bp insert size) was prepared and sequenced on the Illumina HisSeq4000. Total 38 Gb clean reads were used for assembling *18S* and *28S* based on the following method: 1) reads were mapped to reference genes of rDNA using mrsFAST v3.3.0 with several iterations (Hach et al. 2014) (first iteration referred to genes downloaded from GenBank (NCBI Resource Coordinators 2016); later iterations referred to assembled contigs in the latest iteration); 2) mapped reads were then assembled using SPAdes v3.11 (Bankevich et al. 2012); 3) tandem contigs were filtered using mereps v2.6 because a huge number of repetitive reads greatly lowers assembly efficiency (Kolpakov et al. 2003); 4) steps one to three were automatically performed for 3–10 iterations until all genes were recovered.

The individual genes were aligned using Mafft online version 7 (<https://mafft.cbrc.jp/alignment/server/>) (Kuraku et al. 2013) with default parameters. The alignment was displayed and manually curated in Mega7 (Kumar et al. 2016). All 16 aligned genes were concatenated using SequenceMatrix version 1.7.8 (Vaidya et al. 2011). The concatenated matrix was used to calculate the best-fit evolutionary model (GTR+I+G) using PartitionFinder 2.1.1 (Lanfear et al. 2012, 2017). Maximum likelihood (ML) analysis were carried out using RAxML version 7.0.4. (Stamatakis et al. 2008) with 1000 bootstrap replicates. Phylograms were drawn using Interactive Tree of Life (ITOL) (Letunic and Bork 2016).

Results

Phylogenetic inference

Our phylogenetic analysis recovered similar topology (Fig. 1) to that of Kunderata et al. (2018), only Tetralobinae were placed in an unsupported terminal clade with Car-

diophorinae + Negastrinae, and Dendrometrinae including *Diplophoenicus* Candèze (Morostomatinae) formed a separate clade. Similar to previously published phylogenies, we obtained low statistical support for the backbone of tree. All subfamilies were monophyletic, except for Dendrometrinae (due to the inclusion of *Diplophoenicus*) and Lissominae (due to the inclusion of Thylacosterninae). The newly sequenced luminescent species from China was found in an unsupported clade with Oestodinae and Hemiopinae as follows: *Oestodes tenuicollis* (Randall) + (*Hemiops* sp. + new luminescent taxon), far from other bioluminescent groups like Thylacosterninae and Agrypninae: Pyrophorini.

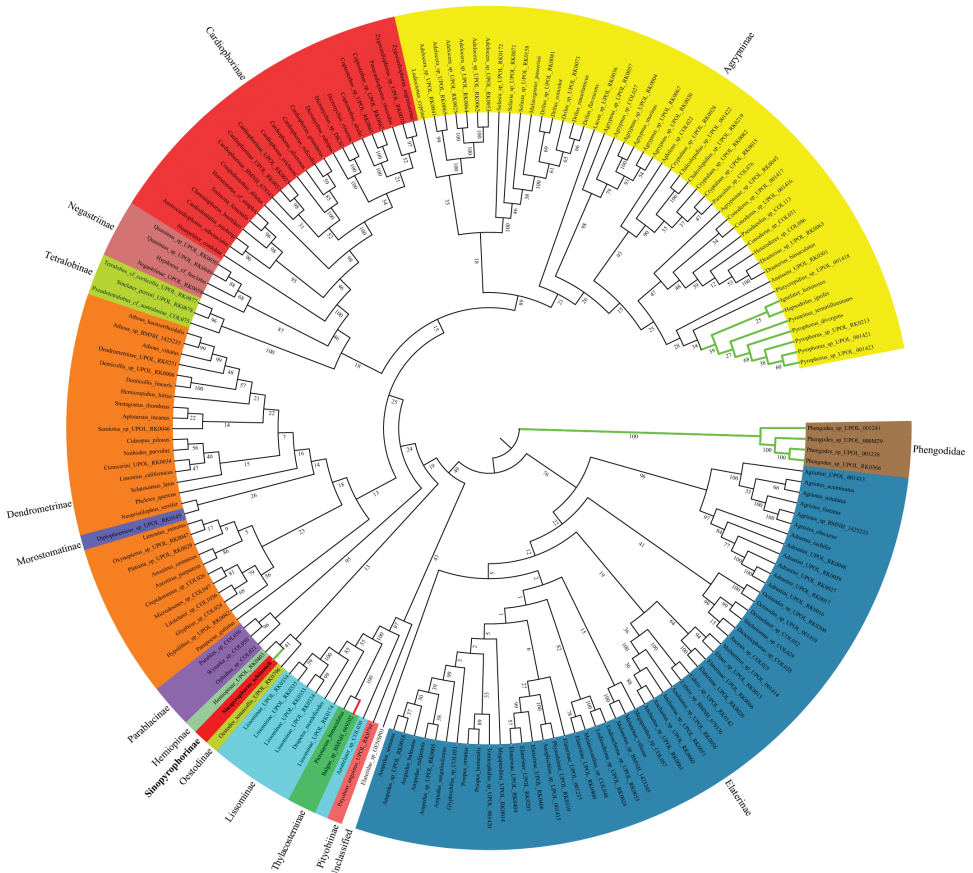


Figure 1. Inferred phylogenetic position of *Sinopyrophorus schimmeli* Bi & Li, gen. et sp. nov. within Elateridae based on the concatenated 14 mitochondrial genes (13 protein-coding genes and *16S*) and two nuclear ribosomal genes (*18S*, *28S*) using the Maximum Likelihood (ML) analysis. Numbers near each branch indicate ML bootstrap values with 1000 replicates. The same colored shaded areas at the terminals denote the same subfamily. Green bold lines indicate luminescent taxa. The bold red line indicates the presence of luminescent species within the same genus.

Taxonomy

Sinopyrophorus Bi & Li, gen. nov.

<http://zoobank.org/6828CC35-47EA-4F3A-994E-4BE4C2C4AF8A>

Figs 2–23

= *Sinopyrophorus* He et al., 2019: 565 [nomen nudum; published without description, unavailable name according to the ICZN (1999, Art. 13)].

Type species. *Sinopyrophorus schimmeli* Bi & Li, sp. nov., here designated.

Diagnosis. Head with frontoclypeal region (Fig. 4) strongly protruding, longitudinally strongly carinate medially; antennomeres II and III short, subequal in length; clicking mechanism (i.e., prosternal process fitting into mesoventral cavity) fully developed; prosternal process straight in lateral view, pretarsal claw (Fig. 13) lacking setae at base; hind wing (Fig. 14) with well-defined wedge cell; abdomen with seven (male) or six (female) ventrites; large transverse luminous organ present on abdominal sternite II (Fig. 16); aedeagus (Fig. 20) with parameres arcuate and median lobe much shorter than parameres.

Description. Male. Body elongate, ~ 4.6 times as long as wide, weakly convex in lateral view. Vestiture of fine, suberect setae.

Head with frontoclypeal region strongly protruding, inflexed at apex, medially longitudinally carinate; carina setose and apparently not joined to supra-antennal carinae, basally half as wide as frons, then narrowed and subparallel-sided, with cuticle between edges flat (Fig. 4). Antennal insertions concealed from above. Labrum free, transverse, anterior margin convex in dorsal view. Maxilla (Fig. 7) with galea scoop-like, anterior part covered with setae, denser on inner edge; lacinia elongate, densely pilose; palp with apical palpomere slightly expanded anteriorly. Labium (Fig. 6) with prementum elongate, trilobed anteriorly. Mandibles (Fig. 5) bidentate, apical tooth narrowly acute, subapical mesal tooth small. Antenna with 11 antennomeres, filiform; antennomeres II and III subequal in length (together 1/3 as long as antennomere IV), globular; remaining antennomeres at least five times longer than wide.

Prothorax with chin piece of prosternum short, bisinuate, not concealing labium; prosternal process slightly constricted between coxae in ventral view, almost straight in lateral view. Pronotosternal suture almost straight. Procoxae narrowly separated, externally broadly open. Scutellar shield (Fig. 9) trapezoidal, moderately elevated, narrowed posteriorly, posterior apex slightly emarginate. Mesocoxal cavities narrowly separated, open laterally to both mesepimeron and mesepisternum; mesotrochantin visible. Mesoventrite (Figs 10, 11) with posterior area lower than metaventrite. Meso-metaventral suture distinct. Metacoxae extending laterally to meet metepimeron, metacoxal plates not covering trochanters when legs withdrawn. Hind wing (Fig. 14) 2.35 times as long as wide; apical field ~ 0.25 times as long as total wing length, apical field with three sclerites forming an epsilon figure; radial cell longer than wide, with inner posterobasal angle acute; cross-vein r3 horizontal;

MP3+4 with basal cross-vein and basal spur; CuA2 meeting MP4; wedge cell present, ~ 3.5 times as long as wide, with obliquely truncate apex. Leg with trochanter-femur joint oblique; tibial spurs double, tarsal formula 5-5-5; pretarsal claws (Fig. 13) simple, lacking setae at base; empodium weakly developed, bisetose.

Abdomen with seven ventrites (sternites III–IX, Figs 2b, 15). Sternite II with transverse, semicircular luminescent organ occupying more than half of its width (Fig. 16). Intercoxal process of ventrite I (i.e., sternite III) narrowly rounded. First five ventrites subequal in length; ventrite V with posterior margin emarginate. Tergite VIII (Fig. 18); sternite VIII (Fig. 17) ~ 0.7 times as long as ventrite V (i.e., sternite VII), posteromedially emarginate, with each lobe slightly emarginate posteriorly; sternite IX (Fig. 19b) acute at base, more sclerotized at anterior half, connected to tergite IX by membrane; tergites IX and X partly fused (Fig. 19a), narrowly pointed anteriorly. Aedeagus (Fig. 20) with median lobe very short, only approximately half as long as aedeagus, with short basal struts; basal half wider, apical half narrow, slightly concave to subparallel-sided, with rounded apex.

Female. Slightly larger than male. Abdomen with six ventrites. Sternite VIII (Fig. 21) with spiculum ventrale 0.8 times total length of sternite. Ovipositor (Fig. 22) long, with paraprocts 3.5 times longer than gonocoxites; gonocoxites partially sclerotized; styli attached subapically. Internal genital tract (Fig. 23) simple; vagina long, membranous, slightly enlarged near entry of common oviduct; bursa copulatrix elongate, slightly widened anteriorly, sclerotized near base, with single spermathecal gland duct and fine spinules internally; colleterial gland absent.

Etymology. The generic name is derived from the Latin prefix *sino-*, which means Chinese, and *Pyrophorus*, a bioluminescent click-beetle genus from Central and South America. Gender masculine.

Distribution. China: Western Yunnan.

***Sinopyrophorus schimmeli* Bi & Li, sp. nov.**

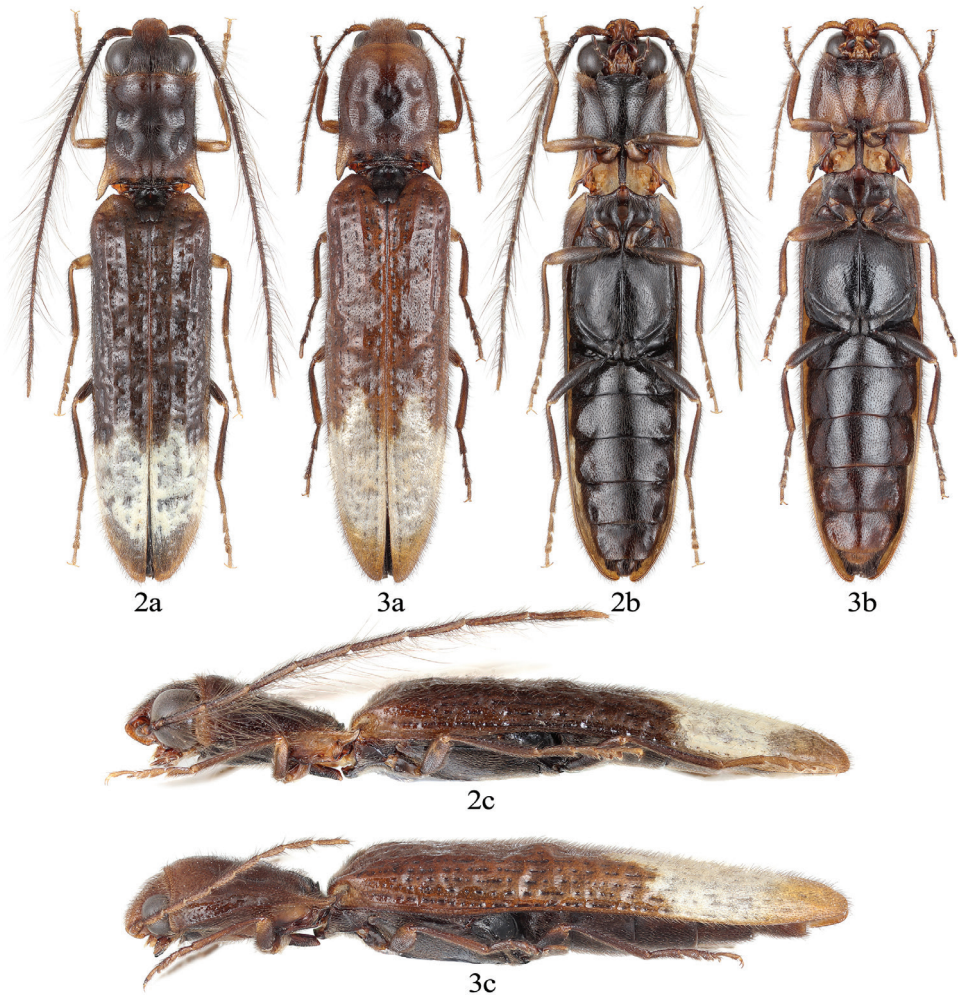
<http://zoobank.org/D8B48DF6-3B0D-45E4-94DD-127CC4C48B43>

Figs 2–23

= *Sinopyrophorus schimmeli* He et al., 2019: 565 [nomen nudum; published without description, unavailable name according to the ICZN (1999, Art. 13)].

Type locality. China, Yunnan, Yingjiang, Shangbangzhong, 24°26'N, 97°45'W, 1650 m.

Type material. Holotype: male, “China, Yunnan, Yingjiang, Shangbangzhong, 24°26'N, 97°45'W, 1650 m, 2017.VI.23, leg. Wen-Xuan Bi”; “Holotype *Sinopyrophorus schimmeli* sp. nov.” [red handwritten label] (SNUC). Paratypes (9 males, 3 females): 1 female, same data as holotype (KIZ-CAS); 1 male, 1 female, “China, Yunnan, Longchuan, Husa, 1770 m, 2017.VI.13–14, leg. Wen-Xuan Bi” (CBWX); 1 male, ditto except 2000 m, 2017.VI.16 (CBWX); 1 male, 1 female, ditto except 1700 m, 2017.VI.24, leg. Yu-Tang Wang (CBWX); 2 males, ditto except 1770 m, 2016.V.31

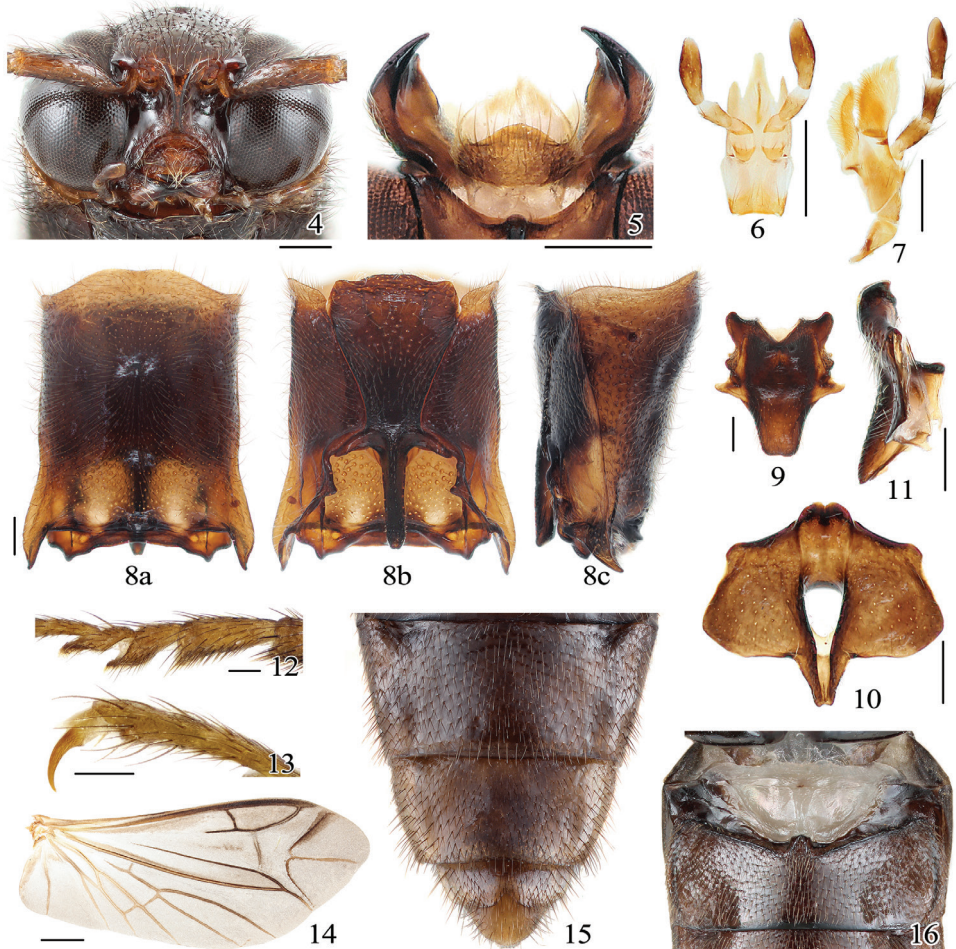


Figures 2–3. Habitus of *Sinopyrophorus schimmeli* Bi & Li, gen. et sp. nov. paratypes **2** male **3** female. **a**, dorsal view; **b**, ventral view; **c**, lateral view.

(CCCC); 1 male, ditto except leg. Xiao-Dong Yang (CCCC); 3 males, ditto except 2017.VI.25, leg. Wen-Xuan Bi (KIZ-CAS).

Other material examined. 2 males, China, Yunnan, Longchuan, Husa, 1770 m, 2017.VI.13–16, leg. Wen-Xuan Bi, damaged, partially used for extracting genomic DNA in a project of mitogenome (accession number MH065615; He et al. 2019); 2 males, China, Yunnan, Longchuan, Husa, 1770 m, 2018.VI.13, leg. Wen-Xuan Bi, the whole body of both specimens was used for the extraction of genomic DNA in an ongoing project of de novo genome sequencing and assembly of 18S and 28S.

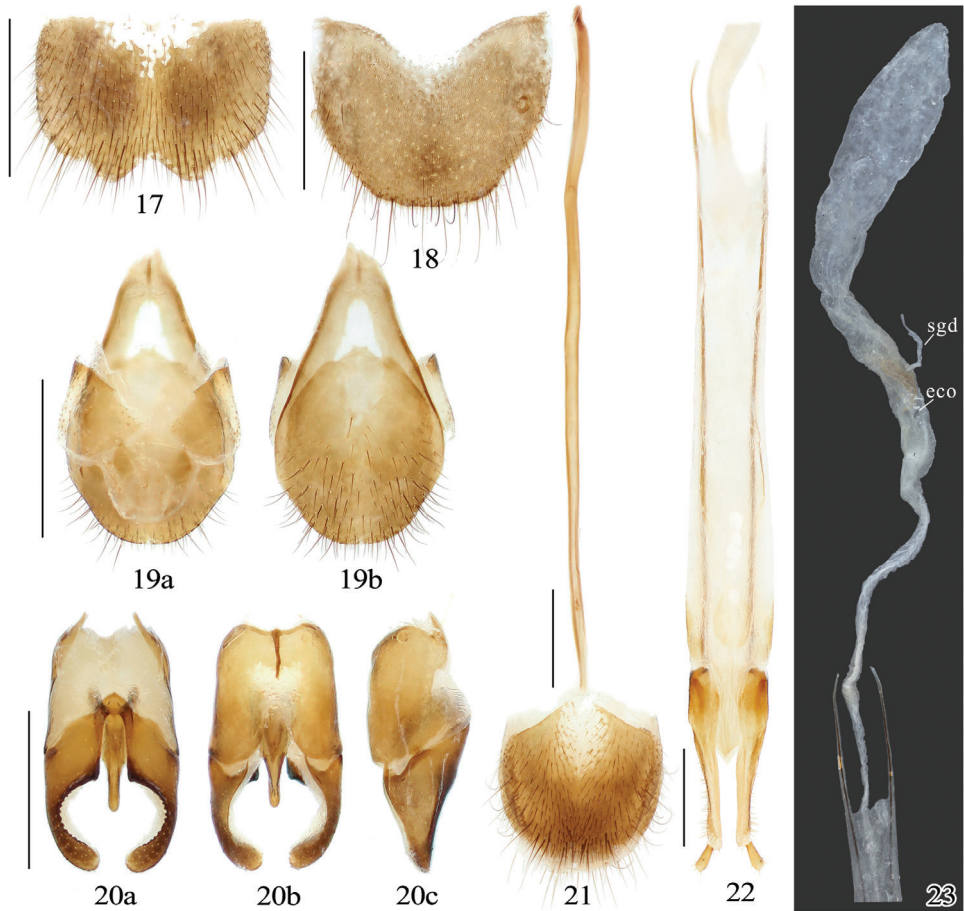
Diagnostic description. Male (Fig. 2). Body length 9.6–11.3 mm (holotype: 11.3 mm). Body brown to dark brown, with posterior portion of prothorax, fore- and mid-legs



Figures 4–16. *Sinopyrophorus schimmeli* Bi & Li, gen. et sp. nov. Male **4** head (anterior view) **5** labrum and mandibles (dorsal view) **6** labium **7** maxilla **8** prothorax **9** scutellum (dorsal view) **10** mesoventrite (ventral view) **11** mesoventrite (lateral view) **12** tarsomeres II–IV (lateral view) **13** tarsal claw (lateral view) **14** hind wing **15** ventrites IV–VII **16** abdominal luminescent organ (pale area above ventrite I). **a**, dorsal view; **b**, ventral view; **c**, lateral view. Scale bars: 0.25 mm (**4–11**); 0.1 mm (**12, 13**); 1 mm (**14**); not to scale (**15, 16**).

paler; elytra with broad subapical pale band, zigzagged anteriorly, rounded posteriorly. Body surface with fine, suberect brown setae, denser on legs; elytral light band with pale setae.

Head transverse, weakly convex, 0.75 times as long as wide, same width as pronotal anterior edge; sparsely and finely punctate. Frons rectangular, 1.4 times longer than width, 0.3 times as wide as head width across the eyes. Frontoclypeal region concave at sides beneath; with one small median depression. Eyes protuberant, median width of each eye ~ 0.7 times interocular distance in dorsal view. Mouthparts directed anteroventrally. Labrum (Fig. 5) 2.2 times wider than long. Antenna long, reaching second half of elytral length, ~ 0.7 times as long as body length; scape 2.3 times as long as



Figures 17–23. *Sinopyrophorus schimmeli* Bi & Li, gen. et sp. nov. Male **17** sternite VIII **18** tergite VIII **19** tergites IX–X with sternite IX **20** aedeagus. Female **21** sternite VIII **22** ovipositor (dorsal view) **23** internal genital tract. Abbreviations: eco, the entry of the common oviduct; sgd, spermathecal gland duct. a, dorsal view; b, ventral view; c, lateral view. Scale bars: 1 mm; not to scale (**23**).

combined length of antennomeres II and III, and of approximately same length as antennomere 4, slightly curved; antennomeres 4–11 successively weakly lengthened, with fine and very long, distinct setae; setae almost as long as apical antennomere.

Prothorax (Fig. 8) slightly convex in lateral view, tallest anteriorly; ~ 1.2 times as long as wide in dorsal view, weakly narrowed anteriorly, slightly narrower than elytral humeral width; sides slightly sinuate; pronotal lateral carina complete; anterior angles short, subacute; hind angles narrowly acute, moderately produced posterolaterally, each with short carina; posterior edge straight from dorsal view, medially elevated; pronotal disk sparsely and finely punctate, with eight shallow depressions: single median and posteromedian, and three pairs at sides. Prosternum and hypomeron more coarsely punctate than pronotum. Elytra ~ 3.0 times as long as combined width, ~ 2.9 times

as long as pronotum, parallel-sided; each elytron with three low and evenly spaced swellings, longitudinally arranged at basal half near suture; with nine punctate striae; apices conjointly rounded; epipleura short, abruptly narrowed near metacoxa. Legs long; tarsomeres I–III elongate, tarsomere I \sim 1.4 times as long as tarsomere II, tarsomere II as long as combined lengths of tarsomeres III and IV or as long as tarsomere V; tarsomeres III and IV ventrally lobate (Fig. 12).

Abdomen with each ventrite with paired depressions posterolaterally. Aedeagus (Fig. 20) robust, \sim 1.6 times as long as wide. Phallobase slightly longer than wide, narrowed dorsally, emarginate posteriorly. Median lobe approximately half as long as aedeagus, with basal struts 0.25 times total length of median lobe. Parameres \sim 1.5 times longer than median lobe, shorter than phallobase, with dorsal surface \sim 1.6 times longer than ventral one, partially fused basally in dorsal view; each paramere with dorsal surface angulate on inner margins at basal 2/5, strongly narrowed and curved mesad with dentate inner margin near apical 1/3 and rounded apex; bearing 20–30 fine setae near apex, longer on ventral surface.

Female (Fig. 3). Body length 12.1–14.5 mm. Similar to male in its general appearance but with integument paler. Eyes smaller, median width of each eye \sim 0.4 times interocular distance in dorsal view. Antenna shorter, only reaching elytral humeri, \sim 0.3 times as long as body length. Pronotum relatively shorter with lateral margins more rounded, narrowed anteriorly, with rounded anterior angles. Elytra relatively longer, \sim 3.3 times as long as wide, \sim 3.0 times as long as pronotum. Legs relatively shorter. Abdominal luminescent organ smaller, occupying approximately one third of basal abdominal sternite width.

Immature stages. Unknown.

Etymology. This species is named in honor of late Mr. Rainer Schimmel, a specialist in Elateridae, who kindly provided valuable comments at the beginning of this study.

Biological notes. All specimens of the new species were collected during the late May to June (i.e., the middle of the rainy season) from the mountain area in vicinity of Longchuan County or Yingjiang County, western Yunnan in subtropical evergreen broadleaf forests by searching for flashes or by light trapping during night. The adults of both sexes emitted a continuous yellowish green light from the abdominal luminous organs while in flight, or during a short time when preparing for flight or afterwards. During this process the luminous organ is exposed ventrally by raising and extending the abdomen from the metaventrite (Suppl. material 2, Movie S1). The reaction of the adults when disturbed during a flight is to retract their abdomen, hide their luminous organ, and show a death-feigning behavior (thanatosis). Thanatoid adults remained inactive for a long time, which was obviously different from the observation in Pyrophorini because the latter begin to emit light and are very active after being disturbed (Costa 1975). At least three lampyrid species (*Luciola* sp., *Diaphanes* sp., and *Pyrocoelia* sp.) occurred sympatrically with the new elaterid species and can be found simultaneously during night but can be easily distinguished by different flash patterns. Although some specimens of *S. schimmeli* were previously collected using light traps in 2016, this species was found to be luminescent only in 2017 when its bioluminescent behavior

was observed in the field. This was caused by the abdominal luminescent organ being hidden when the beetle is not active.

Nomenclatural notes. He et al. (2019) reported the mitochondrial genome of *S. schimmeli* gen. et sp. nov. and used the genus and species name of the here described taxon in their study. The paper of He et al. (2019) was intended to be published after the formal description of *S. schimmeli* Bi & Li, gen. et sp. nov. but unfortunately, it was published earlier, causing nomenclatural problems by reporting the genus and species names without available descriptions and thus unavailable according to the Code (ICZN 1999).

Sinopyrophorinae Bi & Li, subfam. nov.

<http://zoobank.org/8964AB43-FA98-4FB3-8D9A-2E95150E94AE>

Type genus. *Sinopyrophorus* Bi & Li, gen. nov., here designated.

Diagnosis. The molecular phylogenetic analysis (Fig. 1) and morphology (Figs 2–23) justify the establishment of a new monogeneric subfamily Sinopyrophorinae Bi & Li, subfam. nov. within Elateridae. Sinopyrophorinae are easily recognizable by the strongly protruding frontoclypeal region (Fig. 4), which is medially distinctly longitudinally carinate, antennomeres II and III subequal in length and together less than half as long as antennomeres IV–XI, pronotal hind angles (Fig. 8) acute, produced posterolaterally, prosternal process (Fig. 8c) straight in lateral view, tarsomeres III and IV (Fig. 12) with ventral lobes, abdomen with seven (male) or six (female) ventrites, with a luminous organ (Fig. 16) on sternite II, and aedeagus (Fig. 20) with a median lobe shorter than phallobase, and arcuate parameres.

Discussion

Phylogenetic placement and morphology of *Sinopyrophorus schimmeli* Bi & Li, gen. et sp. nov.

He et al. (2019) provided the first preliminary phylogenetic hypothesis for *S. schimmeli* based on the analysis of 13 protein-coding mitochondrial genes. They found this species sister to a clade containing Dendrometrinae and Elaterinae; however, their sampling of the click-beetle lineages was limited and the position of *S. schimmeli* was not statistically supported.

Here, we used the most comprehensive dataset of Elateridae to date to elucidate the phylogenetic position of the first known Asian luminescent species. Our analysis (Fig. 1) placed *S. schimmeli* in a clade with *Hemiops* and *Oestodes*, which are both the type genera of the subfamilies Hemiopinae and Oestodinae, respectively, and which were not included in the study by He et al. (2019). However, the relationships among these lineages are not statistically supported and the long branches (see Kundrata et al.

2016) indicate a long-term independent evolution of these groups, which is supported by their distinct morphology. Sinopyrophorinae differ from both Hemiopinae and Oestodinae by having the strongly protruding frontoclypeal region with median longitudinal carina, the antennomeres II and III subequal in length and much shorter than remaining antennomeres (present only in the hemiopine genus *Plectrosternus* Lacordaire), the posterior margin of pronotum simple, without sublateral incisions or carinae, the prosternal process straight in lateral view, the posterior end of scutellar shield emarginate, the wide mesoventrite with an elongate mesoventral cavity which is only gradually narrowed posteriorly, the bisetose empodium (present in *Oestodes*, multisetose in Hemiopinae), the abdomen with six or seven ventrites and with a luminous organ, the male genitalia with a median lobe shorter than parameres, and each paramere strongly curved mesad with a dentate inner margin, the female genitalia with a more sclerotized ovipositor, longer paraprocts and styli attached subapically to gonocoxites (apically in *Oestodes* and Hemiopinae; A. Prosvirov, pers. comm.). These morphological differences in combination with the molecular phylogeny support the subfamilial rank of Sinopyrophorinae, especially when there are no obvious synapomorphies which would define the clade of Sinopyrophorinae + Oestodinae + Hemiopinae, or placement of *Sinopyrophorus* in any other subfamily. Since the backbone of the Elateridae phylogenetic tree is not or only weakly supported (Kundrata et al. 2016, 2018; this study), future genomic or transcriptomic data might help to resolve the relationships among the deep splits including Sinopyrophorinae.

Our molecular analysis in combination with the morphological investigation confirmed that *S. schimmeli* does not belong to any of described subfamilies containing bioluminescent species. The clade of Sinopyrophorinae, Oestodinae and Hemiopinae formed one of the basal radiations in Elateridae, far from the Agrypninae: Pyrophorini, which contains the majority of luminescent click beetles (Fig. 1). The position of *S. schimmeli* far from Pyrophorini is additionally supported by the morphological features such as the pretarsal claws without setae at base (present in Pyrophorini), hind wings with a well-defined wedge cell (absent in Pyrophorini), abdomen with six or seven ventrites (five in Pyrophorini) and the presence of styli on the gonocoxites of ovipositor (styli absent in Pyrophorini). Thylacosterninae, which include the luminescent *Balgus schnusei*, are regularly recovered inside Lissominae in recent DNA-based analyses (Kundrata et al. 2014, 2016, 2018; Bocak et al. 2018; this study). They differ from Sinopyrophorinae in having the flabellate antennae, deep antennal cavities lying beneath the hypomera, and membranous tarsal lobes (Costa 1984a, Costa et al. 2010). The members of the subfamily Campyloxeninae, which have not been included in any DNA-based study to date, differ from Sinopyrophorinae by much wider frontoclypeal region with a complete frontal carina (frontoclypeal region strongly protruding, relatively narrow and high, longitudinally carinate medially in *S. schimmeli*), narrowed apical portions of lateral lobes of mesoventrite (wide in *S. schimmeli*) oval-shaped mesoventral cavity (elongate, gradually narrowed posteriorly in *S. schimmeli*), abdomen with five ventrites and without a luminous organ (six or seven ventrites, and a large abdominal luminous organ in *S. schimmeli*), distinctly longer paraprocts, differently shaped aedeagus with the median lobe longer than parameres, and the

paramere elongate, with a subapical hook, and apex oriented posteriorly (Costa 1975, Arias-Bohart 2015).

Southern China including Yunnan is a world biodiversity hotspot (Myers et al. 2000) and hosts many endemic beetle species including Elateridae. Intensive entomological research in southern China and neighboring regions is necessary to find out if the newly established Sinopyrophorinae contains more species. Additionally, the discovery of a larva of *S. schimmeli* may help to better understand the morphological distinctiveness and systematic position of this interesting beetle lineage.

Evolution of bioluminescence in Elateridae

Bioluminescence has evolved independently many times in various organisms (Day et al. 2004). Within Coleoptera, bioluminescence is best known in Lampyridae (fireflies), but also present in Phengodidae, Rhagophthalmidae, and some Elateridae, all within the superfamily Elateroidea (e.g., Oba 2009). Additionally, it was reported also for the larvae of two species belonging to Staphylinidae (Costa et al. 1986, Rosa 2010), which are not closely related to Elateroidea (e.g., Zhang et al. 2018). Within the Elateroidea, bioluminescence independently evolved several times (Bocakova et al. 2007, Sagegami-Oba et al. 2007, Amaral et al. 2014, Fallon et al. 2018) but despite the recent progress in elucidating the phylogenetic relationships within this superfamily (Kundrata et al. 2014), the relationships between the luminescent lineages remain unresolved.

Within Elateridae, nearly all luminescent taxa belong to the agrypnine tribe Pyrophorini, and each of the remaining three smaller groups contain only a single bioluminescent species. All other bioluminescent subfamilies, except Sinopyrophorinae, also include non-luminescent species. Campyloxeninae were placed into Pyrophorini by Stibick (1979) but this was not accepted by later authors (see e.g., Costa et al. 2010). In fact, the members of Campyloxeninae differ diagnostically from Pyrophorini in e.g., the absent setae on tarsal claws, presence of the wedge cell in the hind wing venation and the ovipositor with styli (Costa 1975, Arias-Bohart 2015). Current molecular phylogeny suggests at least three independent origins of bioluminescence within Elateridae, i.e., in Agrypninae: Pyrophorini, Sinopyrophorinae and Thylacosterninae. The presence of a single luminous organ located on abdomen without any prothoracic bioluminescent organs, which is shared by *S. schimmeli* and the pyrophorine genus *Hifo*, is therefore an apparent homoplasy. Sequences of the fresh DNA-grade material of Campyloxeninae would help us to better understand the position of this group and if it represents a fourth origin of bioluminescence in Elateridae. All available phylogenetic analyses indicate that the ancestral state of Elateridae was nonluminescent and the luminescence was later obtained in several independent lineages (Bocakova et al. 2007, Sagegami-Oba et al. 2007, Douglas 2011, Kundrata and Bocak 2011, Kundrata et al. 2014).

In Lampyridae, bioluminescence was first gained by larvae as an aposematic warning display, and subsequently gained by adults and co-opted as a sexual signal; the overall trend of courtship is the use of pheromones in ancestral species, then pheromones used in conjunction with photic signals, then the sole use of photic signal (Branham and

Wenzel 2001, 2003; Ohba 2004; Stanger-Hall et al. 2018). Males of *S. schimmeli* have a large luminous organ on abdomen plus very long antennae (longer than in females, hypothesized to be for pheromone detection) and large eyes (larger than in females, and hypothesized to be for bioluminescence detection), which suggest the use of multiple communication channels for mate attraction (Stanger-Hall et al. 2018, and references therein). It is hypothesized that in elaterids, bioluminescence of the abdominal lantern is an optical signal for the intraspecific sexual communication, while the signals from the prothoracic lanterns (if present) serve to warn predators and may also provide illumination in flight (Lall et al. 2000, 2010). Additionally, antennae are usually relatively longer in species which rely greatly on pheromones as sexual signals (Stanger-Hall et al. 2018). Therefore, the external morphology of *S. schimmeli* suggests the combined sexual communication of both light signals and pheromones. The relatively larger sexual signal sensors of *S. schimmeli* males in comparison to conspecific females are in agreement with situation in many other insect groups, in which males are the more actively searching sex, with more sensitive sensors (Steinbrecht 1987, Stanger-Hall et al. 2018).

The discovery of *S. schimmeli* as the first record of a bioluminescent click beetle in Asia shed new light on the geographic distribution and evolution of luminescent click beetles. As a representative of a unique lineage, only distantly related to all other luminescent click beetles, *S. schimmeli* may serve as a new model taxon in the research of bioluminescence within Coleoptera. A project of *de novo* genome sequencing of *S. schimmeli* has already started and should help answer the questions related to the genome characteristics of this taxon (e.g., genome size, heterozygosity etc.), its genomic difference from those of luminescent pyrophorine click beetles, and the genomic basis of the origin of its bioluminescence.

Acknowledgements

We give special thanks to Mr. Yu-Tang Wang (Taiwan, China) for his proposal to collect the specimens of Lampyridae, which enabled the discovery of the new luminescent click beetle, and for his assistance in collecting specimens. We also thank Mr. Xiao-Dong Yang (Sichuan, China) for collecting specimens, Dr. Zi-Wei Yin (SNUC, China) for capturing the photomicrographs of the new species, Mr. Xing Chen (Yunnan, China) for assembling nuclear ribosomal DNA, Dr. Alexander Prosvirov (Moscow, Russia) for the photographs of genitalia of Hemiopinae and Oestodinae, Prof. Cleide Costa (São Paulo, Brazil) for the discussion on the abdominal luminous organ in Pyrophorini, Dr. Kathrin Stanger-Hall (Athens, USA) and Dr. Luiz Silveira (Athens, USA) for their comments on earlier versions of the draft, and Dr. Hume Douglas (Ottawa, Canada) for valuable comments leading to the improvement of our manuscript. We also thank Prof. Wen Wang (Yunnan, China) and other members in his lab for their helps and supports in this study. Special thanks are due to the late Mr. Rainer Schimmel (Vinningen, Germany) for his valuable comments at the beginning of this study. This work was supported by grants from the National Natural Science Foundation of China (No. 31472035), Yunnan Provincial Science and Technology Department (No. 2014FB179) and Chinese Academy of Sciences (CAS “Light of West China” Program) to LX.Y.

References

- Amaral DT, Arnoldi FGC, Rosa SP, Viviani VR (2014) Molecular phylogeny of Neotropical bioluminescent beetles (Coleoptera: Elateroidea) in southern and central Brazil. *Luminescence* 29: 412–422. <https://doi.org/10.1002/bio.2561>
- Arias-Bohart ET (2015) *Malalcahuello ocaresi* gen. & sp. n. (Elateridae, Campyloxeninae). *ZooKeys* 508: 1–13. <https://doi.org/10.3897/zookeys.508.8926>
- Bankevich A, Nurk S, Antipov D, Gurevich AA, Dvorkin M, Kulikov AS, Lesin VM, Nikolenko SI, Pham S, Prjibelski AD, Pyshkin AV, Sirotkin AV, Vyahhi N, Tesler G, Alekseyev MA, Pevzner PA (2012) SPAdes: A new genome assembly algorithm and its applications to single-cell sequencing. *Journal of Computational Biology* 19: 455–477. <https://doi.org/10.1089/cmb.2012.0021>
- Bocak L, Motyka M, Bocek M, Bocakova M (2018) Incomplete sclerotization and phylogeny: The phylogenetic classification of *Plastocerus* (Coleoptera: Elateroidea). *PLoS ONE* 13: e0194026. <https://doi.org/10.1371/journal.pone.0194026>
- Bocakova M, Bocak L, Hunt T, Teräväinen M, Vogler AP (2007) Molecular phylogenetics of Elateriformia (Coleoptera): evolution of bioluminescence and neoteny. *Cladistics* 23: 477–496. <https://doi.org/10.1111/j.1096-0031.2007.00164.x>
- Branham MA, Wenzel JW (2001) The evolution of bioluminescence in cantharoids (Coleoptera: Elateroidea). *Florida Entomologist* 84: 565–586. <https://doi.org/10.2307/3496389>
- Branham MA, Wenzel JW (2003) The origin of photic behavior and the evolution of sexual communication in fireflies (Coleoptera: Lampyridae). *Cladistics* 19: 1–22. [https://doi.org/10.1016/S0748-3007\(02\)00131-7](https://doi.org/10.1016/S0748-3007(02)00131-7)
- Calder AA (1996) Click Beetles: Genera of Australian Elateridae (Coleoptera). *Monographs on Invertebrate Taxonomy*. CSIRO Publishing, Collingwood, 401 pp. <https://doi.org/10.1071/9780643105171>
- Costa C (1975) Systematics and evolution of the tribes Pyrophorini and Heligmini with description of Campyloxeninae, new subfamily (Coleoptera, Elateridae). *Arquivos de Zoologia* 26: 49–190. <https://doi.org/10.11606/issn.2176-7793.v26i2p49-190>
- Costa C (1984a) Note on the bioluminescence of *Balgus schnusei* (Heller, 1974) (Triaxagidae, Coleoptera). *Revista Brasileira de Entomologia* 28: 397–398.
- Costa C (1984b) On the systematic position of *Hifo* Candèze, 1881 (Elateridae, Coleoptera). *Revista Brasileira de Entomologia* 28: 399–402.
- Costa C, Vanin SA, Colepicolo Neto P (1986) Larvae of Neotropical Coleoptera. XIV. First record of bioluminescence in the family Staphylinidae (Xantholinini). *Revista Brasileira de Entomologia* 30: 101–104.
- Costa C, Lawrence JF, Rosa SP (2010) Elateridae Leach, 1815. In: Leschen RAB, Beutel RG, Lawrence JF (Eds) *Handbook of Zoology, Coleoptera, Beetles, vol 2: Morphology and Systematic (Elateroidea, Bostrichiformia, Cucujiformia partim)*. Walter de Gruyter GmbH & Co. KG, Berlin and New York, 75–103. <https://doi.org/10.1515/9783110911213.75>
- Day JC, Tisi LC, Bailey MJ (2004) Evolution of beetle bioluminescence: the origin of beetle luciferin. *Luminescence* 19: 8–20. <https://doi.org/10.1002/bio.749>

- Douglas H (2011) Phylogenetic relationships of Elateridae inferred from adult morphology, with special reference to the position of Cardiophorinae. *Zootaxa* 2900: 1–45. <https://doi.org/10.11646/zootaxa.2900.1.1>
- Douglas H, Kundera R, Janosikova D, Bocak L (2018) Molecular and morphological evidence for new genera in the click-beetle subfamily Cardiophorinae (Coleoptera: Elateridae). *Entomological Science* 21: 292–305. <https://doi.org/10.1111/ens.12306>
- Fallon TR, Lower SE, Chang C, Bessho-Uehara M, Martin GJ, Bewick AJ, Behringer M, Debat HJ, Wong I, Day JC, Suvorov A, Silva CJ, Stanger-Hall KF, Hall DW, Schmitz RJ, Nelson DR, S.M. L, Shigenobu S, Bybee SM, Larracuenta AM, Oba Y, Weng JK (2018) Firefly genomes illuminate parallel origins of bioluminescence in beetles. *Elife* 7: e36495. <https://doi.org/10.7554/eLife.36495>
- Hach F, Sarrafi I, Hormozdiari F, Alkan C, Eichler EE, Sahinalp SC (2014) MrsFAST-Ultra: a compact, SNP-aware mapper for high performance sequencing applications. *Nucleic Acids Research* 42: W494–W500. <https://doi.org/10.1093/nar/gku370>
- He JW, Bi WX, Dong ZW, Liu GC, Zhao RP, Wang W, Li XY (2019) The mitochondrial genome of the first luminous click-beetle (Coleoptera: Elateridae) recorded in Asia. *Mitochondrial DNA Part B-Resources* 4: 565–567. <https://doi.org/10.1080/23802359.2018.1555019>
- Kolpakov R, Bana G, Kucherov G (2003) Mreps: Efficient and flexible detection of tandem repeats in DNA. *Nucleic Acids Research* 31: 3672–3678. <https://doi.org/10.1093/nar/gkg617>
- Kumar S, Stecher G, Tamura K (2016) MEGA7: Molecular Evolutionary Genetics Analysis version 7.0 for bigger datasets. *Molecular Biology and Evolution* 33: 1870–1874. <https://doi.org/10.1093/molbev/msw054>
- Kukalova-Peck J, Lawrence JF (1993) Evolution of the hind wing in Coleoptera. *Canadian Entomologist* 125: 181–258. <https://doi.org/10.4039/Ent125181-2>
- Kukalova-Peck J, Lawrence JF (2004) Relationships among coleopteran suborders and major endoneopteran lineages: Evidence from hind wing characters. *European Journal of Entomology* 101: 95–144. <https://doi.org/10.14411/eje.2004.018>
- Kundera R, Bocak L (2011) The phylogeny and limits of Elateridae (Insecta, Coleoptera): is there a common tendency of click beetles to soft-bodiedness and neoteny? *Zoologica Scripta* 40: 364–378. <https://doi.org/10.1111/j.1463-6409.2011.00476.x>
- Kundera R, Bocakova M, Bocak L (2014) The comprehensive phylogeny of the superfamily Elateroidea (Coleoptera: Elateriformia). *Molecular Phylogenetics and Evolution* 76: 162–171. <https://doi.org/10.1016/j.ympev.2014.03.012>
- Kundera R, Gunter NL, Douglas H, Bocak L (2016) Next step toward a molecular phylogeny of click-beetles (Coleoptera: Elateridae): redefinition of Pityobiinae, with a description of a new subfamily Parablacinae from the Australasian Region. *Austral Entomology* 55: 291–302. <https://doi.org/10.1111/aen.12185>
- Kundera R, Gunter NL, Janosikova D, Bocak L (2018) Molecular evidence for the subfamilial status of Tetralobinae (Coleoptera: Elateridae), with comments on parallel evolution of some phenotypic characters. *Arthropod Systematics & Phylogeny* 76: 137–145.
- Kuraku SC, Zmasek M, Nishimura O, Katoh K (2013) aLeaves facilitates on-demand exploration of metazoan gene family trees on MAFFT sequence alignment server with enhanced interactivity. *Nucleic Acids Research* 41: W22–W28. <https://doi.org/10.1093/nar/gkt389>

- Lall AB, Cronin TW, Carvalho AA, de Souza JM, Barros MP, Stevani CV, Bechara EJH, Ventura DE, Viviani VR, Hill AA (2010) Vision in click beetles (Coleoptera: Elateridae): pigments and spectral correspondence between visual sensitivity and species bioluminescence emission. *Journal of Comparative Physiology A - Neuroethology Sensory Neural and Behavioral Physiology* 196: 629–638. <https://doi.org/10.1007/s00359-010-0549-x>
- Lall AB, Ventura DSE, Bechara EJH, de Souza JM, Colepicolo-Nito P, Viviani VR (2000) Spectral correspondence between visual spectral sensitivity and bioluminescence emission spectra in the click beetle *Pyrophorus punctatissimus* (Coleoptera : Elateridae). *Journal of Insect Physiology* 46: 1137–1141. [https://doi.org/10.1016/S0022-1910\(99\)00224-3](https://doi.org/10.1016/S0022-1910(99)00224-3)
- Lanfear R, Calcott B, Ho SYW, Guindon S (2012) PartitionFinder: Combined selection of partitioning schemes and substitution models for phylogenetic analyses. *Molecular Biology and Evolution* 29: 1695–1701. <https://doi.org/10.1093/molbev/mss020>
- Lanfear R, Frandsen PB, Wright AM, Senfeld T, Calcott B (2017) PartitionFinder 2: New methods for selecting partitioned models of evolution for molecular and morphological phylogenetic analyses. *Molecular Biology and Evolution* 34: 772–773. <https://doi.org/10.1093/molbev/msw260>
- Letunic I, Bork P (2016) Interactive tree of life (iTOL) v3: an online tool for the display and annotation of phylogenetic and other trees. *Nucleic Acids Research* 44: W242–W245. <https://doi.org/10.1093/nar/gkw290>
- Myers N, Mittermeier RA, Mittermeier CG, da Fonseca GAB, Kent J (2000) Biodiversity hotspots for conservation priorities. *Nature* 403: 853–858. <https://doi.org/10.1038/35002501>
- NCBI Resource Coordinators (2016) Database resources of the National Center for Biotechnology Information. *Nucleic Acids Research* 44: D7–D19. <https://doi.org/10.1093/nar/gkv1290>
- Rosa SP (2010) Second record of bioluminescence in larvae of *Xantholinus* Dejean (Staphylinidae, Xantholinini) from Brazil. *Revista Brasileira de Entomologia* 54: 147–148. <https://doi.org/10.1590/S0085-56262010000100022>
- Oba Y (2009) On the origin of beetle luminescence. In: Meyer-Rochow VB (Ed) *Bioluminescence in focus - A collection of illuminating essays*. Research Signpost, Kerala, 277–290.
- Ohba N (2004) Flash communication systems of Japanese fireflies. *Integrative and Comparative Biology* 44: 225–233. <https://doi.org/10.1093/icb/44.3.225>
- Sagegami-Oba R, Oba Y, Ôhira H (2007) Phylogenetic relationships of click beetles (Coleoptera: Elateridae) inferred from 28S ribosomal DNA: Insights into the evolution of bioluminescence in Elateridae. *Molecular Phylogenetics and Evolution* 42: 410–421. <https://doi.org/10.1016/j.ympev.2006.07.017>
- Stamatakis A, Hoover P, Rougemont J (2008) A rapid bootstrap algorithm for the RAxML web servers. *Systematic Biology* 57: 758–771. <https://doi.org/10.1080/10635150802429642>
- Stanger-Hall KF, Lower SES, Lindberg L, Hopkins A, Pallansch J, Hall DW (2018) The evolution of sexual signal modes and associated sensor morphology in fireflies (Lampyridae, Coleoptera). *Proceedings of the Royal Society B-Biological Sciences* 285: 20172384. <https://doi.org/10.1098/rspb.2017.2384>
- Steinbrecht RA (1987) Functional morphology of pheromone-sensitive sensilla. In: Prestwich GD, Blomquist GJ (Eds) *Pheromone biochemistry*. Academic Press, Orlando, FL, 353–384. <https://doi.org/10.1016/B978-0-12-564485-3.50016-6>

- Stibick JNL (1979) Classification of the Elateridae (Coleoptera) - Relationships and classification of the subfamilies and tribes. *Pacific Insects* 20: 145–186.
- Vaidya G, Lohman DJ, Meier R (2011) SequenceMatrix: concatenation software for the fast assembly of multi-gene datasets with character set and codon information. *Cladistics* 27: 171–180. <https://doi.org/10.1111/j.1096-0031.2010.00329.x>
- Viviani VR (2002) The origin, diversity, and structure function relationships of insect luciferases. *Cellular and Molecular Life Sciences* 59: 1833–1850. <https://doi.org/10.1007/PL00012509>
- Zhang SQ, Che LH, Li Y, Liang D, Pang H, Ślipiński A, Zhang P (2018) Evolutionary history of Coleoptera revealed by extensive sampling of genes and species. *Nature Communications* 9: 205. <https://doi.org/10.1038/s41467-017-02644-4>

Supplementary material 1

Table S1.

Authors: Jin-Wu He

Data type: molecular data

Explanation note: The GenBank accession numbers of mitochondrial genes (PCGs and *16S*) and nuclear rRNA genes (*18S* and *28S*) in Elateridae and outgroup used for the phylogenetic analysis and references in rRNA assembly.

Copyright notice: This dataset is made available under the Open Database License (<http://opendatacommons.org/licenses/odbl/1.0/>). The Open Database License (ODbL) is a license agreement intended to allow users to freely share, modify, and use this Dataset while maintaining this same freedom for others, provided that the original source and author(s) are credited.

Link: <https://doi.org/10.3897/zookeys.864.26689.suppl1>

Supplementary material 2

Movie S1.

Authors: Wen-Xuan Bi

Data type: multimedia

Explanation note: Luminescent behavior of *Sinopyrophorus schimmeli*.

Copyright notice: This dataset is made available under the Open Database License (<http://opendatacommons.org/licenses/odbl/1.0/>). The Open Database License (ODbL) is a license agreement intended to allow users to freely share, modify, and use this Dataset while maintaining this same freedom for others, provided that the original source and author(s) are credited.

Link: <https://doi.org/10.3897/zookeys.864.26689.suppl2>

Supplementary material 3

Sequence/Matrix data.

Copyright notice: This dataset is made available under the Open Database License (<http://opendatacommons.org/licenses/odbl/1.0/>). The Open Database License (ODbL) is a license agreement intended to allow users to freely share, modify, and use this Dataset while maintaining this same freedom for others, provided that the original source and author(s) are credited.

Link: <https://doi.org/10.3897/zookeys.864.26689.suppl3>

A new genus and species of berothids (Insecta, Neuroptera) from the Late Cretaceous Myanmar amber

Qiang Yang¹, Chaofan Shi², Dong Ren³

1 School of Life Sciences, Guangzhou University, #230 Waihuanxi Road, Guangzhou Higher Education Mega Center, Guangzhou 510006, China **2** School of Earth Sciences and Engineering, Sun Yat-sen University, Guangzhou 510275, China **3** College of Life Sciences, Capital Normal University, Xisanhuanbeilu 105, Haidian District, Beijing 100048, China

Corresponding author: *Qiang Yang* (yq11_1984@126.com)

Academic editor: *Shaun Winterton* | Received 9 April 2019 | Accepted 24 June 2019 | Published 18 July 2019

<http://zoobank.org/9F207A95-C905-444F-BB5D-19F69E9C7549>

Citation: Yang Q, Shi C, Ren D (2019) A new genus and species of berothids (Insecta, Neuroptera) from the Late Cretaceous Myanmar amber. *ZooKeys* 864: 99–109. <https://doi.org/10.3897/zookeys.864.35271>

Abstract

A new genus and species of Berothidae is described from the Late Cretaceous (Cenomanian) Myanmar amber. *Ansoberotha jiewenae* **gen. et sp. nov.** can be easily distinguished from other berothid genera by the long antenna, the scape with ca. 100 flagellomeres, the forewing with four ra-rp, MP and CuA are pectinately branched, and the hind wing with one oblique cua-cup between CuA stem and the distal branch of CuP.

Keywords

Beaded lacewing, Burmese, fossil, long scape, Mesozoic

Introduction

Berothidae is a small family of Neuroptera, comprising approximately 110 extant species assigned to 24 genera, which were divided into six subfamilies (Aspöck and Randolph 2014, Oswald 2019). The family are distributed over all the biogeographic realms except for the Oceania and Antarctica. They are mainly restricted to the tropics and subtropics, with a few occurring in the temperate zone between 50°. Berothidae form a neuropteran

clade with Rhachiberothidae and Mantispidae, although the phylogenetic relationships among the three families are still controversial (Tjeder 1959; Willmann 1990; Aspöck and Mansell 1994; Aspöck et al. 2001; Beutel et al. 2010; Zimmermann et al. 2011; Randolph et al. 2013, 2014; Aspöck and Randolph 2014; Haring and Aspöck 2004; Winterton et al. 2010; Engel et al. 2018). In particular, the disagreement on the familial status of Rhachiberothidae resulted in the questionable assignment of the extinct subfamily Paraberothinae (Nel et al. 2005; Makarkin and Kupryjanowicz 2010; Makarkin 2015). Herein, we tentatively follow the cladograms of Neuroptera in Wang et al. (2017), and exclude Rhachiberothidae including Paraberothinae from the family Berothidae.

Berothidae have a fossil history dating back to the Middle Jurassic. Approximately 22 genera with 33 species have been described, mainly distributed in the Eurasia, North and South America (as shown in Table 1). Among them, ten genera with 13 species have been described from the Myanmar amber, representing the most abundant and diverse morphology of the fossil berothids (Engel 2004; Engel and Grimaldi 2008; Yuan et al. 2016; Makarkin 2018; Huang et al. 2019). Herein, a new genus and species of Berothidae is described from the Late Cretaceous Myanmar amber.

Materials and methods

This study is based on one female specimen from Myanmar amber. The amber pieces were collected in the Hukawng Valley (the state of Kachin in northern Myanmar). A detailed map of the Hukawng Valley is given by Grimaldi et al. (2002: fig. 1). The volcanoclastic matrix of the amber is estimated to be -98.79 ± 0.62 million years old, i.e., near the Albian/Cenomanian (Early/Late Cretaceous) boundary (Shi et al. 2012). The biological inclusions of Myanmar amber represent a sample of a tropical forest community in equatorial southeastern Asia at -12°N paleolatitude (Grimaldi et al. 2002; Poinar et al. 2008; Zhang et al. 2018; Chen et al. 2019; Lin et al. 2019). The specimen was deposited by Ms Dan Zuo in the collections of the Key Laboratory of Insect Evolution & Environmental Changes, College of Life Sciences, Capital Normal University, Beijing, China (**CNUB**; Dong Ren, Curator). The specimen was examined using a Zeiss Discovery V20 stereomicroscope and photographed with an AxioCam HRc digital camera attached to the Zeiss Discovery V20 stereomicroscope (both instruments Carl Zeiss Light Microscopy, Göttingen, Germany). Line drawings were prepared with the Adobe Illustrator CS6 and with the aid of Adobe Photoshop CS6.

Venational terminology generally follows Kukalová-Peck and Lawrence (2004) as interpreted by Yang et al. (2012, 2014). Terminology of details of venation (e.g., spaces, veinlets, traces) follows Oswald (1993). Crossveins are designated after the longitudinal veins with which they connect and are numbered in sequence from the wing base.

Abbreviations:

- AA1–AA3** first to third anterior anal vein;
- CuA** anterior cubitus;
- CuP** posterior cubitus;

Table 1. List of named fossil Berothidae.

Species	Age	Locality	Reference
<i>Sinosmylites pectinatus</i> Hong, 1983	Middle Jurassic Bathonian to Callovian	Inner Mongolia, China (Jiulongshan Formation)	Hong 1983
<i>Sinosmylites fumosus</i> Makarkin, Yang & Ren, 2011	Middle Jurassic Bathonian to Callovian	Inner Mongolia, China (Jiulongshan Formation)	Makarkin et al. 2011
<i>Sinosmylites nasnitsyni</i> Makarkin, Yang & Ren, 2011	Middle Jurassic Bathonian to Callovian	Inner Mongolia, China (Jiulongshan Formation)	Makarkin et al. 2011
<i>Berothone protea</i> (Panfilov, 1980)	Upper Jurassic Upper Callovian–Kimmeridgian	Karatau, Kazakhstan (Karabastau Formation)	Khramov 2015
<i>Berothone gracilis</i> (Panfilov, 1980)	Upper Jurassic Upper Callovian–Kimmeridgian	Karatau, Kazakhstan (Karabastau Formation)	Khramov 2015
<i>Krokhatbone parva</i> Khramov, 2015	Upper Jurassic Upper Callovian–Kimmeridgian	Karatau, Kazakhstan (Karabastau Formation)	Khramov 2015
<i>Krokhatbone tristis</i> Khramov, 2015	Upper Jurassic Upper Callovian–Kimmeridgian	Karatau, Kazakhstan (Karabastau Formation)	Khramov 2015
<i>Sinosmylites karatavicus</i> Khramov, 2015	Upper Jurassic Upper Callovian–Kimmeridgian	Karatau, Kazakhstan (Karabastau Formation)	Khramov 2015
<i>Sinosmylites auliensis</i> Khramov, 2015	Upper Jurassic Upper Callovian–Kimmeridgian	Karatau, Kazakhstan (Karabastau Formation)	Khramov 2015
<i>Sinosmylites hotgoricus</i> Khramov, 2015	Upper Jurassic	Khoutiyn-Khotgor, Mongolia (Ulan-Ereg Formation)	Khramov 2015
<i>Epimesoberotha parva</i> Jepson, Makarkin & Coram	Early Cretaceous Early Berriasian	Durlston Bay, England (Lulworth Formation)	Jepson et al. 2012
<i>Banoberotha enigmatica</i> Whalley, 1980	Early Cretaceous Valanginian/Hauterivian	Lebanese amber (Jezzine)	Whalley 1980
<i>Sibelliberotha rihanensis</i> Azar & Nel, 2013	Early Cretaceous Valanginian/Hauterivian	Lebanese amber (Jezzine)	Azar and Nel 2013
<i>Oloberotha sinica</i> Ren & Guo, 1996	Early Cretaceous Barremian	Liaoning, China (Yixian Formation)	Ren and Guo 1996
<i>Ansoberotha jiewenae</i> gen. & sp. n.	Late Cretaceous lowermost Cenomanian	Myanmar amber	This paper
<i>Dasyberotha eucharis</i> Engel & Grimaldi, 2008	Late Cretaceous lowermost Cenomanian	Myanmar amber	Engel and Grimaldi 2008
<i>Ethiroberotha elongata</i> Engel & Grimaldi, 2008	Late Cretaceous lowermost Cenomanian	Myanmar amber	Engel and Grimaldi 2008
<i>Haploberotha carsteni</i> Makarkin, 2018	Late Cretaceous lowermost Cenomanian	Myanmar amber	Makarkin 2018
<i>Haploberotha persephone</i> Engel & Grimaldi, 2008	Late Cretaceous lowermost Cenomanian	Myanmar amber	Engel and Grimaldi 2008
<i>Iceloberotha kachinensis</i> Engel & Grimaldi, 2008	Late Cretaceous lowermost Cenomanian	Myanmar amber	Engel and Grimaldi 2008
<i>Iceloberotha simulatrix</i> Engel & Grimaldi, 2008	Late Cretaceous lowermost Cenomanian	Myanmar amber	Engel and Grimaldi 2008
<i>Jersiberotha myanmarensis</i> Engel & Grimaldi, 2008	Late Cretaceous lowermost Cenomanian	Myanmar amber	Engel and Grimaldi 2008
<i>Jersiberotha tauberorum</i> Engel & Grimaldi, 2008	Late Cretaceous lowermost Cenomanian	Myanmar amber	Engel and Grimaldi 2008
<i>Protoberotha minuta</i> Huang, Ren & Wang, 2019	Late Cretaceous lowermost Cenomanian	Myanmar amber	Huang et al. 2019
<i>Systemoberotha magillae</i> Engel & Grimaldi, 2008	Late Cretaceous lowermost Cenomanian	Myanmar amber	Engel and Grimaldi 2008
<i>Telisoberotha libitina</i> Engel & Grimaldi, 2008	Late Cretaceous lowermost Cenomanian	Myanmar amber	Engel and Grimaldi 2008
<i>Maculoberotha nervosa</i> Yuan, Ren & Wang, 2016	Late Cretaceous lowermost Cenomanian	Myanmar amber	Yuan et al. 2016
<i>Magniberotha recurrens</i> Yuan, Ren & Wang, 2016	Late Cretaceous lowermost Cenomanian	Myanmar amber	Yuan et al. 2016
<i>Jersiberotha luzzii</i> Grimaldi, 2000	Late Cretaceous Turonian	Raritan (New Jersey) amber	Grimaldi 2000
<i>Jersiberotha similis</i> Grimaldi, 2000	Late Cretaceous Turonian	Raritan (New Jersey) amber	Grimaldi 2000
<i>Nascimberotha picta</i> Grimaldi, 2000	Late Cretaceous Turonian	Raritan (New Jersey) amber	Grimaldi 2000
<i>Microberotha macculloughi</i> Archibald & Makarkin, 2004	Early Eocene	Hat Creek amber, British Columbia	Archibald and Makarkin 2004
<i>Elektroberotha groehni</i> Makarkin & Ohl, 2015	Late Eocene	Baltic amber	Makarkin and Ohl 2015
<i>Xenoberotha angustialata</i> Makarkin, 2017	Early Eocene late Ypresian	Colorado, USA (Green River Formation)	Makarkin 2017

MA / MP	anterior and posterior branches of media;
RA	anterior radius;
RP	posterior radius;
RP1	proximal-most branch of RP;
RP2	branch of RP distal to RP1;
ScA	subcosta anterior;
ScP	subcosta posterior.

Systematic paleontology

Class Insecta Linnaeus, 1758

Order Neuroptera Linnaeus, 1758

Family Berothidae Handlirsch, 1906

Genus *Ansoberotha* gen. nov.

<http://zoobank.org/A9486E3A-C995-430F-9D54-F45F1DC9279B>

Type (and only) species. *Ansoberotha jiewenae* gen. et sp. nov.

Etymology. The generic name is a combination of the Latin *ansa* (meaning haft, handle), and *Berotha*, the type genus of the family, in reference to the long scapus. Gender feminine.

Diagnosis. Antenna long, more than 6.6 mm, longer than body or forewings; scape elongate, ca. 0.64 mm, almost 12 times as long as wide; flagellum with about 100 flagellomeres. Pronotum elongate, about three times as long as wide. Forewing with one basal sc-r and four ra-rp, M forked distal to the separation of RP; MP, CuA pectinately branched. Hind wing with one r-m between RP stem and MA; one oblique cua-cup between CuA stem and distal branch of CuP.

***Ansoberotha jiewenae* gen. et sp. nov.**

Figures 1, 2

<http://zoobank.org/08878C7B-AC2C-48D8-BD01-824134515A83>

Etymology. The specific epithet is named after Ms Jiewen Zhao (Hunan, China), the daughter of this amber's owner (Ms Dan Zuo). Her mother hopes that this honour will promote Jiewen's interests in natural history.

Diagnosis. As for the genus.

Holotype. CNU-NEU-MA2018072, female, a nearly complete and well-preserved specimen.

Locality and horizon. Hukawng Valley, Kachin State, northern Myanmar; lower-most Cenomanian, Upper Cretaceous.

Description. Holotype CNU-NEU-MA2018072. Total body length 4.0 mm. Head and body with numerous scattered, fine setae; head about as wide as long. Com-

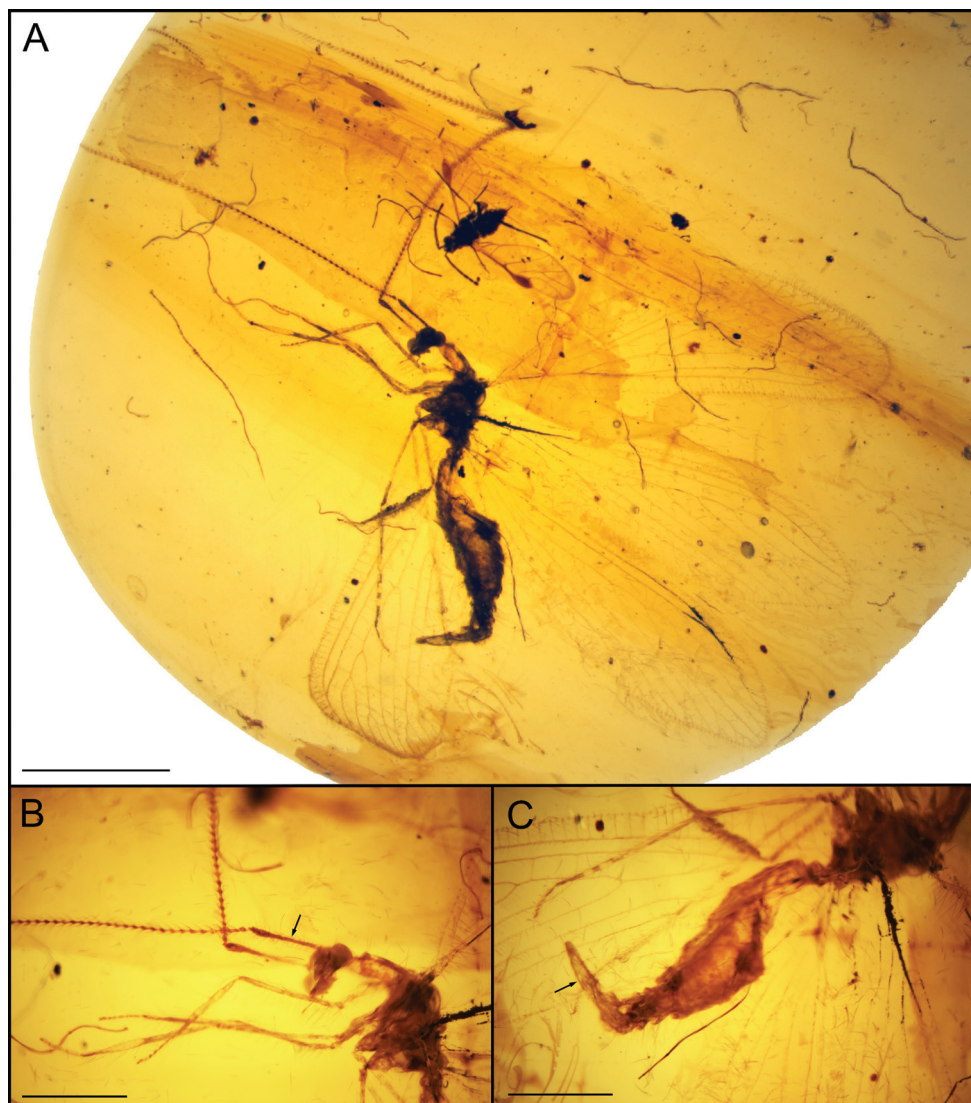


Figure 1. *Ansoberotha jiewenae* gen. et sp. nov., holotype CNU-NEU-MA2018072 **A** photograph of holotype **B** detailed photograph of antenna, arrow shows the long scape **C** detailed photograph of abdomen, arrow shows the gonapophysis lateralis. Scale bars 2 mm (**A**) and 1 mm (**B, C**).

pound eyes large. Antenna filiform, over 6.6 mm, with scattered setae all over; scape elongate, ca. 0.64 mm, almost 12 times as long as wide; pedicel as long as wide, slightly thicker than flagellum; flagellum with approximately 100 flagellomeres, the last few flagellomeres tapering. Pronotum elongate, narrower than head, about three times as long as wide; pro-, meso-, and metanotum with scattered, long, fine setae. Legs relatively long and slender, with numerous short setae intermixed with long setae. Forelegs: coxa elongated; femur long and slender; tibia slightly inflated nearly as long as femur; basitarsus nearly three times as long as the second tarsomere, the last four tarsomeres

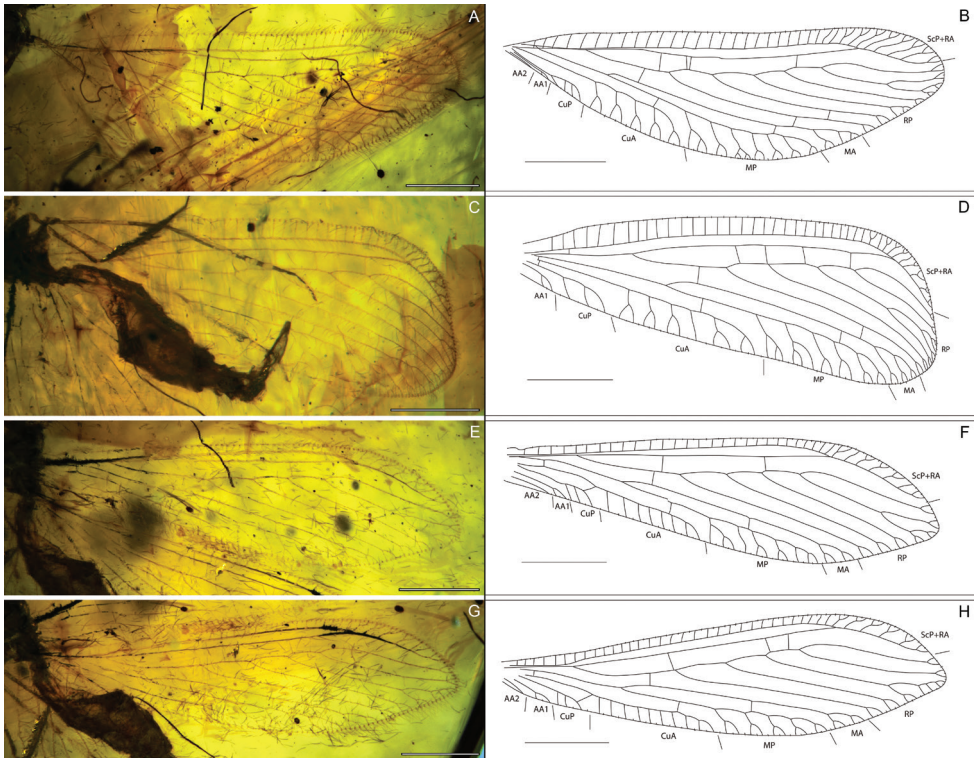


Figure 2. *Ansoberotha jiewenae* gen. et sp. nov., holotype CNU-NEU-MA2018072 **A, B** photograph of left forewing and line drawing **C, D** photograph of right forewing and line drawing **E, F** photograph of left hind wing and line drawing **G, H** photograph of right hind wing and line drawing. Scale bars 1 mm.

of the same length, each tarsomeres with two ended spur. Mid- and hind legs coxa coniform, thicker than forelegs. Each leg with two pretarsal claws, one big arolium. Abdomen nine segments, with scattered short setae; gonapophysis lateralis elongate.

Forewing length 5.5 mm, width 1.5 mm (left forewing/LFW); length 4.9 mm, width 1.8 mm (right forewing/RFW); elongated ovoid, apex rounded, with dense relatively short setae on veins and longer setae on margins; trichosors prominent along entire wing margin. Humeral vein crossvein-like; presumable ScA not detected; costal space relatively broad; most subcostal veinlets simple, not forked, only three (LFW) or four (RFW) distal apex subcostal veinlets forked once, pterostigma not present. ScP and RA fused distally, entering margin before wing apex; ScP+RA with five forked veinlets. Subcostal space slightly narrower than costal space, basally narrowed; only one sc-r present in right forewing, left forewing not detected due to preservation; four ra-rp crossveins located proximal to the fusion of ScP and RA. RP separated from R distal to sc-r, with six (LFW) or five (RFW) branches; RP4 (LFW) dichotomously forked, RP3 (RFW) pectinately forked, with three branches; only one crossveins detected between RP1, RP2 in LFW. M divided into MA and MP distal to the origin of RP and proximal to the separation of RP1 from RP stem, one ma-mp crossvein present; MA distally pectinately forked, with three branches; MP pectinately forked, with seven (LFW) or

six (RFW) branches; two crossveins between stem RP, MA and RP1, MA. Cu divided into CuA and CuP near wing base, with one m-cu detected in LFW, two in RFW; CuA pectinately forked, with five (LFW) or six (RFW) distal forked branches; CuP pectinately forked, with three or four simple branches, one crossvein between CuA, CuP in RFW detected. AA1 with a distal fork; AA2, AA3 not detected; no crossveins detected between AA region. Membrane without colour pattern.

Hind wing elongate, length 5.1 mm, width 1.5 mm (left hind wing/LHW); length 5.2 mm, width 1.5 mm (right hind wing/RHW). Trichosors prominent along entire wing margin. Costal space narrow, dilated distal to the fusion of ScP and RA; subcostal veinlets simple, widely spaced, pterostigma not present. Subcostal space no crossveins detected. ScP and RA fused distally, entering margin before wing apex; ScP+RA with seven (LHW) or five (RHW) veinlets, most with distal fork. RA space wider than subcostal space, with two (LHW) or three (RHW) ra-rp located proximal to the fusion of ScP and RA. RP originated slightly distal to wing base, with five pectinate branches, most forked distally; RP4 of LHW, RP3 of RHW dichotomously forked distally; no crossveins between RP branches; one r-m between RP stem and MA. M forked distal to origin of RP and proximal to the origin of RP1; MA dichotomously branched distally; MP pectinately forked, with six (LHW) or five (RHW) branches, most with distal fork; one ma-mp between MA and MP. Cu divided into CuA and CuP near wing base; with two m-cu detected, one near wing base, another located between RP and CuA branches; CuA long, parallel with the posterior margin, pectinately branched with eight (LHW) or 10 (RHW) simple branches; CuP with three distal simple pectinate branches; one oblique cua-cup between CuA stem and distal branch of CuP. AA1 with a distal fork; AA2 simple; AA3 not detected; no crossveins detected between AA region. Membrane without colour pattern.

Remarks. *Ansoberotha* gen. nov. is distinctly different from the other Burmese amber berothid genera by having following characters: (1) *Ansoberotha* gen. nov. antenna is very long, over 6.6 mm, longer than body or forewings; the scape is elongate, ca. 0.64 mm, almost 12 times as long as wide; the flagellum with approximately 100 flagellomeres; other genera without such long antenna, scape, or so many flagellomeres; (2) the forewing of *Ansoberotha* gen. nov. with four ra-rp; *Ethiroberotha* and *Protoberotha* without ra-rp; *Haploberotha* and *Maculaberotha* with only one ra-rp; *Jersiberotha*, *Iceloberotha*, *Telistoberotha*, and *Dasyberotha* with two ra-rp; (3) the forewing MP and CuA are pectinately branched, with no less than five branches; (4) the hind wing of *Ansoberotha* gen. nov. with one oblique cua-cup between CuA stem and the distal branch of CuP; other genera do not have this crossvein.

Acknowledgements

We appreciate the valuable comments and useful suggestions on our manuscript from the editor (Dr. Shaun L. Winterton), the reviewer (Dr. Vladimir N. Makarkin), and another anonymous reviewer. We thank Ms Dan Zuo (Changsha, Hunan, China) for donated of the type specimen to us for study. This study was supported by National Natural Sci-

ence Foundation of China (grant nos. 41602014, 31501881, 31730087), Program for Changjiang Scholars and Innovative Research Team in University (grant no. IRT-17R75), Project of High-level Teachers in Beijing Municipal Universities (IDHT20180518), Scientific Research Foundation of Guangzhou University (69-18ZX10150).

References

- Archibald SB, Makarkin VN (2004) A new genus of minute Berothidae (Neuroptera) from Early Eocene amber of British Columbia, Canada. *Canadian Entomologist* 136: 61–76. <https://doi.org/10.4039/n03-043>
- Aspöck U, Mansell MW (1994) A revision of the family Rhachiberothidae Tjeder, 1959, stat. n. (Neuroptera). *Systematic Entomology* 19: 181–206. <https://doi.org/10.1111/j.1365-3113.1994.tb00587.x>
- Aspöck U, Plant JD, Nemeschkal HL (2001) Cladistic analysis of Neuroptera and their systematic position within Neuropterida (Insecta: Holometabola: Neuropterida: Neuroptera). *Systematic Entomology* 26: 73–86. <https://doi.org/10.1046/j.1365-3113.2001.00136.x>
- Aspöck U, Randolph S (2014) Beaded lacewings – a pictorial identification key to the genera, their biogeographics and a phylogenetic analysis (Insecta: Neuroptera: Berothidae). *Deutsche Entomologische Zeitschrift* 61: 155–172. <https://doi.org/10.3897/dez.61.8850>
- Azar D, Nel A (2013) A new beaded lacewing from a new Lower Cretaceous amber outcrop in Lebanon (Neuroptera: Berothidae). In: Azar D, Engel MS, Jarzembowski E, Krogmann L, Nel A, Santiago-Blay J (Eds) *Insect Evolution in an Amberiferous and Stone Alphabet. Proceedings of the 6th International Congress on Fossil Insects, Arthropods and Amber*. Brill, Leiden and Boston, 111–130. https://doi.org/10.1163/9789004210714_009
- Beutel RG, Friedrich F, Aspöck U (2010) The larval head of Nevrothidae and the phylogeny of Neuroptera (Insecta). *Zoological Journal of the Linnean Society* 158: 533–562. <https://doi.org/10.1111/j.1096-3642.2009.00560.x>
- Chen S, Deng SW, Shih CK, Zhang WW, Zhang P, Ren D, Zhu YN, Gao TP (2019) The earliest Timematids in Burmese amber reveal diverse tarsal pads of stick insects in the mid-Cretaceous. *Insect Science* <https://doi.org/10.1111/1744-7917.12601>
- Engel MS (2004) Thorny lacewings (Neuroptera: Rhachiberothidae) in Cretaceous amber from Myanmar. *Journal of Systematic Palaeontology* 2: 137–140. <https://doi.org/10.1017/S1477201904001208>
- Engel MS, Grimaldi DA (2008) Diverse Neuropterida in Cretaceous amber, with particular reference to the paleofauna of Myanmar (Insecta). *Nova Supplementa Entomologica* 20: 1–86.
- Engel MS, Winterton SL, Breitenkreuz LCV (2018) Phylogeny and evolution of Neuropterida: Where have wings of lace taken us? *Annual Review of Entomology* 63(1): 531–551. <https://doi.org/10.1146/annurev-ento-020117-043127>
- Grimaldi DA (2000) A diverse fauna of Neuropterodea in amber from the Cretaceous of New Jersey. In: Grimaldi DA (Ed.) *Studies on Fossil in Amber, with Particular Reference to the Cretaceous of New Jersey*. Backhuys Publishers, Leiden, 259–303. <https://doi.org/10.1021/ja00303a021>

- Grimaldi DA, Engel MS, Nascimbene PC (2002) Fossiliferous Cretaceous amber from Myanmar (Burma): its rediscovery, biotic diversity, and paleontological significance. *American Museum Novitates* 3361: 1–72. [https://doi.org/10.1206/0003-0082\(2002\)361<0001:FC AFMB>2.0.CO;2](https://doi.org/10.1206/0003-0082(2002)361<0001:FC AFMB>2.0.CO;2)
- Handlirsch A (1906–1908) Die fossilen Insekten und die Phylogenie der rezenten Formen. Ein Handbuch für Palaeontologen und Zoologen. W Engelmann, Leipzig, 1430 pp. [issued in 1906 (1–640); 1907 (641–1140); 1908 (1120–1430)]
- Haring E, Aspöck U (2004) Phylogeny of the Neuropterida: a first molecular approach. *Systematic Entomology* 29: 415–430. <https://doi.org/10.1111/j.0307-6970.2004.00263.x>
- Hong Y (1983) Middle Jurassic fossil insects in North China. Geological Publishing House, Beijing, 223 pp. [in Chinese, English summary]
- Huang S, Ren D, Wang YJ (2019) A new basal beaded lacewing (Neuroptera: Berothidae) from mid-Cretaceous Myanmar amber. *Cretaceous Research* 95: 1–7. <https://doi.org/10.1016/j.cretres.2018.10.025>
- Jepson JE, Makarkin VN, Coram RA (2012) Lacewings (Insecta: Neuroptera) from the Lower Cretaceous Purbeck Limestone Group, Dorset, UK. *Cretaceous Research* 34: 31–47. <https://doi.org/10.1016/j.cretres.2011.10.001>
- Khranov AV (2015) Jurassic beaded lacewings (Insecta: Neuroptera: Berothidae) from Kazakhstan and Mongolia. *Paleontological Journal* 49(1): 26–34. <https://doi.org/10.1134/S0031030115010062>
- Klimaszewski J, Kevan DKM (1986) A new lacewing-fly (Neuroptera: Planipennia) from Canadian Cretaceous Amber, with an analysis of its fore wing characters. *Entomological News* 97: 124–132.
- Krüger L (1923) Neuroptera succinica baltica. Die im baltischen Bernstein eingeschlossenen Neuroptera des Westpreussischen Provinzial-Museums (heute Museum für Naturkunde und Vorgeschichte) in Danzig. *Stettiner Entomologische Zeitung* 84: 68–92.
- Kukalová-Peck J, Lawrence JF (2004) Relationships among coleopteran suborders and major endoneopteran lineages: evidence from hind wing characters. *European Journal of Entomology* 101: 95–144. <https://doi.org/10.14411/eje.2004.018>
- Lin XD, Labandeira CC, Shih CK, Hotton LC, Ren D (2019) Life habits and evolutionary biology of new two-winged long-proboscid scorpionflies from mid-Cretaceous Myanmar amber. *Nature Communications* <https://doi.org/10.1038/s41467-019-09236-4>
- Linnaeus C (1758) *Systema naturae per regna tria naturae secundum classes, ordines, genera, species, cum characteribus, differentiis, synonymis, locis*. 10th Edition. Vol. 1. Salvii, Holmiae, 824 pp. <https://doi.org/10.5962/bhl.title.542>
- Makarkin VN (1994) Upper Cretaceous Neuroptera from Russia and Kazakhstan. *Annales de la Societe Entomologique de France* 30(3): 238–292.
- Makarkin VN (2015) A new genus of the mantispid-like Paraberothinae (Neuroptera: Berothidae) from Burmese amber, with special consideration of its probasitarsus spine-like setation. *Zootaxa* 4007(3): 327–342. <https://doi.org/10.11646/zootaxa.4007.3.2>
- Makarkin VN (2017) An interesting new genus of Berothinae (Neuroptera: Berothidae) from the early Eocene Green River Formation, Colorado. *Zootaxa* 4226(4): 594–600. <https://doi.org/10.11646/zootaxa.4226.4.9>

- Makarkin VN (2018) A new species of *Haploberotha* (Neuroptera: Berothidae) from mid-Cretaceous Burmese amber. *Cretaceous Research* 90: 375–381. <https://doi.org/10.1016/j.cretres.2018.06.011>
- Makarkin VN, Kupryjanowicz J (2010) A new mantispid-like species of Rhachiberothinae from Baltic amber (Neuroptera, Berothidae), with a critical review of the fossil record of the subfamily. *Acta Geologica Sinica* 84: 655–664. <https://doi.org/10.1111/j.1755-6724.2010.00238.x>
- Makarkin VN, Ohl M (2015) An important new fossil genus of Berothinae (Neuroptera: Berothidae) from Baltic amber. *Zootaxa* 3946(3): 401–415. <https://doi.org/10.11646/zootaxa.3946.3.7>
- Makarkin VN, Yang Q, Ren D (2011) Two new species of *Sinosmylites* Hong (Neuroptera: Berothidae) from the Middle Jurassic of China, with notes on Mesoberothidae. *ZooKeys* 130: 199–215. <https://doi.org/10.3897/zookeys.130.1418>
- Nel A, Perrichot V, Azar D, Néraudeau D (2005) New Rhachiberothidae (Insecta: Neuroptera) in Early Cretaceous and Early Eocene ambers from France and Lebanon. *Neues Jahrbuch für Geologie und Paläontologie Abhandlungen* 235: 51–85. <https://doi.org/10.2113/gsmicropal.51.6.487>
- Oswald JD (1993) Revision and cladistic analysis of the world genera of the family Hemerobiidae (Insecta: Neuroptera). *Journal of the New York Entomological Society* 101: 143–299. <http://biostor.org/reference/41781>
- Oswald JD (2019) Neuropterida Species of the World. Version 6.0. <http://lacewing.tamu.edu/SpeciesCatalog/Main> [accessed 2019.04.01]
- Poinar Jr GO, Buckley R, Brown AE (2008) The secrets of Burmite amber. *MAPS Digest* 20: 20–29.
- Randolf S, Zimmermann D, Aspöck U (2013) Head anatomy of adult *Sisyra terminalis* (Insecta: Neuroptera: Sisyridae) – functional adaptations and phylogenetic implications. *Arthropod Structure and Development* 42: 565–582. <https://doi.org/10.1016/j.asd.2013.07.004>
- Randolf S, Zimmermann D, Aspöck U (2014) Head anatomy of adult *Nevrorthus apatelioides* and basal splitting events in Neuroptera (Neuroptera: Nevrothidae). *Arthropod Systematics and Phylogeny* 72(2): 111–136.
- Ren D, Guo ZG (1996) On the new fossil genera and species of Neuroptera (Insecta) from the Late Jurassic of northeast China. *Acta Zootaxonomica Sinica* 21: 461–479.
- Shi GH, Grimaldi DA, Harlow GE, Wang J, Wang J, Yang MC, Lei WY, Li QL, Li XH (2012) Age constraint on Burmese amber based on UePb dating of zircons. *Cretaceous Research* 37: 155–163. <https://doi.org/10.1016/j.cretres.2012.03.014>
- Tjeder B (1959) Neuroptera-Planipennia. The Lace-wings of Southern Africa. 2. Family Berothidae. In: Hanstrom B, Brinck P, Rudebec G (Eds) *South African animal life*. Vol. 6. Swedish Natural Science Research Council, Stockholm, 256–314.
- Wang YY, Liu XY, Garzón-Orduña IJ, Winterton SL, Yan Y, Aspöck U, Aspöck H, Yang D (2017) Mitochondrial phylogenomics illuminates the evolutionary history of Neuropterida. *Cladistics* 33: 617–636. <https://doi.org/10.1111/cla.12186>
- Whalley PES (1980) Neuroptera (Insecta) in amber from the Lower Cretaceous of Lebanon. *Bulletin of the British Museum of Natural History (Geology)* 33: 157–164.

- Willmann R (1990) The phylogenetic position of the Rhachiberothinae and the basal sister-group relationships within the Mantispidae (Neuroptera). *Systematic Entomology* 15: 253–265. <https://doi.org/10.1111/j.1365-3113.1990.tb00316.x>
- Winterton SL, Hardy NB, Wiegmann BM (2010) On wings of lace: phylogeny and Bayesian divergence time estimates of Neuropterida (Insecta) based on morphological and molecular data. *Systematic Entomology* 35: 349–378. <https://doi.org/10.1111/j.1365-3113.2010.00521.x>
- Yang Q, Makarkin VN, Winterton SL, Khramov AV, Ren D (2012) A remarkable new family of Jurassic insects (Neuroptera) with primitive wing venation and its phylogenetic position in Neuropterida. *PLoS ONE* 7(9): e44762. <https://doi.org/10.1371/journal.pone.0044762>
- Yang Q, Makarkin VN, Ren D (2014) Two new species of *Kalligramma* Walther (Neuroptera: Kalligrammatidae) from the Middle Jurassic of China. *Annals of the Entomological Society of America* 107: 917–925. <https://doi.org/10.1603/AN14032>
- Yuan DD, Ren D, Wang YJ (2016) New beaded lacewings (Neuroptera: Berothidae) from Upper Cretaceous Burmese amber. *Cretaceous Research* 68: 40–48. <https://doi.org/10.1016/j.cretres.2016.08.007>
- Zhang WT, Li H, Shih CK, Zhang AB, Ren D (2018) Phylogenetic analyses with four new Cretaceous bristletails reveal inter-relationships of Archaeognatha and Gondwana origin of Meinertellidae. *Cladistics* 34: 384–406. <https://doi.org/10.1111/cla.12212>
- Zimmermann D, Randolph S, Metscher BD, Aspöck U (2011) The function and phylogenetic implications of the tentorium in adult Neuroptera (Insecta). *Arthropod Structure and Development* 40: 571–582. <https://doi.org/10.1016/j.asd.2011.06.003>

Genetic delimitation of *Pristimantis orestes* (Lynch, 1979) and *P. saturninoi* Brito et al., 2017 and description of two new terrestrial frogs from the *Pristimantis orestes* species group (Anura, Strabomantidae)

Veronica L. Urgiles^{1,2}, Paul Székely^{3,4}, Diana Székely^{4,5,6},
Nicholas Christodoulides¹, Juan C. Sanchez-Nivicela^{2,7,8}, Anna E. Savage¹

1 Department of Biology, University of Central Florida, 4110 Libra Drive, Orlando, Florida, 32816, USA
2 Instituto Nacional de Biodiversidad del Ecuador INABIO, Rumipamba 341 y Av. De los Shyris, Quito, Ecuador
3 Museo de Zoología, Universidad Técnica Particular de Loja, San Cayetano Alto, calle Paris s/n, 11-01-608, Loja, Ecuador
4 EcoSs Lab, Departamento de Ciencias Biológicas, Universidad Técnica Particular de Loja, San Cayetano Alto, calle Marcelino Champagnat s/n, 11-01-608, Loja, Ecuador
5 Faculty of Natural and Agricultural Sciences, Ovidius University Constanța, Constanța, Romania
6 Laboratory of Fish and Amphibian Ethology, Behavioural Biology Unit, FOCUS, University of Liège, Liège, Belgium
7 Grupo de Investigación Evolución y Ecología de Fauna Neotropical (EEFN), Universidad Nacional de Colombia, Bogotá D.C., Colombia
8 Museo de Zoología, Universidad del Azuay, Cuenca, Ecuador

Corresponding author: Paul Székely (jpszekely@utpl.edu.ec)

Academic editor: Johannes Penner | Received 3 April 2019 | Accepted 23 June 2019 | Published 18 July 2019

<http://zoobank.org/D564AD43-593A-4E71-946D-2366A878B1EE>

Citation: Urgiles VL, Székely P, Székely D, Christodoulides N, Sanchez-Nivicela JC, Savage AE (2019) Genetic delimitation of *Pristimantis orestes* (Lynch, 1979) and *P. saturninoi* Brito et al., 2017 and description of two new terrestrial frogs from the *Pristimantis orestes* species group (Anura, Strabomantidae). ZooKeys 864: 111–146. <https://doi.org/10.3897/zookeys.864.35102>

Abstract

In the genus *Pristimantis*, species are often combined into taxonomic units called species groups. The taxonomy of these groups is frequently inaccurate due to the absence of genetic data from type series and repeated misidentifications generated by high morphological resemblance between taxa. Here, we focus on the *P. orestes* species group, providing the first genetic assessment of *P. orestes* sensu stricto from individuals collected from the type locality, with a reviewed diagnosis and description of advertisement calls. We find that two lineages previously named *P. orestes* are genetically distinct and should be separated into two different species. Based on genetic and morphological data, we name one of these species *P. cajanuma* **sp. nov.** This new species is morphologically distinct from other members of the group by having shagreen dorsal skin, evident dorsolateral folds, broader discs on toes and fingers and pale gray ventral coloration. Ad-

ditionally, *P. saturninoi* is placed within the *P. orestes* species group based on genetic data from its type series. However, we find that one of its paratypes is genetically distinct and belongs to a clade containing a new species we name *P. quintanai* **sp. nov.** This new species is morphologically distinguished by lacking a tympanic membrane and vocal sacs in males, and by having expanded discs on toes and fingers, finely tuberculated dorsal skin and irregular white or cream spots in the groin and concealed surfaces of thighs. Our findings highlight the importance of providing genetic characterization and placement from the type series in taxonomic challenging groups, such as *Pristimantis*. We also suggest that the diversity of species within the *P. orestes* group will increase as more sampling is achieved in the southern Andes of Ecuador.

Resumen

Las especies pertenecientes al género *Pristimantis* usualmente están agrupadas en unidades taxonómicas llamadas grupos de especies. A menudo la taxonomía de estos grupos es problemática debido a la ausencia de información genética de las series tipo de las especies o debido a identificaciones erróneas generadas por la elevada similitud morfológica entre especies. Aquí nos enfocamos en el grupo de especies *P. orestes* y proveemos la primera evaluación genética de *P. orestes* sensu stricto en base a individuos colectados en la localidad tipo de la especie con una diagnosis revisada y descripción de vocalizaciones. Encontramos que dos linajes previamente nombrados como *P. orestes* son genéticamente distintos y deberían ser considerados como dos distintas especies. En base a evidencia genética y morfológica nombramos a una de estas especies *P. cajanuma* **sp. nov.** La nueva especie es distinta de otras especies del grupo por presentar piel dorsal con textura finamente granular, pliegues dorsolaterales evidentes, discos amplios en dedos de pie y manos y una coloración ventral gris pálido. Adicionalmente, *P. saturninoi* es colocada dentro del grupo de especies *P. orestes* en base a información genética de especímenes tipo. Sin embargo, encontramos que uno de los paratipos es genéticamente distinto y está dentro de un clado que incluye a una nueva especie morfológicamente similar que nombramos como *P. quintanai* **sp. nov.** Esta nueva especie se distingue de otros *Pristimantis* del grupo por carecer de una membrana timpánica diferenciada, machos sin sacos vocales y por presentar discos expandidos en los dedos de pies y manos, una piel dorsal con textura finamente tubercular y manchas irregulares blancas o crema-blancuecinas en las ingles y superficies ocultas de los muslos. Nuestros resultados resaltan la importancia de proveer caracterizaciones genéticas de especímenes tipos en grupos taxonómicamente complejos como los *Pristimantis*. Sugerimos que la diversidad de especies dentro del grupo de especies *P. orestes* incrementara a medida que más expediciones de campo se realicen en el sur de los Andes de Ecuador.

Keywords

Andes, Ecuador, new species, *P. cajanuma* sp. nov., *P. quintanai* sp. nov.

Palabras clave

Andes, Ecuador, nuevas especies, *P. cajanuma* sp. nov., *P. quintanai* sp. nov.

Introduction

Pristimantis is a species-rich genus of terrestrial frogs that inhabit Central and South America (Hedges et al. 2008, Pinto-Sanchez et al. 2012). Although the genus is distributed broadly across this area, most of the diversity is restricted to the Andean regions of Ecuador, Colombia and Peru (Kieswetter and Schneider 2013). In Ecuador, 228 species of *Pristimantis* have been described to date, which remarkably represent over 40% of the known amphibians in the country (Ron et al. 2019).

Due to the extraordinary diversity and taxonomic complexity of the genus, *Pristimantis* species were grouped into phenetic taxonomic categories called species groups (Lynch and Duellman 1997). These groups were delimited based on a handful of morphological characteristics and resulted in the recognition of 11 species groups (Lynch and Duellman 1997). Such classifications are imperfect because they do not account for genetic and intraspecific variation or character plasticity within *Pristimantis*, yet they are useful in allowing us to recognize potentially diagnostic aspects of the morphology and natural history of individual species. The incorporation of molecular data in an increasing number of taxonomic analyses has recovered some species groups within *Pristimantis* as monophyletic, such as the *P. myersi* species group (Hedges et al. 2008). However, taxonomic resolution within most species groups remains unclear (Padial et al. 2014, Guayasamin et al. 2018), particularly in those groups where sufficient taxon sampling has not been accomplished and where molecular data from type series of described species (holotypes or paratypes) is not available.

Within this context, an interesting taxon that was recently recovered as a monophyletic clade using molecular phylogenetics is the *Pristimantis orestes* species group (Brito et al. 2017). When first proposed, the group included only three species from the south of Ecuador. As more samples were analyzed, a total of 14 species from southern Ecuador and northern Peru were suggested to be part of the group (Duellman and Lehr 2009). Only four of these species were included in the comprehensive Terrarana systematic revision proposed by Hedges et al. (2008) and in the later work of Padial et al. (2014). In both studies, the group was not recovered as monophyletic. Recently, Brito et al. (2017) provided a phylogenetic analysis of the group including a larger number of samples, and recovered monophyly but suggested that the *P. orestes* species group is restricted to the south of Ecuador and includes *P. andinognomus* (Lehr & Coloma, 2008), *P. bambu* (Arteaga & Guayasamin, 2011), *P. mazar* (Guayasamin & Arteaga, 2013), *P. muranunka* (Brito et al., 2017), *P. orestes* (Lynch, 1979) and *P. simonbolivari* (Wiens & Coloma, 1992). In contrast, the Peruvian species *P. melanogaster* (Duellman & Pramuk, 1999) and *P. simonsii* (Boulenger, 1900), which were previously placed in the *P. orestes* group by Lynch and Duellman (1997), are members of different clades. Similar results were found by Székely et al. (2018), with the inclusion of the newly described species *P. tiktik* (Székely et al., 2018) within the *P. orestes* group.

While the analyses of Brito et al. (2017) and Székely et al. (2018) have increased our knowledge of the phylogenetic relationships in the *P. orestes* group, these molecular analyses have also identified polytomies generated by erroneous assignment of species to multiple different clades due to morphological misidentifications and because good quality DNA samples are unavailable from formalin-fixed type specimens (most notably, *P. orestes*). Thus, further genetic characterizations are essential to accurately delimit species within the *P. orestes* species group. Molecular systematics is also necessary to accurately place those taxa that were suggested to be part of the *P. orestes* group but were described using morphological data only, such as *P. saturninoi* (Brito et al., 2017). Here, we present a novel exploration of the nuclear and mitochondrial molecular diversification of the *P. orestes* species group using broad spatial sampling across

high elevation ecosystems in the southern Andes of Ecuador. Specifically, we provide (1) a redescription and genetic delimitation of *P. orestes* sensu stricto, representing the first genetic assessment of the species from its type locality, (2) a revised placement of *P. saturninoi*, and (3) a description of two new species that are part of the *P. orestes* species group.

Materials and methods

Amphibians were collected under authorization from the Ecuadorian Environmental Ministry (MAE): MAE-DNB-CM-2015-0016, MAE-DNB-CM-2016-0045 and MAE-DPC-AIC-B-2018-003. All animal research was carried out under the University of Central Florida's IACUC protocol #18-16W and approved by the Ethics Committee of Universidad Técnica Particular de Loja (UTPL-CBEA-2016-001). Specimens were euthanized with a solution of 2% lidocaine following McDiarmid et al. (1994), fixed in 10% formalin, and preserved in 70% ethanol. Tissue samples from liver were extracted and preserved in 96% ethanol. Geographic coordinates and elevation were recorded with a GPS unit (WGS84 datum). Descriptions of the habitat where specimens were collected and coloration patterns in life are based on the authors' field notes and photographs. Individuals collected in the province of Cañar were deposited at the Museo de Zoología de la Universidad del Azuay (MZUA), Ecuador, whereas individuals collected in the Loja Province were deposited in the Museo de Zoología, Universidad Técnica Particular de Loja (MUTPL), Ecuador.

Because we aimed to provide a genetic delimitation of *P. orestes* sensu stricto, we collected specimens from the type locality of *P. orestes* described in Lynch (1979) at 11 km NE Urdaneta, Loja Province in Ecuador. We reviewed the morphological characteristics of the collected specimens with the original descriptions and with the type specimens (holotypes and paratypes) available in the Kansas Museum of Natural History (KU). We also included individuals collected in Cajanuma, Loja Province, that were previously identified as *P. orestes* in earlier phylogenetic analyses. Finally, we included samples from the type series of *P. saturninoi* as well as from individuals from three nearby localities in the province of Cañar that shared similar morphological characteristics and where previously identified as *P. saturninoi*.

DNA extraction, amplification and sequencing

Total DNA was extracted from liver tissue using DNeasy Blood & Tissue kits (Qiagen, Valencia, California, USA) following the manufacturer's protocol. We amplified two mitochondrial genes (12S and 16S) and one nuclear gene (RAG-1). We obtained a 658 bp fragment of 12S using forward primer 12L29 (5'-AAAGCRTAGCACT-GAAAATGCTAAGA-3') and reverse primer 12H46 (5'-GCTGCACYTTGAC-CTGACGT-3') (Heinicke et al. 2007). To obtain a 1080 bp fragment for 16S, we

aligned the fragment obtained with forward primer 16L19 (5'-AATACCTAAC-GAACTTAGCGATAGCTGGTT-3') and reverse primer 16H36 (5'-AAGCTC-CAWAGGGTCTTCTCGTC-3') (Heinicke et al. 2007), and the fragment obtained with forward primer 16SC (5'-GTRGGCCTAAAAGCAGCCAC-3') and reverse primer 16Sbr-H (5'-CCGGTCTGAACTCAGATCACGT-3') (Darst and Cannatella 2004, Palumbi et al. 1991). We also obtained a 654 bp fragment of RAG-1 using forward primer R182 (5'-GCCATAACTGCTGGAGCATYAT-3') and reverse primer R270 (5'-AGYAGATGTTGCCTGGGTCTTC-3') (Heinicke et al. 2007). PCR conditions follow those specified by Heinicke et al. (2007) for 12S, RAG-1, and the 16S fragment obtained with primers 16L19 and 16H36. For the 16S fragment obtained with primers 16SC and 16SBR, we used PCR conditions specified in Guayasamin et al. (2017). For the samples we could not amplify under these conditions, the annealing temperature was lowered to 49 °C. The final volume of each PCR reaction was 20 µL and contained 2 µL of 10mM dNTP, 3.6 µL of OneTaq PCR buffer, 2 µL of each primer (10 µM) and 0.3 µL of 1 U OneTaq Polymerase and 1µM of DNA. PCR amplification products were cleaned using ExoSAP PCR Product Cleanup Reagent (Thermo Fisher scientific) and Sanger sequenced in both directions by Eurofins Genomics (Kentucky, USA).

Phylogenetic analysis and genetic distances

In addition to newly generated sequence data, we conducted BLAST searches to identify similar sequences of 12S, 16S and RAG-1 in GenBank. The searches show most similarity with the *Pristimantis orestes* species group: *P. simonbolivari* (identity 95%, accession number: EF493671), *P. mazar* (identity 96%, accession number KY967664), *P. orestes* (identity 99%, accession number EF493388), *P. tiktik* (identity 94%, accession number MH668274). Therefore, we included all available sequences of the *Pristimantis orestes* species group available in GenBank. To correctly place the *P. orestes* group within the broader *Pristimantis* phylogeny, we included sequences from close congeneric clades based on the phylogeny proposed by Padial et al. (2014) and defined *Strabomantis biporcatus* and *Lynchius flavomaculatus* as outgroups. A summary of GenBank accession numbers, museum collection identifiers and localities are given in Table 1.

Sequences were cleaned, assembled and aligned in GeneiousPro v. 9.1.6 (Biomatters Ltd.) using the MAFFT algorithm (Kato and Standley 2013). Manual posterior corrections of the alignment were performed to remove unnecessary gaps and to adjust the correct reading frame in the RAG-1 gene alignment. To detect possible alignment errors and significant incongruences, we first constructed single-gene trees. A Maximum Likelihood (ML) phylogenetic analysis was performed in IQ-TREE (Nguyen et al. 2015) with each individual gene alignment. Nodal support was obtained after generating 1000 samples for ultrafast bootstrap. Next, we concatenated 12S, 16S and RAG-1 alignments into a single matrix to conduct phylogenetic analyses based on all

Table 1. Species of *Pristimantis* included in this analysis. For each specimen, we provide the museum number, source, locality and GenBank accession number. (*) indicates the outgroup taxa. Museum abbreviations are as follows: MZUA (Museo de Zoología-Universidad del Azuay, Ecuador), MUTPL (Museo de Zoología, Universidad Técnica Particular de Loja, Ecuador), MEPN (Museo de Historia Natural de la Escuela Politécnica Nacional, Ecuador), KU (Kansas Museum of Natural History, USA), QCAZ (Museo de Zoología-Pontificia Universidad Católica del Ecuador, Ecuador), DHMECN (Departamento de Herpetología, Instituto Nacional de Biodiversidad del Ecuador, Ecuador).

Species	Museum number	GenBank accession number			Locality
		12S	16S	RAG-1	
<i>Pristimantis andinognomus</i>	QCAZ45661	–	KY967671	KY967690	Ecuador: Zamora Chinchipe, Tapichalaca Reserve
	QCAZ45534	–	KY967669	KY967688	Ecuador: Loja, Podocarpus National Park, guardianía Cajanuma
<i>P. bambu</i>	QCAZ46744	–	KY967659	KY967693	Ecuador: Cañar, Reserva Mazar
	QCAZ46708	–	KY967673	–	Ecuador: Cañar, Reserva Mazar
<i>P. cajanuma</i>	MUTPL160	MK993333	MK604537	–	Ecuador: Loja, Cajanuma, Podocarpus National Park, Los Miradores Trail
	MUTPL157	MK993331	MK604535	–	Ecuador: Loja, Cajanuma, Podocarpus National Park, Los Miradores Trail
	MUTPL158	MK993332	MK604536	MK602184	Ecuador: Loja, Cajanuma, Podocarpus National Park, Los Miradores Trail
<i>P. ceuthospilus</i>	KU212216	EF493520	EF493520	–	Peru: Cajamarca, Chota, 12 km W Llama
<i>P. chalceus</i>	KU177638	EF493675	EF493675	–	Ecuador: Carchi, Maldonado
<i>P. cryophilus</i>	KU217863	EF493672	EF493672	–	Ecuador: Azuay, 4 km W Laguna Torcadorn
<i>P. diadematus</i>	KU221999	EU186668	EU186668	–	Peru: Loreto, Teniente Lopez
<i>P. galdi</i>	QCAZ32368	EU186670	EU186670	EU186746	Ecuador: Zamora Chinchipe, El Pangui
<i>P. imitatrix</i>	KU215476	EF493824	EF493667	–	Peru: Madre de Dios, Cuzco Amazonico, 15 km E Puerto Maldonado
<i>P. mazar</i>	QCAZ27559	–	KY967664	KY967683	Ecuador: Cañar, Reserva Mazar, La Libertad
	QCAZ27572	JF906315	KY967666	KY967685	Ecuador: Cañar, Reserva Mazar, La Libertad
<i>P. melanogaster</i>	MHNSM56846	EF493826	EF493664	–	Peru: Amazonas, N. Slobe Abra Barro Negro, 28 km SSW Leimebambe
<i>P. munanunka</i>	MEPN14737	–	KY967661	KY967680	Ecuador: Zamora Chinchipe, Cerro Plateado
	MEPN14722	–	KY967660	KY967679	Ecuador: Zamora Chinchipe, Cerro Plateado
<i>P. orestes</i>	KU218257	EF493388	EF493388	–	Ecuador: Azuay, 7 km E Sigsig
	QCAZ45464	JF906323	–	–	Ecuador: Loja, Podocarpus National Park, guardianía Cajanuma
	QCAZ45646	JF906324	–	–	Ecuador: Loja, Podocarpus National Park, guardianía Cajanuma
	MUTPL242	–	MK604538	MK602185	Ecuador: Loja, 11 km NE Urdaneta
	MUTPL248	MK993330	MK604539	MK602186	Ecuador: Loja, 11 km NE Urdaneta
	MUTPL249	–	MK604540	–	Ecuador: Loja, 11 km NE Urdaneta
	MZUA.AN.2488	–	MK604545	MK602190	Ecuador: Loja, 11 km NE Urdaneta
QCAZ45556	–	KY967670	KY967689	Ecuador: Loja, Podocarpus National Park, Lagunas del Compadre	
<i>P. parvillus</i>	KU177821	EF493352	EF493352	–	Ecuador: Pichincha
<i>P. phoxocephalus</i>	KU218025	EF493349	EF493349	–	Ecuador: Chimborazo, 70 km W Riobamba via Pallatanga
<i>P. quintanai</i>	MZUA.AN.1748	–	MK604542	MK602187	Ecuador: Cañar, Rivera
	MZUA.AN.1881	MK993335	MK604541	MK602188	Ecuador: Cañar, Comunidad Guangras
	MZUA.AN.1878	MK993334	MK604543	–	Ecuador: Cañar, Guangras
	MZUA.AN.2705	MK993337	MK604546	MK602191	Ecuador: Cañar, Llavircay
	MZUA.AN.1900	MK993336	MK604544	MK602189	Ecuador: Cañar, Llavircay

<i>P. rhodoplichus</i>	KU219788	EF493674	EF493674	–	Peru: Piura, Le Tambo
<i>P. saturninoi</i>	DHMECN 12237	MK993329	MK604534	–	Ecuador: Morona–Santiago, Sangay National Park
	DHMECN 12232	MK993327	MK604533	–	Ecuador: Morona–Santiago, Sangay National Park
	DHMECN 12214	MK993328	MK604532	–	Ecuador: Morona–Santiago, Sangay National Park
<i>P. simonbolivari</i>	QCAZ56567		KY967676	KY967695	Ecuador: Bolívar, Bosque Protector Cashca Totoras
	KU218254	EF493671	EF493671	–	Ecuador: Bolívar, Bosque Protector Cashca Totoras
<i>P. simonsii</i>	KU212350	EU186665	EU186665	–	Peru: Cajamarca, S slope Abra Quilsh, 28 km NNW Cajamarca
<i>Pristimantis</i> sp.	QCAZ56535	–	KY967675	KY967694	Ecuador: Azuay, Laguna Patocochea
<i>Pristimantis</i> sp.	DHMECN3112	–	KY967658	KY967677	Ecuador: Zamora Chinchipe, Reserva Tapichalaca
<i>P. spinosus</i>	KU218052	EF493673	EF493673	–	Ecuador: Morona–Santiago, 10.6 km W Plan de Milogio
<i>P. tiktik</i>	MUTPL239	MH668274	MH668275	MH708575	Ecuador: Loja, 21 km E Urdaneta
	MUTPL247	MH668161	MH668276	MH708576	Ecuador: Loja, 14 km E Urdaneta
<i>P. unistrigatus</i>	KU218057	EF493387	EF493387	EF493444	Ecuador: Imbabura, 35 km E Pquela
<i>Lynchius flavomaculatus</i>	KU218210*	EU186667	EU186667	EU186745	Ecuador: Morona–Santiago, Yangana
<i>Strabomantis biporcatus</i>	CVULA7073*	EU186691	EU186691	EU186754	Venezuela: Sucre, Parque Nacional de Paria, Les Melenas, Peninsula de Paria

genes. We used PartitionFinder2 (Lanfear et al. 2016) under the corrected Bayesian information criterion to find the best model of evolution. Molecular phylogenetic relationships with the concatenated matrix were inferred using ML and Bayesian inference. ML analysis were conducted in IQ-TREE in the CIPRES Science Gateway portal (Miller et al. 2010). Nodal support was obtained after generating 1000 samples for ultrafast bootstrap. Bayesian inference was conducted in MrBayes v.3.1.2 (Ronquist et al. 2012) under Markov chain Monte Carlo sampling. We performed two independent runs of 50,000,000 generations and four chains sampling every 100 generations. The first 100,000 generations were discarded as burn-in. To visualize the generated samples from the Bayesian analysis and confirm that the posterior probability had reached a stationary local maximum, we used TRACER (Rambaut et al. 2014). The average standard deviation of split frequencies was < 0.05 and effective sample size was > 2000 for all parameters. We compared genetic distance between clades and between each individual sequence using uncorrected p distances for the 16S fragment in MEGA X (Kumar et al. 2018).

Morphological analysis

The format of the description follows Lynch and Duellman (1997) and the format of the diagnostic characters follows Duellman and Lehr (2009). Sex of each specimen was determined via direct observation of secondary sexual traits (vocal slits and vocal sac)

and gonadal inspection through abdominal incisions. Morphometric variables are based on Watters et al. (2016). We measured each variable three times using a digital caliper to the nearest 0.1 mm. We present the average, maximal, and minimal values of each morphometric character. Abbreviations for measurements are as follows: eye to nostril distance (EN), head length (HL), head width (HW), interorbital distance (IOD), internarial distance (IND), snout vent length (SVL), tibia length (TL), foot length (FL), tympanum diameter (TD), eye diameter (ED) and upper eyelid width (EW).

For the species comparison we reviewed morphological characteristics, measurements and coloration patterns of morphologically similar members of the *P. orestes* species group (Lynch and Duellman 1997) and additional similar terrestrial frogs that occur in southern Ecuador: *P. andinognomus*, *P. bambu*, *P. mazar*, *P. orestes*, *P. vidua* (Lynch, 1979), *P. simonbolivari*, *P. tiktik* and *P. saturninoi*. We based our comparisons on original descriptions of the species and via direct examination of type material available in the Kansas Museum of Natural History (KU, USA), the Zoology Museum of the Catholic University of Ecuador (QCAZ, ECU), Zoology Museum of Azuay University (MZUA, ECU), and the Instituto Nacional de Biodiversidad del Ecuador (DHMECN, ECU). Reviewed specimens are listed in Suppl. material 1.

Call recording

The calls of four *P. orestes* sensu stricto males were recorded in the field in August 2016 using an Olympus LS-11 Linear PCM Recorder and a RØDE NTG2 condenser shotgun microphone at 44.1 kHz sampling frequency and 16-bit resolution, in WAV file format (Suppl. material 2). Air temperature and humidity were measured with a data logger (Lascar Electronics, model EL-USB-2-LCD, accuracy: ± 0.5 °C; $\pm 5\%$). The original, analyzed call recordings are deposited in full length in the Fonoteca UTPL (Suppl. material 3). Acoustic analysis was conducted using Raven Pro 1.4 (<http://www.birds.cornell.edu/raven>). We measured the temporal parameters from the oscillograms and the spectral parameters from spectrograms obtained through Hanning window function, DFT: 512 samples, 3 dB filter bandwidth: 124 Hz, 50% overlap and 86.1 Hz frequency resolution.

The terminology and procedures for measuring call parameters follow Cocroft and Ryan (1995), Toledo et al. (2015) and Köhler et al. (2017) and a call-centered approach was used to distinguish between a call and a note (sensu Köhler et al. 2017). The following temporal and spectral parameters were measured and analyzed: (1) call duration: time from the beginning to the end of a call; (2) inter-call interval: the interval between two consecutive calls, measured from the end of one call to the beginning of the consecutive call; (3) call rate: number of calls per second, measured as the time between the beginning of the first call and the beginning of the last call; (4) dominant frequency: the frequency containing the highest sound energy, measured along the entire call; and (5) the 90% bandwidth, reported as frequency 5% and frequency 95%, or the minimum and maximum frequencies, excluding the 5% below and above the total energy in the selected call.

Results

Molecular systematics

Phylogenetic analyses were based on newly generated sequences from 16 individuals. The final dataset (46 terminals) including the three concatenated gene fragments consisted of 2393 bp, including 658 bp of 12S, 1080 bp of 16S and 654 bp of RAG-1. We recovered some minor differences between the RAG-1 single-gene tree and our concatenated tree, but only for very poorly supported nodes (Suppl. material 4). The best partition scheme included four subsets. The first partition subset included the 12S sequences and the best substitution model was GTR+G, and the second partition subset included 16S sequences and the best substitution model was GTR+I+G. The subset for RAG-1 was partitioned according to codon positions. Subset three included RAG-1 1st and 2nd codon positions and the best substitution model was GTR+G. Subset four included RAG-1 3rd codon positions and the best substitution model was

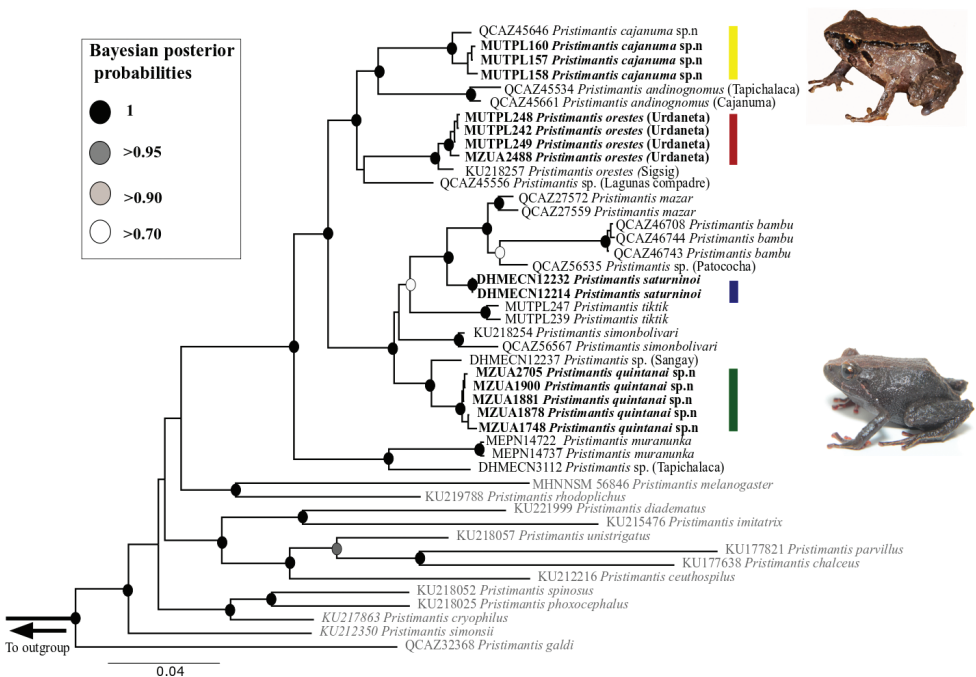


Figure 1. Bayesian phylogeny of the *Pristimantis orestes* species group based on 2393 base pairs of concatenated DNA from 12S, 16S, and RAG-1 gene fragments. Bayesian posterior probability support values are shown for each node, except when they are less than 0.70. Bolded names represent new sequences obtained in this study. Colored bars represent the following species: *P. cajanuma* sp. nov. (yellow), *P. orestes* (dark red), *P. saturninoi* (blue) and *P. quintanaei* sp. nov. (green). We rooted the tree with *Lynchiuss flavomaculatus* and *Strabomantis biporcatus*. Names in grey represent closely related clades of the *Pristimantis orestes* species group based on the phylogeny of Padial et al. (2014). Photographs of the new species *P. cajanuma* and *P. quintanaei* are shown.

Taxonomic treatment

Class Amphibia Linnaeus, 1758

Order Anura Fischer von Waldheim, 1813

Superfamily Brachycephaloidea Günther, 1858

Family Strabomantidae Hedges, Duellman & Heinicke, 2008

Subfamily Pristimantinae Pyron & Wiens, 2011

Genus *Pristimantis* Jiménez de la Espada, 1870

Pristimantis orestes (Lynch, 1979)

Fig. 2

Common English name: Urdaneta Robber Frog

Common Spanish name: Cutín de Urdaneta

Eleutherodactylus orestes Lynch, 1979

Eleutherodactylus (Eleutherodactylus) orestes: Lynch and Duellman 1997

Pristimantis orestes: Heinicke et al. 2007

Pristimantis (Pristimantis) orestes: Hedges et al. 2008

Etymology. Greek, Orestes, a mountaineer.

Type material. Holotype. KU141998, an adult female, obtained 11 km NE Urdaneta, Provincia Loja, Ecuador, 2970 m, 24 July 1971 by William E. Duellman and Bruce MacBryde.

Paratypes. KU141999–KU142003, collected syntopically with the holotype.

Diagnosis. *Pristimantis orestes* is a small species distinguished by the following combination of traits: (1) skin on dorsum finely tuberculated (in life the skin tuberculated texture is more evident); evident dorsolateral folds absent but sometimes a continuous row of pustules is present; low middorsal fold present; skin on venter areolate; discoidal fold weak, more evident posteriorly; (2) tympanic membrane absent but tympanic annulus evident, its length about 45% of the length of eye; supratympanic fold present; (3) snout short, subacuminate in dorsal view, rounded in profile; canthus rostralis weakly concave in dorsal view, rounded in profile; (4) upper eyelid bearing several small tubercles, similar in size and shape with the ones from the dorsum, about 90% IOD in females and 60% IOD in males; cranial crests absent; (5) dentigerous processes of vomers prominent, oblique, slightly ovoid, separated medially by distance lower than width of processes; each processes bearing 3 to 6 teeth; (6) males with a subgular vocal sac and small vocal slits; nuptial pads absent; (7) Finger I shorter than Finger II; discs on fingers just slightly expanded, rounded; circumferential grooves present; (8) fingers lacking lateral fringes; subarticular tubercles prominent; supernumerary palmar tubercles present, smaller than subarticular tubercles; palmar tubercle completely divided into a larger (inner) and a smaller (outer) tubercles; thenar tubercle oval, smaller than the inner palmar tubercle; (9) small, inconspicuous, ulnar tubercles present (trait more visible in life); (10) heel with small

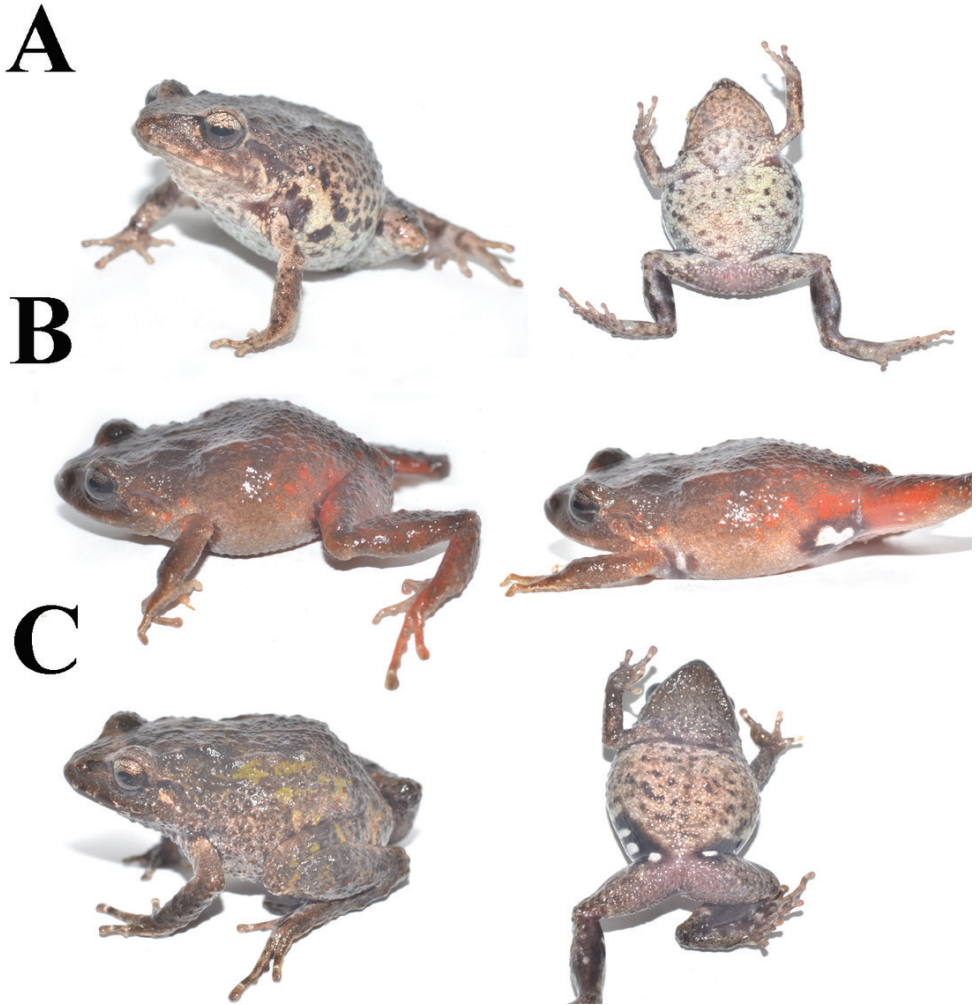


Figure 2. *Pristimantis orestes* variation in life. **A** MZUA.AN.2488, profile and ventral view **B** MZUA.AN.2493, profile view **C** MZUA.AN.2497, profile and ventral view.

tubercles; outer edge of tarsus with a row of small tubercles; inner tarsal tubercles coalesced into a short tarsal fold (traits more visible in life); (11) inner metatarsal tubercle broadly ovoid, about 2× ovoid, subconical (in profile), outer metatarsal tubercle; supernumerary plantar tubercles present; (12) toes lacking lateral fringes; webbing basal; Toe V slightly longer than Toe III; discs on toes just slightly expanded, rounded, about same size as those on fingers; circumferential grooves present; (13) in life, dorsum varies from gray, copper-brown and brown; venter gray to pale brown spotted with cream and/or brown; groin, anterior and posterior surfaces of thigh, concealed shank and axillae are dark brown or black enclosing large white spots; iris whitish gray, with a reddish broad median horizontal streak, and with fine black re-

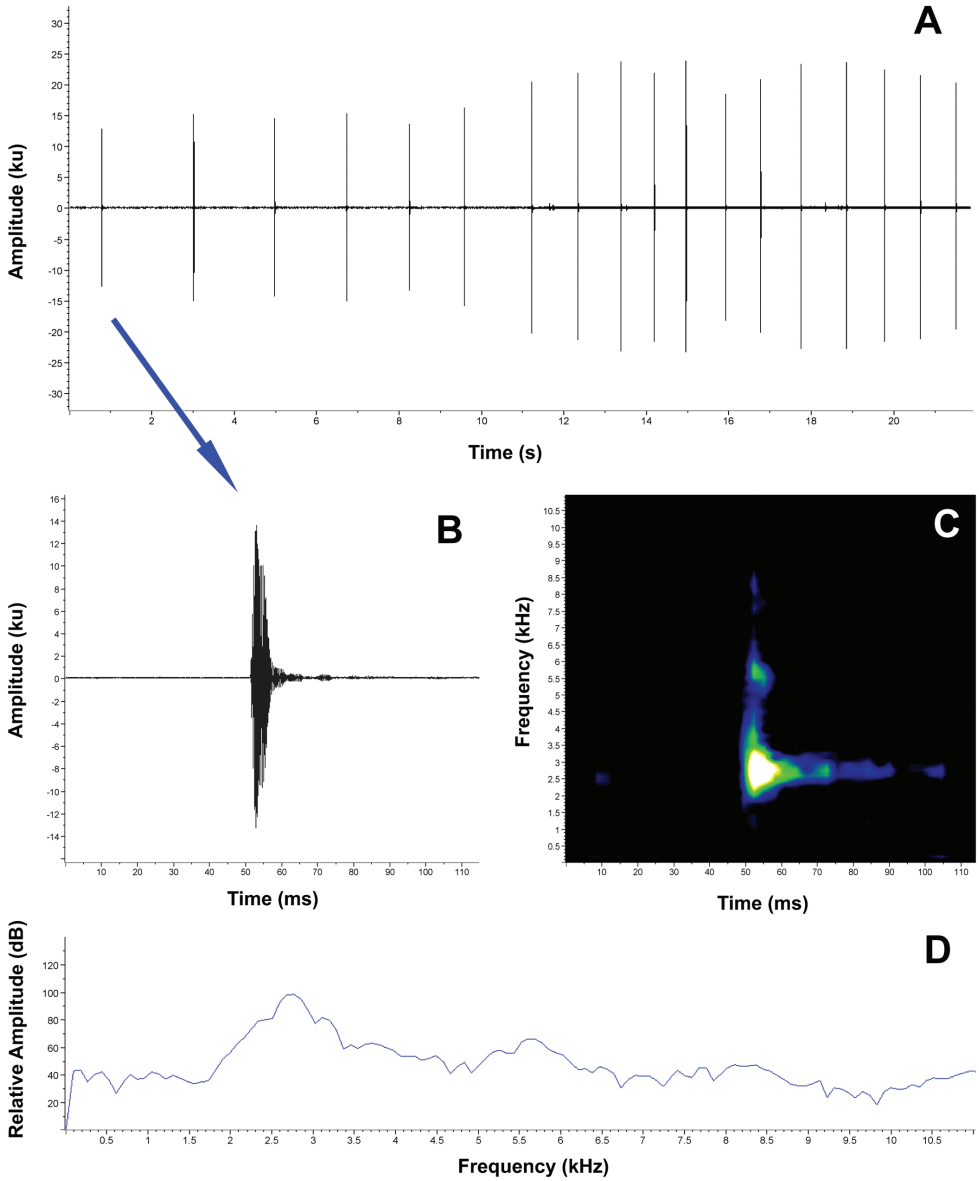


Figure 3. Advertisement call of *Pristimantis orestes*. **A** Oscillogram of a 12-call section of the call series **B** Oscillogram of a single call **C** Spectrogram of a single call **D** Power spectrum of a single call.

ticulations; (14) SVL 22.4–23.7 mm in adult females ($N = 2$) and 16.5–22.3 mm in adult males (20.1 ± 2.16 SD, $N = 5$).

Variation. Morphometric variation is shown in Table 3. In one male (MZUA.AN.2497) the discoidal fold is more visible but the ulnar tubercles are barely distinguishable both in life and in preservative. In one female (MZUA.AN.2493) a vague

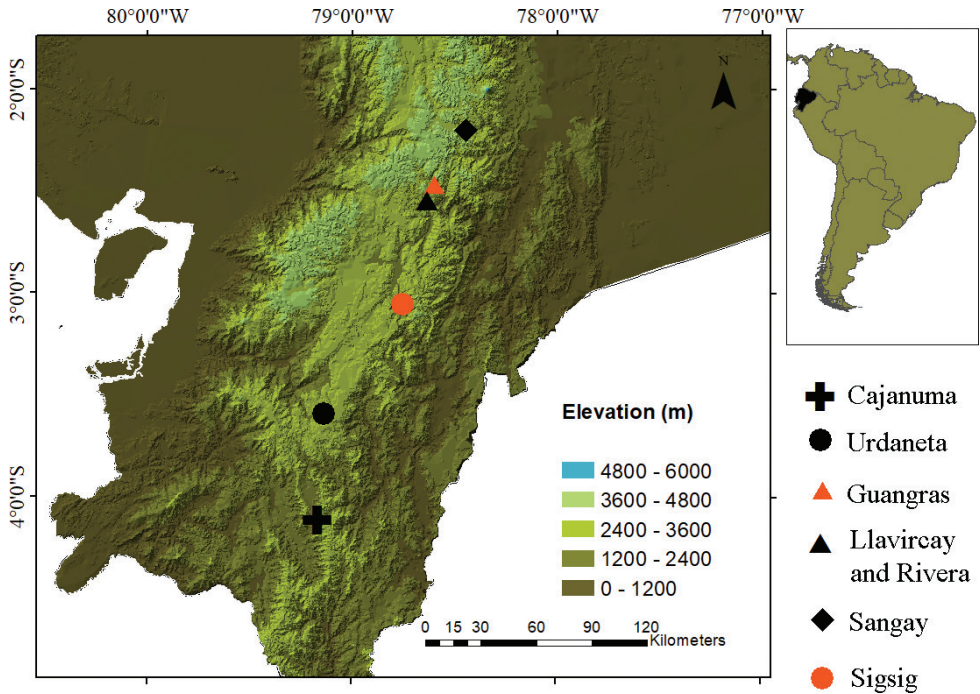


Figure 4. Map of southern Ecuador showing recording localities of *Pristimantis saturninoi*, *P. quintanai* sp. nov., *P. orestes*, and *P. cajanuma* sp. nov.

dorsolateral fold (formed by a continuous row of pustules) is present in the anterior half of dorsum and the middorsal fold is not distinguishable; in this same individual the ulnar tubercles are more notorious than in the other preserved specimens. In a female (MZUA.AN.2497), the dorsum and dorsal surfaces of limbs display a brownish-green coloration; the flanks and lips are dark brown with irregular cream blotches. One male (MZUA.AN.2488) presents orange spots over a brown background in the dorsum, flanks and limbs and a continuous orange blotch in the groin and anterior surfaces of thighs (Fig. 2).

Advertisement call. Two of the analyzed recordings (FUTPL-A-130 and FUTPL-A-131) are from the same unvouchered male. *Pristimantis orestes* has an advertisement call characterized by a call series composed by clicking calls repeated for long periods of time (Fig. 3). Because the males can call continuously for long periods of time, the call series duration is unknown. The calls are characterized by a duration of (range and mean \pm SD in parenthesis): 0.008–0.013 s (0.011 ± 0.0009 , $N = 190$), an inter-call interval of 0.705–3.824 s (1.680 ± 0.650 , $N = 185$) and a call rate of 0.50–0.73 calls/s (0.58 ± 0.110 , $N = 4$). The 90% bandwidth ranged from 2325.6–2756.2 Hz (2605.7 ± 88.555 , $N = 190$) to 2756.2–3186.9 Hz (2989.2 ± 115.100 , $N = 190$), with the dominant frequency being at 2670.1–2928.5 Hz (2773.5 ± 77.359 , $N = 190$). The fundamental frequency is not recognizable, but 2 to 3 harmonics are sometimes visible.

Table 3. Measurements (in mm) of adult males and females of *Pristimantis orestes* collected from Urdaneta. The mean and standard deviation (SD) of each morphological character are shown for males ($N = 5$) but not females due to sample size ($N = 1$). Abbreviations of the morphometric measurements are presented in Materials and methods.

	MZUA 2488 ♀	MZUA 2493 ♂	MZUA 2497 ♂	MUTPL 242 ♂	MUTPL 248 ♂	MUTPL 249 ♂	Mean \pm SD (range) ♂
SVL	22.4	20.0	16.5	20.7	20.8	22.3	20.1 \pm 2.2 (16.5–22.3)
EN	2.2	1.7	1.5	1.7	1.7	1.8	1.7 \pm 0.1 (1.5–1.8)
TD	1.5	0.9	0.8	1.2	1.3	1.4	1.1 \pm 0.3 (0.7–1.4)
ED	2.5	2.3	2.0	2.4	2.4	2.5	2.3 \pm 0.2 (2.0–2.5)
EW	1.8	1.8	1.4	1.6	1.8	2.0	1.7 \pm 0.2 (1.4–2.0)
IOD	3.1	2.4	2.2	2.9	2.9	3.1	2.7 \pm 0.4 (2.2–3.1)
IND	1.8	1.8	1.4	1.9	1.6	2.1	1.8 \pm 0.3 (1.4–2.1)
HL	6.7	5.5	6.1	7.4	7.4	7.6	6.8 \pm 0.9 (5.5–7.6)
HW	6.5	8.3	6.8	7.7	7.5	7.9	7.6 \pm 0.6 (6.8–8.3)
TL	9.2	9.0	8.2	9.0	9.0	9.4	8.9 \pm 0.4 (8.2–9.4)
FL	8.2	8.3	7.8	8.7	8.7	8.9	8.5 \pm 0.4 (7.8–8.9)

Three of the four recorded males increased the call rate at the end of their calls (Fig. 3), intensifying the call emissions in the last 20–30 seconds. The call rate increased, and the inter-call interval decreased from 0.35–0.63 calls/s (0.47 ± 0.145 , $N = 3$) to 0.70–1.06 calls/s (0.88 ± 0.177 , $N = 3$), respectively, and from 1.063–3.824 s (2.111 ± 0.672 , $N = 64$) to 0.705–2.087 s (1.253 ± 0.401 , $N = 88$).

Distribution. Lynch (1979) states that this species occurs on the eastern Andean Cordillera from the Cuenca hoya to the Loja hoya in southern Ecuador. However, we suggest that this distribution might be inaccurate and needs to be reviewed, as many of the records are probably erroneous belonging to very similar, but in fact different species. For example, additional localities previously reported by Lynch (1979) from the Loja Province include Saraguro, but this record is likely erroneous, and refers to observations of an undescribed, very similar species. Guayasamin and Arteaga (2013) also reported *P. orestes* from Susudel in the Azuay province (MZUTI 706), but this record needs to be reviewed via molecular and morphological analysis to confirm identity of this specimens. Thus, we recommend limiting the distribution of *P. orestes* to the confirmed localities in Urdaneta and in Sigsig, in an elevational range between 2940 to 3100 m (Fig. 4).

Natural history. We found all the specimens in a pastureland in a subpáramo habitat. Specimens were encountered at night on grassy vegetation (usually at 10–20 cm above the ground) near the road. Calling males were encountered between May and August. The only sympatric frog species registered was *Gastrotheca pseustes*.

Conservation status. *Pristimantis orestes* is categorized as endangered based on criteria B1b(iii) (IUCN 2018). We suggest maintaining this category because the species i) has only been found in two localities, and ii) its natural habitat (páramo and

subpáramo) has been heavily damaged and fragmented by grazing, fires and roads. Also, in its type locality, *P. orestes* is not locally abundant, only few individuals were registered at every visit to the population. However, additional information is needed to evaluate population trends and to assess the presence and impact of pathogenic infections in this species.

Remarks. Lynch (1979) provides an accurate and detailed description of this species, including a brief description of the cranial osteology. Our diagnosis concurs with all the morphological features described by the author, but we also focus on characters that were not detailed in the original description but that are useful to distinguish *P. orestes* from other similar species (e.g., condition of discoidal fold and nuptial pads in males). The only significant difference is that the outer tarsal tubercles are not prominent, and we consider the color of the iris to be whitish gray instead of gray-bronze (Fig. 2). The diagnosis provided herein is based on four specimens from the original description (KU 141998, 141999, 142000, 142002): one adult female (MZUA.AN.2488) and five adult males (MUTPL 242, 248, 249 and MZUA.AN.2493, 2497) collected from the type locality.

***Pristimantis cajanuma* sp. nov.**

<http://zoobank.org/B00AB277-06B5-4F73-84E1-38EBC5E870D8>

Figs 5–8

Common English name: Cajanuma Rain Frog

Common Spanish name: Cutín de Cajanuma

Type material. Holotype. MUTPL 346 (Figs 5–7), field no. SC 159, adult female from Ecuador, Loja Province, Loja canton, Cajanuma entrance to the Podocarpus National Park, on Los Miradores trail (4.1176S, 79.1663W; datum WGS84), 3022 m above sea level, collected by Diana Székely and Paul Székely on 28 June 2018.

Paratypes (Fig. 8) 16 specimens collected in the type locality: MUTPL 343 (SC 156) an adult female and MUTPL 344 (SC 157) a juvenile (4.1170S, 79.1668W; datum WGS84), 2974 m, MUTPL 345 (SC 158) a juvenile (4.1176S, 79.1663W; datum WGS84), 3022 m, MUTPL 347 (SC 160) an adult female and MUTPL 353 (SC 166) a subadult male (4.1177S, 79.1658W; datum WGS84), 3042 m, and MUTPL 352 (SC 165) a subadult male and MUTPL 355 (SC 168) an adult male (4.1177S, 79.1647W; datum WGS84), 3098 m collected by Diana Székely and Paul Székely on 28 June 2018; MUTPL 573 (SC 331) a subadult female (4.1166S, 79.1691W; datum WGS84), 2890 m collected by Diana Székely and Paul Székely on 09 December 2018; MUTPL 583 (SC 903) an adult female and MUTPL 584 (SC 904) a subadult female (4.1167S, 79.1690W; datum WGS84), 2883, MUTPL 588 (SC 908) and MUTPL 592 (SC 912) two juveniles, MUTPL 589 (SC 909) and MUTPL 591 (SC 911) two subadult females, and MUTPL 593 (SC 913) and MUTPL 594 (SC 914) two adult males (4.1169S, 79.1666W; datum WGS84), 2984 m collected by Diana Székely and Paul Székely on 05 January 2019.

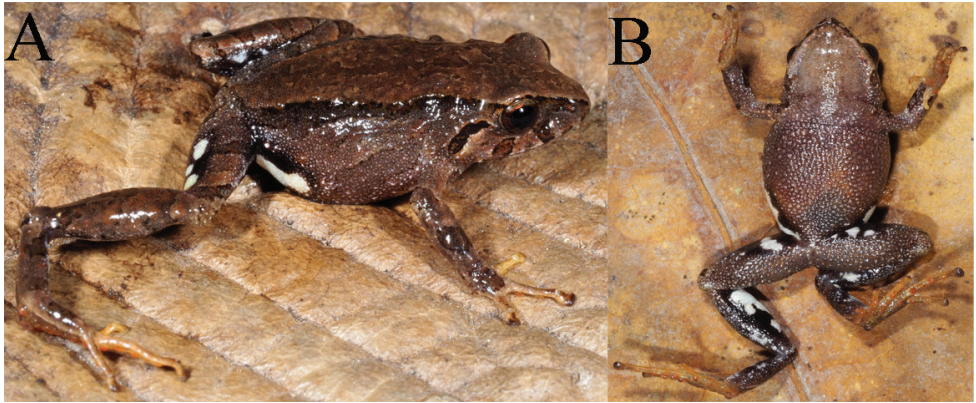


Figure 5. Holotype of *Pristimantis cajanuma* sp. nov. in life. **A** dorsolateral view **B** ventral view.

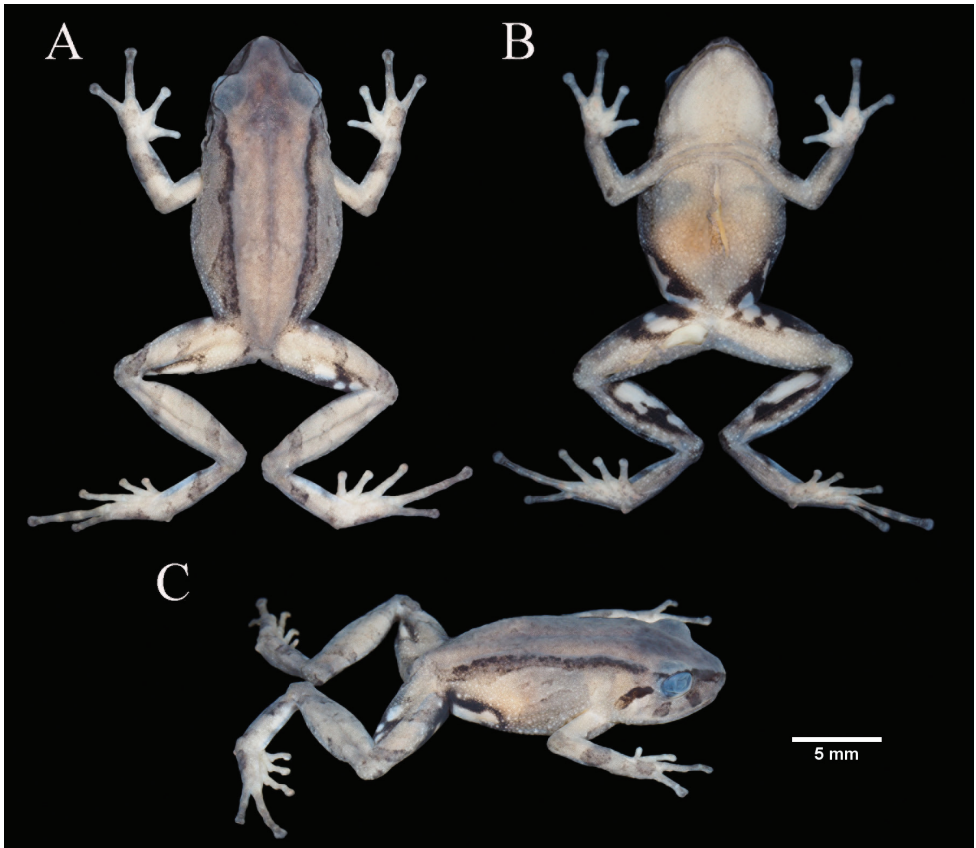


Figure 6. Holotype of *Pristimantis cajanuma* sp. nov. in preservative, adult female MUTPL 346: **A** dorsal view **B** ventral view **C** lateral view.

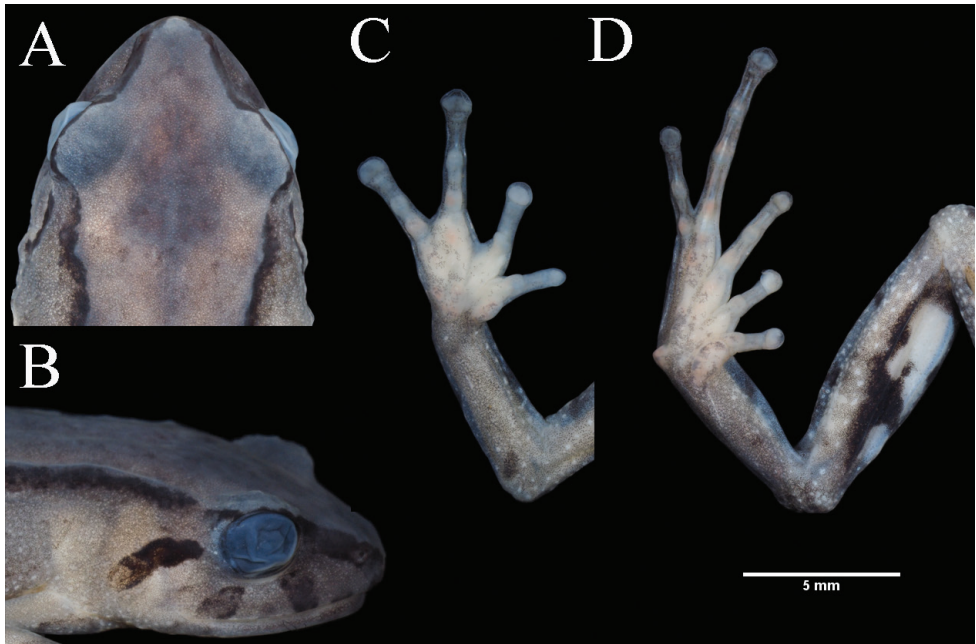


Figure 7. Holotype of *Pristimantis cajanuma* sp. nov. in preservative, adult female MUTPL 346: **A** dorsal view of head **B** profile view of head **C** palmar surfaces **D** plantar surfaces.

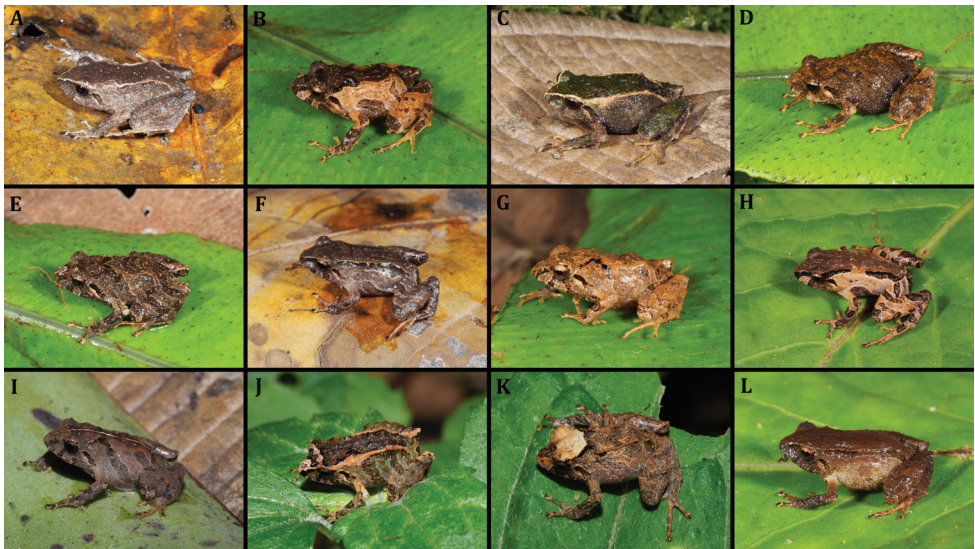


Figure 8. Color variation of *Pristimantis cajanuma* sp. nov. in life. **A–E** females: **A** MUTPL 343 **B** MUTPL 591 **C** MUTPL 347 **D** MUTPL 583 **E** MUTPL 584; **F–H** juveniles: **F** MUTPL 345 **G** MUTPL 588 **H** MUTPL 592 **I–L** males: **I** MUTPL 353 **J** MUTPL 352 **K** MUTPL 355 **L** MUTPL 594.

Diagnosis. *Pristimantis cajanuma* is a small species distinguished by the following combination of traits: (1) skin on dorsum shagreen; skin on venter areolate (trait more visible in life); discoidal fold weak; dorsolateral folds present; low middorsal fold present; (2) tympanic membrane absent but tympanic annulus evident, its length about 45% of the length of eye; supratympanic fold present; (3) snout short, subacuminate in dorsal view, rounded in profile; canthus rostralis concave in dorsal view, angular in profile; (4) upper eyelid bearing several small tubercles, about 60% IOD in females and 65% IOD in males; cranial crests absent; (5) dentigerous processes of vomers prominent, triangular, without space between the processes; each processes bearing 4 to 7 teeth; (6) males with subgular vocal sac and vocal slits; nuptial pads absent; (7) Finger I shorter than Finger II; discs on fingers expanded, rounded; circumferential grooves present; (8) fingers lacking lateral fringes; subarticular tubercles prominent; supernumerary palmar tubercles present, rounded, smaller than subarticular tubercles; palmar tubercle bifurcated (partially divided distally); thenar tubercle oval; (9) small, inconspicuous, ulnar tubercles present (trait more visible in life); (10) heel with small tubercles; outer edge of tarsus with a row of small tubercles; inner tarsal tubercles coalesced into a short tarsal fold; (11) inner metatarsal tubercle broadly ovoid, about 2× round, subconical (in profile) outer metatarsal tubercle; supernumerary plantar tubercles present; (12) toes lacking lateral fringes; webbing basal; Toe V slightly longer than Toe III; discs on toes expanded, rounded, about same size as those on fingers; circumferential grooves present; (13) in life, dorsum of various shades of brown, gray or sometimes green, with or without darker bands or bars; flanks various shades of brown or gray, usually lighter than the dorsum coloration; venter light gray with or without dark flecks; groin, anterior and posterior surfaces of thighs, concealed shanks and axillae are black enclosing large white spots; iris bronze with a reddish broad median horizontal streak, and with fine black reticulations; SVL 17.6–22.1 mm in adult females (19.8 ± 1.81 SD, $N = 8$) and 14.4–16.4 mm in adult males (15.4 ± 0.83 SD, $N = 5$).

Comparison with similar species. *Pristimantis cajanuma* is morphologically similar to its closest relatives, the species from the recently redefined *P. orestes* group (sensu Brito et al. 2017), but its characteristic morphological features readily distinguish it from all resembling species. *Pristimantis cajanuma* is most similar to *P. orestes* sensu stricto but can be easily distinguished by having evident dorsolateral folds (absent in *P. orestes*), a shagreen skin on dorsum (finely tuberculated in *P. orestes*), broader discs on the fingers and toes (e.g. width of disc on Finger III in *P. cajanuma*: 0.8–1 mm, $N = 3$; in *P. orestes*: 0.6–0.7 mm, $N = 3$), palmar tubercle bifurcated, only partially divided distally (completely divided into a larger and a smaller tubercle in *P. orestes*) and by the more widespread black coloration in the groin and concealed shanks (Fig. 9). Its sister species, *P. andinognomus* is significantly smaller (females up to 17 mm, males up to 14 mm; Lehr and Coloma 2008), has the Toe V much longer than Toe III (Toe V slightly longer than Toe III in *P. cajanuma*) and lacks the typical black enclosing large white spots coloration of the groin, anterior and posterior surfaces of thighs, concealed shanks and axillae of *P. cajanuma*.

Pristimantis simonbolivari has a similar coloration of the groin, anterior and posterior surfaces of thighs, concealed shanks and axillae but lacks dorsolateral folds (present

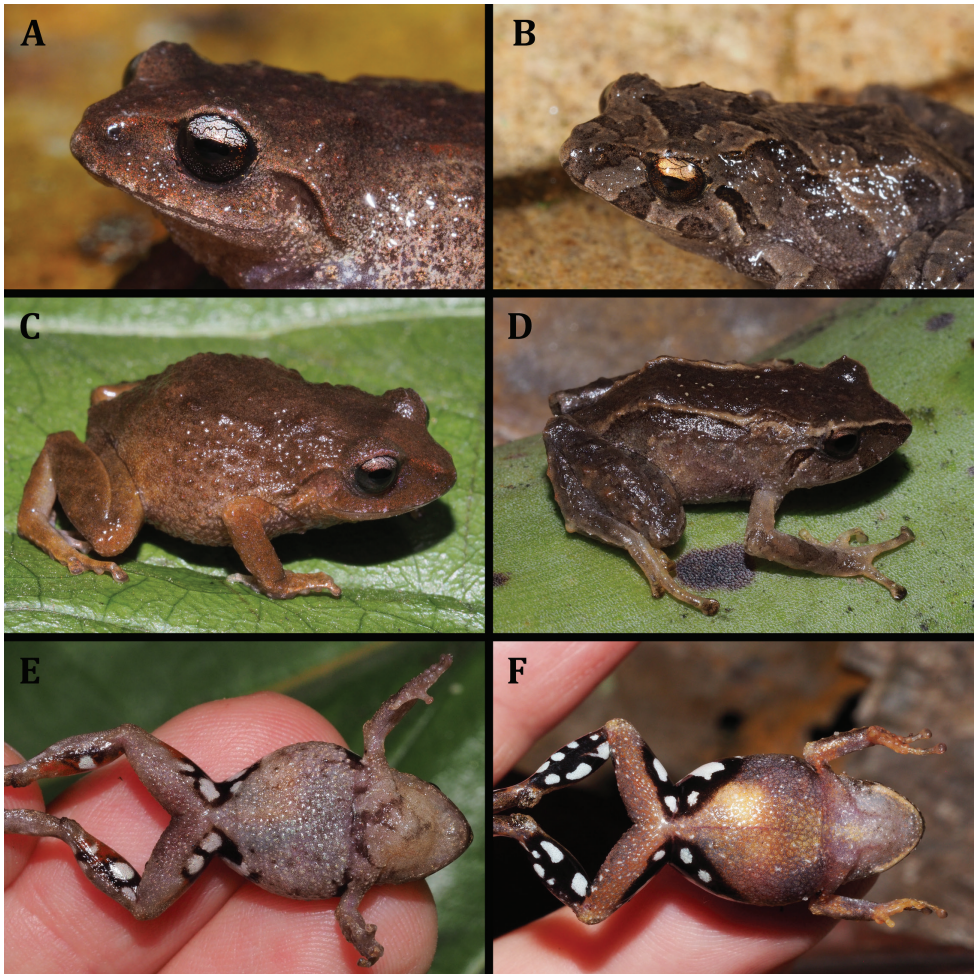


Figure 9. Morphological differences between *Pristimantis orestes* sensu stricto (A, C, E) and *P. cajanuma* sp. nov. (B, D, F): whitish gray iris (A) vs. bronze iris (B) dorsolateral folds absent (C) vs. dorsolateral folds present (D); and limited black coloration in the groin and concealed surfaces of shanks (E) vs. wide-spread black coloration (F).

in *P. cajanuma*) and its venter coloration is darker, orange or brown (light gray in *P. cajanuma*). *Pristimantis saturninoi* and *P. quintanai* sp. nov. also have similar coloration of the groin, thighs and shanks but *P. saturninoi* has a black or blackish-amber venter (venter light gray in *P. cajanuma*) and green iris (bronze in *P. cajanuma*). *Pristimantis quintanai* sp. nov. is different by having a finely tubercular dorsum skin (shagreen in *P. cajanuma*), and by having a black, reddish-brown or reddish-cream venter coloration.

All other species of the *P. orestes* group (sensu Brito et al. 2017) lack the typical coloration of the groin, thighs, shanks and axillae of *P. cajanuma*: *Pristimantis bambu* has large yellow spots; *P. mazar* has a reticulated pattern, *P. tiktik* presents a black reticulum

in the females and whitish/pinkish yellow coloration in the males and *P. muranunka* shows a brown or dark brown uniform coloration.

Description of holotype. Adult female (MUTPL 346) (Figs 5–7) with head narrower than body, wider than long, HL 92% of HW, HW 36% of SVL; HL 33% of SVL; snout short (snout to eye distance 16% of SVL), subacuminate in dorsal view, rounded in profile (Fig. 7A, B); canthus rostralis concave in dorsal view, angular in profile; loreal region flat; ED notably greater than eye-nostril distance; nostrils not protuberant; lips not flared; cranial crests absent; upper eyelid bearing several small tubercles (one slightly larger than the others), width of upper eyelid 64% of IOD; half of tympanic annulus evident (Fig. 7B), oval (slightly higher than wider), its upper and posterodorsal part obscured by rounded supratympanic fold; tympanic membrane absent; diameter of tympanum 52% of the length of eye; postictal tubercles are fused and form a short ridge situated posteroventrally to tympanic annulus; choanae small, round, partially concealed by palatal shelf of maxillary arch; dentigerous processes of vomers prominent, triangular in outline, much larger than the choanae, without space between the processes, each bearing 4 or 5 teeth; tongue 1.5× as long as wide, slightly notched posteriorly, posterior half not adherent to floor of mouth.

Skin on dorsum shagreen, that on flanks is finely tuberculated; thin, low middorsal fold starting at tip of snout and ending at cloaca; long, continuous dorsolateral folds present (Fig. 6A); skin of throat shagreen, that on chest and belly areolate; discoidal fold weak, barely visible (Fig. 6B); ornamentation in cloacal region absent.

Ulnar tubercles small, inconspicuous (trait more visible in life); outer palmar tubercle inconspicuous, bifurcated (partially divided distally); thenar tubercle oval; subarticular tubercles prominent, round and subconical in section; supernumerary palmar tubercles rounded, smaller than subarticular tubercles; fingers lacking lateral fringes; Finger I shorter than Finger II; discs on fingers expanded, rounded; all fingers bearing pads well defined by circumferential grooves (Fig. 7C).

Hindlimbs short; TL 50% of SVL; FL 47% of SVL; heel with small tubercles (one slightly larger than the others); outer edge of tarsus with a row of small tubercles (trait more visible in life); inner edge of tarsus bearing a short fold; inner metatarsal tubercle broadly ovoid, about 2× round and subconical (in profile) outer metatarsal tubercle; subarticular tubercles prominent, round and subconical in section; plantar supernumerary tubercles rounded, smaller than subarticular tubercles; toes lacking lateral fringes; webbing basal; discs on toes expanded, rounded, about same size as those on fingers; toes with ventral pads well defined by circumferential grooves; relative length of toes I < II < III < V < IV; Toe V slightly longer than Toe III (tip of Toe III not reaching the penultimate subarticular tubercle on Toe IV, tip of Toe V not reaching the proximal edge of distal subarticular tubercle on Toe IV) (Fig. 7D).

Measurements of holotype. SVL 20.6; HW 7.5; HL 6.9; IOD 2.4; internarial distance 1.7; upper EW 1.5; ED 2.3; eye-nostril distance 1.8; snout to eye distance 3.2; TD 1.2; TL 10.2; FL 9.7.

Body mass of holotype: 1.01 g.

Coloration of holotype. In life (Fig. 5) the dorsum is brown with dark mottling and with the dorsolateral folds blackish-dark brown. Flanks grayish-brown with white flecks. Dorsal surfaces of hindlimbs and arms the same color as the dorsum but with dark brown transverse bars. The head bears blackish-dark brown canthal, labial and supratympanic stripes. The throat is whitish gray and the venter is brownish-gray with white flecks. Groin, anterior and posterior surfaces of thighs, concealed shanks and axillae are black enclosing large white spots. The dorsal and ventral surfaces of the hands and feet are reddish-orange. The iris is bronze with a reddish broad median, horizontal streak, and with fine black reticulations.

In preservative (Figs 6, 7) the dorsum is brownish gray and the flanks whitish gray with white flecks. All the blackish-dark brown coloration of the dorsolateral folds, canthal, labial and supratympanic stripes in life became dark gray in preservative. Also, the black enclosing the large white spots of the groin, anterior and posterior surfaces of thighs, concealed shanks and axillae in life turned to dark gray in preservative. The dorsal and ventral surfaces of the hands and feet are whitish gray.

Variation. Morphometric variation is shown in Table 4. The dorsolateral folds were fragmented in some of the specimens (Figs 8E, G, I, 9B) and thus not so evident, but all encountered individuals (probably more than 50) had dorsolateral folds. *Pristimantis cajanuma* displays a considerable variation in the dorsal coloration (Figure 8). We encountered individuals with a general gray (Fig. 8A, E, F, I, K), light brown (Fig. 8G), dark brown (Fig. 8D, L), light brown with a dark brown middorsal band (Fig. 8B, H) and even green (Fig. 8C, J) coloration. Some of the individuals had chevrons on the dorsum (Fig. 8E) and/or dark transverse bars on the flanks and limbs (Fig. 8E, I, J), white or yellowish dorsolateral folds (Fig. 8A, C, J), white middorsal fold (Fig. 8I) and even completely whitish-yellow head (Fig. 8K). As for the sexual dimorphism, besides the size difference (the males are significantly smaller), the only identified coloration difference is that the males are lacking the characteristic large white spots enclosed by black of the groin, anterior and posterior surfaces of thighs, concealed shanks and axillae. From the encountered individuals, only the specimen MUTPL 353 had a similar coloration of the groin, but significantly fainter.

The dorsolateral folds are already visible in the juveniles (Fig. 8F, G, H), but the large white spots enclosed by black in the groin, anterior and posterior surfaces of thighs, concealed shanks and axillae are not so conspicuous and probably become darker and more evident as the animals mature. The identity of all the specimens was confirmed molecularly using the 16S mitochondrial gene.

Etymology. The specific epithet *cajanuma* (in Quechua language “*cajan*” means cold and “*uma*” peak, or head, in other words the cold peak, referring to the cold climate of the area) is used as a noun in apposition and refers to the region where the species is found. Cajanuma is the highest entrance to the Podocarpus National Park, which is one of the largest and most diverse protected area from Ecuador. By naming this species *cajanuma* we also want to honor and recognize the Podocarpus National Park rangers for their extraordinary and tireless work protecting this incredible reserve.

Table 4. Measurements (in mm) of adult males and females of *Pristimantis cajanuma* sp. nov. Mean and standard deviation (SD) values of each morphological character are shown for females ($N = 8$) and males ($N = 5$). Abbreviations of the morphometric measurements are presented in Materials and methods.

	MUTPL													Mean \pm SD (range) ♀	Mean \pm SD (range) ♂
	343 ♀	346 ♀	347 ♀	573 ♀	583 ♀	584 ♀	589 ♀	591 ♀	352 ♂	353 ♂	355 ♂	593 ♂	594 ♂		
SVL	20.7	20.6	22.0	18.5	22.1	18.4	18.1	17.6	14.4	14.9	16.1	16.4	15.2	19.8 \pm 1.8 (17.6–22.1)	15.4 \pm 0.8 (14.4–16.4)
EN	1.7	1.8	1.7	1.7	1.7	1.6	1.6	1.6	1.3	1.3	1.3	1.3	1.3	1.7 \pm 0.1 (1.6–1.8)	1.3 (1.3)
TD	1.1	1.2	1.2	0.9	1.2	0.8	0.9	0.9	0.7	0.9	0.9	0.8	0.7	1.1 \pm 0.7 (0.8–1.2)	0.8 \pm 0.1 (0.7–0.9)
ED	2.3	2.3	2.4	2.3	2.5	2.2	2.2	2.2	1.9	2.0	2.1	1.9	1.7	2.3 \pm 0.1 (2.2–2.5)	1.9 \pm 0.1 (1.7–2.1)
EW	1.5	1.5	1.6	1.2	1.7	1.4	1.2	1.3	1.2	1.2	1.3	1.2	1.2	1.4 \pm 0.2 (1.2–1.7)	1.2 \pm 0.1 (1.2–1.3)
IOD	2.5	2.4	2.5	2.4	2.5	2.2	2.4	2.1	1.7	1.8	2.0	2.0	1.9	2.4 \pm 0.2 (2.1–2.5)	1.9 \pm 0.1 (1.7–2.0)
IND	1.8	1.7	1.9	1.7	2.0	1.7	1.7	1.7	1.4	1.5	1.6	1.6	1.6	1.8 \pm 0.1 (1.7–2.0)	1.5 \pm 0.1 (1.4–1.6)
HL	6.8	6.9	7.6	5.8	7.5	5.8	5.8	5.7	5.2	5.4	5.7	5.7	5.3	6.5 \pm 0.8 (5.7–7.6)	5.5 \pm 0.2 (5.2–5.7)
HW	7.5	7.5	8.1	6.5	7.8	6.9	6.7	6.3	4.9	5.2	5.6	5.9	5.7	7.2 \pm 0.7 (6.3–8.1)	5.5 \pm 0.4 (4.9–5.9)
TL	10.5	10.2	10.7	9.5	10.8	9.3	9.2	9.1	7.3	7.7	8.0	8.0	7.9	9.9 \pm 0.7 (9.1–10.8)	7.8 \pm 0.3 (7.3–8.0)
FL	9.1	9.0	9.6	8.9	10.2	8.9	8.4	8.2	6.8	7.4	7.6	7.5	7.4	9.1 \pm 0.6 (8.2–10.2)	7.3 \pm 0.3 (6.8–7.6)

Distribution and natural history. *Pristimantis cajanuma* is known only from the Cajanuma entrance to the Podocarpus National Park, in an altitudinal range between 2882 and 3097 m a.s.l. in a Mountain Cloud Forest ecosystem. All specimens were encountered during the night, perching on the vegetation (usually at 10–40 cm above the ground), near the Los Miradores trail. No calling males were encountered. Other sympatric frog species include *Pristimantis andinognomus*, *P. vidua* and an undescribed species of *Pristimantis*.

Conservation status. Even though *Pristimantis cajanuma* is currently known only from the type locality in the Podocarpus National Park, we recommend that this species to be categorized as Near Threatened following the IUCN criteria. This is due the fact that the species is locally abundant and its habitat does not face any major threats (because it is situated within a national protected area). However, at present its distribution is limited to only one locality, therefore there is some level of threat.

***Pristimantis quintanai* sp. nov.**

<http://zoobank.org/33697F57-D0C2-470F-8750-5ECF80546904>

Figs 10–12

Common English name: Quintana's Rain Frog

Common Spanish name: Cutín de Quintana

Type material. Holotype. MZUA.AN.1881 (Figs 10–12), an adult female collected in Guangras, Rivera parish, Azogues canton, Cañar Province, Ecuador (2.4826S, 78.6019W; datum WGS84), 2527 m above sea level, by Juan C. Sanchez-Nivicela, Amanda Quezada Bruno Timbe and Jhonny Cedeño.

Paratypes. Two males MZUA.AN.1880, MZUA.AN.1900, three females MZUA.AN.1873, MZUA.AN.1885, MZUA.AN.1874 and a subadult female MZUA.



Figure 10. Holotype of *Pristimantis quintanai* sp. nov. in life.

AN.1890 collected with the holotype. Two females MZUA.AN.1746, MZUA.AN.1748 and a subadult female MZUA.AN.1747 collected from Rivera, Rivera parish, Azogues canton, Cañar Province, Ecuador (2.5459S, 78.6303W; datum WGS84), 2699 m by Juan C. Sanchez-Nivicela, Eduardo Toral and Veronica L. Urgiles and a female MZUA.AN.2705 collected from Llavircay Rivera parish, Azogues canton, Cañar Province, Ecuador (2.5637S, 78.5957W; datum WGS84), 2830 m by Amanda Quezada and Jhonny Cedeño.

Diagnosis. *Pristimantis quintanai* is a small species characterized by: (1) skin of dorsum finely tuberculated with low and rounded tubercles that vary in size (character more noticeable in life), notorious dermal crests, elevated; skin on venter coarsely areolate, dorsolateral folds present, low, middorsal fold low, discoidal fold barely noticeable; low sinusoidal scapular fold; (2) tympanic membrane indistinct, tympanic annulus differentiated, visible, rounded (57% of ED), postrictal tubercles present; (3) short snout, slightly subacuminate in dorsal view, rounded in profile, canthus rostralis concave; (4) upper eyelid with one or two rounded tubercles and with several low ones, cranial crest absent; (5) dentigerous processes of vomer oblique, with one to two teeth, rounded choana; (6) males have small vocal slits but lack vocal sac and nuptial pads; (7) Finger I shorter than Finger II, discs rounded, with dilated pads in all fingers, well defined circumferential grooves; (8) lateral fringes of finger barely noticeable; (9) ulnar tubercles present, lacking antebrachial tubercles; (10) heel with one rounded and several low tubercles, shank lacking tubercles, tarsal tubercles low and small; (11) lateral fringes on toes barely noticeable, webbing absent; Toe V longer than Toe III; discs of toes rounded, dilated pads in all toes, well defined circumferential grooves; (12) inner

metatarsal tubercles ovoid two times bigger than outer one, rounded; supernumerary plantar tubercles very low and small, smaller than subarticular tubercles; (13) iris grayish-gold with thin dark reticulations and a horizontal reddish stripe in the middle of the eye, dorsal coloration varies between dark brown, or light brown with cream; flanks vary between dark brown with minute white spots to light cream or yellowish-cream with minute white spots; ventral coloration varies between black, light reddish-brown or reddish-cream; groin and concealed surfaces of thighs are black with white irregular spots (whitish-cream and smaller in males); (14) SVL 19.0–21.8 mm in adult females (20.5 ± 0.90 SD, $N = 6$) and 15.5–16.4 mm in adult males (16.0 ± 0.64 SD, $N = 2$).

Comparison with similar species. *Pristimantis quintanai* is morphologically most similar to *P. simonbolivari*, *P. orestes*, and *P. saturninoi* from the *P. orestes* complex. The new species is similar to *P. saturninoi*, *P. orestes* sensu stricto, and *P. cajanuma* and *P. simonbolivari* in having white spots on the groin. However, it can be distinguished from *P. saturninoi* by having expanded discs in fingers and toes (narrower in *P. saturninoi*), by lacking tympanic membrane, and because males lack nuptial pads. The new species differs from *P. orestes* sensu stricto by having a low dorsolateral fold, a ventral coloration that varies between black, reddish-brown or reddish-cream (gray to pale brown spotted with cream and brown in *P. orestes*), and because males lack vocal sacs. *Pristimantis quintanai* is different from *P. cajanuma* by having a finely tuberculated dorsal skin and a ventral coloration that can vary between black, reddish-brown or reddish-cream (light gray with or without dark flecks and skin texture shagreen in *P. cajanuma*). *Pristimantis quintanai* differs from *P. simonbolivari* by having a finely tuberculated dorsal skin (smooth in *P. simonbolivari*), males with vocal sacs, and a row of ulnar tubercles (indistinct in *P. simonbolivari*).

Pristimantis bambu is different from the new species by having a finely granular dorsal skin, ulnar tubercles coerced into a fold, vocal sacs in males (absent in *P. quintanai*), yellow coloration in the groin, and by lacking tubercles on the heel (one small rounded and several low in *P. quintanai*). *Pristimantis mazar* is different by lacking tubercles on the upper eyelid (one or two small rounded and several low in *P. quintanai*) and by having a well differentiated tympanic membrane, a dark reticulated pattern in the groin, a creamish-gray to dark brownish gray dorsal coloration and a whitish-cream coloration in the venter. *Pristimantis andinognomus* is different from the new species by having enlarged conical tubercles on heel and upper eyelids (one or two rounded and several low in *P. quintanai*), a differentiated tympanic membrane, males with vocal sacs and pale copper dorsal coloration. *Pristimantis vidua* is different by having a finely granular dorsal skin and by lacking ulnar tubercles. Finally, *P. tikitik* is different by lacking dorsolateral folds (present, low in *P. quintanai*) and because males have vocal sacs, a reddish coloration on the groin (irregular white or whitish-cream in *P. quintanai*) and a ventral coloration that varies between various shades of gray, brown, orange or green (black, reddish-brown or reddish-cream in *P. quintanai*).

Description of holotype. Adult female (Figs 10–12) with head narrower than body and wider than long. HL is 87% of HW, HW 36% of SVL; HL 31% of SVL; snout short (snout to eye distance 6% of SVL), subacuminate in dorsal view, rounded



Figure 11. Holotype of *Pristimantis quintanai* sp. nov. in preservative, adult female MZUA.AN.1881. **A** dorsal view **B** ventral view **C** profile view.

in profile (Fig. 12A, B); canthus rostralis concave in dorsal view, angular in profile; loreal region flat; ED 60% of eye-nostril distance; nostrils oriented laterally; lips not flared; cranial crests absent; upper eyelid bearing one small subconical tubercle and low small tubercles, width of upper eyelid 57% of IOD; tympanic annulus, rounded, its upper and posterodorsal part obscured by a low and short supratympanic fold; tympanic membrane absent (Fig. 12B); diameter of tympanum 63% of ED; one postrictal tubercle posteroventral to the tympanic annulus; choanae small, round, no concealed by palatal shelf of maxillary arch; dentigerous processes of vomers triangular, slightly larger than the choanae, without space between the processes, bearing one teeth on the left one and two teeth on the right one; tongue 1.4× as long as wide, slightly notched posteriorly, posterior half not adherent to floor of mouth.

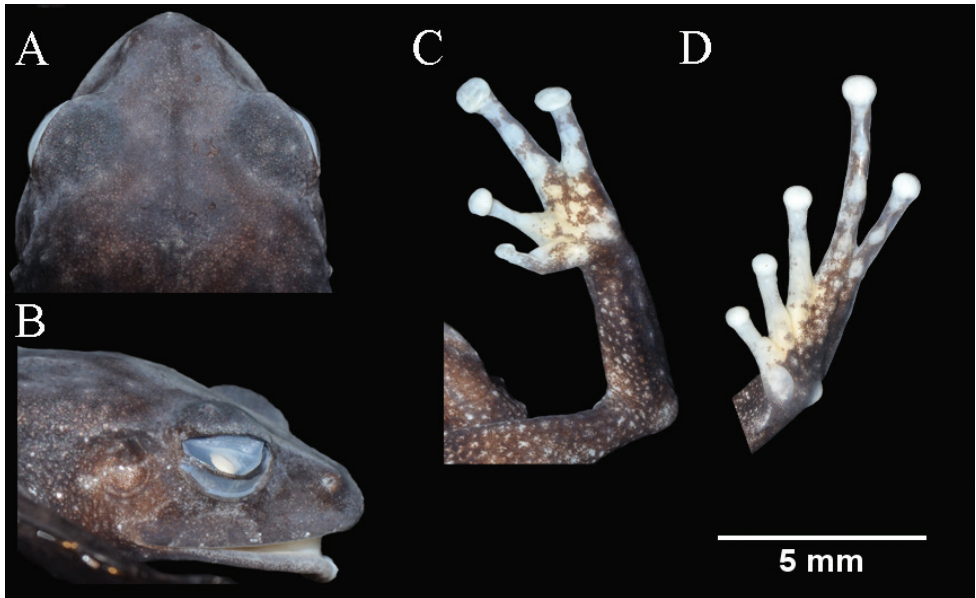


Figure 12. Holotype of *Pristimantis quintanai* sp. nov. in preservative, adult female MZUA.AN.1881. **A** head in dorsal view **B** head in profile view **C** palmar surfaces **D** plantar surfaces.

Skin on dorsum finely tuberculated; middorsal fold present; low dorsolateral folds (more noticeable toward the end of dorsum); sinusoidal scapular fold present (Fig. 11A) skin of throat shagreen with few small scattered tubercles, skin on chest and belly coarsely areolate; discoidal fold low, barely noticeable (Fig. 11B); cloacal region with enlarged warts.

Ulnar tubercles present, outer palmar tubercle bifurcated (divided distally); the- nar tubercle rounded; subarticular tubercles not projected, round and subconical in section; supernumerary palmar tubercles low and rounded, smaller than subarticular tubercles; fingers bearing lateral fringes; Finger I shorter than Finger II; discs on fingers laterally expanded, rounded; all fingers bearing dilated pads well defined by circumferential grooves (Fig. 12C).

Hindlimbs short; TL and FL are 40% of SVL; heel with two small subconical tubercles (the one closest to the tarsus bigger); outer edge of tarsus with a row of small and low tubercles; inner edge of tarsus bearing a fold; inner metatarsal tubercle broadly ovoid, about 2× the rounded outer metatarsal tubercle; subarticular tubercles not projected; plantar supernumerary tubercles low, barely noticeable; toes bearing lateral fringes; webbing absent; discs on toes laterally expanded, rounded, wider than those on fingers; toes with dilated pads well defined by circumferential grooves; relative length of toes $I < II < III < V < IV$ (Fig. 12D).

Measurements of holotype. SVL 20.2; HW 7.2; HL 6.3; IOD 2.6; internarial distance 1.8; upper EW 1.5; ED 2.2; eye-nostril distance 1.3; TD 1.4; TL 8.8; FL 8.5.

Coloration of holotype. In life (Fig. 10) the dorsum is brown, but it becomes darker toward the flanks. The tips of the tubercles, that cover most of the dorsal surfaces, are slightly pinkish. A dark brown strip is visible in the supratympanic region. The loreal region, nostrils and upper lips have vertical dark brown chevrons. The dorsal surfaces of finger tips are dark cream. The throat is dark brown with minute pinkish-cream spots, the venter is dark brown, the groin and concealed surfaces of the thighs and tibia are black with irregular white spots (larger in the groin region). The venter is black. The ventral surfaces of hands are cream with dark brown spots. Toes I, II and III and the tips of Toes IV and V are cream, the plantar surfaces as well as Toes IV and V present a dense brown spatter. The iris is grayish-gold with dark reticulations and a reddish horizontal bar in the middle. The cloacal region presents a dark triangle delimited by a thin gray strip that extends to the thighs.

In preservative (Fig. 11) the dorsum and flanks are dark brown with tiny light brown dots (the tip of the tubercles is light gray). The head and upper eyelids are grayish-brown, the dorsal surfaces of the limbs present the same coloration as the dorsum. The dorsal surfaces of hands and foot are light brown with cream spots, the dorsal surfaces of the tips in Fingers I and II are cream. The dorsal surfaces of toes I, II and III are cream with a tiny brown spatter. The throat and chest are light brown, the venter is dark brown, the groin and concealed surfaces of thighs and tibia are dark brown with white irregular spots. The ventral surfaces of hands are white whit brown spatter. Toes I, II and III and the tips of Toes IV and V are white, the plantar surface as well as Toes IV and V show a dense brown spatter. The cloacal region presents a dark triangle delimited by a thin gray strip that extends to the thighs.

Variation. Morphometric variation is detailed in Table 5. In the males MZUA.AN.1900 (Fig. 13A) and MZUA.AN.1880 (Fig. 13B), the tubercles on the dorsum and on the upper eyelid are less distinguishable (character more notorious in life in these specimens). One individual, MZUA.AN.2705 (Fig. 13C) has smaller blueish-white spots on the groin, the dorsal surfaces of finger tips and toes and the ventral surfaces of hands and foot are pink. The throat is dark brown with minute dark gray spots. In the male MZUA.AN.1900, the flanks and posterior limbs have dark brown vertical chevrons delimited by cream. The throat, chest and the region of the flanks next to the belly is yellowish-cream, the venter is reddish-cream. The male, MZUA.AN.1880 presents a lighter dorsal coloration with a light brown and yellowish-cream pattern.

Etymology. The specific epithet honors Dr Pedro Quintana-Ascencio for his contributions teaching young scientists from Ecuador and the USA and for promoting conservation studies in endangered ecosystems in the south of Ecuador. This is our tribute to Pedro as an ecologist, professor and friend.

Distribution and natural history. *Pristimantis quintanai* is known from three localities in the Province of Cañar: Guangras, Rivera and Llavircay in an elevation range between 2500 and 2800 m. The ecosystem where the species is found is categorized as an evergreen high montane forest from the eastern Andes of Ecuador (Ministerio de Ambiente del Ecuador 2012). All specimens were encountered during the night between small shrubs and in leaf litter. Some specimens were observed in small branches



Figure 13. Morphological variation of *Pristimantis quintanai* sp. nov. in live. **A** MZUA.AN.1900, profile and dorsal view **B** MZUA.AN.1880, profile and ventral view **C** MZUA.AN.2705, profile view.

Table 5. Measurements (in mm) of adult males and females of *Pristimantis quintanai* sp. nov. The mean, standard deviation (SD) and range of each morphological character are shown for females ($N = 6$). The mean of each character is show for males ($N = 2$). Abbreviations of the morphometric measurements are presented in Materials and methods.

	MZUA								Mean \pm SD (range) ♀	Mean ♂
	1881 ♀	1746 ♀	1885 ♀	1873 ♀	2705 ♀	1874 ♀	1900 ♂	1880 ♂		
SVL	20.2	20.7	20.6	21.8	19.0	20.6	15.5	16.4	20.5 \pm 0.9 (19.0–21.8)	16.0
EN	1.3	1.2	1.7	1.9	1.7	1.6	1.0	1.1	1.6 \pm 0.3 (1.2–1.9)	1.1
TD	1.4	1.4	1.1	1.1	1.1	1.1	0.8	0.9	1.2 \pm 0.2 (1.1–1.4)	0.9
ED	2.2	2.2	2.1	2.1	2.0	2.1	1.7	1.7	2.1 \pm 0.1 (2.0–2.2)	1.7
EW	1.5	1.7	1.4	1.8	1.6	1.6	1.0	1.3	1.6 \pm 0.1 (1.5–1.8)	1.2
IOD	2.6	2.4	2.8	3.0	2.5	2.5	1.9	2.0	2.6 \pm 0.2 (2.4–3.0)	2.0
IND	1.8	2.0	2.0	2.0	1.7	1.8	1.4	1.7	1.9 \pm 0.1 (1.8–2.0)	1.6
HL	6.3	6.5	6.5	7.0	5.9	6.2	4.5	4.8	6.4 \pm 0.4 (5.9–6.5)	4.7
HW	7.2	7.4	7.5	7.8	6.8	7.2	5.6	5.8	7.3 \pm 0.3 (6.8–7.0)	5.7
TL	8.8	9.0	9.4	9.5	8.8	8.9	7.0	7.4	9.1 \pm 0.3 (8.8–9.5)	7.2
FL	8.5	7.7	8.5	8.9	8.4	8.7	6.5	7.2	8.5 \pm 0.4 (7.7–8.9)	6.9

between 0 and 25 cm above ground. Other sympatric frogs include *P. pycnodermis* and two other unidentified species of *Pristimantis*.

Conservation status. The localities where *P. quintanai* has been registered cover an estimated area of 40 km². The landscape is highly fragmented and includes extensive areas of both active and abandoned paddocks and has been directly influenced by the infrastructure of the Mazar hydroelectric project. In all the localities, the montane forest has been drastically reduced, particularly next to villages and cities. *Pristimantis quintanai* is not a locally abundant species given that only a handful of individuals (<7) were found in each of the visited localities. We therefore recommend that this species be categorized as Endangered B1ab (iii), following the IUCN criteria, because its extent of occurrence is less than 5000 km² and its natural habitat has been severely fragmented.

Discussion

Recent phylogenies published by Brito et al. (2017) and Székely et al. (2018) have advanced our understanding of the *P. orestes* species group but continue to recover *P. orestes* as three different lineages from three localities of southern Ecuador: 1) Cajanuma (Loja), 2) Lagunas del Compadre (Loja) and 3) Sigsig (Azuay). The issue of paraphyly arises from a lack of molecular data from the type species that was collected in 1971 by William E. Duellman and Bruce MacBride (Lynch 1979) in the locality of Urdaneta, province of Loja. In our study, we provide for the first time genetic sequences of *P. orestes* sensu stricto from four specimens collected at the type locality. Notably, the *P. orestes* specimens from Urdaneta cluster together with the specimen from Sigsig in a strongly supported clade. Thus, in our analysis, we found no evidence to suggest that the individual from the Sigsig locality is genetically distinct from those in Urdaneta and therefore we maintain the identity of KU18257 as *P. orestes*. In contrast, we found evidence to suggest that the specimen from the nearby locality Lagunas del Compadre is genetically distinct and should therefore not be considered part of *P. orestes* sensu stricto. We aim to provide a complete description of the new species from Lagunas del Compadre based on a larger number of specimens in a future study.

Our analyses show that *Pristimantis saturninoi* consists of two genetically distinct lineages. One lineage includes the holotype and one paratype from the description of Brito et al. (2017), and as such, we consider this clade as *P. saturninoi* sensu stricto. A second paratype (DHMECN 12237) clusters together with *P. quintanai* in a distinct clade and therefore should be considered as a distinct species from *P. saturninoi*. Although we find a moderate genetic distance (2.3%, based on the 16S fragment) between DHMECN 12237 and *P. quintanai*, we still need genetic, morphological and behavioral evidence (i.e., calls) from a larger number of individuals to determine relationships with *P. quintanai*. This conflict within *P. saturninoi* is most likely the result of convergent morphological resemblance between the collected specimens that prevents their separation based on morphological characteristics only. Similar issues with type series that are found to consist of different species have been reported in other clades within *Pristimantis* (Ortega-Andrade and Venegas 2014), highlighting the importance of obtaining different lines of evidence

including genetic, morphological and ecological data when dealing with complex cryptic groups of species (Araujo De Oliveira et al. 2017) such as the *P. orestes* species group.

A handful of morphological characters including the characteristic white spots in the groin are shared between *P. orestes* and the newly described species *P. cajanuma* and *P. quintanai*. Here, we find evidence of strong genetic differentiation between these species and provide a combination of additional morphological characters that can help to easily distinguish between these species in the field. Our phylogeny suggests that true diversity within the *P. orestes* species group is yet to be fully uncovered, and that formal descriptions for several new taxa (e.g., DHMECN 3112, QCAZ 45556) are still needed. Moreover, as detailed here for *P. saturninoi* and *P. orestes* sensu stricto, additional genetic data are also needed from other potential members such as *P. colodactylus*, *P. vidua*, and *P. tinajillas* to infer the evolutionary history of the group. As we conduct more field expeditions in the southern highlands of the Ecuadorean Andes with a focus on the type localities, we are confident that the diversity as well as our understanding of phylogenetic relationships of the *P. orestes* species group will significantly increase.

Acknowledgements

For providing access to herpetological collections under their care we thank Santiago R. Ron (Pontificia Universidad Católica del Ecuador), Luke Welton (Kansas Museum of Natural History), Amanda Quezada (MZUA) and Mario Yanez-Muñoz (DHMECN, ECU). We are immensely grateful to the environmental promoters “CUTIN” and to Johnny Cedeño, Homero Abad, Eduardo Toral, Zaira Vicuna, Karina Gutierrez and Bruno Timbe for providing help and logistic support during our field expeditions in Cañar. Special thanks to Enrique Armijos Cano and all the other rangers of Podocarpus National Park for their support during our fieldwork. Jorge Brito kindly provided tissue samples of type series of *P. saturninoi* for our study. Barbara Sharanowski, Miles Zhang, Alexa Trujillo and Ryan Ridenbaugh provided valuable help and comments on our phylogenetic analysis. We thank Edgar Lehr and Santiago Ron for the constructive comments that significantly improved our manuscript. This study was funded by a National Geographic Society early career grant, an Explorers Club student grant, a Linnaean Society grant, a UCF Biology travel award, the Fondo Ambiental para la Protección del Agua (FONAPA), and the Fulbright Foreign Student Program, all awarded to VLU.

References

- Arteaga AF, Guayasamin JM (2011) A new frog of the genus *Pristimantis* (Amphibia: Strabomantidae) from the high Andes of southeastern Ecuador, discovered using morphological and molecular data. *Zootaxa* 2876: 17–29. <https://doi.org/10.11646/zootaxa.3616.4.3>
- Boulenger GA (1900) Descriptions of new batrachians and reptiles collected by Mr. P. O. Simons in Peru. *Annals and Magazine of Natural History, Series 7*(6): 181–186. <https://doi.org/10.1080/00222930008678355>

- Brito J, Almendariz A, Batallas D, Ron SR (2017) Nueva especie de rana bromelícola del género *Pristimantis* (Amphibia: Craugastoridae), meseta de la cordillera del Cóndor, Ecuador. *Papeis Avulsos de Zoologia* 57(15): 177–195. <https://doi.org/10.11606/0031-1049.2017.57.15>
- Brito J, Batallas D, Yanez-Munoz MH (2017) Ranas terrestres *Pristimantis* (Anura: Craugastoridae) de los bosques montanos del rio Upano, Ecuador: Lista anotada, patrones de diversidad y descripción de cuatro especies nuevas. *Neotropical Biodiversity* 3: 125–156. <https://doi.org/10.1080/23766808.2017.1299529>
- Cocroft RB, Ryan MJ (1995) Patterns of advertisement call evolution in toads and chorus frogs. *Animal Behaviour* 49: 283–303. <https://doi.org/10.1006/anbe.1995.0043>
- Darst CR, Cannatella DC (2004) Novel relationships among hyloid frogs inferred from 12S and 16S mitochondrial DNA sequences. *Molecular Phylogenetics and Evolution* 31: 462–475. <https://doi.org/10.1016/j.ympev.2003.09.003>
- Duellman WE, Lehr E (2009) Terrestrial-breeding frogs (Strabomantidae) in Peru. *Nature und Tier Verlag, Münster*, 382 pp.
- Duellman WE, Pramuk JB (1999) Frogs of the genus *Eleutherodactylus* (Anura: Leptodactylidae) in the Andes of northern Peru. *Scientific Papers. Natural History Museum, University of Kansas* 13: 1–78. <https://doi.org/10.5962/bhl.title.16169>
- Guayasamin JM, Arteaga AF (2013) A new species of the *Pristimantis orestes* group Amphibia: Strabomantidae) from the high Andes of Ecuador, Reserva Mazar, *Zootaxa*. 3616 (4): 345–356. <https://doi.org/10.11646/zootaxa.3616.4.3>
- Guayasamin JM, Arteaga A, Hutter CR (2018) A new (singleton) rainfrog of the *Pristimantis myersi* Group (Amphibia: Craugastoridae) from the northern Andes of Ecuador. *Zootaxa*, 4527(3): 323–334. <https://doi.org/10.11646/zootaxa.4527.3.2>
- Guayasamin JM, Hutter CR, Tapia EE, Culebras J, Peñafiel N, Pyron RA, Morochz C, Funk C, Arteaga A (2017) Diversification of the rainfrog *Pristimantis ornatissimus* in the lowlands and Andean foothills of Ecuador. *PLoS ONE* 12(3): e0172615. <https://doi.org/10.1371/journal.pone.0172615>
- Hedges SB, Duellman WE, Heinicke MP (2008) New World direct-developing frogs (Anura: Terrarana): molecular phylogeny, classification, biogeography, and conservation. *Zootaxa* 1737: 1–182. <https://doi.org/10.11646/zootaxa.3986.2.1>
- Heinicke MP, Duellman WE, Hedges SB (2007) Major Caribbean and Central American frog faunas originated by ancient oceanic dispersal. *Proceedings of the National Academy of Sciences* 104(24): 10092–10097. <https://doi.org/10.1073/pnas.0611051104>
- IUCN (2018) The IUCN Red List of Threatened Species. Version 2018-2. <http://www.iucn-redlist.org>
- Jiménez de la Espada M (1870) Fauna neotropicalis species quaedam nondum cognitae. *Jornal de Ciências, Matemáticas, Physicas e Naturaes* 3: 57–65.
- Katoh K, Standley DM (2013) MAFFT multiple sequence alignment software version 7: improvements in performance and usability. *Molecular Biology and Evolution* 4: 772–80. <https://doi.org/10.1093/molbev/mst010>
- Kieswetter CM, Schneider CJ (2013) Phylogeography in the northern Andes: complex history and cryptic diversity in a cloud forest frog, *Pristimantis w-nigrum* (Craugastoridae). *Molecular Phylogenetics and Evolution*. 69(3): 417–29. <https://doi.org/10.1016/j.ympev.2013.08.007>

- Köhler J, Jansen M, Rodríguez A, Kok PJR, Toledo LF, Emmrich M, Glaw F, Haddad CFB, Rödel MO, Vences M (2017) The use of bioacoustics in anuran taxonomy: theory, terminology, methods and recommendations for best practice. *Zootaxa* 4251: 1–124. <https://doi.org/10.11646/zootaxa.4251.1.1>
- Kumar S, Stecher G, Li M, Knyaz C, Tamura K (2018) MEGA X: Molecular Evolutionary Genetics Analysis across Computing Platforms, *Molecular Biology and Evolution* 35(6): 1547–1549. <https://doi.org/10.1093/molbev/msy096>
- Lanfear R, Frandsen PB, Wright AM, Senfeld T, Calcott B (2016) PartitionFinder 2: new methods for selecting partitioned models of evolution for molecular and morphological phylogenetic analyses. *Molecular biology and evolution*. <https://doi.org/10.1093/molbev/msw260>
- Lehr E, Coloma LA (2008) A minute new Ecuadorian Andean frog (Anura: Strabomantidae, *Pristimantis*). *Journal of Herpetology* 64(3): 354–367. <https://doi.org/10.1655/07-089.1>
- Lynch JD (1979) Leptodactylid frogs of the genus *Eleutherodactylus* from the Andes of southern Ecuador. *Miscellaneous Publications, Museum of Natural History, University of Kansas* 66: 1–62. <https://doi.org/10.5962/bhl.title.16268>
- Lynch JD, Duellman WE (1997) Frogs of the genus *Eleutherodactylus* in western Ecuador: systematics, ecology, and biogeography. *Special Publication Natural History Museum University of Kansas* 23: 1–236. <https://doi.org/10.5962/bhl.title.7951>
- McDiarmid RW (1994) Preparing amphibians as scientific specimens. In: Heyer WR, Donnelly MA, McDiarmid RW, Hayek LC, Foster MS (Eds) *Measuring and Monitoring Biological Diversity Standard Methods for Amphibians*, Smithsonian Press, Washington, DC, 289–297.
- Miller MA, Pfeiffer W, Schwartz T (2010) “Creating the CIPRES Science Gateway for inference of large phylogenetic trees” in *Proceedings of the Gateway Computing Environments Workshop (GCE)*, New Orleans, LA, 14 November 2010, 1–8. <https://doi.org/10.1109/GCE.2010.5676129>
- Ministerio de Ambiente del Ecuador (2012) *Sistema de Clasificación de los Ecosistemas del Ecuador Continental*. Subsecretaría de Patrimonio Natural, Quito, 143 pp.
- Nguyen LT, Schmidt HA, von Haeseler A, Minh BQ (2015) IQ-TREE: a fast and effective stochastic algorithm for estimating maximum-likelihood phylogenies. *Molecular Biology and Evolution* 32(1): 268–74. <https://doi.org/10.1093/molbev/msu300>
- Oliveira EA, Rodrigues LR, Kaefer IL, Pinto KC, Hernández-Ruz EJ (2017) A new species of *Pristimantis* from eastern Brazilian Amazonia (Anura, Craugastoridae). *Zookeys* 687: 101–29. <https://doi.org/10.3897/zookeys.687.13221>
- Ortega-Andrade HM, Venegas PJ (2014) A new synonym for *Pristimantis luscombei* (Duellman and Mendelson 1995) and the description of a new species of *Pristimantis* from the upper Amazon basin (Amphibia: Craugastoridae). *Zootaxa* 3895(1): 31–57. <https://doi.org/10.11646/zootaxa.3895.1.2>
- Padial JM, Grant T, Frost DR (2014) Molecular systematics of terraranas (Anura: Brachycephaloidea) with an assessment of the effects of alignment and optimality criteria. *Zootaxa* 3825(1): 1–132. <https://doi.org/10.11646/zootaxa.3825.1.1>
- Palumbi SR, Martin A, Romano S, McMillan WO, Stice L, Grabowski G (1991) *The Simple Fool's Guide to PCR*. Version 2.0. University of Hawaii, Honolulu.
- Pinto-Sanchez NR, Ibanez R, Madrinan S, Sanjur OI, Bermingham E, Crawford AJ (2012) The Great American Biotic Interchange in frogs: multiple and early colonization of Central

- America by the South American genus *Pristimantis* (Anura: Craugastoridae). *Molecular Phylogenetics and Evolution* 62: 954–972. <https://doi.org/10.1016/j.ympev.2011.11.022>
- Pyron RA, Wiens JJ (2011) A large-scale phylogeny of Amphibia with over 2,800 species, and a revised classification of extant frogs, salamanders, and caecilians. *Molecular Phylogenetics and Evolution* 61: 543–583. <https://doi.org/10.1016/j.ympev.2011.06.012>
- Rambaut A, Suchard MA, Xie D, Drummond AJ (2014) Tracer v1.5, Available from: <http://beast.bio.ed.ac.uk/Tracer>
- Ron SR, Merino-Viteri A, Ortiz DA (2019) Anfibios del Ecuador. Version 2019.0. Museo de Zoología, Pontificia Universidad Católica del Ecuador. <https://bioweb.bio/faunaweb/amphibiaweb>
- Ronquist F, Teslenko M, van der Mark P, Ayres DL, Darling A, Hohna S, Larget B, Liu L, Suchard MA, Huelsenbeck JP (2012) MrBayes 3.2: efficient Bayesian phylogenetic inference and model choice across a large model space. *Systematics Biology* 61(3): 539–42. <https://doi.org/10.1093/sysbio/sys029>
- Székely P, Eguiguren JS, Székely D, Ordonez-Delgado L, Armijos-Ojeda D, Riofrio-Guaman ML, Cogălniceanu D (2018) A new minute *Pristimantis* (Amphibia: Anura: Strabomantidae) from the Andes of southern Ecuador. *PLoS ONE* 13(8): e0202332. <https://doi.org/10.1371/journal.pone.0202332>
- Toledo LF, Martins IA, Bruschi DP, Passos MA, Alexandre C, Haddad CFB (2015) The anuran calling repertoire in the light of social context. *Acta Ethologica* 18: 87–99. <https://doi.org/10.1007/s10211-014-0194-4>
- Watters JL, Cummings ST, Flanagan RL, Siler CD (2016). Review of morphometric measurements used in anuran species descriptions and recommendations for a standardized approach. *Zootaxa* 4072(4): 477–495. <https://doi.org/10.11646/zootaxa.4072.4.6>
- Wiens JJ, Coloma LA (1992) A new species of the *Eleutherodactylus myersi* (Anura: Leptodactylidae) assembly from Ecuador. *Journal of Herpetology* 26: 196–207. <https://doi.org/10.2307/1564862>

Supplementary material I

Specimens used for morphological comparisons

Authors: Veronica L. Urgiles, Paul Székely, Diana Székely, Nicholas Christodoulides, Juan C. Sanchez-Nivicela, Anna E. Savage

Data type: species data

Explanation note: For each specimen we present the museum number and locality.

Copyright notice: This dataset is made available under the Open Database License (<http://opendatacommons.org/licenses/odbl/1.0/>). The Open Database License (ODbL) is a license agreement intended to allow users to freely share, modify, and use this Dataset while maintaining this same freedom for others, provided that the original source and author(s) are credited.

Link: <https://doi.org/10.3897/zookeys.864.35102.suppl1>

Supplementary material 2

Advertisement call of *Pristimantis orestes sensu stricto*

Authors: Veronica L. Urgiles, Paul Székely, Diana Székely, Nicholas Christodoulides, Juan C. Sanchez-Nivicela, Anna E. Savage

Data type: species data

Copyright notice: This dataset is made available under the Open Database License (<http://opendatacommons.org/licenses/odbl/1.0/>). The Open Database License (ODbL) is a license agreement intended to allow users to freely share, modify, and use this Dataset while maintaining this same freedom for others, provided that the original source and author(s) are credited.

Link: <https://doi.org/10.3897/zookeys.864.35102.suppl2>

Supplementary material 3

Data of call recordings used in the present study

Authors: Veronica L. Urgiles, Paul Székely, Diana Székely, Nicholas Christodoulides, Juan C. Sanchez-Nivicela, Anna E. Savage

Data type: species data

Explanation note: Dist. = distance from the focal male; Call = call duration; Temp. = air temperature; H. = air humidity.

Copyright notice: This dataset is made available under the Open Database License (<http://opendatacommons.org/licenses/odbl/1.0/>). The Open Database License (ODbL) is a license agreement intended to allow users to freely share, modify, and use this Dataset while maintaining this same freedom for others, provided that the original source and author(s) are credited.

Link: <https://doi.org/10.3897/zookeys.864.35102.suppl3>

Supplementary material 4

Single gene trees for 12S, 16S and RAG-1 for the *Pristimantis orestes* species group, inferred with Maximum Likelihood

Authors: Veronica L. Urgiles, Paul Székely, Diana Székely, Nicholas Christodoulides, Juan C. Sanchez-Nivicela, Anna E. Savage

Data type: molecular data

Explanation note: Bootstrap support is shown for nodes over 70%.

Copyright notice: This dataset is made available under the Open Database License (<http://opendatacommons.org/licenses/odbl/1.0/>). The Open Database License (ODbL) is a license agreement intended to allow users to freely share, modify, and use this Dataset while maintaining this same freedom for others, provided that the original source and author(s) are credited.

Link: <https://doi.org/10.3897/zookeys.864.35102.suppl4>

Supplementary material 5

Maximum Likelihood tree inference of the *Pristimantis orestes* species group

Authors: Veronica L. Urgiles, Paul Székely, Diana Székely, Nicholas Christodoulides, Juan C. Sanchez-Nivicela, Anna E. Savage

Data type: statistical data

Explanation note: Bootstrap support values are shown for nodes over 70%. The bar coloration indicates the following: *P. cajanuma* sp. nov. (yellow), *P. orestes* (dark red), *P. saturninoi* (blue), and *P. quintanai* sp. nov. (green).

Copyright notice: This dataset is made available under the Open Database License (<http://opendatacommons.org/licenses/odbl/1.0/>). The Open Database License (ODbL) is a license agreement intended to allow users to freely share, modify, and use this Dataset while maintaining this same freedom for others, provided that the original source and author(s) are credited.

Link: <https://doi.org/10.3897/zookeys.864.35102.suppl5>

Discovery and description of a mysterious Asian flying squirrel (Rodentia, Sciuridae, *Biswamoyopterus*) from Mount Gaoligong, southwest China

Quan Li^{1,2}, Xue-You Li¹, Stephen M. Jackson^{3,4,5,6}, Fei Li⁷, Ming Jiang⁸,
Wei Zhao⁸, Wen-Yu Song^{1,2}, Xue-Long Jiang¹

1 State Key Laboratory of Genetic Resources and Evolution, Kunming Institute of Zoology, Chinese Academy of Sciences, Kunming, China **2** Kunming College of Life Science, University of Chinese Academy of Sciences, Kunming, China **3** Biosecurity NSW, NSW Department of Primary Industries, Orange, New South Wales 2800, Australia **4** School of Biological, Earth and Environmental Sciences, University of New South Wales, Sydney, New South Wales 2052, Australia **5** Division of Mammals, National Museum of Natural History, Smithsonian Institution, Washington, DC 20013-7012, United States of America **6** Australian Museum Research Institute, Australian Museum, 1 William St. Sydney, New South Wales 2010, Australia **7** Kadoorie Conservation China, Kadoorie Farm & Botanic Garden, Lam Kam Road, Tai Po, Hong Kong, China **8** Baoshan Management Bureau of Gaoligongshan National Nature Reserve, Baoshan, Yunnan, China

Corresponding author: *Xuelong Jiang* (jiangxl@mail.kiz.ac.cn)

Academic editor: *R. López-Antoñanzas* | Received 5 February 2019 | Accepted 30 April 2019 | Published 18 July 2019

<http://zoobank.org/246FA0BE-1170-4DB6-94C7-6C24043A9C4C>

Citation: Li Q, Li X-Y, Jackson SM, Li F, Jiang M, Zhao W, Song W-Y, Jiang X-Y (2019) Discovery and description of a mysterious Asian flying squirrel (Rodentia, Sciuridae, *Biswamoyopterus*) from Mount Gaoligong, southwest China. ZooKeys 864: 147–160. <https://doi.org/10.3897/zookeys.864.33678>

Abstract

The flying squirrels of the tribe Pteromyini (Family Sciuridae) currently include 15 genera of which the genus *Biswamoyopterus* comprises two recognized species, *B. biswasi* Saha, 1981 and *B. laoensis* Sanamxay et al., 2013. These two species were each described from only one specimen that are separated from each other by 1,250 kilometres in southern Asia, where they occur in northeast India and central Lao PDR respectively. In 2017 and 2018, two specimens of *Biswamoyopterus* were discovered from Mount Gaoligong, west Yunnan province, southwest China (between the type locality of the two recognized species). This study aimed to evaluate the taxonomic status of these two newly acquired specimens of *Biswamoyopterus* by comparing their morphology with the two described species of the genus. The results of this study showed that the specimens from Yunnan province (China) differed from

both *B. laoensis* and *B. biswasi* in both pelage colour and craniology, and should be recognised as a distinct species, *B. gaoligongensis* **sp. nov.**, which is formally described here. This study contributes to the understanding of the flying squirrels of southern Asia and identifies an additional species that appears to be endemic to southwest China; however, more research is required to provide details of its ecology, distribution, and conservation status.

Keywords

Biodiversity, conservation, mammal, Pteromyini, systematics, taxonomy, threatened, wildlife, Yunnan

Introduction

The flying squirrels of the tribe Pteromyini (Family Sciuridae) currently comprise 52 species of recent mammals that are placed in 15 genera. A number of fossil species have also been described and includes in several of the genera containing extant species as well as 13 additional extinct genera (Jackson and Thorington 2012; Jackson and Schouten 2012; Koprowski et al. 2016). The genus *Biswamoyopterus* Saha, 1981 is the most recently described in the tribe and initially only included *Biswamoyopterus biswasi* Saha, 1981 based on a single specimen collected in Namdapha National Park, northeast India (Saha 1981). *Biswamoyopterus biswasi* was placed in its own genus by Saha (1981) as it was considered to exhibit a unique combination of characters that distinguish it from other genera including: 1) large body size, cylindrical tail, and well-developed uropatagium (tail membrane or interfemoral membrane) similar to *Petaurista*, *Aeretes* and *Aeromys*; 2) the presence of ear tufts similar to *Belomys* and *Trogopterus*; and 3) cuspidate brachyodont dentition similar to *Hylopetes* and *Aeromys*. In addition to these characters, *Biswamoyopterus* was recognised to have pale-yellow incisors similar to *Aeromys* and *Eupetaurus* (Corbet and Hill 1992). In reference to these characters, Sanamxay et al. (2013) described a second species of *Biswamoyopterus* (*B. laoensis*) based on a single specimen collected from central Lao PDR. So far, all knowledge of *Biswamoyopterus* comes from the morphological description of these two holotypes. As a result, the International Union for Conservation of Nature (IUCN) listed *Biswamoyopterus biswasi* as critically endangered due to hunting and habitat loss from logging (Molur 2016) and *Biswamoyopterus laoensis* as data deficient (Kennerley 2017).

There is a gap of 1,250 km between the type localities of the two described *Biswamoyopterus* species (Sanamxay et al. 2013). Western Yunnan, southwest China occurs between the two type localities of *Biswamoyopterus* (Fig. 1). In 2017 and 2018, two specimens of *Biswamoyopterus* sp. were collected in Mount Gaoligong (the watershed of the Irrawaddy River and the Nu River [Salween River]), west Yunnan (Fig. 1) that appeared to have different pelage and cranial characters from the two described species of *Biswamoyopterus*. Therefore, the aim of this study was to: 1) undertake a detailed comparison of the specimens collected in Yunnan province, China with the two described species; and 2) if these Yunnan specimens proved to be distinct, formally describe and name a new species of *Biswamoyopterus*.

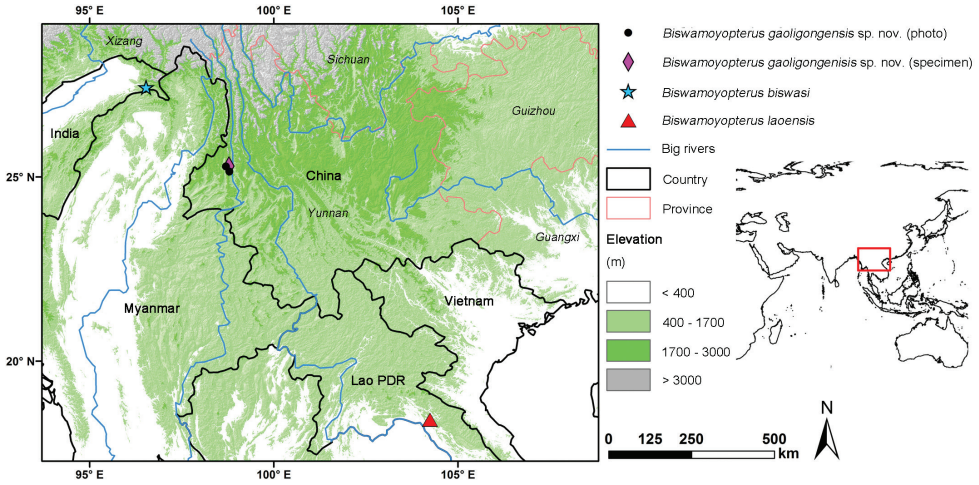


Figure 1. Known localities of three species of *Biswamoyopterus*.

Materials and methods

Ethics statement

Animals used for this study were approved by the Animal Ethics Committee of the Kunming Institute of Zoology, Chinese Academy of Sciences (approval ID: SMKX2018021).

Repositories

ZSI Zoological Collection of the Zoological Survey of India, Kolkata [Calcutta], India.

NUoL Zoological collection of the Faculty of Environmental Sciences, National University of Laos, Vientiane, Lao PDR.

KIZ Kunming Natural History Museum of Zoology, Kunming Institute of Zoology, Chinese Academy of Sciences, Kunming, China.

Specimens examined

Holotype

CHINA • 1♂, holotype of *Biswamoyopterus gaoligongensis* sp. nov., skin and skull available; Yunnan province, Baoshan city, Longyang county, Lujiang township, Baihua-lin village; 25.298N, 98.785E; 2040 m a.s.l.; Jan. 2017; Quan Li leg.; Broad-leaved evergreen forests; KIZ 034924 (field No. bs1628).

INDIA • 1♂, holotype of *Biswamoyopterus biswasi*, skin and skull available; Tirap District, Namdapha, 26 km east of Miao, Deban; ca. 350 m a.s.l.; Apr. 1981; Shyamrup Biswas leg.; collected from a tall Nahar tree (*Mesua ferrea*) at 20:15 pm; ZSI 20705.

LAO PDR • 1 ♀, holotype of *Biswamoyopterus laoensis*, skin and skull available; Bolikhamxai Province, Pak Kading District, Ban (village) Thongnami, Thongnami market (Purchased from the market by the collectors. The collectors speculated that the original collection site might be Nam Kading National Biodiversity Conservation Areas or Khammouan Limestone National Biodiversity Conservation Areas (NBCA), which is about 5 km Northeast of Thongnami and Khammouan Limestone NBCA, and about 25 km Southeast of Ban village); 18.172N, 104.24E; Sep. 2012; Daosavanh Sanamxay, Sysouphanh Xayavong, and Vilakhan Xayaphet leg.; NUoL FES.MM.12.163.

Paratype

CHINA • 1 sex unknown, paratype of *Biswamoyopterus gaoligongensis* sp. nov., skin of head and skull available; same locality as for KIZ 034924; Dec. 2018; a native of the area leg.; KIZ 035622 (field No. 201812001).

Morphological techniques

The external and craniodental measurements of type specimen of *Biswamoyopterus biswasi* and *Biswamoyopterus laoensis* were employed from the literature (Saha 1981; Sanamxay et al. 2013). External measurements of *Biswamoyopterus* sp. nov. were copied from the label tied on the specimen, included body mass, head and body length, tail length, hind feet length, and ear length. Craniodental measurements of *Biswamoyopterus* sp. nov. were taken with digital caliper to the nearest 0.01 mm; the mensural points follow Saha (1981) and Sanamxay et al. (2013) to facilitate the subsequent comparison (Fig. 2). A total of 28 craniodental measurements were used, including:

BB	Breadth of braincase,	OB	Orbit breadth,
BH	Braincase height,	ONL	Occipitonasal length,
CBL	Condylbasal length,	PL	Palate length,
DL	Diastema length,	POB	Postorbital breadth,
FL	Frontal length,	PPL	Postpalatal length,
GPB	Greatest palatal breadth,	RB	Rostrum breadth,
IBG	Inter bullae gap,	WAAM	Width of auditory bullae across the external auditory meati,
IOB	Interorbital breadth,	WPFM	Width of the bony palate at the first upper molar,
LAB	Length of auditory bulla,	ZB	Zygomatic breadth,
LBP	Length of bony palate,	ZH	Zygomatic height.
LIF	Length of the incisive foramina,	P	Premolars,
MB	Mastoid breadth,	M	Molars;
MH	Mandible height,		Superscript (P ^x , M ^x) upper premolars and upper molars, and
ML	Mandible length,		Subscript (P _x , M _x) lower premolars and lower molars.
MRTL	Mandibular tooth row length,		
MWN	Maximum width of nasals,		
MYTL	Maxillary tooth row length,		
NL	Nasal length,		

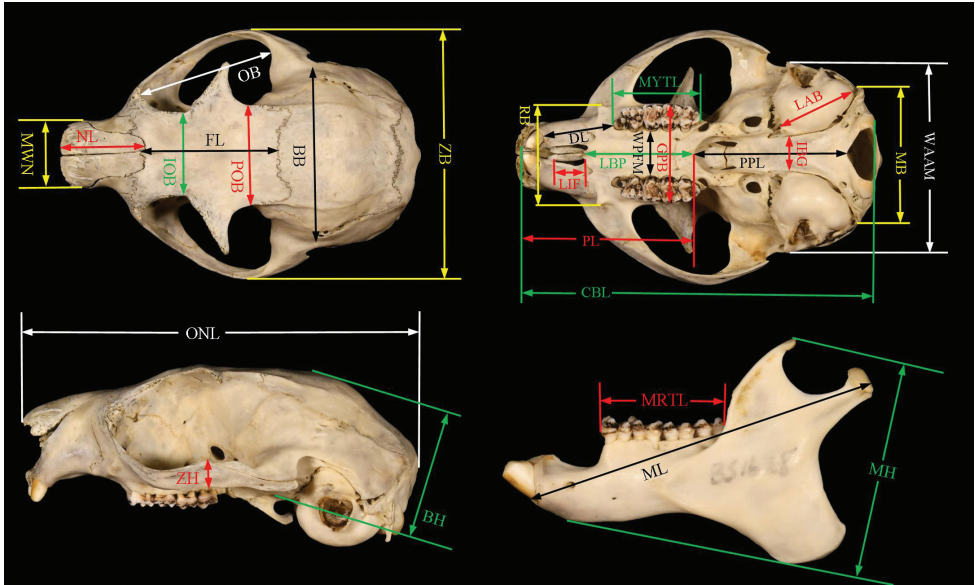


Figure 2. Twenty-eight craniodental measurements taken for this study. See text for definitions. The different coloured arrows have no special meaning, they make it easier to see the starting and ending points of different measurements. Photo credit: Sanamxay et al. (2013).

The nomenclature of cheek teeth structures followed Tong (2007) and Thorington et al. (1996) (Fig. 3).

Pelage colour comparisons were made among all four available specimens. Skull and teeth were studied using a stereo binocular microscope. As only four skull specimens were available, statistical analysis was not possible.

Taxonomy

Class Mammalia Linnaeus, 1758

Order Rodentia Bowdich, 1821

Family Sciuridae Fischer, 1817

Subfamily Sciurinae Fischer, 1817

Tribe Pteromyini Brandt, 1855

Genus *Biswamoyopterus* Saha, 1981

***Biswamoyopterus gaoligongensis* sp. nov.**

<http://zoobank.org/21C9D58C-EDC9-4016-8148-3F81DB51D9D3>

Common name. Mount Gaoligong Flying Squirrel. Chinese common name "高黎贡比氏鼯鼠".

Holotype. Specimen KIZ: 034924 (field number bs1628), an adult male, skull, dried skin, baculum, and remaining body part in alcohol deposited in the Kunming

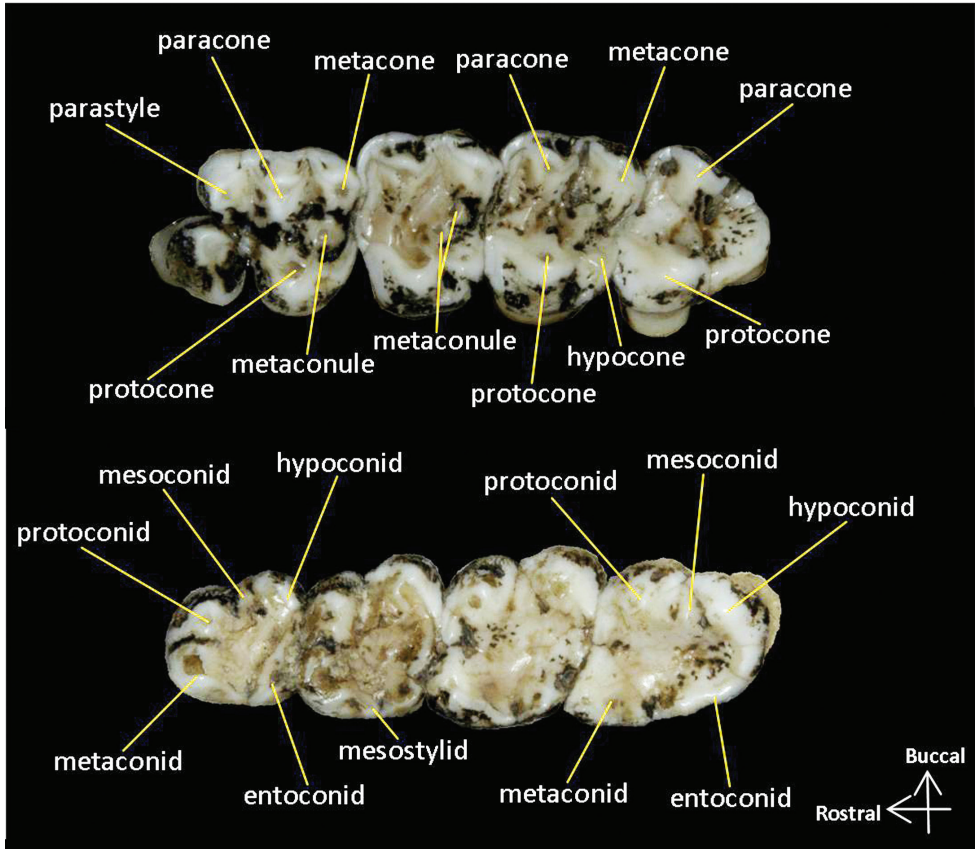


Figure 3. Nomenclature of cheek teeth of *Biswamoypterus*. Maxillary tooth row (top), Mandibular tooth row (bottom).

Natural History Museum of Zoology, Kunming Institute of Zoology, Chinese Academy of Science (KIZ).

Type locality. Baihualin village [25.298167N, 98.784683E], Lujiang township, Longyang County, Baoshan City, Yunnan, China. The locality is located on the eastern slope of the southern Mount Gaoligong.

Etymology. The specific name is derived from Mount Gaoligong, the type locality of the new species and *-ensis*, Latin for belonging to.

Diagnosis. *Biswamoypterus gaoligongensis* sp. nov. can be distinguished from the other two described species of *Biswamoypterus* by the following combination of traits: 1) The ear tufts at the base of the posterior margins of ears are bicolored, basally white and terminal black. The scrotum is dark brown which strongly contrasts with the yellowish-white abdominal pelage. 2) The muzzle is very short, and the zygomatic arch is distinctly expanding outward, making the outline of the skull short and wide. The outer margin of the nasal bone, the orbital margin of the frontal bone, and the post-orbital margin of the frontal bone are almost parallel to the midline of skull on the

dorsal view. The central point of the posterior margin of the palatal bones lies in front of the posterior margin of M^3 . 3) M^1 and M^2 are sub-square in outline, and as large as P^4 . The hypoconid of P_4 - M_2 are very developed, strongly pointed towards posterior buccal side.

Description. *Biswamoyopterus gaoligongensis* sp. nov. is a large flying squirrel (head and body length: 440 mm, tail length: 520 mm, and body mass: 1370 g) with a very developed uropatagium that extends approximately one-third of the proximal tail length in fresh specimen (Fig. 4). The back and upper surface of patagium are predominantly reddish brown, while the back between the shoulder and uropatagium is speckled with numerous white-tip furs that are absent from the head, shoulder, plagiopatagium, outer edge of uropatagium, limbs, and tail (Fig. 4). Similar to the shoulder, the head is reddish brown, but showing some yellowish grey in the crown. The ear is naked, with two bunches of long hairs (i.e., ear tufts) at the ear base, the anterior tufts are black, and the posterior tufts are basally white and terminal black. The back of each manus is reddish brown and the digits are black, while the whole pes and digits are black. The tail is cylindrical, the part beyond the uropatagium is black, and the part within the uropatagium is the same colour as the uropatagium. Throat, belly, and ventral surface of patagium are yellowish white. However, the scrotum is dark brown which strongly contrasts with the abdominal pelage.

Skull is large with a short muzzle and an expanded outward zygomatic arch, making the outline of skull short and wide (Fig. 5). The frontal depression is deep and postorbital processes are large and well developed. The outer margin of the nasal bone, the orbital margin of the frontal bone, and the post-orbital margin of the frontal bone are almost parallel to the midline of skull on the dorsal view. The auditory bullae are relatively large, with a honeycomb pattern of complex septae. The interpremaxillary foramen is well opened, which is not common in most flying squirrel genera. The mandible is generally similar to that of other flying squirrels. The coronoid process is less developed, only slightly higher than condylar process when the mandible is placed on a plane.

The anterior surface of incisors is pale yellow. Cheek teeth are strongly cuspidate brachyodont, with slightly pitted enamel.

Maxillary teeth: P^3 is strong and unicuspid. Parastyle is prominent on P^4 and dwindle on the following molars in an anterior to posterior gradient. Paracone is prominent on P^4 , M^1 , M^2 , and M^3 . Metacone is prominent on P^4 , M^1 , and M^2 , and indistinct on M^3 . Between protocone and metacone, at the exit of the middle valley of P^4 , M^1 , M^2 , and M^3 , there are two mesostyles form a projecting gutter. Protocone is prominent on P^4 , M^1 , M^2 , and M^3 . Hypocone is small, separated from protocone by a notch, distinct on M^1 and M^2 , small on P^4 , and absent on M^3 . The anteroloph and posteroloph are indistinct on P^4 and M^3 ; distinct on M^1 and M^2 , but they do not develop into a ridge as high as the protoloph and metaloph. A protoloph connecting the protocone with the paracone on M^1 , M^2 , and M^3 , and notched on P^4 . A metaloph connecting the protocone with the metacone on M^2 , interrupted by one big or two small metaconules on P^4 and M^1 , and absent on M^3 .

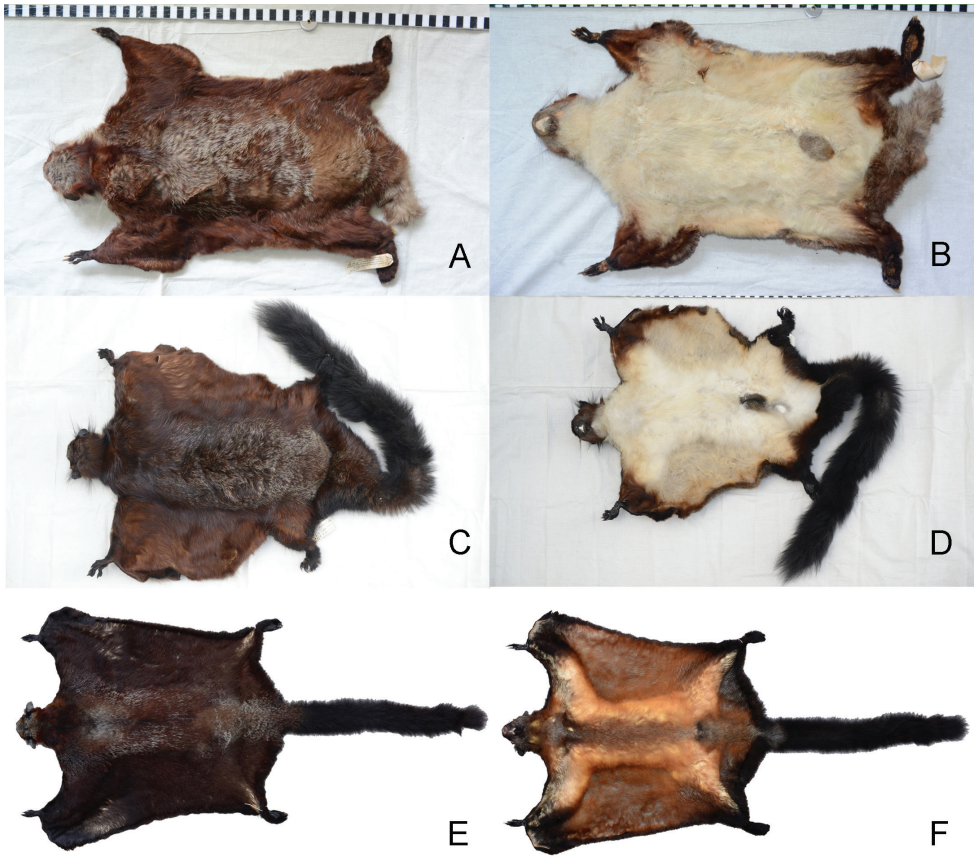


Figure 4. Skins of the three known *Biswamoyopecterus* species **A, B** (ZSI 20705, holotype) *Biswamoyopecterus biswasi* **C, D** (KIZ 034924, holotype) *Biswamoyopecterus gaoligongensis* sp. nov. **E, F** (NUoL FES. MM.12.163, holotype) *Biswamoyopecterus laoensis*. The images **E, F** were derived from Sanamxay et al. (2013).

Mandibular teeth: Four main cusps (protoconid, hypoconid, metaconid, and entoconid) are all distinct on P_4 , M_1 , M_2 , and M_3 . Mesoconid is present on the buccal side of P_4 , M_1 , M_2 , and M_3 , the notch between mesoconid and hypoconid is distinct, seems to be formed by the intense wear and tear. Mesostylid is small and fused with metaconid on P_4 and M_1 , indistinct on M_2 and M_3 .

Comparison. Body size, *B. gaoligongensis* sp. nov. is similar to *B. biswasi* but clearly smaller than *B. laoensis* (Table 1). Pelage colour becomes dark gradually from *B. biswasi* to *B. gaoligongensis* sp. nov. and to *B. laoensis*. The back, *B. biswasi* is morocco-red speckled with white, *B. gaoligongensis* sp. nov. is reddish brown speckled with white, and *B. laoensis* is dark reddish brown speckled with white. The belly, *B. biswasi* is white, *B. gaoligongensis* sp. nov. is yellowish-white, and *B. laoensis* is pale orange. The tail beyond uropatagium, *B. biswasi* is pale smoky grey, with a dark tip, both *B. gaoligongensis* sp. nov. and *B. laoensis* are black (Fig. 4). The ear tufts, *B. biswasi* are white, *B. gaoligongensis*

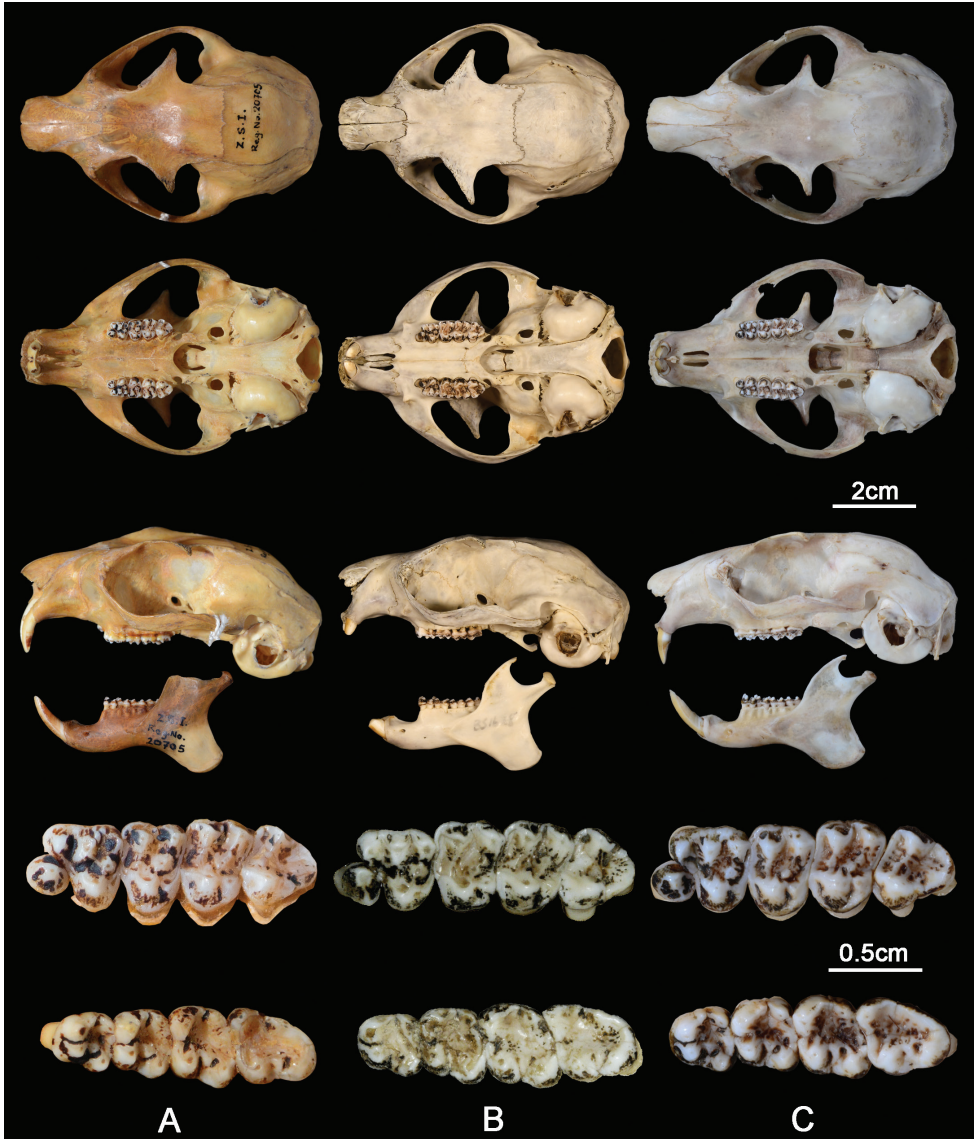


Figure 5. Skulls, left maxillary (above) and left mandibular (below) tooth rows of the three known *Biswamoyopterus* species. **A** (ZSI 20705, holotype) *Biswamoyopterus biswasi* **B** (KIZ 034924, holotype) *Biswamoyopterus gaoligongensis* sp. nov. **C** (NUoL FES.MM.12.163, holotype) *Biswamoyopterus laoensis*. The images of **C** were derived from Sanamxay et al. (2013).

sp. nov. are bicolour (the anterior tufts are black, and the posterior tufts are basally white and terminal black), and *B. laoensis* are black (Fig. 6).

The muzzle of *B. gaoligongensis* sp. nov. is very short, *B. biswasi* is intermediate, and *B. laoensis* is much longer (Fig. 5, Table 1). As a result, the outline of skull of *B. gaoligongensis* sp. nov. is short and wide, *B. biswasi* is relatively short, and *B. laoensis* appears

Table 1. Body Mass (in grams), external and skull measurements (in mm) of four specimens of genus *Biswamoyopterus*.

Measurements	<i>B. biswasi</i> (ZSI 20705)	<i>B. gaoligongensis</i> sp. nov. (KIZ 034924)	<i>B. gaoligongensis</i> sp. nov. (KIZ 035622)	<i>B. laoensis</i> (NUoL FES.MM.12.163)
Body Mass	–	1370.0	–	1800.0
Head and body length	405.0	440.0	–	455.0
Tail length	605.0	520.0	–	620.0
Hind feet length	78.0	75.0	–	74.5
Ear length	46.0	47.0	46.0	52.0
Occipitonasal length (ONL)	72.40	69.75	71.11	74.39
Condylobasal length (CBL)	70.10	66.37	67.73	70.99
Mastoid breadth (MB)	–	30.72	33.50	30.79
Zygomatic breadth (ZB)	47.50	48.41	48.30	47.72
Zygomatic height (ZH)	–	4.61	4.58	4.86
Breadth of braincase (BB)	–	33.86	34.46	32.84
Braincase height (BH)	–	22.90	24.15	22.55
Rostrum breadth (RB)	–	19.61	19.62	17.04
Nasal length (NL)	20.90	19.35	20.70	22.57
Maximum width of nasals (MWN)	–	13.15	12.51	13.37
Interorbital breadth (IOB)	19.00	15.75	16.38	14.06
Postorbital breadth (POB)	–	18.87	20.55	17.19
Length of the incisive foramina (LIF)	6.40	5.65	5.86	5.85
Length of bony palate (LBP)	–	20.08	22.01	23.83
Post palatal length (PPL)	–	28.72	29.68	28.77
Length of auditory bulla (LAB)	15.50	14.68	14.57	17.33
Width of auditory bullae across the external auditory meati (WAAM)	–	35.88	36.76	35.96
Inter bullae gap (IBG)	–	6.52	6.76	5.01
Maxillary tooth row length (MYTL)	15.50	15.92	16.23	16.33
Greatest palatal breadth (GPB)	–	18.26	18.61	19.37
Width of the bony palate at the first upper molar (WPFM)	–	8.58	8.03	8.05
Mandibular tooth row length (MRTL)	–	15.24	15.41	15.33
Mandible length (ML)	–	44.44	46.53	45.36
Mandible height (MH)	–	27.10	27.37	29.78
Palate length (PL)	34.70	32.60	32.87	–
Diastema length (DL)	15.70	13.70	15.03	–
Orbit breadth (OB)	24.60	26.17	26.50	–
Frontal length (FL)	28.60	27.66	30.63	–

long. On the dorsal view of skull, the outer margin of the nasal bone, the orbital margin of the frontal bone, and the post orbital margin of the frontal bone of *B. gaoligongensis* sp. nov. are almost parallel to the midline of skull, while *B. biswasi* slanted, and *B. laoensis* slanted even more. The postorbital processes of *B. gaoligongensis* sp. nov. and *B. biswasi* are clearly larger than *B. laoensis*. The preglenoid process of *B. gaoligongensis* sp. nov. and *B. laoensis* are almost flat, whereas that of *B. biswasi* obviously protruding forward (Fig. 7). The sutures of frontal and squamosal bone of *B. gaoligongensis* sp. nov. are bulging, while *B. biswasi* and *B. laoensis* are almost flat. The auditory bullae of



Figure 6. Ear tufts of the three *Biswamoyopterus* species, the red arrow indicates the anterior tufts, and the yellow arrow indicates the posterior tufts **A** (ZSI 20705, holotype) *Biswamoyopterus biswasi* **B** (KIZ 034924, holotype) *Biswamoyopterus gaoligongensis* sp. nov. **C** (NUoL FES.MM.12.163, holotype) *Biswamoyopterus laoensis*. The image **C** was derived from Sanamxay et al. (2013).

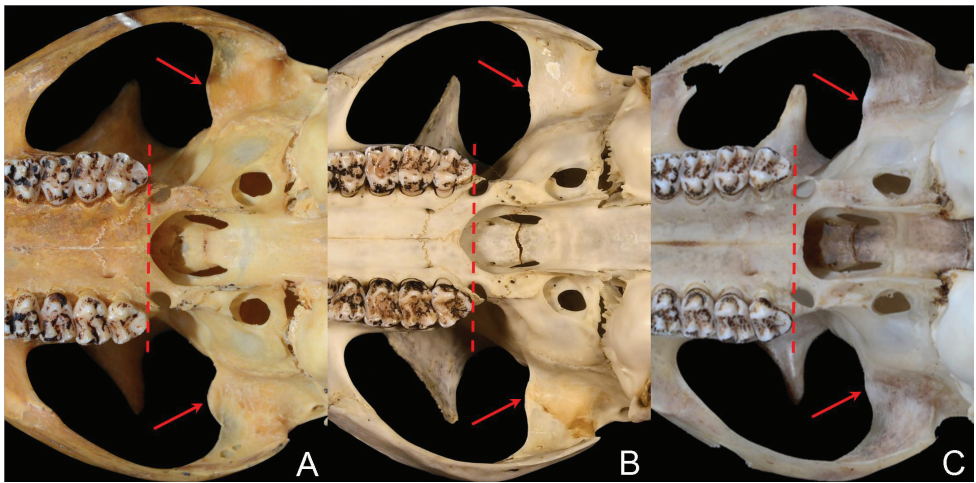


Figure 7. The posterior margin of the palatal bones relative to the posterior margin of M^3 (dotted line) and shape of the pregenoid process (arrow) of the three *Biswamoyopterus* species **A** (ZSI 20705, holotype) *Biswamoyopterus biswasi* **B** (KIZ 034924, holotype) *Biswamoyopterus gaoligongensis* sp. nov., **C** (NUoL FES.MM.12.163, holotype) *Biswamoyopterus laoensis*. The image **C** was derived from Sanamxay et al. (2013).

B. gaoligongensis sp. nov. and *B. biswasi* are distinctly smaller than those of *B. laoensis*. The posterior margin of the palatal bones of *B. gaoligongensis* sp. nov. and *B. biswasi* is concave forward, while *B. laoensis* is flat. The central point of the posterior margin of the palatal bones of *B. gaoligongensis* sp. nov. lies in front of the posterior margin of M^3 , *B. biswasi* just meet, and *B. laoensis* lies behind (Fig. 7).

The metacone and hypocone of M^1 and M^2 of *B. gaoligongensis* sp. nov. are most developed among three species, followed by *B. laoensis*, again *B. biswasi*. As a result, M^1 and M^2 of *B. gaoligongensis* sp. nov. are almost equal to P^4 , while those of *B. laoensis* and *B. biswasi* are smaller than P^4 . In addition, the outline of M^1 and M^2 of *B. gaoligongensis* sp. nov. is sub-square, *B. laoensis* is sub-rectangle, and *B. biswasi* is sub-triangular. The hypoconid of *B. gaoligongensis* sp. nov. is strongest among three species, followed by *B. biswasi*, again *B. laoensis* (Fig. 5).

Distribution. Apart from the locality of the holotype, there are two more localities in Yunnan, China, where the *Biswamoyopterus gaoligongensis* sp. nov. was photographed. These include Linjiapu (25.28693N, 98.70102E), 10 km west of the type locality; and Banchang (25.145876N, 98.796026E), 9 km south of the type locality (Fig. 1). Although these three localities cover the east and west slopes of Mount Gaoligong (the watershed of the Irrawaddy River and the Nu River [Salween River]), they are all restricted in a small area of southern Mount Gaoligong.

Natural history. Little is known about the natural history of *Biswamoyopterus gaoligongensis* sp. nov. The holotype was collected from evergreen broad-leaved forest at an altitude of 2,000 meters above sea level. A set of photos taken in Linjiapu showed a *Biswamoyopterus gaoligongensis* sp. nov. resting on the branches of *Daphniphyllum* sp. *Petaurista yunnanensis*, *P. elegans*, and *Hylopetes alboniger* were also collected in the same habitat where the holotype was collected.

Conservation status. The limited available information suggests that *Biswamoyopterus gaoligongensis* sp. nov. has a relatively low abundance. Because low-altitude forests inhabited by *Biswamoyopterus gaoligongensis* sp. nov. are close to human settlements, they are vulnerable to human activities. The currently known threats are agricultural reclamation and poaching.

Key to the three known species of *Biswamoyopterus*

- 1 Pale orange belly and marked with numerous, black, discontinuous lines; ear tufts black; long muzzle; large auditory bulla; the posterior edge of the palatal bones is flat..... *Biswamoyopterus laoensis*
- Light-coloured belly; ear tufts bicolor or white; short muzzle; smaller auditory bulla; the posterior edge of the palatal bones is concave forward..... **2**
- 2 Parti-coloured tail with a dark tip; ear tufts white; the central point of the posterior margin of the palatal bones just meet the posterior margin of M³; the outline of M¹ and M² is sub-triangular; smaller hypoconid *Biswamoyopterus biswasi*
- Black tail; ear tufts bicolor; the central point of the posterior margin of the palatal bones lies in front of the posterior margin of M³; the outline of M¹ and M² is sub-square; strong hypoconid *Biswamoyopterus gaoligongensis* sp. nov.

Discussion

This study describes a third species of *Biswamoyopterus* in the middle of the isolated ranges of two previously known species, suggesting that the distribution of *Biswamoyopterus* is much broader than previously known. Although the genetic analysis within *Biswamoyopterus* was not available in this study, the morphological comparison shows that *Biswamoyopterus gaoligongensis* sp. nov. markedly differs from *Biswamoyopterus bis-*

Table 2. Comparison of the three species of *Biswamoyopterus*.

Species	<i>B. biswasi</i>	<i>B. gaoligongensis</i> sp. nov.	<i>B. laoensis</i>
Size	Relatively small	Relatively small	Large
Dorsal coloration	Morocco-red speckled with white	Reddish brown speckled with white	Dark reddish brown speckled with whitish-grey
Ventral Coloration	White	Yellowish-white	Pale orange and marked with numerous, black, discontinuous lines
Coloration of tail beyond the uropatagium	Pale smoky grey with a dark tip	Black	Black
Ear tufts	White	The anterior tufts are black, and the posterior tufts are basally white and terminal black	Black
Muzzle	Short	Shorter	Long
Outer margin of the nasal bone, orbital margin of the frontal bone, and post-orbital margin of the frontal bone vs. midline of the skull	Inclined	Almost parallel	More inclined
Postorbital processes	Large	Large	Relatively small
Preglenoid process	Forward protruding	Almost flat	Almost flat
Sutures of frontal and squamosal bone	Almost flat	Bulge	Almost flat
Auditory bulla	Relatively small	Relatively small	Large
Posterior margin of the palatal bones	Concave forward, the central point just meets the posterior margin of M ³	Concave forward, the central point lies in front of the posterior margin of M ³	Flat, the central point lies behind the posterior margin of M ³
M ¹ and M ²	Feeble metacone and hypocone, outline of M ¹ and M ² is sub-triangular	Most developed metacone and hypocone, outline of M ¹ and M ² is sub-square	Second developed metacone and hypocone, outline of M ¹ and M ² is sub-rectangle
M ₁ and M ₂	Second developed hypoconid	Most developed hypoconid	Feeble hypoconid

wasi and *Biswamoyopterus laoensis* in pelage colour and craniodental traits (Figs 4, 5; Table 2). Within the distribution of *Biswamoyopterus* and adjacent areas (Fig. 1), they occur sympatrically with a number of flying squirrels including *Belomys pearsonii*, *Eupetaurus* sp., *Hylopetes alboniger*, *H. phayrei*, *Petaurista alborufus*, *P. caniceps*, *P. elegans*, *P. petaurista*, *P. philippensis*, *P. yunnanensis* and *Trogopterus xanthipes* (Jackson and Thorington 2012; Jackson and Schouten 2012). This high diversity of both genera and species may be the result of the region acted both as refugia and diversification centre since the late Miocene (Lu et al. 2013; Mercer and Roth 2003).

Acknowledgements

We thank Mr. Dazhou Peng, Mr. Jinlin Qian, and Mr. Chunliao Qian for their assistance in the field. We are grateful to Dr. Rong Li for identification of plant species, and Dr. Qigao Jiangzuo for some morphologic terms. We appreciate Baoshan Management Bureau of Gaoligongshan National Nature Reserve for their assistance in field work. Our research is supported by National Key Research and Development Program of China (#2017YFC0505202) and the Yunnan University “Double First-Class” Construction Program (C176240107).

References

- Corbet GB, Hill JE (1992) The Mammals of the Indomalayan Region: A Systematic Review. Oxford University Press, New York, 307 pp.
- Jackson SM, Schouten P (2012) Gliding Mammals of the World. CSIRO Publishing, Melbourne, 58–160. <https://doi.org/10.1071/9780643104051>
- Jackson SM, Thorington RW (2012) Gliding mammals: Taxonomy of living and extinct species. Smithsonian Contributions to Zoology, Washington DC, 32–72. <https://doi.org/10.5479/si.00810282.638.1>
- Kennerley R (2017) *Biswamoyopterus laoensis*. The IUCN Red List of Threatened Species 2017: e.T88700294A88700297. <https://doi.org/10.2305/IUCN.UK.2017-2.RLTS.T88700294A88700297.en> [Downloaded on 28 March 2019]
- Koprowski JL, Goldstein EA, Bennett KR, Mendes CP (2016) Family Sciuridae (tree, flying and ground squirrels, chipmunks, marmots and prairie dogs). In: Wilson DE, Mittermeier RA, Ruff S, Martínez-Vilalta A, Cavallini P (Eds) Handbook of the Mammals of the World: Lagomorphs and Rodents I Lynx Editions, Barcelona, 648–837.
- Lu X, Ge D, Xia L, Zhang Z, Li S, Yang Q (2013) The evolution and paleobiogeography of flying squirrels (Sciuridae, Pteromyini) in response to global environmental change. *Evolutionary Biology* 40(1): 117–132. <https://doi.org/10.1007/s11692-012-9191-6>
- Molur S (2016) *Biswamoyopterus biswasi* (errata version published in 2017). The IUCN Red List of Threatened Species 2016: e.T2816A115063959. <https://doi.org/10.2305/IUCN.UK.2016-3.RLTS.T2816A22271554.en> [Downloaded on 28 March 2019]
- Mercer JM, Roth VL (2003) The effects of Cenozoic global change on squirrel phylogeny. *Science* 299(5612):1568–1572. <https://doi.org/10.1126/science.1079705>
- Saha SS (1981) A new genus and a new species of flying squirrel (Mammalia: Rodentia: Sciuridae) from northeastern India. *Bulletin of the Zoological Survey of India* 4(3): 331–336.
- Sanamxay D, Douangboubpha B, Bumrungsri S, Xayavong S, Xayaphet V, Satasook C, Bates PJJ (2013) Rediscovery of *Biswamoyopterus* (Mammalia: Rodentia: Sciuridae: Pteromyini) in Asia, with the description of a new species from Lao PDR. *Zootaxa* 3686(4): 471–481. <https://doi.org/10.11646/zootaxa.3686.4.5>
- Thorington RW, Musante AL, Anderson CG, Darrow K (1996) Validity of Three Genera of Flying Squirrels: *Eoglaucomys*, *Glaucomys*, and *Hylopetes*. *Journal of Mammalogy* 77(1): 69–83. <https://doi.org/10.2307/1382710>
- Tong H (2007) *Aeretes melanopterus* (Pteromyinae, Rodentia) from Tianyuan Cave near Zhoukoudian (Choukoutien) in China. *Geobios* 40(2): 219–230. <https://doi.org/10.1016/j.geobios.2006.04.006>